FATE AND EFFECT OF PERACETIC ACID SOLUTIONS ON BIOLOGICAL WASTEWATER TREATMENT SYSTEMS

A Dissertation
Presented to
The Academic Faculty

by

Jinchen Chen

In Partial Fulfillment
of the Requirements for the Degree
Doctor of Philosophy in the
School of Civil and Environmental Engineering

Georgia Institute of Technology
August 2021

FATE AND EFFECT OF PERACETIC ACID SOLUTIONS ON BIOLOGICAL WASTEWATER TREATMENT SYSTEMS

Approved by:

Dr. Spyros G. Pavlostathis, Advisor
School of Civil and Environmental
Engineering
Georgia Institute of Technology

Dr. Ching-Hua Huang
School of Civil and Environmental
Engineering
Georgia Institute of Technology

Dr. Sotira Yiacoumi
School of Civil and Environmental
Engineering
Georgia Institute of Technology

Dr. Xing Xie
School of Civil and Environmental
Engineering
Georgia Institute of Technology

Dr. Yuanzhi Tang
School of Earth and Atmospheric
Science
Georgia Institute of Technology

Date Approved: [May 04, 2021]

ACKNOWLEDGEMENTS

I, from deep inside, thank my advisor, Dr. Spyros G. Pavlostathis, for all his support and education in my graduate studies. From the first day I started my graduate research and my journey in the lab, he patiently shared his wisdom and knowledge, educated me to be a careful, thoughtful, and open-minded researcher. Beyond research, he encouraged and guided me to be a positive, grateful, tolerant, and strong person. I truly appreciate all the opportunities and challenges he provided with in my research and all his trust and encouragement on my way to be a better person. His perseverance in tough time and dedication to excellence hearten my faith in all my dreams and will always light up my way whenever I fall in the dark again in the future.

In addition to my advisor, I would like to thank the members of my thesis committee: Dr. Ching-Hua Huang, Dr. Sotira Yiacoumi, Dr. Xing Xie and Dr. Yuanzhi Tang. I would also like to thank Dr. Guangxuan Zhu and Dr. Chaoyang Huang for their tremendous support in the laboratory.

I thank Dr. Christine M. Dykstra for patiently training me in various experiments and helping me on all the lab instruments. I thank Sha Long and Dr. Xiaoguang Liu for all of the critical thinking and discussions in our co-work and their companionship inside the lab. I also thank Dr. Cheng Cheng and my other labmates for all of their support.

Last but not least, I would like to thank my mother for giving me life, raising me up, and educating me to aim high, to break limits, to fight for the summit and to never give up. I also thank all my other families and my friends for all their support and love.

TABLE OF CONTENT

LIST OF TABLES

LIST OF FIGURES

LIST OF SYMBOLS AND ABBREVIATIONS

AA	Acetic acid
AOB	Ammonia oxidizing bacteria
ARR	Ammonia removal rate
BNR	Biological nitrogen removal
COD	Chemical oxygen demand
DBP	Disinfection by-product
DO	Dissolved oxygen
H_2O_2	Hydrogen peroxide
CO_2	Carbon dioxide
DAF	Dissolved air floatation
N_2	Nitrogen
N_2O	Nitrous oxide
NOB	Nitrite oxidizing bacteria
NPR	Nitrate production rate
NRR	Nitrite removal rate
O_2	Oxygen
OTU	Operational taxonomic unit
OUR	Oxygen uptake rate
PAA	Peracetic acid
ROS	Reactive oxygen species
VFA	Volatile fatty acid

SUMMARY

PAA, as a wide-spectrum effective disinfectant, has been extensively and increasingly used in many industries, especially in poultry processing to control food-borne pathogens. However, the information related to the fate and effect of PAA in poultry processing wastewater and its biological treatment is extremely limited. Therefore, the objectives of the present study were to assess the fate of PAA in poultry processing wastewater streams, investigate dominant factors contributing to PAA decomposition, and evaluate the effect of PAA on biological wastewater treatment processes typically used in poultry processing plants, such as organic matter degradation, nitrification, and denitrification.

First, this research reported that PAA was not detected in any dissolved air flotation (DAF) influent and effluent samples collected at mid plant operation shifts, as a result of wastewater dilution and PAA decomposition during the wastewater conveyance to the DAF unit. However, up to 25 mg/L PAA was detected in the DAF effluent at the end of the operation shift coinciding with emptying chiller tanks where PAA levels in excess of 1,000 mg/L are typically maintained. The PAA decomposition rate correlated positively with pH, temperature, wastewater strength and organic content, and negatively with initial PAA concentration. PAA decomposition followed one-step and two-step pseudo-first order decomposition kinetics above and below pH 6, Acetic acid at equimolar concentration was the main product resulting from PAA decomposition in poultry processing wastewater. H_2O_2 decomposition in poultry waste streams was

negatively correlated to the initial H_2O_2 concentration and the decomposition rate was faster in DAF underflow than in process water.

The short-term evaluation of the effect of PAA on organic matter degradation, nitrification and denitrification using a mixed heterotrophic/autotrophic culture revealed that all the impact was dose-dependent, with significant inhibition at PAA greater than 20 mg/L, predominantly by PAA alone or in combination with H_2O_2. Minor inhibition was caused by indirect addition of PAA solution, a direct result of fast PAA decomposition in the complex, organic feed.

The long-term evaluation of the effect of PAA on organic matter degradation, nitrification, and denitrification using a mixed heterotrophic/autotrophic culture indicated that the impact was dose-dependent, with significant inhibition at PAA greater than 40 mg/L. Fast recovery of organic matter degradation, nitrification, and denitrification was achieved after PAA and/or H_2O_2 direct addition ended in both aerobic and anoxic reactors. Microbial acclimation to PAA did not take place in the aerobic reactors, but a low degree of acclimation was observed in anoxic reactors over the long-term operation. The observed decrease in nitrification rates in the aerobic reactors is predominantly attributed to enzyme inhibition than to loss of nitrifiers, but the impact of denitrification in the anoxic reactors is attributed to both enzyme inhibition and loss of culture viability. Intracellular ROS was not the cause of the observed deterioration of nitrification in the aerobic reactors, but was related to the decrease in denitrification activity in the anoxic reactors; nevertheless, the capacity of the microbial community to manage PAA-induced cell oxidative stress increased in both aerobic and anoxic reactors over the long-term operation. In both aerobic and anoxic reactors, the microbial community composition

significantly shifted over the long-term operation with addition of PAA solution, but shifted slightly to moderately with addition of H_2O_2.

Long-term evaluation of PAA with a continuously-fed, three-reactor biological nitrogen removal (BNR) system revealed that continuous, direct addition of PAA at 80 to 200 mg/L in the first, anaerobic reactor did not affect the BNR system performance, but both organic matter degradation and nitrogen removal were severely affected by continuous feeding with wastewater carrying residual PAA at 80 and 200 mg/L. Fast recovery of organic matter degradation and N removal was achieved within three hydraulic retention times feeding with PAA/H_2O_2-free DAF wastewater. The BNR system was more susceptible to residual PAA without the anaerobic reactor, i.e., a two-reactor system. Fast recovery of the BNR system performance after two upsets suggest that the BNR system's performance was not worsened during the long-term operation with PAA; however, acclimation to PAA was not established either. Microbial community analysis showed that the major orders *Lactobacillales, Synergistales, Bacteroidales*, and *Pseudomonadales* in the first, anaerobic reactor were all negatively impacted by PAA; the PAA impact on *Synergistales* and *Bacteroidales* was reversed while was not on *Lactobacillales* and *Pseudomonadales* after operation with PAA solution free DAF wastewater. In contrast, *Campylobacterales* and *Sphingomonadales* were enriched, attributed to their antioxidizing ability reported previously by other studies. However, both *Campylobacterales* and *Sphingomonadales* were not favored during the PAA-free system operation. The microbial communities in the second, anoxic reactor, and the third, aerobic reactor were very similar, due to the continuous mixed liquor cycling between them. All major orders in these two reactors,

Betaproteobacteriales, Sphingobacteriales and *Rhodobacterales*, were negatively affected by PAA.

The in-depth assessment of PAA effect on nitrification using an enriched nitrifying culture revealed that the impact on nitrification was predominantly related to the inhibitory effect of PAA on related enzymes, rather than to loss of cell viability or excessive cell oxidative stress. The inhibitory effect of PAA on both ammonia and nitrite oxidation was quantitatively successfully described by a Michaelis-Menten, non-competitive inhibition model. The transcriptional activities of the PAA and H_2O_2-amended nitrifying culture suggests that N metabolism related genes, such as *Nxr* and *Hao*, were downregulated under the effect of PAA, especially at a relatively high PAA level (i.e., 3 mg/L). The downregulation of all major ATPases genes and the upregulation of ATP synthases genes suggests that culture cells tended to store ATP rather than use ATP under the effect of PAA and/or H_2O_2. The upregulation of ATP-dependent protease indicates that protein damage occurred in the PAA and H_2O_2-amended nitrifying culture and the damage caused by PAA was worse than that by H_2O_2.

Overall, the long-term evaluation of the effect of PAA suggests that organic matter degradation, nitrification and denitrification of poultry processing wastewater will not be affected during the normal plant operation when residual PAA and H_2O_2 are not present in the wastewater, but will be affected when wastewater with high residual PAA concentrations is expected at the end of plant operation shifts due to emptying of chiller tanks, or in the case of accidental PAA solution spills.

Overall, the results of the study enhance our understanding relative to the fate and effect of PAA solutions in poultry processing wastewater treatment systems, information

crucial for the rational design and operation of biological treatment processes, especially those related to biological nutrient removal. The outcome of the study provides systematic information to the poultry processing industry to develop a sound methodology that will ensure the continuous use of PAA solutions to achieve pathogen-free products, while avoiding upsets of biological processes typically used in poultry processing plants, especially in the case biological treatment of PAA-bearing wastewater.

INTRODUCTION

1.1 Preface

Peracetic acid (PAA) has become a common alternative sanitizer in many

industries, such as, food, healthcare, water and wastewater treatment, fine chemicals, and

pulp and paper (Luukkonen and Pehkonen, 2017). There are many qualities that

contribute to PAA becoming an ideal disinfectant, including high oxidation potential,

toxicity to microorganisms, but not to higher forms of life, absence of persistent toxic or

mutagenic residuals or by-products, effectivity at ambient temperatures, stability and long

shelf life, low corrosivity, deodorizing ability, widespread availability, and reasonable

cost (Tchobanoglous et al., 2014).

PAA is commercially available as a quaternary equilibrium mixture containing

acetic acid (CH_3COOH), hydrogen peroxide (H_2O_2), PAA (CH_3COOOH) and water.

PAA is the peroxide of acetic acid, in a clear and colorless aqueous form, with a strong

pungent acidic odor. Pure PAA solution is not thermodynamically stable, and usually

spontaneously decomposes to produce acetic acid and O_2 at pH below its pK_a value of 8.2

(Yuan et al., 1997). Due to the high oxidation potential, PAA is a highly effective

bactericidal, virucidal, fungicidal and sporicidal agent used in various industries

(Luukkonen and Pehkonen, 2017). Current research has focused on the disinfection

efficiency of PAA, while information on the fate and effect of PAA in biological

wastewater treatment systems, where PAA-bearing wastewater is processed, is limited.

As H_2O_2 is always present in PAA solutions and given the biocidal property of H_2O_2,

1

there is potential that H_2O_2 can also impact biological treatment processes where PAA-and/or H_2O_2-bearing wastewater is processed. Thus, it is important to assess the fate and effect of PAA and H_2O_2 on biological wastewater treatment systems where PAA and H_2O_2 may cause upsets of biological processes. This study focused on the fate and effect of PAA and H_2O_2 in biological wastewater treatment systems typically used by the poultry processing industry. Specifically, the PAA and H_2O_2 decomposition kinetics in various wastewater matrices and the dominant factors contributing to their decomposition have been studied. Furthermore, the short- and long-term effect of PAA and H_2O_2 on biological treatment processes, including organic matter degradation, nitrification, denitrification, and the corresponding biological responses to PAA and H_2O_2 reflected by cell viability, cellular oxidative stress, respiration activities, and their microbial community structure and transcriptional activity, have been studied.

1.2 Research Objectives

The overall objective of this research was to assess the fate and effect of PAA and H_2O_2 on biological wastewater treatment systems. The specific objectives of this study were to:

1. Assess the fate of PAA and H_2O_2 in complex wastewater matrices.

2. Assess the short-term effect of PAA and H_2O_2 on aerobic degradation, nitrification and denitrification in batch bioassays.

3. Evaluate the long-term effect of PAA and H_2O_2 on bench-scale semi-continuously-fed bioreactors for an in-depth assessment of the three sub-processes (i.e., organic carbon removal, nitrification, and denitrification), as well

as biological responses (i.e., cell viability and intracellular reactive oxygen species) and microbial community structure.

4. Evaluate the short-term effect of PAA and H_2O_2 on an enriched nitrifying culture in batch nitrifying bioassays, for an in-depth assessment of nitrification activity, cellular level responses (i.e., cell viability and intracellular reactive oxygen species), as well as genetic responses (i.e., microbial community structure and transcriptomics).

5. Evaluate the long-term effect of PAA solution on a bench-scale continuously-fed biological nitrogen removal (BNR) system.

1.3 Approach

1.3.1 Assessment of PAA Fate and Decomposition in Poultry Processing Wastewater Streams

The fate and decomposition of PAA in different poultry processing wastewater streams was assessed. Dominant factors, such as pH, temperature, wastewater strength, and PAA/H_2O_2 concentration, contributing to PAA decomposition in these streams were investigated. PAA decomposition products were also identified.

1.3.2 Assessment of Short-term Effect of PAA Solution on Batch Bioassays

Mixed liquor withdrawn from a stock culture was used to assess the effect of PAA and H_2O_2 on the aerobic degradation of organic substrates, as well as nitrification and denitrification in batch bioassays amended with a range of PAA//H_2O_2 and H_2O_2 Concentrations.

1.3.3 Assessment of Long-term Effect of PAA Solution on Semi-Continuously Fed Bioreactors

Aerobic and anoxic bioreactors, semi-continuously fed with poultry processing wastewater, amended with PAA solution and H_2O_2 at increasing concentrations, were operated for 166 d. In addition, the effect of direct PAA solution and H_2O_2 addition to the bioreactors was assessed. The effect of PAA and H_2O_2 on aerobic degradation and nitrification in the aerobic reactors and organics degradation and denitrification in the anoxic reactors were evaluated, quantified in terms of chemical oxygen demand (COD) removal and nitrification as well as denitrification rates. Microbial responses to PAA solution, such as culture viability and intracellular reactive oxygen species (ROS), were also evaluated. Complementary aerobic and anoxic batch assays were conducted with single, direct PAA addition to determine potential acclimation taking place over the long-term operation with addition of PAA solution. Finally, the microbial community diversity and composition over the long-term operation with PAA and H_2O_2 addition were evaluated.

1.3.4 Assessment of Long-term Effect of PAA Solution on an Enriched Nitrifying Culture

Mixed liquor withdrawn from an enriched nitrifying culture was used to assess the effect of PAA and H_2O_2 on nitrification activity, respiration activities, cell viability, and cell oxidative stress, as well as microbial community structure and transcriptomics in batch bioassays.

4

1.3.5 Assessment of Long-term Effect of PAA Solution on a Continuous-flow Biological

Nitrogen Removal (BNR) System

The effect of PAA solution on a continuous-flow BNR system was evaluated, quantified in terms of extent of COD removal, denitrification and nitrification rates. The effect of direct PAA addition to the system, as well as poultry processing wastewater with residual PAA was assessed. The microbial community structure over the long-term operation with PAA addition was evaluated.

CHAPTER 2. BACKGROUND

2.1 PAA Physicochemical Properties

Table 2.1 summarizes the physicochemical properties of PAA (CAS: 79-21-0). PAA is a colorless liquid with pungent acidic odor, thermodynamically unstable, which spontaneously decomposes or explodes when concentrated. It is heavier and miscible with water, has a higher boiling point and lower melting point than water. PAA has a high redox potential (1.96 V vs. SHE), which is only lower than that of ozone (2.01 V) and hydroxyl radical (2.02 V), which can also be formed as a secondary oxidizer as a result of PAA decomposition. Table 2.2 summarizes the half reactions and oxidizing potential of commonly used oxidizers (Luukkonen and Pehkonen, 2017).

Table 2.1. Physicochemical properties of PAA.

Property	Value	Reference
Molecular Weight	76.051 g/mol	
Viscosity	3.28 cP at 25°C	*U.S. Coast Guard, Department of Transportation. CHRIS - Hazardous Chemical Data. Volume II. Washington, D.C.: U.S. Government Printing Office, 1984-5.*
Boiling Point	110°C at1 atm	*Lide, D.R. CRC Handbook of Chemistry and Physics 88TH Edition 2007-2008. CRC Press, Taylor & Francis, Boca Raton, FL 2007, p. 3-420*
Melting Point	-0.2 °C at 1 atm	*Lide, D.R. CRC Handbook of Chemistry and Physics 88TH Edition 2007-2008. CRC Press, Taylor & Francis, Boca Raton, FL 2007, p. 3-420*
Solubility	1000 mg/mLwater at 25°C	URL: http://www.hmdb.ca/metabolites/HMDB0031608
Density	1.226 g/cm^3 at 15°C	*Lide, D.R. CRC Handbook of Chemistry and Physics 88TH Edition 2007-2008. CRC Press, Taylor & Francis, Boca Raton, FL 2007, p. 3-420*
Vapor Density	(Air = 1): 2.6	URL: http://www.ilo.org/dyn/icsc/showcard.display?p_card_id=1031
Vapor Pressure	2.6 kPa at 20	URL: http://www.ilo.org/dyn/icsc/showcard.display?p_card_id=1031
log K$_{ow}$	-1.07	US EPA; Estimation Program Interface (EPI) Suite. Ver. 4.0. Jan, 2009. *http://www.epa.gov/oppt/exposure/pubs/episuitedl.htm*
Henry's Constant	660 mol/kg-bar	Cugley J., Infrared spectra, force constants and thermodynamic functions of matrix isolated peroxyacetic acid, Chem. Phys., 1976, 18, 281-292.
Enthalpy of Vaporization	44.2 kJ/mol at 15	Stephenson, R. M.; Stanislaw, M. Handbook of the Thermodynamics of Organic Compounds, 1987. [doi:10.1007/978-94-009-3173-2]
Enthalpy of Dissociation	428.0 kJ/mol at 25	Cottrell, T.L. *The Strengths of Chemical Bonds*, 2d ed., Butterworth, London, 1958; B. S. W. Benson, *J. Chem. Educ.* **42:**502 (1965); and J. A. Kerr, *Chem. Rev.* **66:**465 (1966).

Table 2.2. Half-reactions and oxidation potentials (vs. Ag/AgCl electrode) of oxidizers commonly used in water treatment applications (Luukkonen and Pehkonen, 2017).

Oxidant	Half-Reaction	E^0 (V)
Hydroxyl Radical (·OH)	$\cdot OH + e^- \leftrightarrow OH^-$	2.02
Ozone (O$_3$)	$O_3 + 2H^+ + 2e^- \leftrightarrow O_2 + H_2O$	2.076
PAA	$CH_3CO_3H + 2H^+ + 2e^- \leftrightarrow CH_3CO_2H + O_2$	1.96
H$_2$O$_2$	$H_2O_2 + 2H^+ + 2e^- \leftrightarrow 2H_2O$	1.776
Permanganate (MnO4$^-$)	$MnO_4^- + 4H^+ + 3e^- \leftrightarrow MnO_2 + 2H_2O$	1.679
	$MnO_4^- + 8H^+ + 5e^- \leftrightarrow Mn^{2+} + 4H_2O$	1.507
Chlorine gas (Cl$_2$)	$Cl_2(g) + 2e^- \leftrightarrow 2Cl^-$	1.358
Hypochlorous acid	$HOCl + H^+ + 2e^- \leftrightarrow Cl^- + H_2O$	1.482
Chlorine Dioxide	$ClO_2 + H^+ + e^- \leftrightarrow HClO_2$	1.277
	$HClO_2 + 3H^+ + 4e^- \leftrightarrow Cl^- + 2H_2O$	1.57

2.2 PAA Decomposition

PAA solution is commercially available as a quaternary equilibrium mixture of acetic acid (CH_3COOH), hydrogen peroxide (H_2O_2), peracetic acid (CH_3COOOH) and water:

$$CH_3COOH + H_2O_2 \leftrightarrow CH_3COOOH + H_2O \qquad (2.1)$$
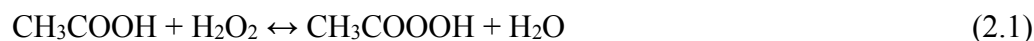
PAA in aqueous solution at a pH range of 5.5-9 may decompose according to the following three reactions (Yuan et al., 1997; Pereira et al., 2020):

1) Spontaneous decomposition to form acetic acid and oxygen:

$$CH_3COOOH \rightarrow 1/2\ CH_3COOH + 1/2\ O_2 \qquad (2.2)$$
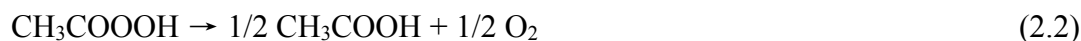
2) Hydrolysis to form acetic acid and hydrogen peroxide:

$$CH_3COOOH + H_2O \rightarrow CH_3COOH + H_2O_2 \qquad (2.3)$$
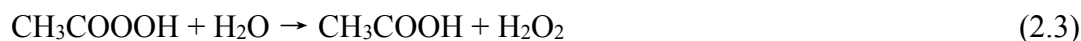
3) Transition metal catalyzed decomposition:

$$M^{n+}$$

$$CH_3COOOH \rightarrow CH_3COOH + 1/2\ O_2\ (+ \text{ other decomposition products}) \qquad (2.4)$$
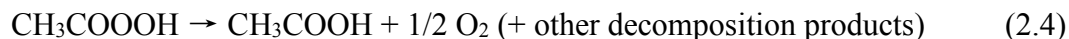
The contribution of reaction 2.3 to PAA decomposition decreases with increasing pH and is negligible at pH $\geqslant$ 9.5; in contrast, reaction 2.4 is more pronounced at higher pH values and is the only reaction occurring at pH $\geqslant$ 9.5 (Yuan et al., 1997). Thus, the participation of peracetic acid and peracetate in the above-mentioned reactions depends on the relative distribution between the two species, which in turn depends on the solution pH and the PAA pKa value of 8.2. Under strong acidic conditions, the spontaneous decomposition of PAA is a three-step reaction: protonation of the oxygen atom, formation of an active intermediary (a C_4 compound resulting from the attack of the oxygen atom of the hydroxyl in a PAA molecule on the activated carbonyl carbon of

another PAA molecule), and finally formation of acetic acid and oxygen (Zhao et al., 2008). However, spontaneous decomposition of PAA under acidic conditions was found to be insignificant below 55°C (Zhao et al., 2008). At neutral and alkaline conditions, the peracid anion ($R\text{-}COOO^-$) induces spontaneous decomposition of peracids, which explains the increase in the PAA decomposition rate with increasing pH. The decomposition of PAA is affected or catalyzed by many factors, such as pH, temperature, organic materials and transition metals (Luukkonen and Pehkonen, 2017). It should be noted that the term decomposition is used hereafter as an all-inclusive term without any specific reference to exact reaction mechanisms. In addition to acetic acid, O_2 and H_2O_2, PAA spontaneously and/or by reaction with other reactive chemical species may lead to the production of hydroxyl radical (HO•), acetoxyl radical ($CH_3COO•$), peroxyacetoxyl radical ($CH_3COOO•$), acetaldehyde (CH_3COH), and methyl radical ($H_3C•$) (Tolleson et al., 2012). None of the above-mentioned peracetic acid degradation products is considered to be toxic and all should be readily degraded under the prevailing conditions of biological processes commonly use in biological wastewater treatment systems.

PAA can react with various agents in aqueous systems. Figure 2.1 is a summary of reactions of peracids with physical or chemical agents in aqueous environments (Luukkonen and Pehkonen, 2017). Transition metals, such as, permanganate, cobalt, copper, silver and iron, can catalyze PAA decomposition by different mechanisms. For instance, the catalyzing effect of cobalt on PAA is by the formation of organic radicals, and the effect of iron on PAA is by the Fenton reaction, while catalysis by permanganate proceeds by complicated redox reactions rather than radicals (Popov et al., 2005). PAA was reported to react with Fe(II) more rapidly than H_2O_2, and the combination of

PAA/Fe(II) was applied to degrade micropollutant, such as methylene blue and naproxen (Kim et al., 2019). Phosphate accelerates the decomposition of PAA due to its radical quenching capacity (Mattle et al., 2011). In addition to the above-mentioned reactions, PAA reacts with peptide bonds of intact proteins (i.e., polypeptides) and free amino acids (Tolleson et al., 2012). Du et al. (2018) reported that most amino acids showed sluggish reactivity towards PAA, except cysteine reacting very fast with PAA; methionine and histidine followed second-order kinetics. They also found that the reaction of amino acids with PAA is affected by pH (faster at pH 5 and 7 than at pH 9), because the lower the pH is, the higher the protonated PAA concentration, which is the effective form towards amino acids.

The observed decomposition kinetics of PAA in aqueous systems vary in different matrices because the rate is the result of multiple, complex interactions of PAA with matrix components, but pseudo-first order kinetics are common. In DI water, Yuan et al. (1997a) found that PAA decomposition followed second-order kinetics with a maximum rate at pH 8.2. In their later study, Yuan et al. (1997b) reported that PAA hydrolysis followed first-order kinetics, with an increasing rate as pH increased. Pederson et al. (2009) reported PAA decomposition followed first-order kinetics in the aqueous phase of submerged aquaculture biofilters; the higher the PAA dosage the slower its decomposition.
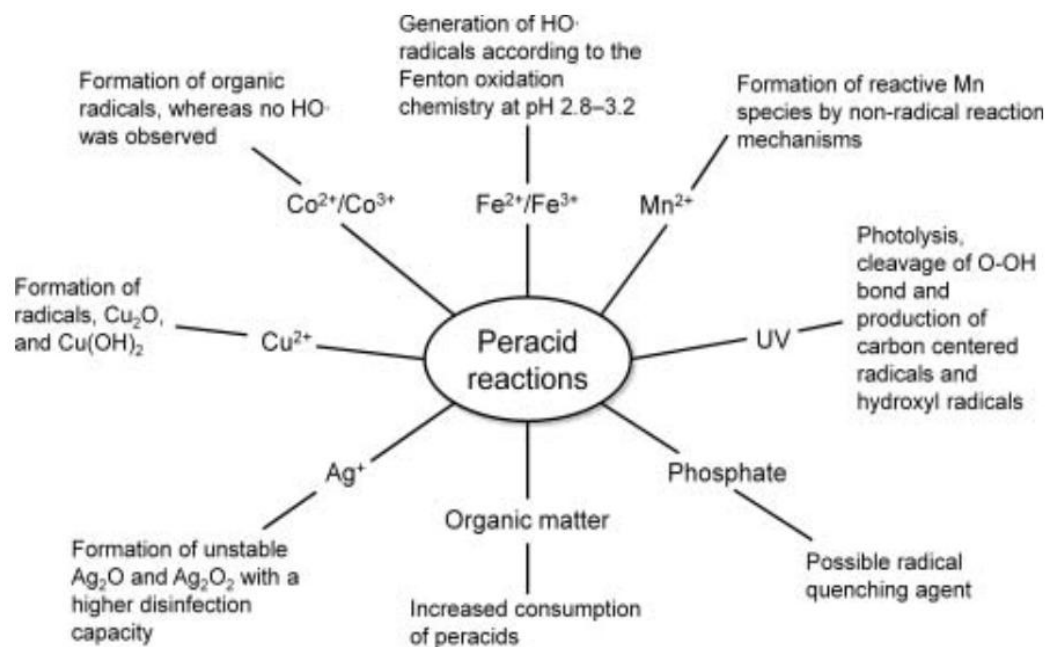
Figure 2.1. Reaction of peracids with various physical and chemical agents in aqueous environments (Luukkonen and Pehkonen, 2017).

2.3 PAA Disinfection

PAA is a wide-spectrum, strong disinfectant, effective against bacteria, viruses, and fungi. The advantages of PAA as a disinfectant are: ease of implementation without specialized equipment, broad spectrum antimicrobial activity at relatively low doses, lack of toxic or mutagenic byproducts, relatively low dependence on pH compared to chlorine due to its high pK_a value (8.2), and short contact time (Wagner et al., 2002; Kitis, 2004; Santoro et al., 2007; Mattle et al., 2011). The above-stated advantages and benefits of using PAA have been tested and realized with treated municipal wastewater effluent, especially for its suitability for water recycle and reuse (Luukkonen and Pehkonen, 2017).

Although H_2O_2 is always present in the equilibrium mixture of PAA solutions, also a disinfectant contributing to the disinfection power of the PAA mixture, PAA is a more potent antimicrobial agent than H_2O_2, being rapidly active at low concentrations

11

against a wide spectrum of microorganisms (Baldry, 1983; Baldry and French, 1989b;
Fraser et al., 1984). It was found that H_2O_2 required much larger doses than PAA for the
same level of disinfection (Wagner et al., 2002).

So far very limited research has been performed on the mode of action of PAA as
an antimicrobial agent, and there are only speculations that it functions much as other
peroxides and oxidizing agents (Block, 1991). Its disinfectant activity is based on the
release of active oxygen species (Liberti and Notarnicola, 1999). Several types of specific
reactions by PAA have been described by Kitis (2004) and references therein: a)
Sulfhydryl (-SH), disulfide (S-S), and double bonds in proteins, enzymes, and other
biomolecules are oxidized; b) inactivation of the enzyme catalase, which inhibits
hydroxyl radical oxidation; c) chemiosmotic function of the lipoprotein cytoplasmic
membrane is disrupted; d) protein denaturation occurs; and e) DNA denaturation.

2.4 PAA Inhibition of Biological Treatment Processes

PAA has been an effective antimicrobial agent for the poultry industry, used
primarily in chiller tanks. Wastewater generated in poultry processing facilities,
combined with other wastewater, is typically treated by dissolved air floatation (DAF) to
remove suspended solids, the underflow (or effluent) of which is typically treated by a
biological wastewater treatment process (Hajaya and Pavlostathis, 2012). Anecdotal
reports make reference to PAA in poultry processing wastewater causing severe upsets to
biological wastewater treatment processes, making it difficult to meet effluent discharge
requirements. Pederson et al. (2009) reported that minor impact was caused by 1 mg/L
PAA on a submerged aquaculture biofilter, whereas increased nitrite levels were

12

observed over a prolonged period under the effect of both 2 and 3 mg/L PAA application. Current research has focused on the disinfection efficacy of PAA and PAA decomposition in relatively clean systems, mostly in treated municipal secondary and tertiary effluents (Gehr et al., 2003; Koivunen and Heinone-Tanski, 2005; Falsanisi et al., 2006; Santoro et al., 2007; Soares Cavallini et al., 2013; Luukkonen et al., 2015). However, little information is available relative to possible adverse effect of PAA on biological wastewater treatment processes. Takashi et al. (2017) illustrated the gradual cell-structure collapse after 5- and 30-min PAA treatment against *Staphylococcus aureus* and *Pseudomonas aeruginosa* biofilm models in vitro via transmission electron photomicrographs, which suggested that there is potential PAA causes damage to cell membrane via reacting with the phospholipid bilayer and/or membrane proteins. However, no more information is available regarding the inhibition mechanism of PAA on a cellular level. PAA and chlorine both partially destroyed plasmid DNA while PAA was more efficient than chlorine in preventing bacterial regrowth (Zhang et al., 2019). Aldehyde formation by PAA disinfection was reported at a very low concentration; for instance, 10 mg/L of PAA was able to form a maximum 6.1 μg/L of formaldehyde in surface water (Nurizzo et al., 2005). However, it has been found that an increase in the PAA concentration promotes the formation of halogenated disinfection by-products (DBPs), through the oxidation of halogens (Cl^-, Br^-, or I^-) to hypohalous acids (HOCl, HOBr, or HOI), subsequently reacting with dissolved organic matter to form halogenated DBPs (Booth and Lester, 1995). Formaldehyde is known as a highly toxic compound, while halogenated DBPs are mutagenic. Biological processes may also be inhibited by the DBPs formed by PAA in addition to PAA itself.

2.5 Poultry Processing and Wastewater Treatment

Poultry processing plant follows typical practices for the processing of broilers, which in sequence include slaughtering, scalding and plucking, evisceration and organ removal, carcass washing, chilling, and rinsing. The chilling compartment commonly consists of three chiller tanks in series (i.e., pre-chiller, main chiller, and finishing chiller). Bird carcasses enter the pre-chiller and exit the finishing chiller while clean process water flows continuously countercurrent to the birds, i.e., enters the finishing chiller and exits the pre-chiller as chiller overflow (Figure 2.2). The chiller overflow along with other wastewater streams are treated by a dissolved air floatation (DAF) unit to remove suspended solids, such as fat, protein, feathers and flocs formed by the addition of flocculants (Dlangamandla et al., 2018). The DAF underflow (or effluent) is typically treated by a biological wastewater treatment process (Hajaya and Pavlostathis, 2012). PAA is increasingly used by the poultry processing industry, primarily applied on poultry carcasses during spray washing, chilling, or post chilling as an effective antimicrobial agent to suppress and control food-borne pathogens, thus ensuring food safety along with prolonged meat shelf life. However, anecdotal reports make reference to PAA in poultry processing wastewater causing severe upsets to biological wastewater treatment processes, making it difficult to meet effluent discharge requirements.
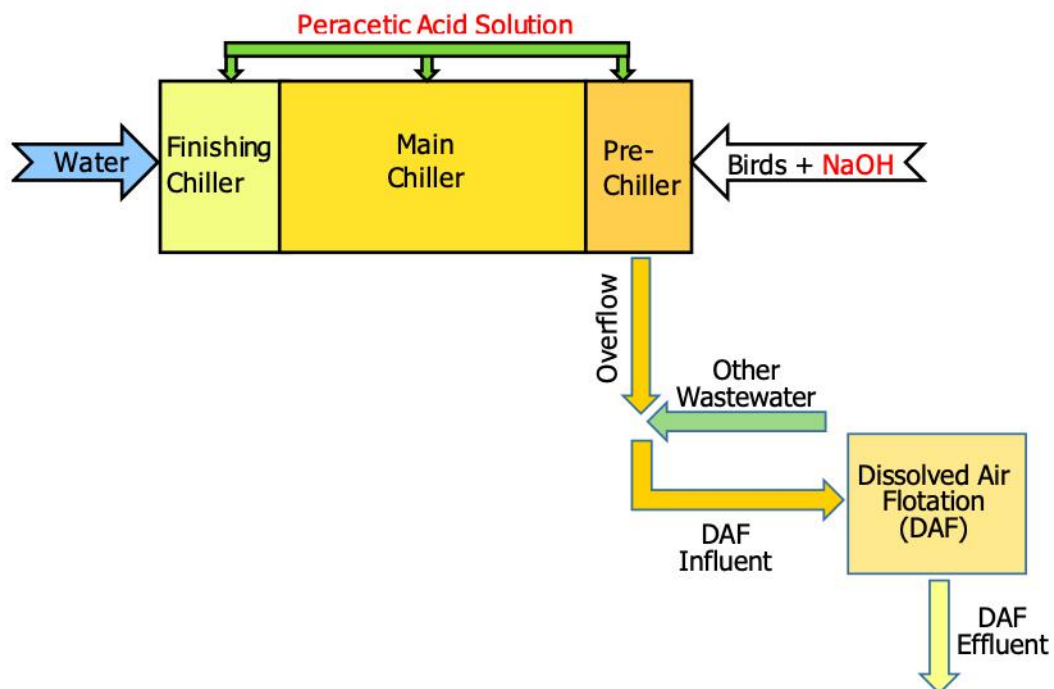
Figure 2.2. Schematic diagram of three chiller tanks and wastewater flow to the dissolved air flotation (DAF) unit.

CHAPTER 3. MATERIALS AND METHODS

3.1 General Analytical Methods

3.1.1 pH

All pH measurements were performed using the potentiometric method with a ATI Orion Model 370 digital pH meter (Orion Research Inc., Boston, MA) and a gel-filled combination pH electrode (VWR International, West Chester, PA). The meter was calibrated weekly with pH 4.0, 7.0, and 10.0 standard buffer solutions (Fisher Scientific, Pittsburg, PA).

3.1.2 Chemical Oxygen Demand (COD)

COD was measured using the closed reflux, colorimetric method as described in *Standard Methods* (Eaton et al., 2005). An aliquot of 2 mL of sample was added to the vial containing 3 mL pre-made digestion solution (HACH Company, Loveland, CO). After tumbling the vial for 4-8 times, the content in the vials was digested at 150°C for 2 h and then cooled down to room temperature. The absorbance was measured at 620 nm with a spectrophotometer (DR3900, HACH Company, Loveland, CO). Samples were centrifuged and filtered through a 0.45 μm polypropylene membrane filter if the soluble COD was measured, otherwise well-mixed samples were used after appropriate dilution for total COD measurements. All samples were prepared and measured in either triplicate (total COD) or duplicate (soluble COD).

3.1.3 N Species

Ammonium was determined by the salicylate method (HACH Method 10031; HACH, Loveland, CO, USA). Nitrite was determined by the ferrous sulfate method (HACH Method 10019). Nitrate was determined by the chromotropic acid method (HACH Method 10020). Total nitrogen (TN) was measured by the persulfate digestion method (HACH Method 10208). Organic nitrogen was calculated as the difference between TN and inorganic N (i.e., the sum of ammonium, nitrite, and nitrate). Crude protein was estimated as the organic nitrogen multiplied by a conversion factor of 6.25 (equivalent to 0.16 grams of N per gram of protein, based on the general protein formula of $C_{16}H_{24}O_5N_4$) (Grady et al., 2011).

3.1.4 P Species

Total phosphorus (TP) and soluble orthophosphate were measured following the molybdovanadate/acid persulfate digestion method (HACH Method 10127).

3.1.5 Anions

Anion concentrations were measured using a Dionex ICS-3000 ion chromatography unit (Dionex Corporation, Sunnyvale, CA) equipped with a suppressed conductivity detector, a Dionex IonPac AG14A (4x50mm) precolumn, and a Dionex IonPac AS14A (4x250 mm) analytical column. The unit was operated in autosupression mode with 1 mM $NaHCO_3$/8 mM Na_2CO_3 eluent and a flow rate of 1 mL/min. All samples were filtered through 0.2 μm membrane filters prior to injection. The minimum detection limit for sulfate was 0.05 mM.

3.1.6. Cations

Cations (i.e., common and trace metal cations) were measured by inductively coupled plasma mass spectrometry (ICP-MS, Agilent 7500a series). Samples were diluted in 2% trace metal grade HNO_3 (Fisher Scientific, Inc.; Waltham, MA) containing 20 ppb scandium (Sc) as an internal standard to correct for instrument drift. All measurements were conducted in duplicate. Calibration standards were prepared with a certified stock solution (SPEX CertiPrep; Metuchen, NJ) in 2% HNO_3 containing the internal standard and analyzed every 15–20 samples as quality controls.

3.1.7 Total and Volatile Solids (TS and VS)

Total solids content of samples was determined according to procedures outlined in *Standard Methods* (Eaton et al., 2005). Samples were weighed in pre-ignited (550°C) and cooled ceramic crucibles using a PG503-S balance (METTLER TOLEDO, Columbus, OH). The samples were then dried at 105°C for 24 h in a Fisher Isotemp Model 750G oven. After drying, the crucibles were transferred to a desiccator until cooled, and then the dry weight was measured. To measure VS, the crucibles were transferred to a Fisher Isotemp Model 550-126 muffle furnace and ignited at 550°C for 20 min. After ignition, the samples were cooled in a desiccator and the remaining solids weight was measured. TS was calculated as the difference between the weight of the crucible after the sample was dried at 105°C and the tare weight of the crucible divided by the sample volume. VS was calculated as the difference between the weight of the crucible after the sample was dried at 105°C and the weight of the crucible after the sample was combusted at 550°C divided by the sample volume.

3.1.8 Total and Volatile Suspended Solids (TSS and VSS)

TSS and VSS were determined according to procedures described in *Standard Methods* (Eaton et al., 2005). Whatman GF/C glass fiber filters (47 mm diameter and 1.2 μm nominal pore size; Whatman, Florham Park, NJ) were washed with deionized (DI) water and ignited at 550oC for 20 min in a Fisher Isotemp Model 550-126 muffle furnace before use. The filters were then cooled in a desiccator and weighed. Samples of known volume were filtered through the glass fiber filters. The filters were then rinsed with 10 mL DI water to remove dissolved organics and inorganic salts. The filters containing the samples were dried at 105°C for 90 min. After cooling in a desiccator, the dry weight was recorded and the filters containing the dry samples were ignited at 550°C for 20 min. After ignition, the samples were cooled down in a desiccator and the weight was measured. TSS and VSS concentrations were then calculated. TSS was calculated as the difference between the weight of the filter after the sample was dried at 105°C and the tare weight of the filter divided by the sample volume. VSS was calculated as the difference between the weight of the filter after the sample was dried at 105°C and the weight of the filter after the sample was combusted at 550°C divided by the sample volume.

3.1.9 Total Gas Production

Total gas production in closed assay bottles and large volume reactors was measured by either the acid brine displacement method or with a Sper Scientific (Scottsdale, AZ) pressure transducer (resolution −1 atm to 1.974 atm with an accuracy of 0.002 atm).

3.1.10 Gas Composition

The gas composition was determined by a gas chromatography (GC) unit (Agilent Technologies, Model 6890N; Agilent Technologies, Inc., Palo Alto, CA) equipped with two columns and two thermal conductivity detectors. Methane (CH_4) and dinitrogen (N_2) were separated with a 15 m HP-Molesieve fused silica, 0.53 mm i.d. column (Agilent Technologies, Inc.). Carbon dioxide (CO_2) and hydrogen sulfide (H_2S) were separated with a 25 m Chrompac PoraPLOT Q fused silica, 0.53 mm i.d. column (Varian, Inc., Palo Alto, CA). Helium was used as the carrier gas at a constant flow rate of 6 mL/min. The 10:1 split injector was maintained at 150°C, the oven was set at 40°C and the detector temperature was set at 150°C. All gas analyses were performed by injecting a 200 μL gas sample. The minimum detection limits for CH_4, CO_2, H_2S, and N_2 were 500, 800, 100 and 50 ppmv, respectively.

3.1.11 Volatile Fatty Acids (VFAs)

VFAs (C_1 to C_7; i.e., formic, acetic, propionic, iso-butyric, n-butyric, iso-valeric, n-valeric, iso-caproic, n-caproic, and heptanoic acids) were quantified using a high-performance liquid chromatography (HPLC) unit equipped with a UV-vis detector (Agilent 1100, Santa Clara, CA). A HPX-87H column (BioRad, Hercules, CA) was used with an eluent of 5 mM H_2SO_4 at a flow rate of 0.6 mL/min. The injection volume was 20 μL, and the column was maintained at 65℃. The wavelength of 210 nm was used for all VFAs detection. Samples used for the measurement of VFAs were prepared by centrifugation at 10,000 rpm for 20 min and filtration through 0.2 μm Nuclepore track-etched polycarbonate membranes (Whatman Inc., Florham Park, NJ) prior to injection. A

10 mM VFAs standard solution was obtained from Supelco (Product No. CRM46975; Bellefonte, PA); all VFAs had quantification ranges from 0.25 to 10 mM. The results of VFAs analysis are summarized in Table 3.1.

Table 3.1. Results of VFAs analysis.

VFA	Retention time (min)	Slope[a]	R^2	Molecular Weight (mg/mmol)
Formate	13.085	89.14	1.00	46.03
Acetate	14.267	68.28	1.00	60.05
Propionate	16.722	83.42	1.00	74.08
i-Butyrate	18.807	118.93	1.00	88.11
n-Butyrate	20.285	95.84	0.99	88.11
i-Valerate	23.154	115.42	1.00	102.13
n-Valerate	27.468	96.03	0.99	102.13
i-Caproate	33.963	104.67	1.00	116.16
n-Caproate	39.543	99.81	0.99	116.16
Heptanoate	61.499	94.86	0.99	130.18

[a]Slope = peak area/VFA concentration (mM)

The calculation of VFAs in terms of COD is as follows:

$$VFA\ COD\ \left(\frac{mg}{L}\right) = \frac{peak\ area}{slope} \times molecular\ weight\ \times CODconversion\ factor$$

3.1.12 Dissolved Oxygen (DO)

DO was measured by luminescence using a HACH DO meter (HACH, Loveland, CO, USA). The DO meter was equipped with a measuring LED that emits a pulse of blue light and a photo diode as a light detector.

3.1.13 Total Carbohydrates

Total carbohydrates were measured using the anthrone method (Morris, 1948). The anthrone solution was prepared by dissolving 1 g of anthrone (Sigma Aldrich) in 500

mL 98% H_2SO_4. Each sample was digested in glass digestion vials with the 0.2%

anthrone solution for 15 min in a boiling water bath. Absorbance was measured at 620

nm with a HACH DR3900 spectrophotometer (HACH, Loveland, CO, USA). Well-

mixed samples were used after appropriate dilution for total carbohydrates measurements.

All samples were prepared in triplicates and a calibration curve was prepared using 1 g/L

standard solution of glucose. Figure 3.1. shows the calibration curve. However, this

method was found to overestimate the carbohydrates content of PAA-bearing poultry

processing waste streams. The positive PAA interference on the anthrone method was

evaluated and data corrected by subtracting 0.465 [PAA] (mg/L) from the total

carbohydrates (mg/L) estimated by the anthrone method.
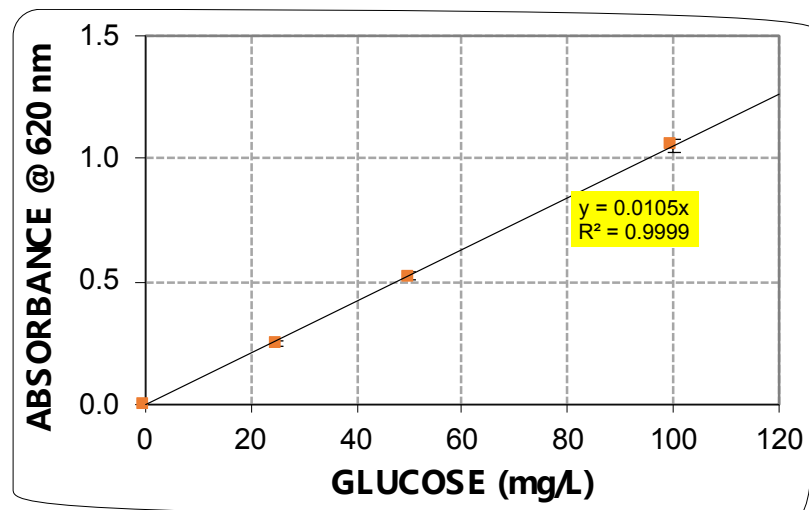
Figure 3.1. Carbohydrates calibration curve using glucose as the standard.

3.1.14 Total Lipids

Total lipids were measured using a gravimetric method after liquid-liquid extraction with chloroform and methanol (Pavlostathis, 1985). A sample aliquot was pre-acidified using 1.0 N HCl to pH 3, and then mixed with 40 and 100 mL chloroform and methanol, respectively, in a blender for 1 min. An additional 60 and 40 mL of chloroform and methanol was added with further mixing. The blender contents were then filtered through a No.40 Whatman® filter, and the filtrate transferred into an extraction funnel and allowed to separate the chloroform phase overnight. The chloroform bottom layer was transferred to a pre-weighed Erlenmeyer flask (initial flask weight) and the chloroform was evaporated by placing the flask on a heating plate set at 80°C. The flask was then placed in a 100°C oven in order to dry the remaining solvent. After being cooled in a desiccator, the flask was weighed again (final flask weight) and the total lipids concentration was calculated by the equation below.

$$Total\ Lipids\left(\frac{mg}{L}\right) = \frac{Final\ flask\ weight\ (mg) - Initial\ flask\ weight\ (mg)}{Sample\ volume\ (L)}$$

3.1.15 Culture Viability and Intracellular ROS

Culture viability, based on cell membrane integrity, was evaluated using the Live/Dead BacLight bacterial viability kit (cat. No. L7012) (Molecular Probes/Invitrogen Corporation, Carlsbad, CA) following the manufacture's protocol.

3.1.16 Intracellular Reactive Oxygen Species (ROS)

Intracellular ROS, an important indicator of oxidative stress, was determined using CellRox Green reagent (cat. No. C10444) (Molecular Probes/Invitrogen Corporation, Carlsbad, CA), were measured following standard protocols.

3.2 PAA and H_2O_2

3.2.1 PAA and H_2O_2 Solutions

Typical commercial PAA solutions used in poultry processing plants contain 5 to 50% PAA, 33 to 50 % CH_3COOH and 5 to 11% H_2O_2 (w/w). Peracetic acid (32% PAA, 45% acetic acid, 6% H_2O_2 w/w) was purchased from Sigma-Aldrich (St. Louis, MO, USA). This PAA solution closely matches typical PAA solutions used in poultry processing, which have relatively low H_2O_2 weight fractions as mentioned above. H_2O_2 (30%, w/w) was purchased from VWR (Pittsburgh, PA, USA). The PAA and H_2O_2 stock and working solutions were stored in the dark at $4^{\circ}C$.

3.2.2 PAA and H_2O_2 Equivalent Weight

In order to compare the effect of PAA and H_2O_2 on the microbial activity during the long-term operation of the aerobic reactors at a same oxidizing capacity, the H_2O_2 dose to R2 was increased to reach an oxidizing capacity equal to that of PAA in R3. The PAA and H_2O_2 decomposition reactions are shown below (Zhao et al., 2007). The equivalent weight of a compound undergoing a redox reaction is calculated as the molecular weight divided by the number of electrons involved in the redox reaction. Based on the oxidation state of each atom in the PAA and H_2O_2 molecule and their

products, one electron is transferred per mole PAA or H_2O_2 decomposed (Reaction 1 and 2 below). Based on the above, the equivalent weight of both PAA and H_2O_2 is equal to their molecular weight (PAA, 76 g/mole; H_2O_2, 34 g/mole). Thus, in terms of equivalents, one mole of H_2O_2 is 2.235-fold stronger oxidant than one mole of PAA.

1) PAA

$$\overset{\text{-III +I +III -II -I -I +I}}{CH_3COOOH} \rightarrow \overset{\text{-III +I +III -II -II +I}}{CH_3COOH} + \overset{0}{\tfrac{1}{2} O_2}$$

+1e⁻ / -1e⁻

2) H_2O_2

$$\overset{\text{+I -I}}{H_2O_2} \rightarrow \overset{\text{+I -II}}{H_2O} + \overset{0}{\tfrac{1}{2} O_2}$$

+1e⁻ / -1e⁻
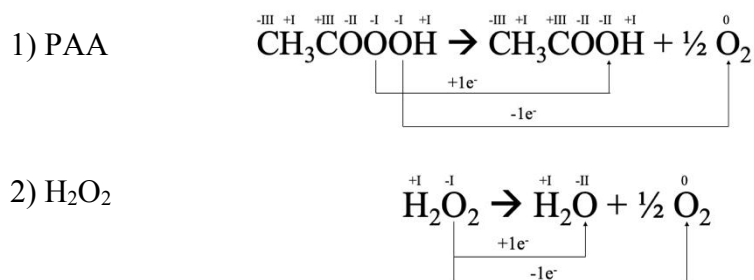
3.2.3 Spectrophotometric Quantification PAA and H_2O_2 (HACH DPD Method)

The PAA spectrophotometric method uses a powder pillow consisting of the N, N-diethyl-p-phenylenediamine (DPD) indicator, phosphate buffer (pH ~ 6.2-6.5) and potassium iodide (KI). KI is oxidized by PAA, liberating iodine (I_2), which oxidizes DPD to its pink product, known as Würster dye (Harp, 2002), that is detected at a wavelength of 515 nm. A spectrophotometer (HACH DR 1900) was used to measure the absorbance, which displays the results in terms of mg/L chlorine (as Cl_2). The factor of 1.07 was used to convert the measurement (mg/L Cl_2) to mg/L PAA, based on the molecular weight ratio of PAA to Cl_2 76:71. A standard curve was created with absorbance values vs. PAA concentration at 0.1, 0.5, 1.0, 5.0, and 10.0 mg/L PAA (Figure 3.2).
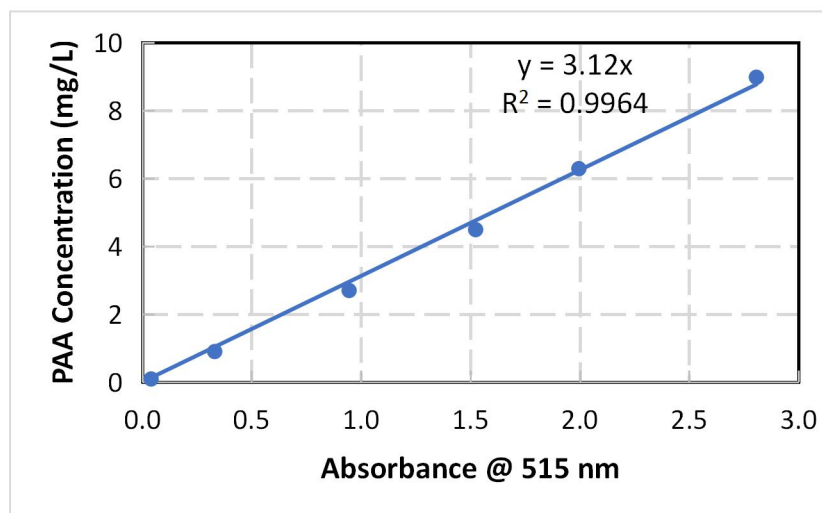
Figure 3. 2. PAA calibration curve.

Even though H_2O_2 exists in PAA solutions at very low concentrations, it also causes a positive error in the measurement of PAA using the DPD method. Because of this, KI and ammonium molybdate were used to first react with H_2O_2 in the samples to release free I_2, followed by the above procedure of PAA reacting with DPD, resulting in the concentration of total PAA and H_2O_2. Then, the H_2O_2 concentration was calculated by subtracting the PAA concentration from the total PAA and H_2O_2 concentration. The minimum detection limits were 0.05 mg/L for H_2O_2 and 0.1 mg/L for PAA. A standard curve was created with absorbance values vs. H_2O_2 concentration at 0.425, 0.85, 1.7, and 3.4 mg/L (Figure 3.3).
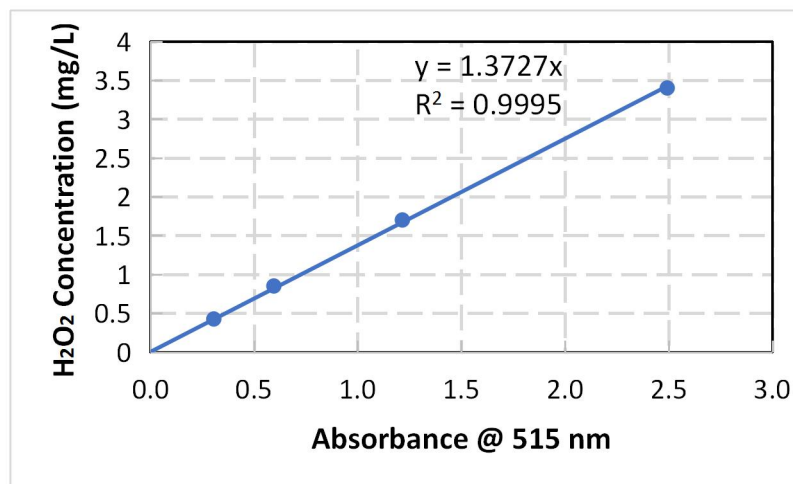
Figure 3.3. H_2O_2 calibration curve.

3.2.4 Simultaneous Quantification of PAA and H_2O_2 by HPLC

Simultaneous determination of PAA and H_2O_2 was achieved following the high-performance liquid chromatography (HPLC) method developed by Pinkernell et al. (1997). This method is based on the successive quantitative reaction of PAA with methyl p-tolyl sulfide (MTS) and H_2O_2 with triphenylphosphine (TPP) yielding the corresponding sulfoxide (MTSO) and phosphine oxide (TPPO). MTS and TPP and their oxides are separated by HPLC on a reverse-phase column (Luna® 5μm C8(2) 100 Å, 150 x 3 mm, Phenomenex, Torrance, CA) with acetonitrile/e-pure water (40:60, v:v) as eluent, at 1 mL/min flow rate for 8 min. The following gradient of acetonitrile in e-pure water was used: 40% for 0 to 3 min, 100% for 3 to 8 min. The injection volume was 5 μL, with needle wash by e-pure water before each run. External calibration with MTSO and TPPO standards leads to a very accurate and reliable method, using 0.1 to 8 mM standard MTSO and 0.01 to 1 mM TPPO. External calibration was also done for MTS and TPP standards, for analyzing residual MTS and TPP in the sample after the successive quantitative reaction. This method is applied at a PAA concentration range from 7.6 to

608 mg/L, and H_2O_2 from 0.34 to 34 mg/L. The calibration curves are shown in Figure 3.4.
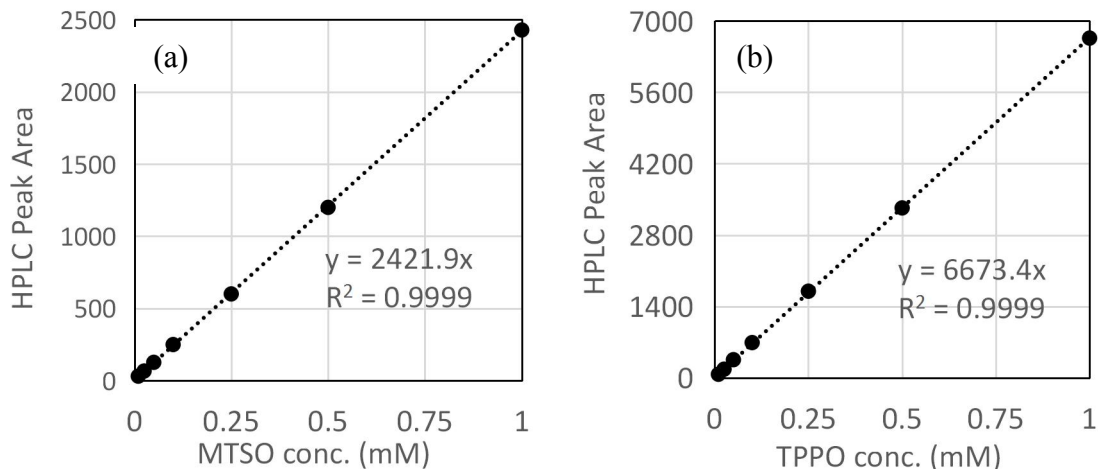
Figure 3.4. Calibration curve for (a) MTSO and (b) TPPO (Optimal quantitative range for both MTSO and TPPO is 0.01 to 1 mM).

To determine the concentration of PAA and H_2O_2 in the PAA working solution or a sample, a blank with deionized water followed the procedures described above was also prepared. The calculation of the concentration of PAA and hydrogen peroxide in the working PAA solution was as follows.

$$PAA \ (mM) = \frac{MTSO \ area_{wk \ sln.} - MTSO \ area_{bk}}{slope_{MTSO}}$$

$$H_2O_2 \ (mM) = \frac{TPPO \ area_{wk \ sln.} - TPPO \ area_{bk}}{slope_{TPPO}}$$

3.2.5 Iodometric Titrimetric Quantification of PAA and H_2O_2

Iodometric titration was used to measure PAA and total peroxides (in this case H_2O_2 and PAA) in aqueous solutions with intense color or high turbidity, taking advantage of the different reaction rates of iodide with PAA and H_2O_2. PAA reacts with KI liberating free I_2 within 30 s, while H_2O_2 needs 1-2 min to liberate free I_2. For the

measurement of PAA only, the titration should be completed within 1 min. Soluble starch solution was used as the I_2 indicator, showing a shade of dark blue and then the I_2 was titrated with a sodium thiosulfate ($Na_2S_2O_3$) solution resulting in a colorless end point of the titration. For the measurement of total peroxides, i.e., PAA and H_2O_2, ammonia molybdate is added to catalyze the reaction of H_2O_2 and KI, after which the produced I_2 is titrated with $Na_2S_2O_3$ using soluble starch as indicator. The minimum detection is 0.1 and 0.05 mg/L for PAA and H_2O_2, respectively. PAA quantification was as follows.

$$C_{PAA}(\frac{mg}{L}) = \frac{\left(\frac{V_1 C_1}{2}\right) * M_{PAA}}{V_S} * 1000$$

where: V_1, volume of $Na_2S_2O_3$ standard solution consumed, L; C_1, standardized actual concentration of $Na_2S_2O_3$ standard solution, mol/L; M_{PAA}, molecular weight of PAA, 76.05 g/mol; V_S, sample volume, L.

3.3 DNA Extraction and 16s Amplicon Sequencing

Bacterial DNA was extracted from the cultures using PowerSoil DNA Isolation Kit (QIAGEN LLC, Germantown, MD) according to the manufacturer's instructions. DNA was quantified using NanoDrop One (Thermo Scientifc, Wilmington, DE) and stored at -80°C until sequencing was performed. Bacterial DNA was amplified using the bacterial universal 16S rRNA gene primers 515F (5'-GTGCCAGCMGCCGCGGTAA-3') and 806R (5'-GGACTACHVGGGTWTCTAAT-3'). Amplified DNA was sequenced using the Illumina MiSeq platform and analyzed (Sangon Biotech, Shanghai, China). Bioinformatic analysis was performed using R packages (Ames, Iowa, USA). Taxonomy

was assigned using 99% operational taxonomic unit (OUT) similarity in GenBank (National Center for Biotechnology Information). To compare community structure, all representative sequences of detected OTUs were trimmed, aligned and a multi samples Taxonomy analysis tree, rarefaction curves using Alpha diversity and a heatmap in order level were constructed using R (R Core Team, 2014). Principle Components Analysis (PCA) and Principle Coordinates Analysis (PCoA) were then conducted and plotted in 2-D using R (R Core Team, 2014). Functions of the microbial communities was predicted using Functional Annotation of Prokaryotic Taxa (FAPROTX).

3.4 RNA Isolation, Transcriptome Sequencing, and Analyses

Culture (100 mL) was withdrawn from all test series amended with 0/0, 0.5/0.07, 3/0.42, 0/0.5, 0/3 mg/L PAA/H_2O_2 at the end of the 24-h incubation of the batch assay (see Section 1.4.2). The culture samples were centrifuged for 5 min at 16,000 × g and the total RNA was extracted from the culture pellets using RNeasy PowerSoil Total RNA kit (QIAGEN LLC, Germantown, MD) according to the manufacturer's instructions. Before constructing the transcriptome library, the total RNA concentration and size distribution was determined on an Agilent 2100 Bioanalyzer (Agilent, USA). Messenger RNA (mRNA) was enriched by removing ribosomal RNA from total RNA with the MICROBExpress™ Bacterial mRNA Enrichment kit (Ambion, Carlsbad, USA). Then the mRNA was fragmented randomly in fragmentation buffer, followed by cDNA synthesis using random hexamers and reverse transcriptase. After first strand synthesis, a custom second-strand synthesis buffer (Illumina) was added, containing dNTPs, RNase H and *E. coli* polymerase I to generate the second strand by nick-translation; AMPure XP

30

beads were used to purify the cDNA. Then the second strand was degraded by USER

Enzyme. The final cDNA library was ready after a round of purification, terminal-repair,

A-tailing, ligation of sequencing adapters, size selection and PCR enrichment. Library

concentration was first quantified using a Qubit 2.0 fluorometer (Life Technologies,

Carlsbad, USA), and then diluted to 2 ng/μL before checking insert size on a Agilent

2100 bioanalyzer and quantifying to greater accuracy by quantitative PCR (library

activity > 2 nm). The libraries were sequenced using Illumina HiSeq Platform and raw

data were generated for the following analysis. The quality of the raw reads was

visualized using FastQC, cleaned and trimmed using SeqPrep

(https://github.com/jstjohn/SeqPrep). Reads that were shorter than 50 base pairs (bp),

contained ambiguous (N) bases, and were of low quality (below 20) were discarded using

Sickle (https:// github.com/najoshi/sickle). rRNA reads were further screened using

SortMeRNA (http://bioinfo.lifl.fr/RNA/sortmerna/). Resulting sequences were filtered to

remove contigs of less than 300 bp in length. TransGeneScan (http://sourceforge.net/

projects/transgenescan/) was used to predict open reading frames. Transcripts were

assigned to taxonomic affiliations by binning to the best hit (BLASTP, e value $\leq 10^{-5}$) in

the non-redundant database. Potential functions were assigned on the basis of the best

homology (BLASTP, e value $\leq 10^{-5}$) to proteins within the Kyoto Encyclopedia of Genes

and Genomes (KEGG) database. Sequences with hits to proteins in eukaryotic organisms

and viruses were identified and removed before statistical analysis. Expression levels of

transcripts were calculated with RNA-Seq by Expectation-Maximization

(http://deweylab.github.io/RSEM/) based on the fragments per kilobase of transcript per

million mapped reads (FPKM).

CHAPTER 4. PAA FATE AND DECOMPOSITION IN POULTRY PROCESSING WASTEWATER

4.1 Introduction

The decomposition of PAA and its disinfection efficacy in relatively clean systems, mostly in treated municipal secondary and tertiary effluents, has been investigated in many studies (Gehr et al., 2003; Koivunen and Heinone-Tanski, 2005; Falsanisi et al., 2006; Santoro et al., 2007; Cavallini et al., 2013; Luukkonen et al., 2015). However, no information is available relative to the fate of PAA in poultry processing wastewater streams and its possible adverse effect on biological wastewater treatment processes. Thus, information on the fate and decomposition of PAA in poultry processing wastewater streams, which is crucial in assessing wastewater PAA levels entering subsequent biological wastewater treatment systems, is urgently needed.

The objectives of the work reported in this chapter were to: (a) assess the fate and decomposition of PAA in different poultry processing wastewater streams; (b) investigate dominant factors contributing to PAA decomposition in these streams; and (c) identify PAA decomposition products.

4.2 Materials and Methods

4.2.1 On-site PAA Monitoring and Wastewater Characterization

A poultry processing plant in the Southeast US was selected for on-site PAA monitoring and wastewater sampling. For on-site monitoring, samples were withdrawn from chiller tank overflow, DAF influent and effluent and tested for both pH and PAA at different time intervals for up to 6.5 h towards the end of a typical plant operation shift. For long-term characterization of poultry processing wastewater, samples from the pre-chiller, main chiller, finishing chiller, chiller overflow, DAF influent and DAF effluent were collected at mid plant operation shift multiple times over a 2-year period. At the participating poultry processing plant, PAA is continuously added only to the chiller tanks, i.e., pre-, main-, and finishing chiller, during the processing cycle. The samples were stored under refrigeration (4°C) in the laboratory and the following analyses were performed in triplicate: pH, total and volatile solids (TS, VS), total and soluble chemical oxygen demand (COD), volatile fatty acids (VFAs), ammonia, total N, total P, total carbohydrates, lipids, anions, and metals.

4.2.2 PAA Decomposition Assays

Batch PAA decomposition assays were conducted with DAF effluent as this wastewater is typically treated further using biological processes in most poultry processing plants. Five PAA decomposition assays were conducted corresponding to five factors: pH, temperature, initial PAA concentration, strength of DAF effluent and organics. Process water from the poultry processing plant and deionized (DI) water were used as controls. The peracetic acid solution used was as described in Section 3.2.1. The assays were performed in completely mixed 2.8 L Spinner cell flasks (Bellco Glass, Inc.,

Vineland, NJ) with a total liquid volume of 2 L kept at room temperature ($22\pm1^\circ$C), except for the temperature assay, for which five series were tested at 4, 10, 15, 20, and 30°C in 2.8 L water-jacketed Spinner cell flask, temperature controlled by a cooling/heating water circulator. All assays were performed at pH 6, except for testing the effect of pH, for which four series were tested at pH 4, 5, 6, and 7, the pH maintained by using a pH controller (HD PH-P, Barnant Company, Barrington, IL) and 1 N NaOH. The initial PAA concentration for each assay was 800 mg/L, except for testing the effect of carbohydrates (10 mg PAA/L) and initial PAA concentration (100, 200, 400, and 800 mg PAA/L). The high initial PAA concentrations used in this study are consistent with PAA concentrations encountered in poultry chiller tanks (see Section 4.3.1, below). In contrast to low, typically below 10 mg/L, PAA concentrations used for the disinfection of municipal secondary effluent, very high PAA concentrations are used in poultry processing because of the significantly higher microbial and organic content of poultry processing streams. Because the organic and inorganic content of poultry processing wastewater, collectively referred hereafter as wastewater strength, varies throughout the processing cycle, in order to assess the effect of DAF effluent strength on the PAA decomposition kinetics, four series were used with undiluted DAF effluent (i.e., 100% strength) and 5-, 2-, and 1.33-fold diluted effluent with DI water (i.e., 20, 50, and 75% strength, respectively).

In order to assess the effect of organics on the PAA decomposition rate, three aqueous matrices were prepared: high-protein-content, carbohydrates and lipids-in-methanol solution. A sample of decanter solids, high in poultry protein content, and a poultry fats sample were prepared by a rendering facility using poultry processing DAF

skimmings, also called secondary processing nutrients (SPN). The high-protein-content

solution was prepared by adding 100 g wet weight of the decanter solids sample to 1 L DI

water, stirred for 20 h, sieved through No. 60 sieve (250 μm openings), centrifuged at

10,000 rpm for 10 min and filtered through a GF/C glass fiber filter, followed by 0.45 μm

membrane filter. The filtrate was analyzed for pH, COD, total N, ammonia, crude protein,

TS/VS, carbohydrates and lipids. The decanter solids filtrate crude protein content was

very high (956 mg/L) compared to its total carbohydrates (34 mg/L) and lipids (67 mg/L)

content. Based on the total COD content (2,253 mg/L), the filtrate was diluted 4-fold with

DI water to match typical DAF effluent total COD concentrations, and used as the high-

protein-content matrix to evaluate the effect of protein on the PAA decomposition rate. In

order to assess the effect of carbohydrates on the PAA decomposition rate and to match

typical DAF effluent carbohydrates concentrations, a 20 mg/L glucose solution was used.

To overcome the limited poultry fat aqueous solubility, a lipids-in-methanol solution was

prepared by dissolving 50 g fat poultry SPN, obtained from the same rendering company

as the above-mentioned decanter solids, in 1 L methanol. Based on the lipids COD

concentration (i.e., the difference between the total COD of the lipids-in-methanol

solution and that of methanol), the lipids concentration was calculated by using the

conversion factor of 2.9 g COD/g lipids, considering $C_8H_{16}O$ as an empirical formula for

lipids (Grady et al., 1999). In order to match typical DAF effluent lipids concentrations,

the lipids-in-methanol solution was diluted 100-fold with DI water and used to assess the

effect of lipids on the PAA decomposition rate. Methanol, diluted 100-fold with DI water,

was used as the control. PAA was added to the 100-fold diluted lipids-in-methanol and

methanol solutions.

For all batch assays, 5 mL of liquid samples were removed at predetermined times and the residual PAA was measured by titration as described in Chapter 3, Section 3.2.5. It should be noted that in all batch assays, over time and for a duration of more than 6 h, the measured acetic acid molar concentration matched by 100% that calculated based on the decomposed molar PAA concentration. Because of the relatively high PAA concentrations used in the batch assays and the PAA disinfection capacity, acetic acid was not degraded during the batch assays, which implies that all microbial activities were blocked. Thus, PAA decomposition rates measured in this study were not microbially-mediated.

4.2.3 PAA Decomposition Product and COD Balance

Acetic acid has been reported to be the predominant PAA decomposition product (Monarca et al., 2002; Richardson et al., 2007). In order to assess the fate of PAA, aliquots of a stock PAA solution were added to DAF effluent at an initial concentration of 800 mg/L, incubated at room temperature (22 ± 1°C), and both PAA and acetic acid were measured at different times during the incubation period. Initially, upon the addition of 800 mg/L PAA to the DAF effluent, the pH dropped from 6 to 4.3 and remained at 4.3 for 70 h, at which point the pH was raised to and kept at 6 for 5 h by manually adding 1 N NaOH in order to achieve complete PAA decomposition. Three samples collected at 6, 70 and 75 h of incubation were analyzed for PAA, immediately filtered through 0.2 μm syringe filters and analyzed for acetic acid by HPLC as described in Section 2.4, below. The acetic acid in the DAF effluent as well as in the stock PAA solution was also measured. Assuming transformation of PAA to acetic acid at 1:1 molar ratio in the

concentrated working solution, the calculated acetic acid concentrations were compared to the measured concentrations. It should be noted that PAA transformation to acetic acid during the HPLC analysis was negligible based on preliminary tests, in which the measured acetic acid in a standard PAA solution was 100±3.5% of the calculated acetic acid. In order to evaluate the COD balance in PAA-amended DAF effluent, five series with DAF effluent (pH ~6) were prepared in 250 mL Erlenmeyer flasks, amended with PAA solution resulting in initial PAA concentrations of 64, 129, 258, 644, and 1,288 mg/L PAA. PAA was measured frequently until it was non-detected in each series and the total COD was measured immediately after PAA had completely decomposed.

4.2.4 Analytical Methods

pH, COD, N species, P species, anions, cations, total solids (TS) and volatile solids (VS), volatile fatty acids (VFAs), and total carbohydrates were measured as described in Chapter 3, Section 3.1. PAA and H_2O_2 were measured by DPD and HPLC methods as described in Chapter 3, Section 3.2.3 and 3.2.4.

4.3 Results and Discussion

4.3.1 Poultry Processing Wastewater Characteristics

The characteristics of the three chiller samples and the three wastewater streams, collected several times at the same poultry processing plant over a 2-year period, are shown in Table 4.1. The pH in the pre-chiller and main chiller was alkaline, whereas it was acidic in the finishing chiller. These results are consistent with the plant practice of

adding caustic solutions (e.g., NaOH) to the pre-chiller, whereas high PAA

concentrations are typically maintained in the finishing chiller, as discussed below. The

pH of the chiller overflow, which is disposed to the main wastewater drain, was

circumneutral (Table 4.1). Both the DAF influent and effluent had a slightly acidic pH,

consistent with the poultry processing plant practice of adding acid (e.g., H_2SO_4) along

with polymers to the wastewater before DAF to achieve wastewater flocculation leading

to high solids removal.

The PAA concentration in the pre-chiller and main chiller tanks was between 52

and 125 mg/L and over 800 mg/L in the finishing chiller (Table 4.1). This is consistent

with the poultry processing plant practice of continuously adding PAA to the three chiller

tanks. The PAA concentration of the chiller overflow ranged from 48 to 75 mg/L, the

variation of which is attributed to the PAA variation in the chiller tanks (Table 4.1). It is

noteworthy that PAA was not detected in any DAF influent and effluent samples in all

samples collected at mid plant operation shifts. Along with the chiller overflow, other

wastewater streams resulting from other plant processes at different times during the

operation shift are also disposed to the same wastewater pipe and the combined

wastewater is carried to the DAF unit. Thus, as a result of wastewater dilution and PAA

decomposition during the wastewater conveyance to the DAF unit, PAA was not detected

in the DAF influent and effluent in all samples collected at mid plant operation (Table

4.1).

Table 4.1. Characteristics of six wastewater streams collected several times over a 2-year period at the study poultry processing plant.

Parameter	Pre-Chiller	Main Chiller
pH	8.3-9.7(9.0)[a]	9.5-9.8(9.7)
PAA (mg/L)	75-125(84)	52-95(75)
TS (g/L)	2.31-3.35(2.83)	1.42-2.38(1.90)
VS (g/L)	1.33-1.43(1.38)	0.84-1.13(0.99)
Total COD (mg/L)	2464-3024(2744)	1712-2122(1917)
Soluble COD (mg/L)	1422-1520(1471)	459-1389(924)
VFAs (mg COD/L)	169-1717(943)	195-2082(1139)
Total N (mg N/L)[c]	102-163(133)	135-217(176)
Ammonia (mg N/L)	17-24(20)	7-13(10)
Organic N (mg N/L)	86-140(113)	128-204(166)
Crude protein (mg/L)	534-872(703)	800-1278(1039)
Total P (mg P/L)	19-28(23)	15-24(20)
Lipids (mg/L)	773-833(803)	343-743(543)
Carbohydrates (mg/L)[d]	34-38(36)	24-33(29)

[a] Range (median); [b] ND, not detected; [c] Total nitrogen, i.e., sum of organic, ammonia, nitrite, and nitrate nitrogen; [d] Expressed as glucose, corrected for PAA interference. Abbreviations: PAA, peracetic acid; TS, total solids; VS, volatile solids; COD, chemical oxygen demand; VFAs, volatile fatty acids.

Table 4.1 (Continued). Characteristics of six wastewater streams collected several times over a 2-year period at the study poultry processing plant.

Parameter	Finishing Chiller	Chiller Overflow
pH	3.8-4.2(4.0)	6.4-7.0(6.7)
PAA (mg/L)	825-1085(1050)	48-75(62)
TS (g/L)	0.94-1.09(1.02)	1.65-2.94(2.82)
VS (g/L)	0.34-0.55(0.45)	1.06-1.91(1.82)
Total COD (mg/L)	4950-5044(4997)	617-2585(2181)
Soluble COD (mg/L)	4082-4548(4315)	1186-1863(1762)
VFAs (mg COD/L)	2947-5191(4069)	1424-2379(2104)
Total N (mg N/L)[c]	105-166(136)	102-163(151)
Ammonia (mg N/L)	13-15(14)	3-6(6)
Organic N (mg N/L)	91-152(122)	100-158(146)
Crude protein (mg/L)	570-949(760)	622-986(910)
Total P (mg P/L)	17-38(28)	24-36(35)
Lipids (mg/L)	600-900(750)	217-790(543)
Carbohydrates (mg/L)[d]	3-14(7)	17-30(27)

[a] Range (median); [b] ND, not detected; [c] Total nitrogen, i.e., sum of organic, ammonia, nitrite, and nitrate nitrogen; [d] Expressed as glucose, corrected for PAA interference. Abbreviations: PAA, peracetic acid; TS, total solids; VS, volatile solids; COD, chemical oxygen demand; VFAs, volatile fatty acids.

Table 4.1 (Continued). Characteristics of six wastewater streams collected several times over a 2-year period at the study poultry processing plant.

Parameter	DAF Influent	DAF Effluent
pH	4.9-5.4(5)	4.8-5.4(5.2)
PAA (mg/L)	ND[b]	ND
TS (g/L)	1.61-1.93(1.80)	0.89-0.98(0.9)
VS (g/L)	1.13-1.52(1.3)	0.50-0.58(0.52)
Total COD (mg/L)	1635-2386(1738)	429-719(639)
Soluble COD (mg/L)	729-850(808)	741-779(746)
VFAs (mg COD/L)	709-1272(1016)	701-1294(1066)
Total N (mg N/L)[c]	100-157(143)	74-89(89)
Ammonia (mg N/L)	11-14(13)	14-17(14)
Organic N (mg N/L)	89-145(140)	60-75(72)
Crude protein (mg/L)	555-904(804)	377-469(452)
Total P (mg P/L)	17-21(21)	16-18(17)
Lipids (mg/L)	240-530(527)	37-63(40)
Carbohydrates (mg/L)[d]	25-41(29)	9-16(10)

[a] Range (median); [b] ND, not detected; [c] Total nitrogen, i.e., sum of organic, ammonia, nitrite, and nitrate nitrogen; [d] Expressed as glucose, corrected for PAA interference. Abbreviations: PAA, peracetic acid; TS, total solids; VS, volatile solids; COD, chemical oxygen demand; VFAs, volatile fatty acids.

In an effort to further assess PAA levels during an 8-h plant operation shift, on-site simultaneous measurements of pH and PAA in chiller overflow and DAF influent and effluent were conducted during a typical plant processing operation shift (Figure 4.1). For 2.5 h after the on-site monitoring started (12:30 pm), the PAA concentration and pH in the chiller overflow was between 70 and 80 mg/L and 6.5 to 6.9, respectively. Then, within 30 min, the PAA concentration increased to 310 mg/L and then declined to 210 mg/L in another 30 min, while the pH decreased to between 3.8 and 4.0. The drastic change in pH and PAA level in the chiller overflow coincided with the emptying of the three chiller tanks at the end of the processing shift as it is practiced routinely before the plant sanitation cycle starts. Emptying of the chiller tanks lasted for approximately 1 h. The PAA concentration in the DAF influent was at or below 5 mg/L for 4.5 h after the on-site monitoring started and then gradually increased to a maximum value of 30 mg/L. The PAA concentration in the DAF effluent followed the same pattern with a 15-min delay, which is the hydraulic retention time of the DAF unit. The maximum DAF effluent PAA concentration was 25 mg/L, corresponding to about 17% decrease in the PAA concentration. The pH in both the DAF influent and effluent was between 4.6 and 5.4 throughout the monitoring period. Based on these results, the estimated travel time of the chiller outflow in the main wastewater pipe, carrying it to the DAF unit, was about 15 min. Thus, elevated PAA concentrations in DAF effluent wastewater, which is subsequently treated biologically, are expected at the end of plant processing shifts during the empting of the chiller tanks in poultry processing facilities, which do not have wastewater equalization tanks upstream of the DAF unit. In addition, accidental spills

and/or equipment cleaning, as well as malfunctioning could result in wastewater streams with elevated PAA concentrations.
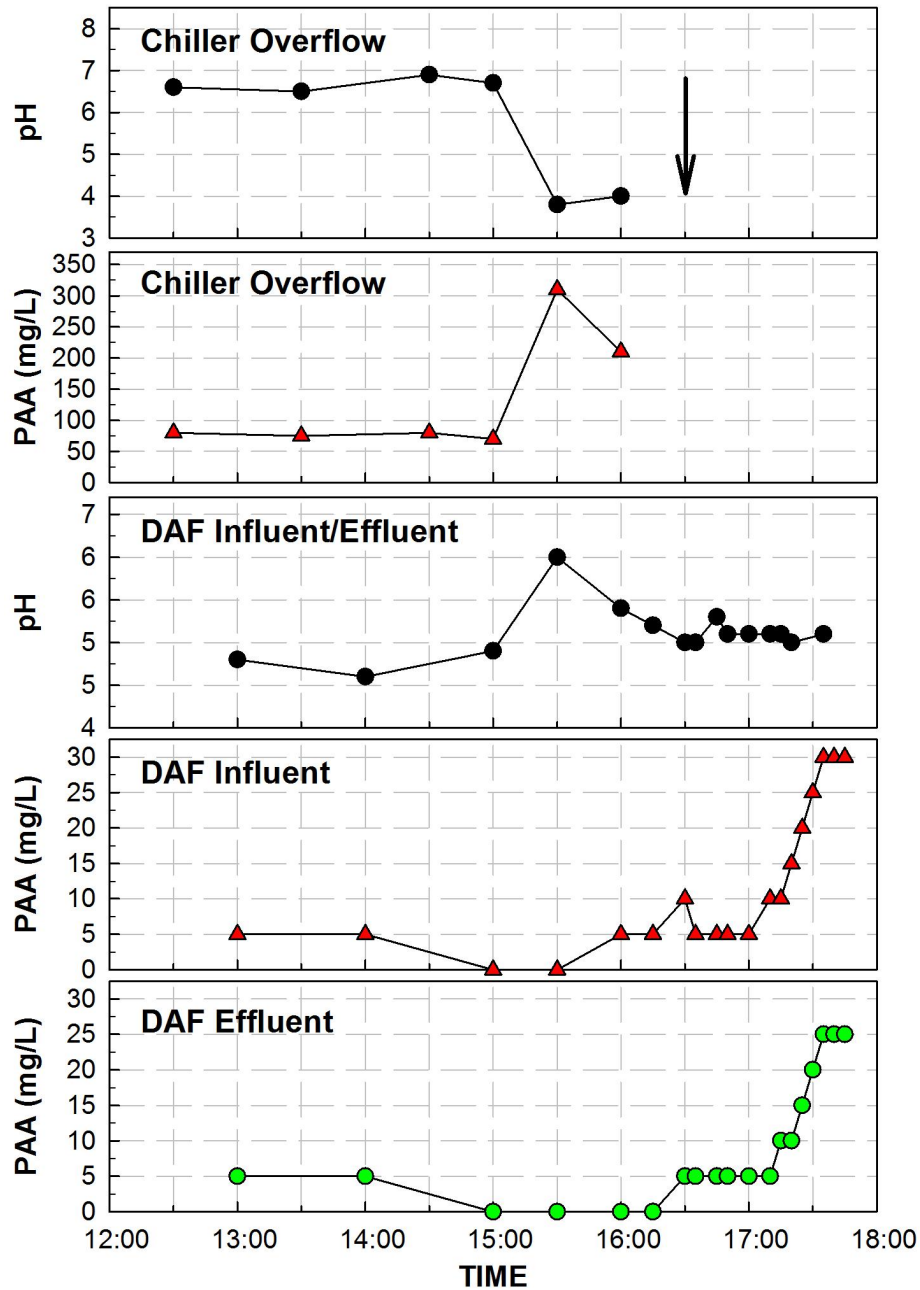
Figure 4.1. pH and PAA concentrations in chiller overflow and DAF influent and effluent measured on-site during a typical plant processing operation shift. Arrow indicates the start of chiller tank empting towards the end of the processing shift.

43

The solids concentrations decreased from the pre- to the finishing chiller and then from the DAF influent to the effluent, corresponding to about 46 and 54% DAF TS and VS solids removal efficiency, respectively. The VS/TS ratio ranged from 32 to 65% in the four chiller samples and from 70 to 79% in the DAF influent, which means that wastewater streams other than chiller overflow with higher organic content are disposed to the main wastewater pipe. The highest COD concentrations were recorded in the finishing chiller wastewater, with median values of 4,997 and 4,315 mg/L for total COD and soluble COD, respectively (Table 4.1). A significant portion of these measured COD values is attributed to the very high levels of PAA solution itself (ca. 18.3 %) typically maintained in finishing chiller as discussed above, as well as the acetic acid (ca. 75.2 %) in the commercial PAA solution used in the study poultry processing plant. The median total COD values in the pre-chiller, main chiller and chiller overflow ranged from 1,917 to 2,744 mg/L (Table 4.1). The total COD concentrations in the DAF influent were much lower than in the chiller wastewater samples, whereas the DAF effluent total COD values were less than 40% of the influent, resulting in more than 60% DAF COD removal efficiency. The soluble/total COD ratio ranged from 0.47 to 0.54 in all wastewater samples, except for 0.86 in the finishing chiller wastewater, attributed to the very high PAA and acetic acid levels, as discussed above. The total VFAs COD represented 64 to 97% of the soluble COD.

The median total N concentrations ranged from 133 to 176 mg/L, which results in a range of organic N from 122 to 166 mg/L when the relatively low ammonia-N concentrations (5-20 mg N/L) and nitrate concentrations (0.8 to 4.9 mg N/L) are taken into account (Table 4.1). The above mentioned range of organic N corresponds to a crude

protein range from 703 to 1,040 mg/L in the four chiller wastewater samples. The DAF unit reduced the influent crude protein from a median concentration of 563 mg/L to an effluent value of 377 mg/L, resulting in more than 33% DAF crude protein removal efficiency (Table 4.1). The median total P concentration ranged from 18 to 32 mg/L without a particular trend along the wastewater train from the chillers to the DAF unit.

The concentrations of common anions in three chiller samples and three wastewater streams (Cl^-, Br^-, NO_2^-, NO_3^-, PO_4^{3-}, and SO_4^{2-}) were measured with results reported in Table 4.2. The median orthophosphate concentration ranged from 21.1 to 30.3 mg/L as P without a particular trend as well, accounted for 81 to 94% of the total P. The median chloride concentration ranged from 78 to 167 mg/L without a particular trend along the wastewater train from the chiller compartment to the DAF unit. Both bromide and nitrite were not detected in all samples. The median sulfate concentration ranged from 12 to 22 mg S/L among the three chiller and chiller overflow samples, whereas ranged from 35 to 42 mg S/L in the DAF influent and effluent.

The lipids concentration in the three chiller wastewater samples ranged from 543 to 803 mg/L and decreased to 411, 453, and 52 in the chiller overflow, DAF influent and effluent, respectively, resulting in more than 88% DAF removal efficiency (Table 4.1). The median total carbohydrates concentration, corrected for PAA interference (see Chapter 3, section 3.1), ranged from 7 to 36 mg/L (Table 4.1). Compared to crude protein and lipids, carbohydrates are a very minor component of poultry processing wastewater, which agrees with previous reports (Hajaya and Pavlostathis, 2012).

The concentrations of common metals (Na, K, and Mg) as well as of trace metals in three chiller samples and three wastewater streams were measured with results

reported in Table 4.3. Among the three common metals, Na concentrations were the highest, ranging from 93 to 319 mg/L. Among the seven trace metals, Mn, Co, and Ni were detected at relatively low concentrations, ranging from 5 to 96 µg/L, 0.1 to 1.7 µg/L, and 0.2 to 61.4 µg/L, respectively. Pb concentrations varied from not detected to 3.5 µg/L. Fe, Cu, and Zn were detected at relatively higher concentrations, ranging from 68 to 277 µg/L, 45 to 227 µg/L, and 34 to 351 µg/L, respectively.

Table 4.2. Results of anion analysis of six wastewater streams collected several times over a 2-year period at the study poultry processing plant.

Anion (mg/L)	Pre-Chiller	Main Chiller
Cl^-	95.7-116.8(106.3)[a]	74.9-80.6(77.8)
Br^-	ND[b]	ND
NO_2^--N	ND	ND
NO_3^--N	1.5-1.8(1.7)	1.2-2.2(1.7)
PO_4^{3-}-P	28.7-30.9(29.8)	24.2-26.8(25.5)
SO_4^{2-}-S	0.7-22.8(11.8)	0.8-23.8(12.3)

[a] Range (median); [b] ND, not detected.

Table 4.2 (Continued). Results of anion analysis of six wastewater streams collected several times over a 2-year period at the study poultry processing plant.

Anion (mg/L)	Finishing Chiller	Chiller Overflow
Cl^-	55.9-117.3(86.6)	101.9-170.6(166.9)
Br^-	ND	ND
NO_2^--N	ND	ND
NO_3^--N	1.7-4.9(3.3)	0.8-1.8(0.9)
PO_4^{3-}-P	29.4-31.1(30.3)	25.9-30.5(28.2)
SO_4^{2-}-S	0.6-42.7(21.7)	12.6-18.9(15.6)

[a] Range (median); [b] ND, not detected.

Table 4.2 (Continued). Results of anion analysis of six wastewater streams collected several times over a 2-year period at the study poultry processing plant.

Anion (mg/L)	DAF Influent	DAF Effluent
Cl^-	117.5-130.5(120.2)	120.5-142.1(127.9)
Br^-	ND	ND
NO_2^--N	ND	ND
NO_3^--N	1.2-3.1(1.5)	0.8-2.4(1.4)
PO_4^{3-}-P	18.4-23.1(21.1)	17.0-23.9(22.0)
SO_4^{2-}-S	36.8-41.8(41.8)	34.6-36.3(36.0)

[a] Range (median); [b] ND, not detected.

Table 4.3. Results of metal analysis of six wastewater streams collected several times over a 2-year period at the study poultry processing plant.

Metal	Pre-Chiller	Main Chiller
Common Metal (mg/L)		
Na	169.6-205.1(187.4) [a]	236.6-318.8(277.7)
K	47.7-81.1(129.5)	71.2-81.6(76.4)
Mg	3.6-6.8(5.2)	3.7-5.5(4.6)
Trace Metal (µg/L)		
Mn	5.1-21.3(13.2)	4.8-12.9(8.9)
Fe	128.4-193.4(160.9)	67.9-193.4(130.7)
Co	0.7-1.7(1.2)	0.1-0.3(0.2)
Ni	14.9-17.6(16.1)	0.2-4.8(2.5)
Cu	95.1-227.2(161.2)	62.1-111.6(86.9)
Zn	34.4-263.9(149.2)	40.2-214.3(127.3)
Pb	ND-2.0(1.0)[b]	0.1-2.7(1.4)

[a] Range (median); [b] ND, not detected.

Table 4.3 (Continued). Results of metal analysis of six wastewater streams collected several times over a 2-year period at the study poultry processing plant.

Metal	Finishing Chiller	Chiller Overflow
Common Metal (mg/L)		
Na	111.4-161.3(136.4)	255.5-306.0(280.8)
K	38.8-68.5(53.7)	93.5-110.2(101.9)
Mg	4.9-6.5(5.7)	4.5-5.8(5.2)
Trace Metal (µg/L)		
Mn	19.6-38.7(29.2)	6.5-19.3(12.9)
Fe	95.2-116.1(105.7)	240.9-258.1(249.5)
Co	0.2-0.9(0.6)	0.5-0.9(0.7)
Ni	4.8-51.7(28.3)	3.1-61.4(32.3)
Cu	111.6-223.8(167.7)	69.6-136.4(103.0)
Zn	34-351(183)	133.3-351.0(242.3)
Pb	1.4-3.5(2.5)	0.1-2.5(1.3)

[a] Range (median); [b] ND, not detected.

Table 4.3 (Continued). Results of metal analysis of six wastewater streams collected several times over a 2-year period at the study poultry processing plant.

Metal	DAF Influent	DAF Effluent
Common Metal (mg/L)		
Na	93.4-129.1(111.3)	116.3-134.7(125.5)
K	45.0-99.1(72.1)	46.1-97.7(71.9)
Mg	2.6-5.2(3.9)	1.3-5.6(3.5)
Trace Metal (µg/L)		
Mn	40.2-96.4(68.3)	53.6-80.7(67.2)
Fe	137.1-258.8(198.0)	210.4-277.2(243.8)
Co	0.1-0.5(0.3)	0.2-0.5(0.4)
Ni	2.4-11.0(6.7)	3.6-9.1(6.4)
Cu	61.6-78.6(70.1)	45.1-56.0(50.6)
Zn	127.1-266.3(196.7)	161.3-302.5(231.9)
Pb	ND-0.3(0.2)	0.1-0.1(0.1)

[a] Range (median); [b] ND, not detected.

PAA was detected in four out of the six wastewater samples collected at mid plant operation shift, multiple times over a 2-year period (Table 4.1). In order to quantify residual PAA decomposition rate under conditions encountered in the study poultry processing plant, representative wastewater samples with residual PAA collected from the pre-chiller, main chiller, finishing chiller, and chiller overflow were placed in an ice chest and transported to the laboratory. Then, aliquots of the four wastewater samples were placed in two sets of 250-mL Erlenmeyer flasks. One set was maintained at 4°C while the second set was maintained at room temperature (22±1°C). The pH as well as the residual PAA were measured over time. The observed pseudo-first order PAA decomposition rates are shown in Table 4.4. The order of the PAA decomposition (chiller overflow > pre-chiller > main chiller > finishing chiller) follows that of the total COD attributed to the samples organic content, corrected for the measured PAA and acetic acid concentrations.

Table 4.4. Pseudo-first order decomposition rate constant (k_{obs1}) values of residual PAA in four chiller wastewater samples collected at the study poultry processing plant and kept at 4 and 22°C.

Wastewater	Initial PAA (mg/L)	Total COD (mg/L)[a]	pH range[b]	Incubation at 4°C		Incubation at 22°C	
				k_{obs1} (d^{-1})	Half-life (d)	k_{obs1} (d^{-1})	Half-life (d)
Pre-Chiller	125	1379	9.7-9.3	0.47±0.03[c]	1.47	1.85±0.1	0.38
Main Chiller	84	210	9.8-9.5	0.37±0.03	1.87	1.09±0.14	0.64
Finishing Chiller	1185	262	3.8-3.8	0.004±0.0008	173.3	0.032±0.003	21.7
Chiller Overflow	48	828	8.1-7.6	0.69±0.03	1.01	2.03±0.19	0.34

[a] COD values corrected for PAA and acetic acid; [b] Initial/final pH values; [c] Mean ± standard error

As shown and discussed in Section 4.3.2, below, increasing pH, wastewater organic constituents, and temperature increase the PAA decomposition rate. The very low PAA decomposition rate in the finishing chiller sample (half-life, i.e., the time required for the PAA concentration to be 50% of its initial concentration, of 21.7 d at 22°C) is attributed to its very low pH as well as to its relatively low non-PAA and non-acetic acid COD concentration (Table 4.4). The remaining three samples had higher PAA decomposition rates (half-life values 0.34 to 0.64 d at 22°C), attributed primarily to alkaline initial pH values (8.1 to 9.8) and secondarily to higher non-PAA and non-acetic acid COD (for the pre-chiller and chiller overflow samples).

4.3.2 PAA Decomposition in DAF Effluent

In order to quantify the PAA decomposition rate under controlled conditions, PAA-free DAF effluent collected at the study poultry processing plant at mid operation

shift was used to assess the effect of four factors: pH, temperature, initial PAA concentration, and DAF effluent strength.

4.3.2.1 Effect of pH on PAA Decomposition Rate

PAA decomposition kinetics are greatly affected by the solution pH. In DI water solutions, between pH 5.5 and 8.2 (the PAA pK_a value), PAA spontaneously decomposes to acetic acid and O_2 with negligible hydrolysis, whereas above pH 8.2, PAA undergoes both spontaneous decomposition and hydrolysis producing acetic acid and H_2O_2 (Yuan et al., 1997). In order to assess the effect of pH on PAA decomposition kinetics relevant to this study, batch assays were conducted at room temperature (22±1°C) with DAF effluent (original pH 5) at four constant pH values: 4, 5, 6, and 7. The initial PAA concentration added to the DAF effluent was 800 mg/L.

The time trend of PAA concentrations in DAF effluent as a function of pH in the batch experimental series were fitted by non-linear regression based on one-step (Eq. 4.4) or two-step (Eq. 4.5) pseudo-first order decomposition kinetics:

$$\frac{d\,[PAA]}{dt} = -\,k_{obs1}[PAA] \tag{4.4}$$

$$\frac{d\,[PAA]}{dt} = -\,k_{obs1}\alpha[PAA] - k_{obs2}(1-\alpha)[PAA] \tag{4.5}$$

where k_{obs1} is the pseudo-first order rate constant (h^{-1}) in either an overall one-step or the first step in a two-step PAA decomposition; k_{obs2} is the second pseudo-first order rate constant (h^{-1}) in a two-step PAA decomposition; and α is the fraction of PAA decomposed in the first step of a two-step PAA decomposition. It should be noted that PAA decomposition in complex wastewater matrices, as was the case in the present study, is the result of multiple, complex interactions of PAA with matrix components; thus, the

reported rate constants are pseudo-first order rate constant values as they are specific to the conditions of each system.

Integration of Eq. 4.4 and Eq. 4.5 results in the following two equations:

$$[PAA]_t = [PAA]_0\, e^{-k_{obs1}\, t} \qquad\qquad (4.6)$$

$$[PAA]_t = [PAA]_0[\alpha e^{-k_{obs1}\, t} + (1-\alpha)e^{-k_{obs2}\, t}] \qquad (4.7)$$

where $[PAA]_0$ and $[PAA]_t$ is the initial and time t PAA concentration (mg/L), respectively. The values of k_{obs1}, k_{obs2}, and α were estimated simultaneously by fitting Eq. 4.6 or Eq. 4.7 to the experimental PAA concentration data using the Levenberg-Marquardt fitting algorithm in SigmaPlot ver. 14 (Table 4.5).

Table 4.5. PAA decomposition rate constant (k) values in DAF effluent at four pH values (controlled pH; 22±1ºC).

pH	Fraction (α)	k_{obs1} (h^{-1})	k_{obs2} (h^{-1})	R^2	Half-life (h)
4.0	0.239 ± 0.024[a]	1.439 ± 0.245	0.017 ± 0.007	0.992	24.7
5.0	0.626 ± 0.059	1.151 ± 0.024	1.862 ± 0.435	0.995	1.7
6.0	1.00	0.939 ± 0.056	0.00	0.992	0.74
7.0	1.00	1.322 ± 0.051	0.00	0.997	0.52

[a] Mean ± standard error

PAA decomposition followed two-step pseudo-first order kinetics at pH 4 and 5, whereas one-step pseudo-first order kinetics described best PAA decomposition at pH 6 and 7. The PAA decomposition rate increased as the pH increased from 4 to 7, which is in agreement with PAA decomposition in DI water at pH 5.5 to 8.2 previously reported by Yuan et al. (1997). The fast PAA decomposition is attributed to reaction with organics, such as proteins that readily react with PAA, whereas reaction with inorganics, such as

transition metals, is relatively slower (Domínguez Henao et al., 2018). The α value, i.e., the fraction of PAA decomposed according to the pseudo-first order rate constant k_{obs1} increased as the solution pH increased from 4 to 5 and became 1.0 at pH 6 and above (Table 4.5). For a PAA pK_a value of 8.2, the fraction of peracetate $[PAA^-]$ to the total peracetic acid and peracetate (i.e., $[PAAH]+[PAA^-]$) molar concentration increases from 0 to 6% for an increase of pH from 4 to 7. Thus, it appears that the value of α increased with increasing peracetate concentration brought about by the increase of the solution pH.

The PAA decomposition in the DAF effluent is affected by both the proton concentration and the PAA reaction with other wastewater components, such as amino acids (Du et al., 2018). The effect of pH solely on PAA decomposition in DI water can be modelled using equation Eq. 4.8 proposed by Yuan et al. (1997), in which PAA decomposition follows second-order kinetics with respect to PAA concentration.

$$-\frac{d[PAA]}{dt} = \frac{2M}{(1+M)^2}(9.21 \times 10^{13}) \exp\left(-\frac{11338.7}{T}\right)[PAA]^2 \qquad (4.8)$$

where $[PAA]$ is the PAA concentration (mol/L), $M = [H^+]/K_a$, and T is temperature (K).

Integration of Eq. 4.8 results in the following equation:

$$[PAA]_t = \frac{1}{\left[\frac{2M}{(1+M)^2}(9.21\times10^{13}) \exp\left(-\frac{11338.7}{T}\right)\right] t + \frac{1}{[PAA]_0}} \qquad (4.9)$$

Based on Eq. 4.8, PAA vs. time data were generated at pH values of 5, 6, and 7 at room temperature (22±1°C) and then regressed using second-order kinetics (Eq. 4.9). Non-linear regression was then performed using the Levenberg-Marquardt fitting algorithm in SigmaPlot ver. 14 (Figure 4.2). The estimated second-order PAA decomposition rate values were 2.4 x 10^{-6}, 2.4 x 10^{-5}, and 2.4 x 10^{-4} L/mg · d at pH 5, 6, and 7, respectively. These rate values correspond to half-life values of 520, 52, and 5.2 d.

The PAA decomposition rate increases by an order of magnitude for each pH unit increase. However, the rate of PAA decomposition by the effect of the proton concentration alone is at least four orders of magnitude lower than that observed in the present study with the DAF effluent (Table 4.5).
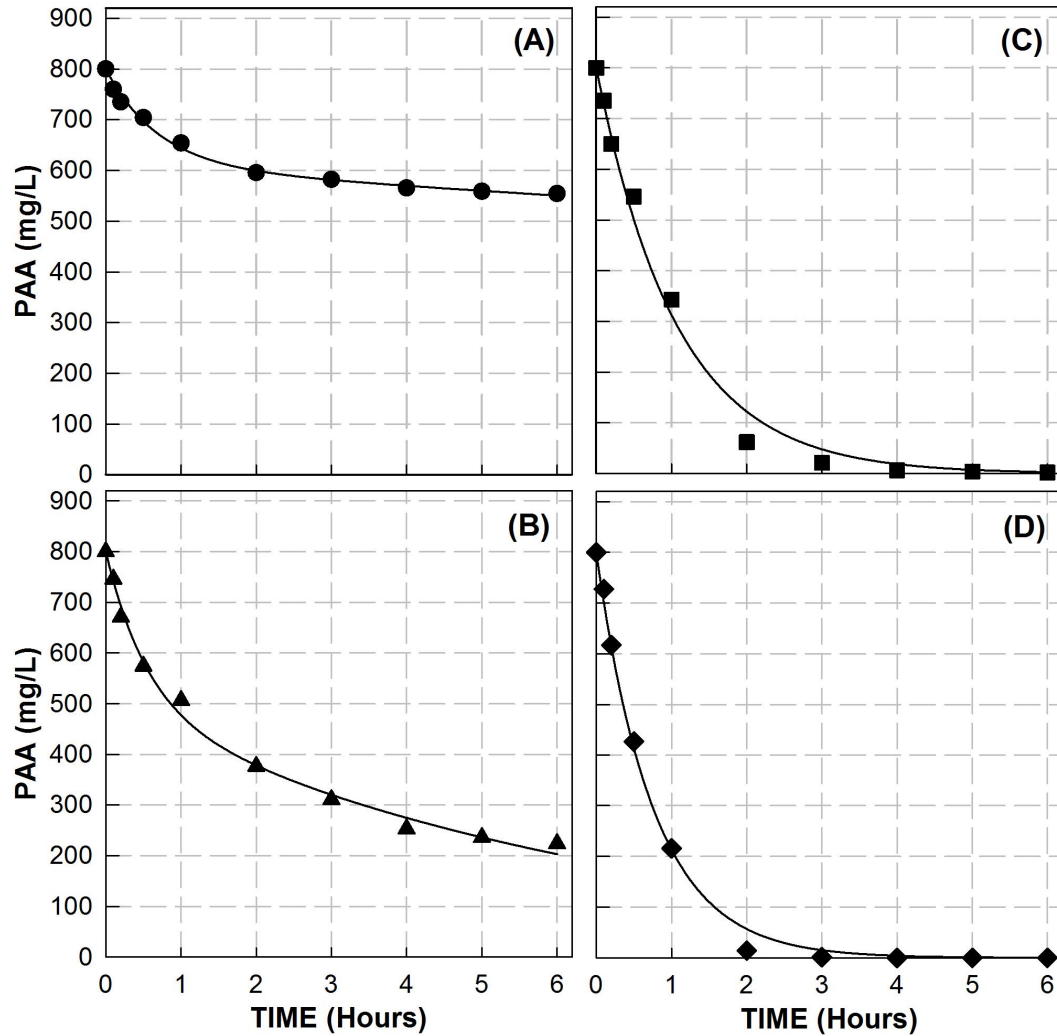
Figure 4.2. Time trend of PAA concentration at constant pH 4 (A), 5 (B), 6 (C), and 7 (D) (Initial PAA concentration 800 mg/L, 22±1ºC). Lines are data fits to double (A and B) and single (C and D) first-order PAA decomposition rate.

In DAF effluent, the PAA decomposition rate is affected by the pH as well as by the PAA reaction with other wastewater components. The overall trend observed is that

PAA decomposed faster at higher pH values, with half-life values decreasing from 24.7 to 0.52 h as the pH increased from 4 to 7 (Table 4.5). PAA decomposition at pH 4 and 5 followed two-step pseudo-first order kinetics, indicating that there are two groups of wastewater components, with one group reacting with PAA much faster than the other group. In contrast, at pH 6 and 7 all components react with PAA at comparable rates, simulated well by one-step pseudo-first order kinetics. PAA decomposition in DI water, plant process water, and DAF effluent from the same poultry processing plant was also investigated at pH 6 with results shown in Figure 4.3. The pseudo-first order PAA decomposition rate was estimated as 0.0009 ± 0.0001, 0.042 ± 0.003, and 1.075 ± 0.007 h^{-1} in DI water, plant process water and DAF effluent, corresponding to half-life values of 32 d, 16.5 h, and 0.6 h, respectively. Compared to PAA decomposition in DAF effluent, decomposition in DI water was negligible ($< 0.1\%$) and in process water was very low (4%). It should be noted that, based on the above-discussed pH effect and the fact that the DAF effluent pH was always below 6, the pH was kept constant at 6 in all assays discussed below and the PAA decomposition is described by one-step pseudo-first order kinetics (Eq. 4.6).
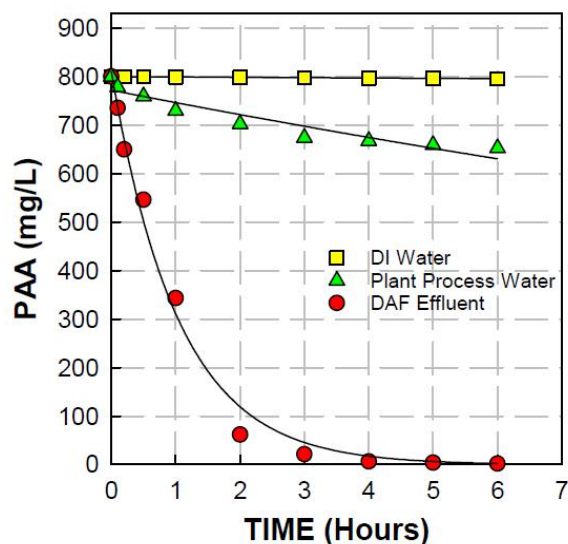
Figure 4.3. Time trend of PAA concentration in DI water, plant process water, and DAF effluent (Initial PAA concentration 800 mg/L, pH 6, 22±1ºC). Lines are data fits to one-step pseudo-first order PAA decomposition rate.

4.3.2.2 Effect of Temperature on PAA Decomposition Rate

The effect of temperature on PAA decomposition at a constant pH of 6 is depicted in Figure 4.4A. As the temperature increased from 4 to 30ºC, the PAA decomposition rate increased from 0.642 to 1.312 h^{-1}, corresponding to half-life values from 1.08 to 0.53 h (Table 4.6). Therefore, the PAA decomposition rate is highly affected by temperature. Based on the Arrhenius plot (Figure 4.4B), the activation energy of the PAA decomposition in the DAF effluent at a constant pH of 6 was estimated as 18.7±0.3 kJ/mol. Kunigk et al. (2012) reported activation energy values of PAA decomposition ranging from 9.7 to 61.2 kJ/mol in the presence of organic matter, such as milk, beer, and tomato juice, with the highest value of 62.1 kJ/mol observed in matrices with the lowest organic matter content. The PAA decomposition activation energy in milk samples, which had the highest protein content among all three matrices tested, was the lowest (9.7 kJ/mol). The activation energy for the PAA decomposition in DAF effluent estimated in

56

this study is relatively low compared to those reported by Kunigk et al. (2012), which may be attributed to the nature of the DAF effluent, in which protein is the major organic component (Table 4.1).

Table 4.6. PAA pseudo-first order decomposition rate constant (k_{obs1}) values in DAF effluent at a range of temperature, initial PAA concentration and DAF effluent strength (pH 6).

Condition	Value	k_{obs1} (h^{-1})	R^2	Half-life (h)
Temperature (°C) *(Initial PAA 800 mg/L Full strength DAF effluent)*	4	0.64±0.03[a]	0.997	1.08
	10	0.81±0.03	0.998	0.86
	15	0.92±0.05	0.956	0.75
	22	1.08±0.07	0.993	0.64
	30	1.31±0.05	0.998	0.53
Initial PAA (mg/L) *(Temperature 22°C Full strength DAF effluent)*	100	5.84±0.55	0.971	0.12
	200	4.08±0.61	0.951	0.17
	400	1.91±0.18	0.994	0.36
	800	1.08±0.07	0.993	0.64
DAF effluent strength (%) *(Initial PAA 800 mg/L Temperature 22°C)*	20	0.20±0.02	0.973	3.47
	50	0.63±0.01	0.999	1.10
	75	0.85±0.05	0.995	0.82
	100	1.08±0.07	0.993	0.64

[a] Mean ± standard error
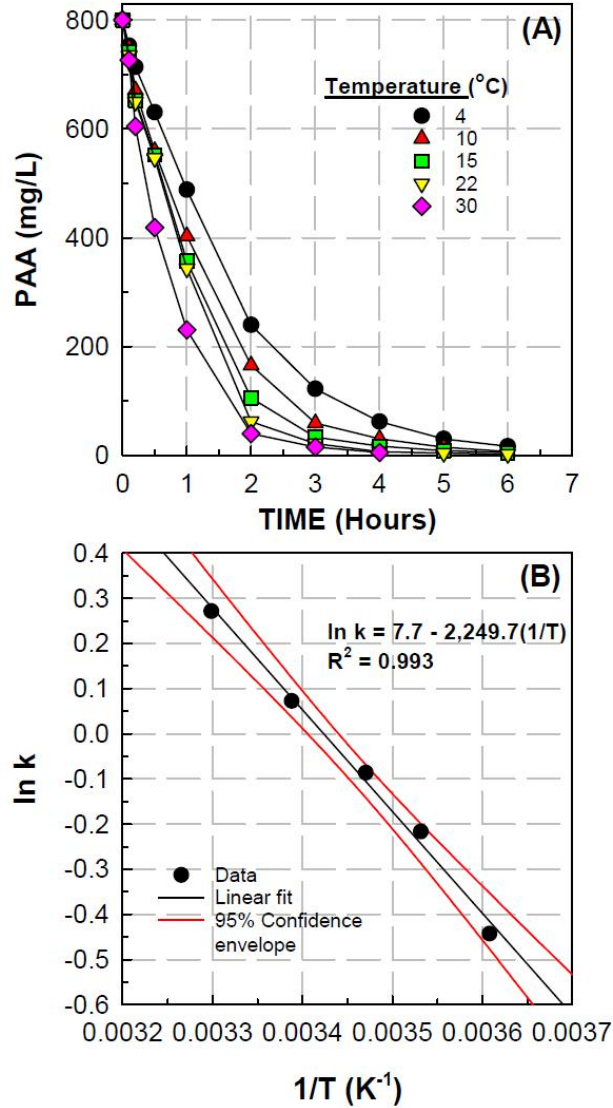
Figure 4.4. Time trend of PAA concentration in DAF effluent at 4, 10, 15, 22 and 30°C (pH 6) (A). Arrhenius plot ln k vs. 1/T (T, temperature, K; k, PAA decomposition rate constant, h^{-1} (B).

The temperature coefficient Q_{10}, i.e., the change in the PAA decomposition rate for a 10°C increase in temperature, is as follows (Eq. 6):

$$Q_{10} = exp\left(\frac{10\,E_a}{R\,T_1 T_2}\right) \qquad (4.10)$$

where E_a is the activation energy (kJ/mol); R is the universal gas constant (8.314 x 10^{-3} kJ/mol · K); and T is temperature (K). Based on the above reported activation energy

for the PAA decomposition in DAF effluent at pH 6, the Q_{10} value is 1.33, which means the PAA decomposition in DAF effluent increases by 33% for a 10°C increase in temperature. Yuan et al. (1997) reported an activation energy of 94.3 kJ/mol for the decomposition of PAA in DI water at pH of 8.2, corresponding to a very high Q_{10} value of 3.44. Zhao et al. (2007) reported that the pH-independent intrinsic activation energy of PAA hydrolysis in DI water was 60.4 kJ/mol, corresponding to a Q_{10} of 2.27, compared to the activation energy of 27.9 kJ/mol obtained in the presence of 0.057 M H_2SO_4 by Dul'neva and Moskvin (2005), which indicates that temperature affects PAA hydrolysis to a higher degree at higher pH.

4.3.2.3 Effect of Initial PAA Concentration and DAF Effluent Strength on PAA Decomposition

The effect of initial PAA concentration on PAA decomposition at a constant pH of 6 is depicted in Figure 4.5. As the initial PAA concentration increased from 100 to 800 mg/L, the PAA decomposition rate decreased from 5.84 to 1.08 h^{-1}, corresponding to half-life values from 0.12 to 0.64 h (Table 4.6). Thus, the initial PAA concentration significantly affects its decomposition rate. Pederson et al. (2009) reported that the PAA decomposition rate in processing water of recirculating aquaculture systems at pH between 7.2 and 7.4 and temperature 17±0.3°C decreased from 1.5 to 0.75 h^{-1} as the initial PAA concentration increased from 1 to 3 mg/L, which is in agreement with the results of the present study. In a subsequent study, Pederson et al. (2013) reported a similar decrease of PAA decomposition rate with increased initial PAA concentration, but an increased PAA decomposition rate with increased COD concentration. Based on

the above, the PAA decomposition rate decreases as the initial PAA concentration increases in complex wastewater streams. As noted in Section 4.3.2.1, above, the measured rate constants in the present study are pseudo-first order constants, specific to the conditions of each system.
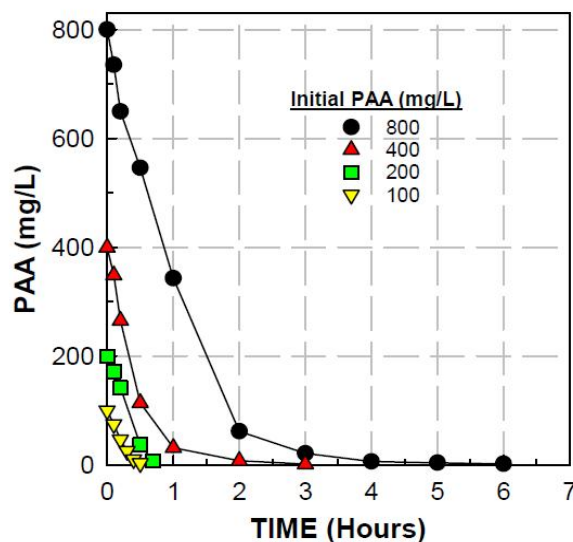
Figure 4.5. Time trend of PAA concentration in DAF effluent at initial PAA concentration of 100, 200, 400 and 800 mg/L (pH 6, 22±1ºC).

The effect of DAF effluent strength on PAA decomposition at constant pH 6 is depicted in Figure 4.6A. As the DAF effluent strength increased from 20 to 100%, the PAA decomposition rate increased from 0.203 to 1.075 h^{-1}, corresponding to half-life values from 3.47 to 0.64 h (Table 4.6). Thus, wastewater strength also plays an important role on the decomposition rate of PAA. Pederson et al. (2013) reported that the PAA decomposition rate was significantly and positively correlated to the wastewater COD concentration. Figure 4.6B illustrates the linearity between the PAA decomposition rate and the strength of the DAF effluent ($R^2 = 0.981$). Domínguez Henao et al. (2018)

reported both the decomposition rate and initial oxidative demand were in good linearity with the concentration of inorganics and organics used in their research. In contrast, no obvious initial demand was observed in the present study. However, the reported linearity between the PAA decomposition rate and the concentration of substances in the water matrices as reported by Domínguez Henao et al. (2018), is in agreement with our results.
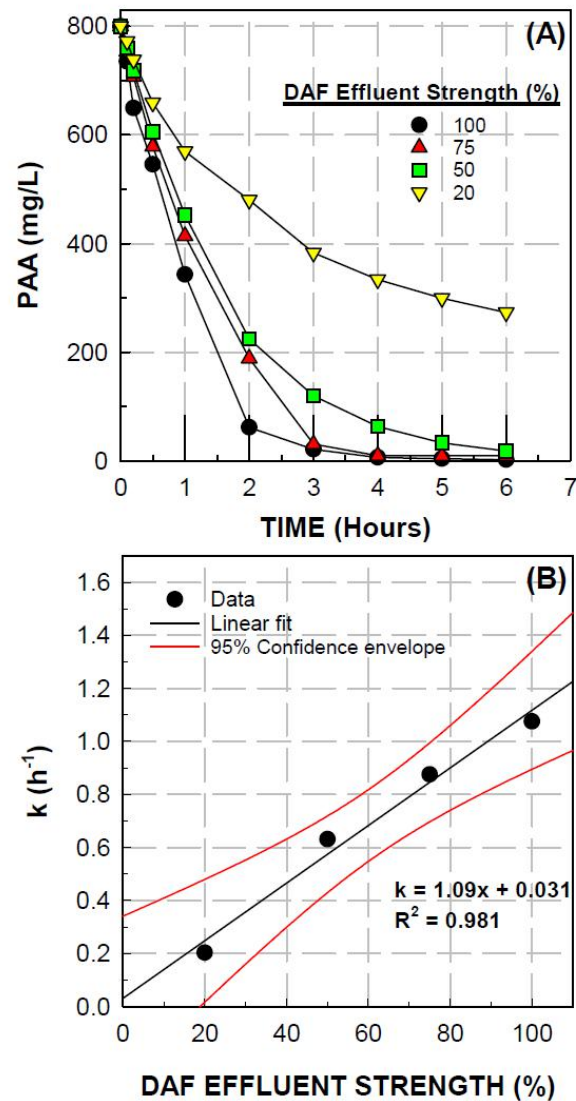
Figure 4.6. Time trend of PAA concentration in DAF effluent of 20, 50, 75, and 100% strength (pH 6, 22±1ºC) (A). PAA decomposition rate value (_k_, h^{-1}) vs. DAF effluent strength (%) (B).

4.3.2.4 Effect of Organics on PAA Decomposition Rate

61

The effect of organics, such as protein, carbohydrates, and lipids, at levels similar to those typically encountered in DAF effluent samples used in the present study, on the decomposition of PAA was investigated at a constant pH 6 and the values of the pseudo-first order PAA decomposition rate were evaluated. Compared to the PAA decomposition rate value in DI water and in 100-fold diluted methanol solution, glucose and lipids had a negligible effect compared to that of the diluted decanter solids filtrate, whose protein content was very high (64% of total COD), assuming a conversion factor of 1.5 g COD/g protein based on $(C_4H_{6.1}O_{1.2}N)x$ as an empirical formula for protein (Grady et al., 1999). The measured PAA decomposition rate value of the decanter solids filtrate, diluted 4-fold to match typical crude protein content of DAF effluent samples (0.974 ± 0.07 h^{-1}), is ca. 91% of the PAA decomposition rate value in the DAF effluent used in this study (1.075 h^{-1}). These results show that PAA reaction with protein is the major contributor to the observed, very high PAA decomposition rate in DAF effluents.

Domínguez Henao et al. (2018) reported that among three classes of organic compounds -- carbohydrates (i.e., glucose and cellulose), protein (i.e., casein and peptone), and fatty acids (i.e., butyric and oleic acid) -- tested at relatively low concentrations (≤ 35 mg COD/L) and an initial PAA concentration of 2 and 10 mg/L, proteins contributed to the PAA decomposition rate much more than the carbohydrates and fatty acids.

4.3.3 PAA Decomposition Product and COD Balance

PAA decomposition to acetic acid in DAF effluent is depicted in Figure 4.7. PAA concentration in the DAF effluent along with the solution pH were monitored with results

shown in Figure 4.7A and 4.7B, respectively. Figure 4.7C illustrates that the sum of PAA

and acetic acid molar concentrations in three samples collected after 6, 70 and 75 h of

incubation was 36.0±0.3, 35.6±0.5, and 35.4±0.5 mM, compared to the initial

concentration of 34.8±0.6 mM. Thus, the molar ratio of PAA transformed to acetic acid

produced was 100±0.9%. Monarca et al. (2002) reported that the major product in the

case of PAA disinfection was acetic acid, both in the original PAA equilibrium solution

and that resulting from PAA decomposition, which is consistent with the results of the

present study, detecting acetic acid at a molar PAA to acetic acid transformation ratio

close to 1. Reported DBPs when PAA was used as the disinfectant are ketones and

aldehydes at ppb levels. For example, formaldehyde and acetaldehyde have been reported

to be formed at low ppb levels during the disinfection of municipal secondary effluents

with PAA (Nurizzo et al., 2005).
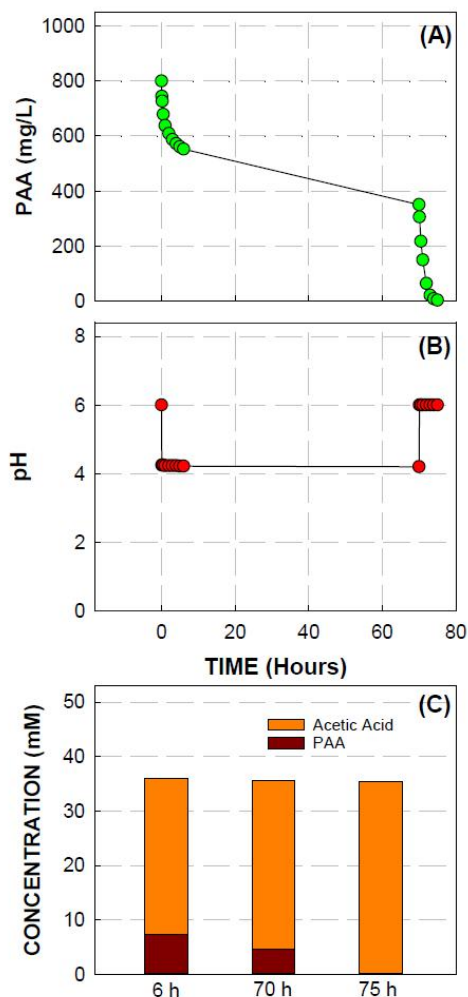
Figure 4.7. Time trend of PAA concentration in DAF effluent with pH adjustment at 75 h (22±1°C) (A). Initial pH drop caused by PAA addition and pH adjustment at 75 h (B). PAA and acetic acid molar concentration in the DAF effluent at 6, 70, and 75 h (C).

Reaction of PAA with organic components in the DAF effluent, leading to a possible overall COD decrease, was evaluated at five initial PAA concentrations of 64, 129, 258, 644, and 1,288 mg/L. The initial and final COD after the complete PAA decomposition were measured. The calculated total COD after the complete PAA decomposition was the sum of total COD of the original DAF effluent, COD of acetic acid as part of the PAA solution added initially, and COD of acetic acid produced by PAA decomposition. The final calculated total COD and the final measured total COD

values agreed well for all PAA doses, except for the two highest doses (i.e., 644 and 1,288 mg PAA/L), for which the measured total COD was lower by ca. 600 mg/L. The initial and final total COD distribution among PAA, acetic acid, and DAF effluent for the two highest PAA doses indicates that the decrease in the total measured COD is attributed to a decrease in the final DAF effluent COD. It is possible that PAA at the relatively high doses reacted with some DAF effluent organic components transforming them to products with an overall lower mean oxidation state and/or some gaseous products. Further confirmation of the nature of the observed decrease of the DAF effluent COD at high PAA doses warrants further investigation.

Overall, based on the results of this study, in order to avoid PAA carryover to biological processes downstream from the DAF unit, monitoring PAA in the DAF influent and effluent along with retention of PAA-bearing wastewater in an equalization tank to provide more time for complete PAA decomposition is recommended. However, as the decomposition of residual PAA, i.e., PAA that is not decomposed by interaction with the wastewater constituents, is very slow at typical wastewater pH values lower than 6.0, increasing the wastewater pH to ≥ 7.0 will result in fast PAA decomposition.

4.3.4 H_2O_2 Decomposition in DAF Effluent

H_2O_2 decomposition in DAF effluent followed two-step pseudo-first order kinetics (Table 4.7), similar to PAA decomposition in DAF effluent at pH 4 and 5, which indicates that there were two groups of substrates, one group reacting much faster with H_2O_2 than the other group. Two initial H_2O_2 concentrations were selected based on the H_2O_2 concentration measured in PAA working solutions. The lowest and highest

measured H_2O_2 concentration in 800 mg/L PAA solution were 64 and 168 mg/L, respectively. In DAF effluent, H_2O_2 overall decomposed faster at an initial concentration of 64 mg/L than at 168 mg/L, resulting in half-life values of 0.09 and 0.11 h of low and high initial H_2O_2, respectively, in the absence of PAA. Furthermore, the fraction α of H_2O_2 decomposed at a higher rate (k_{obs1}) is larger at the lower initial H_2O_2 concentration of 64 mg/L than at 168 mg/L. In the absence of PAA, the fraction of H_2O_2 decomposed at the faster rate k_{obs1} was 0.9 and 0.6 at 64 and 168 mg/L initial H_2O_2 concentration, respectively. The residual H_2O_2 decomposed at comparable rates, 0.6 and 0.7 h^{-1} at 64 and 168 mg/L initial H_2O_2, respectively, suggesting that once the H_2O_2 demand by the faster-reacting substances was satisfied, the residual H_2O_2 decomposition rates (k_{obs2}) were not affected by the residual H_2O_2 concentration. In the presence of PAA, H_2O_2 decomposition in DAF effluent was slower than in the absence of PAA, resulting in half-life values of 0.28 and 0.11 h in the presence and absence of PAA, respectively, at 168 mg/L initial H_2O_2. In poultry processing water, H_2O_2 decomposition also followed two-step pseudo-first order kinetics. The fraction α of 64 mg/L H_2O_2 decomposed at a higher rate (k_{obs1}) is smaller in process water ($\alpha = 0.503$ in the absence of PAA) than in DAF effluent ($\alpha = 0.884$ in the absence of PAA), which is likely due to fewer substances reacting fast with H_2O_2 in the process water than in the DAF effluent.

Table 4.7. H_2O_2 decomposition rate constant (k) values in process water and DAF effluent at low and high initial concentration, with and without PAA (controlled pH 6; 22±1°C).

Matrix	H_2O_2 (mg/L)	PAA (mg/L)	α (fraction)	k_{obs1} (h^{-1})	k_{obs2} (h^{-1})	R^2	Half-Life (h)
DAF Effluent	64	800	0.920	7.08± 0.40[a]	0.40± 0.15[a]	0.999	0.11
	64	0	0.884	9.14±0.63	0.64±0.21	0.999	0.09
	168	800	0.305	11.58±1.06	1.26±0.34	0.989	0.28
	168	0	0.613	12.89±3.66	0.72±0.19	0.989	0.11
Process Water	64	800	0.641	7.26±0.89	0.18±0.03	0.994	0.20
	64	0	0.503	11.37±1.43	0.17±0.01	0.996	0.26

[a] Mean ± standard error

4.4 Summary

PAA has been increasingly used by the poultry processing industry. However, information related to the potential PAA carryover to and effect on biological treatment processes, commonly used in poultry processing wastewater treatment, is limited. The objectives of this work were to assess the fate of PAA in poultry processing wastewater streams, investigate dominant factors contributing to PAA decomposition, and identify major PAA decomposition products. PAA applied to poultry processing chiller tanks does not reach the DAF unit under normal plant operation, except when chillers are emptied at the end of the plant shift and/or in case of an accidental spill. PAA decomposition in poultry waste streams was primarily affected by pH, and secondarily by wastewater strength, wastewater protein content, initial PAA concentration, and temperature. PAA decomposition followed one-step and two-step pseudo-first order decomposition kinetics above and below pH 6, respectively. PAA decomposition resulted in the production of equimolar concentration of acetic acid. Under high PAA dose, a decrease of DAF effluent COD was observed. H_2O_2 decomposition in poultry waste

streams was negatively related to the initial H_2O_2 concentration and the decomposition

rate was faster in DAF underflow than in process water.

CHAPTER 5. SHORT-TERM PAA EFFECT ON BATCH BIOASSAYS

5.1 Introduction

The effect of PAA on biological wastewater treatment processes typically used by the poultry processing industry, such as organic carbon degradation, nitrification and denitrification, is crucial for understanding its potential adverse impact when PAA is carried to the biological process units along with wastewater. However, information related to the effect of PAA on nitrification and denitrification is very limited. The objective of this chapter was to assess the effect of PAA and H_2O_2 on the aerobic degradation of organic substrates, as well as nitrification and denitrification in batch bioassays.

5.2 Materials and Methods

5.2.1 Stock Mixed Heterotrophic Nitrifying/Denitrifying Culture

A stock mixed heterotrophic, nitrifying/denitrifying culture, developed from the activated sludge obtained at a poultry processing facility, was maintained for over 2 years in the laboratory as fed-batch reactor. The reactor was fed twice a week, with a hydraulic retention time (HRT) of 7 d and solids retention time (SRT) of 21 d, in a 5.5-L glass reactor (culture volume 4 L), mixed with a stirring bar and a magnetic stirrer. The stock culture was kept aerobic (3 d) for carbon removal and nitrification, anoxic (1 d) for denitrification and aerobic (3 d) for carbon removal and nitrification again (Figure 4). Before each feeding, an aliquot of mixed liquor was removed and the culture was settled

for 1 h. Then, 3 L supernatant was removed by syphoning and 3 L DAF effluent was added to the reactor, along with 20 mL 1M NaHCO$_3$ to provide alkalinity and inorganic carbon source (NaHCO$_3$ is only added at the beginning of each aerobic phase). The feeding resulted in 500 mg/L initial soluble COD (sCOD), which was degraded to about 100 mg/L by the end of 1 d during the aerobic phase, resulting in a sCOD removal rate of 400 mg/L-d. sCOD was removed at a much lower rate, 200 mg/L-d during the anoxic phase. The feeding resulted in an average initial 50 mg N/L ammonia concentration, and took about 2 d to achieve complete ammonia removal (Figure 5.1). Each 3-d aerobic phase resulted in 110 to 120 mg N/L nitrate production, which was removed completely during the 1-d denitrification during the anoxic phase. Nitrite was always detected at very low levels, 0.2 to 0.5 mg N/L (Figure 5.1). The pH was maintained at 7.5 to 8 with added Na$_2$HCO$_3$ at the beginning of each aerobic phase providing alkalinity for nitrification. The DO level was always kept at 7 to 8 mg/L during the aerobic phases by aeration with pre-humidified compressed air, while during the anoxic phase aeration is turned off. The TSS/VSS was kept at 2.6±0.1/2.1±0.1 g/L, resulting in a VSS/TSS ratio of 82%. The fraction of heterotrophic bacteria, ammonia oxidizing bacteria (AOB) and nitrite oxidizing bacteria (NOB) in the stock culture, determined by selectively inhibiting AOB and NOB and then measuring oxygen uptake rates (Surmacz-Gorska et al., 1996), varied as follows (%): heterotrophs, 92 to 96; AOB, 2 to 5; and NOB, 2 to 3.
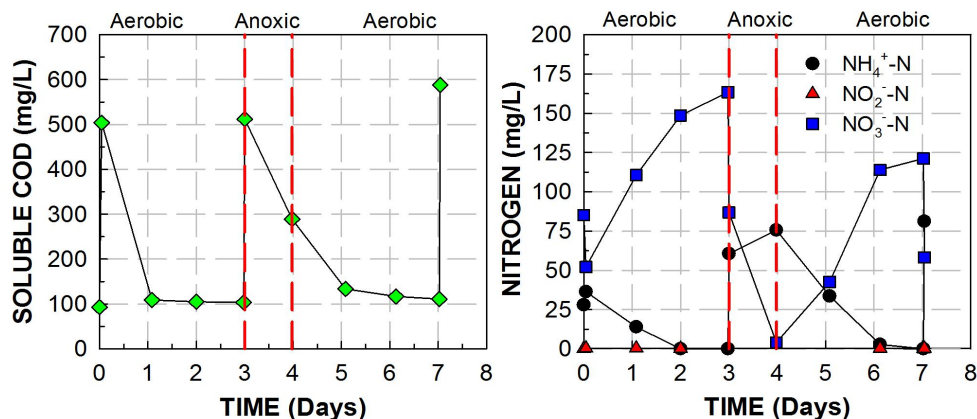
Figure 5.1. Time-trend of soluble COD and nitrogen species during a 1-week characterization of the stock culture.

5.2.2 Batch Nitrification Assays

Five aerobic batch assays were conducted with mixed liquor withdrawn from the stock culture (Section 5.2.1, above). The first assay, consisting of five test series, was setup at an initial PAA/H_2O_2 concentration of 0/0, 5/0.7, 10/1.4, 20/2.8, and 40/5.6 mg/L, all series fed with 300 mg/L glucose, 100 mg N/L NH_4Cl, and 1,200 mg/L $NaHCO_3$, in order to evaluate the effect of direct PAA addition on aerobic degradation and nitrification. The second assay, consisting of five test series, was setup at an initial PAA/H_2O_2 concentration of 0/0, 5/0.7, 10/1.4, 20/2.8, and 40/5.6 mg/L, all series fed with 300 mg/L glucose, 100 mg N/L $NaNO_2$, and 1,200 mg/L $NaHCO_3$, in order to evaluate the effect of direct PAA addition on aerobic degradation and nitrite oxidation (i.e., the second step of nitrification). The third assay, consisting of three test series, was setup with a control without PAA, a series with 20/2.8 mg/L PAA/H_2O_2 pre-decomposed in DAF effluent (indirect PAA solution addition), and a series with 20/2.8 mg/L PAA/H_2O_2 directly added to the culture (direct addition). In the third assay, all series were also fed with 300 mg/L glucose, 100 mg N/L NH_4Cl, and 1,200 mg/L $NaHCO_3$, in order to evaluate the effect of direct and indirect PAA addition on aerobic degradation and

71

nitrification. The fourth assay, consisting of five test series, was setup at an initial H_2O_2 concentration of 0, 5, 10, 20, and 40 mg/L, all series fed with 300 mg/L glucose, 100 mg N/L NH_4Cl, and 1,200 mg/L $NaHCO_3$, in order to evaluate the effect of direct H_2O_2 addition on aerobic degradation and nitrification. The fifth assay, consisting of five test series, was setup at an initial H_2O_2 concentration of 0, 5, 10, 20, and 40 mg/L, all series fed with 300 mg/L glucose, 100 mg N/L $NaNO_2$, and 1,200 mg/L $NaHCO_3$, in order to evaluate the effect of direct H_2O_2 addition on aerobic degradation and nitrite oxidation (i.e., the second step of nitrification). All batch assays were conducted in 500 mL glass aspiration bottles (400 mL liquid volume), mixed magnetically, aerated with pre-humidified compressed air, and incubated at room temperature (22 ± 1^oC). pH, DO, soluble COD, and N species of the batch assays were measured frequently during the incubation. TSS and VSS of the batch assays were measured at the beginning and the end of the incubation. PAA and H_2O_2 were measured immediately after the addition of PAA or H_2O_2 solution and monitored until their complete decomposition.

5.2.3 Batch Denitrification Assays

Two anoxic batch assays were conducted with mixed liquor withdrawn from the stock culture (Section 5.2.1, above). The first assay, consisting of five test series, was setup at an initial PAA/H_2O_2 concentration of 0/0, 5/0.7, 10/1.4, 20/2.8, and 40/5.6 mg/L, all series fed with 600 mg/L glucose and 120 mg/L $NaHCO_3$, in order to evaluate the effect of direct PAA addition on the degradation of organic substrates and denitrification. The second assay, consisting of three test series, was setup with a control without PAA, a series with 20/2.8 mg/L PAA/H_2O_2 pre-decomposed in DAF effluent (indirect addition),

72

and a series with 20/2.8 mg/L PAA/H_2O_2 directly added to the culture (direct addition). All series in the second assay were also fed with 600 mg/L glucose and 120 mg/L NaHCO$_3$, in order to evaluate the effect of direct and indirect PAA addition on the anoxic degradation of organic substrates and denitrification. Nitrate was not added externally to the denitrification assays as the initial nitrate in the mixed liquor was high, ca. 100 mg N/L. Both batch assays were conducted in He-pre-flushed 500 mL glass aspiration bottles (400 mL liquid volume), sealed with rubber stoppers, mixed magnetically, and incubated at room temperature (22±1°C). The pH, soluble COD, gas production and composition, and N species were measured frequently during the incubation. TSS and VSS were measured at the beginning and the end of the incubation. PAA and H_2O_2 were measured immediately after the addition of PAA or H_2O_2 solution and monitored until their complete decomposition.

5.2.4 Analytical Methods

pH, COD, N species, total suspended solids (TSS), volatile suspended solids (VSS), gas production and composition were measured as described in Section 3.1. The fraction of heterotrophic bacteria, ammonia-oxidizing bacteria (AOB), nitrite-oxidizing bacteria (NOB) in the stock mixed heterotrophic/autotrophic culture was determined by using sodium azide (NaN$_3$) and allylthiourea (ATU) to inhibit AOB and NOB, respectively, and then measuring oxygen uptake rates as previously described (Surmacz-Gorska et al., 1996). PAA concentrations were measured using the N, N-diethyl-p-phenylenediamine (DPD) colorimetric method as described in Chapter 3, Section 3.2.1.

5.3 Results and Discussion

5.3.1 Effect of PAA on Aerobic Degradation and Nitrification

The objective of the first nitrification batch bioassay was to evaluate the effect of direct PAA addition on nitrification. PAA and H_2O_2 decayed completely within minutes upon addition in all test series. All series achieved similar COD removal (Figure 5.2B). Complete removal of ammonia was achieved in all series, except the one amended with 40 mg/L PAA (Figure 5.2C). The initial, specific ammonia removal rate (SARR) was 106, 106, 96, 71 and 60 mg N/g VSS-d at an initial PAA of 0, 5, 10, 20 and 40 mg/L, respectively (Table 5.1). An initial PAA concentration of 5 mg/L did not impact the ARR. Based on these results, the effective PAA concentration resulted in 50% inhibition (IC_{50}) of the ARR was 27 mg/L (Figure 5.2F). Series with initial PAA of 0, 5, and 10 mg/L had a transient nitrite concentration reaching 25 to 30 mg N/L. Nitrite reached a level of 43 mg N/L in the series with an initial PAA of 20 mg/L and required 6 d for its complete oxidation to nitrate (Figure 5.2D). After an initial ammonia removal in the series with an initial PAA of 40 mg/L for 1 d, the rate of ammonia oxidation declined significantly forming high levels of nitrite; nitrate was not observed. Compared to the control (i.e., PAA free) series, PAA at 10 mg/L and above resulted in a biomass decrease from 11 to 29%.

Table 5.1. pH, VSS and ammonia removal rates as a function of initial PAA concentration in the first nitrification bioassay.

PAA (mg/L)	pH Initial[a]	pH Final	Final VSS (g/L)	ARR (mg N/L-d)	SARR (mg N/g VSS-d)	Relative ARR
0	8.8	8.6	1.37 ± 0.09[b]	174 ± 14[c]	127 ± 10	1.00
5	8.6	8.6	1.36 ± 0.02	174 ± 10	128 ± 7	1.00
10	8.4	8.7	1.08 ± 0.11	160 ± 4	148 ± 3	0.92
20	7.8	8.5	1.15 ± 0.03	82 ± 2	71 ± 2	0.47
40	7.0	9.0	0.97 ± 0.09	59 ± 10	60 ± 10	0.34

[a] After PAA addition; [b] Mean ± standard deviation; [c] Mean ± standard error
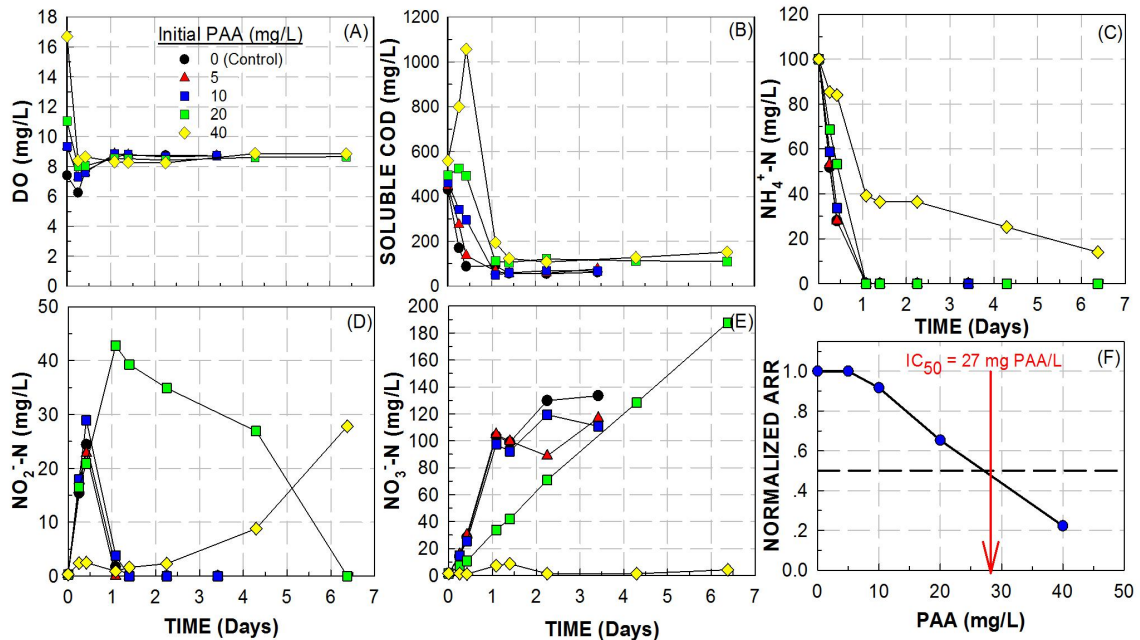
Figure 5.2. Time trend of DO (A), soluble COD (B), ammonia (C), nitrite (D), nitrate (E) concentration in Bioassay 1. Normalized ammonia removal rate (ARR) in each series vs. initial PAA concentration (F).

The objective of the second nitrification batch assay was to evaluate the effect of direct PAA addition on nitrite oxidation. PAA and H_2O_2 decayed below the detection limit of 0.1 mg/L within 2 h upon addition in all test series. All series achieved similar COD removal, except the series amended with 40 mg/L PAA, in which soluble COD increased from 150 mg/L at the end of 5-h incubation to 200 mg/L at the end of 25-h incubation, kept at this level for ~60 h and finally dropped to 139 mg/L at the end of

incubation (Figure 5.3B). Complete transformation of nitrite to nitrate was achieved by all series, except the one amended with 40 mg/L PAA (Figure 5.3C and 5.3D). The initial specific nitrite removal rate (NRR) was 22.3, 23.6, 23.5, 20.8 and 5.6 mg N/g VSS-d corresponding to an initial PAA of 0, 5, 10, 20 and 40 mg/L, respectively. Based on these results, the effective PAA concentration resulting in 50% inhibition (IC_{50}) of the nitrite removal rate was 29 mg/L (Figure 5.3F). The soluble total inorganic N concentration, calculated by adding up the soluble inorganic N species, fluctuated around 130 mg N/L throughout the 120-h incubation in all five series (Figure 5.3E). For all five series, total soluble N measured initially after PAA addition and at the end of incubation is very close to the sum of inorganic N species (ammonia, nitrite and nitrate), which indicates soluble organic N is negligible in all the series. TSS and VSS were measured initially and at the end of incubation, and a loss of 20% VSS was observed in the control reactor throughout the incubation compared to the initial VSS concentration. The series amended with 5 and 10 mg/L PAA had a final VSS concentration similar to the control, whereas the final VSS concentration was ~20% and ~35% lower in the series amended with 20 and 40 mg/L PAA, respectively, compared to the control. Comparing the control at the end of incubation to the seed reactor (initial condition), the fraction of the nitrite oxidizing bacteria (NOB) in the mixed heterotrophic/autotrophic culture increased by 4-fold, while the fraction of the ammonium oxidizing bacteria (AOB) decreased ~50%, caused by the fact that nitrite was supplied as N source rather than ammonia. Additionally, the fraction of heterotrophic bacteria decreased from 80% to 66%. At the end of the incubation, compared to the control, the AOB and NOB fractions were comparable in the series amended with 5 to 20 mg/L PAA, whereas both the AOB and NOB fractions were 4-fold

76

lower in the series amended with 40 mg/L PAA. Thus, these results suggest that AOB and NOB are more susceptible to a high PAA dose (>20 mg/L) than heterotrophs.

Regarding the pathway for ammonia oxidation to nitrite indicates that ammonia is first oxidized to hydroxylamine by ammonia monooxygenase (AMO), mainly located at the cell inner membrane, and then hydroxylamine is oxidized to nitrite by hydroxylamine oxidase (HAO), mainly located at the periplasm (Holmes et al., 2018). Two pathways have been proposed for nitrite oxidation to nitrate by nitrite oxidoreductase (NXR), a periplasmic and a cytoplasmic pathway. Most of the NXR sub-units are located between the inner membrane and periplasm for the periplasmic pathway while located between the inner membrane and cytoplasm for the cytoplasmic pathway (Holmes et al., 2018). In the case of being exposed to PAA, the outer membrane, as the first shield of the cell, will be the first to be exposed and affected, while the periplasm will be the second. Thus, the inhibition caused on ammonia oxidation to nitrite is likely ascribed to that HAO, mainly located in the periplasm, was inhibited by PAA. The periplasmic pathway of nitrite oxidation may also be affected by PAA, whereas the cytoplasmic pathway may still function as long as the NXR in the inner membrane and cytoplasm are not inhibited.

Table 5.2. pH, VSS and nitrite removal rates as a function of initial PAA concentration in the second nitrification bioassay.

PAA (mg/L)	pH Initial[a]	Final	Final VSS (g/L)	NRR (mg N/L-d)	SNRR (mg N/g VSS-d)	Relative NRR
0	9.6	9.2	1.86±0.07[b]	35.6±5[c]	19.1±2.7	1.00
5	9.3	9.3	1.86±0.08	39.9±6.6	21.5±3.5	1.12
10	9.1	9.2	1.84±0.07	42.5±6.1	23±3.3	1.19
20	8.9	9.3	1.51±0.1	31.1±3.4	20.6±2.2	0.87
40	8.4	9.2	1.12±0.04	5.1±0.7	4.5±0.6	0.14

[a] After PAA addition; [b] Mean ± standard deviation; [c] Mean ± standard error
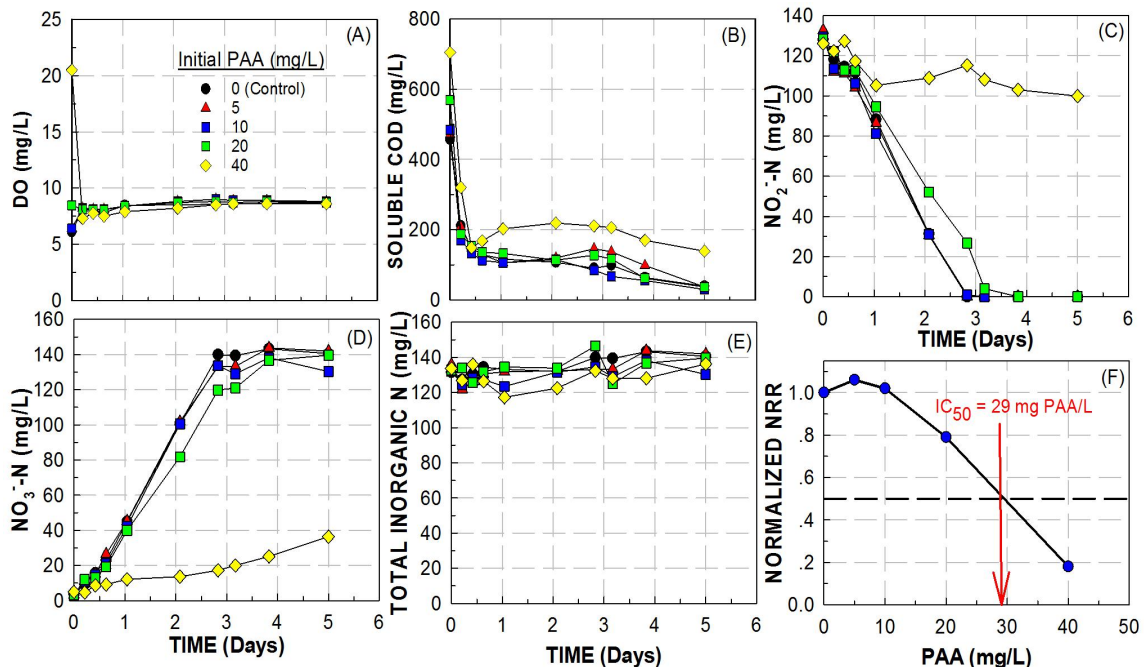
Figure 5.3. Time trend of DO (A), soluble COD (B), nitrite (C), nitrate (D) and total inorganic nitrogen (E) concentration in Bioassay 2. Normalized nitrite removal rate (NRR) in each series vs. PAA (mg/L) (F).

The objective of the third nitrification batch assay was to evaluate the effect of direct and indirect addition of PAA solution at 20 mg PAA/L on nitrification, followed by denitrification. PAA decayed completely within 5 min when was pre-decomposed in DAF effluent and within minutes when it was directly added to the third culture series. During the first aerobic/nitrification phase, the extent of COD removal within 18 h of incubation was 91, 84, and 72% for the control, indirect and direct PAA addition culture series, respectively (Figure 5.4B). Complete removal of ammonia was achieved by all series, with a specific ammonium removal rate (ARR) of 15.1, 14.6 and 8.4 mg N/g VSS-d by the control, indirect and direct culture series, respectively (Figure 5.4C). Transient nitrite levels were observed in the control and indirect culture series, while nitrite reached a maximum level of 26 mg N/L in the series with direct 20 mg/L PAA addition, requiring 7 d for its complete oxidation to nitrate (Figure 5.4D and 5.4E). During the anoxic phase,

all series achieved a similar extent of COD, nitrate and nitrite removal, and ammonium

production from the DAF effluent feed added at the beginning of the anoxic phase.

During the second aerobic/nitrification phase, complete ammonia removal was achieved

by all series in less than 8 d, with a specific ammonium removal rate of 17.8, 12.7 and 7.6

mg N/g VSS-d by the control, indirect and direct PAA addition culture series,

respectively. Nitrite was observed in all culture series reaching a level of 40 to 50 mg

N/L. Nitrite was completely converted to nitrate within 7 d in the control and indirect

PAA addition culture series, while it took 9 d for the complete conversion of nitrite to

nitrate in the direct PAA addition series (Figure 5.4D and 5.4E). At the end of the three-

phase incubation, compared to the control (i.e., PAA free series), 8 and 34% biomass

decrease was observed in the indirect and direct PAA addition culture series.

**Table 5.3. pH, VSS and ammonia removal rates as a function of direct vs. indirect
initial PAA addition in the third nitrification bioassay.**

PAA	pH		Final VSS	ARR	SARR	Relative
(mg/L)	Initial[a]	Final	(g/L)	(mg N/L-d)	(mg N/g VSS-d)	ARR
0	7.3	8.0	1.49±0.03[b]	38.6±2.8[c]	25.9±1.9	1.00
20 direct	6.4	7.9	0.98±0.07	12.2±2.6	12.4±2.7	0.43
20 indirect	6.2	8.0	1.37±0.1	38.3±8.0	28±5.9	0.99

[a] After PAA addition; [b] Mean ± standard deviation; [c] Mean ± standard error
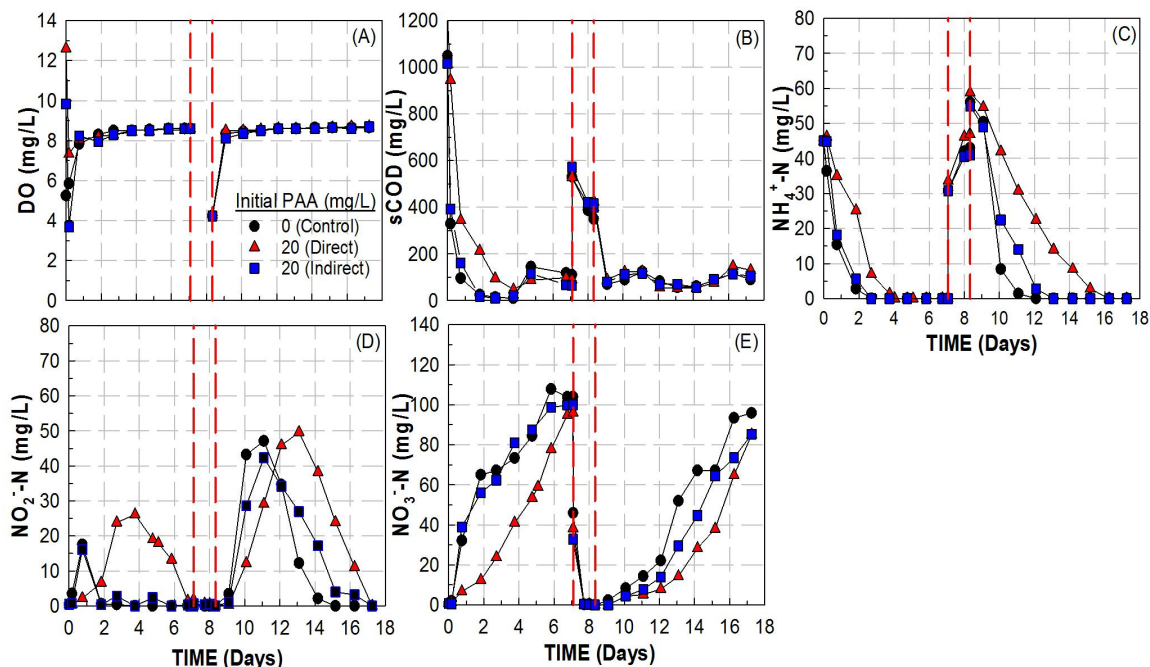
Figure 5.4. Time trend of DO (A), soluble COD (B), ammonia (C), nitrite (D), nitrate (E) concentration in Bioassay 3. The bioassay was conducted in three phases: aerobic (7 d), anoxic (1.4 d) and aerobic (9 d) (broken vertical lines).

5.3.2 Effect of H_2O_2 on Aerobic Degradation and Nitrification

The objective of the fourth nitrification batch bioassay was to evaluate the effect of direct H_2O_2 addition on nitrification. H_2O_2 decayed below the detection limit of 0.1 mg/L within 1 h upon addition to all test series. All series achieved similar COD removal (Figure 5.5B). Negligible effect on ammonia oxidation was observed in series amended with 10 mg/L and lower H_2O_2, while 20 and 40 mg/L H_2O_2 had a mild inhibition on ammonium oxidation (Figure 5.5C). The specific ammonia removal rate (SARR) was 66.7, 67.0, 71.1, 53.1 and 49.2 mg N/g VSS-d in series amended with 0, 5, 10, 20 and 40 mg/L H_2O_2, respectively. The decrease of SARR for the highest H_2O_2 dose was less than 30%. Lower transient nitrite levels were observed in series amended with 20 and 40 mg/L H_2O_2 than in series amended with a lower H_2O_2 dose. The difference in nitrite levels may

be the result of a higher H_2O_2 inhibition on ammonia oxidation to nitrite as the H_2O_2 dose

increased, while nitrite oxidation to nitrate was not affected by the increased H_2O_2 dose.

However, the transient nitrite levels observed in the 20 and 40 mg/L H_2O_2 series lasted

longer than in series amended with a lower H_2O_2 dose. Complete nitrite removal was

achieved within 30 and 42 h in all series (Figure 5.5D). The rate of nitrate formation was

slightly affected by the high H_2O_2 doses (i.e., 20 and 40 mg/L). At the end of the

incubation, 90 to 100 mg N/L nitrate was formed, compared to the initially added 100 mg

/L NH_4^+-N (Figure 5.5E). Overall, the effect of H_2O_2 on nitrification was mild, and was

negligible at 5 and 10 mg/L H_2O_2. Compared with the results of the effect of PAA

solution on nitrification (see Section 5.3.1, above), PAA is the dominant inhibitory factor

on nitrification in the PAA solution rather than H_2O_2.
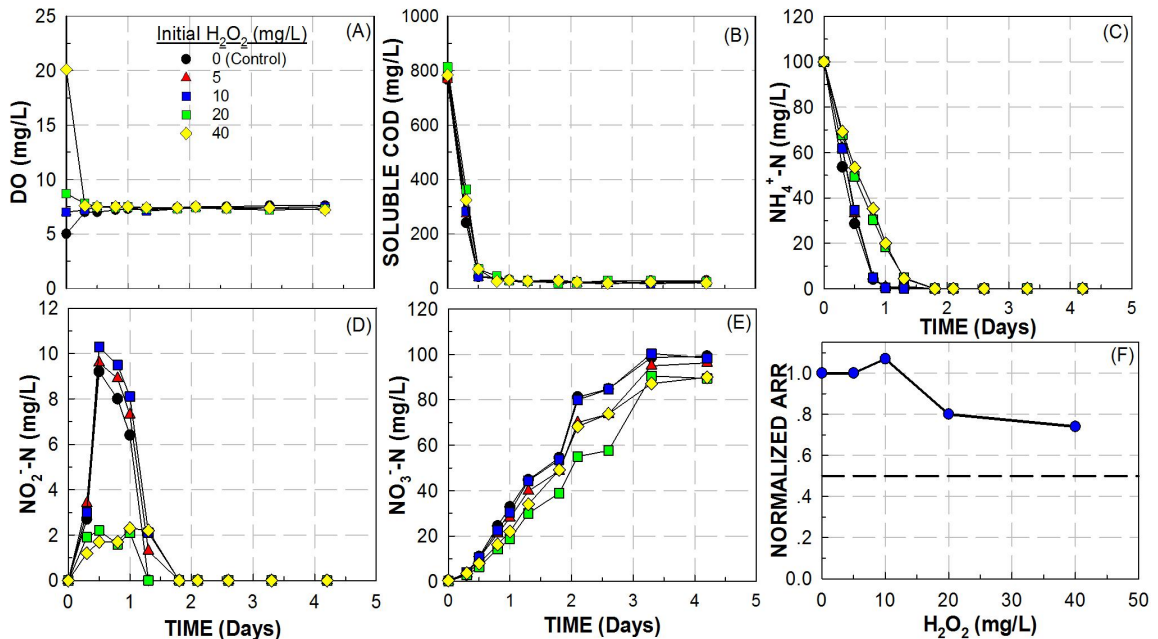
Figure 5.5. Time trend of DO (A), soluble COD (B), ammonia (C), nitrite (D), nitrate (E) concentration in Bioassay 6. Normalized ammonia removal rate (ARR) in each series vs. H_2O_2 (mg/L) (F).

The objective of the fifth batch bioassay was to evaluate the effect of direct and indirect H_2O_2 addition on nitrite oxidation. H_2O_2 decayed below the detection limit of 0.1 mg/L within 1 h upon addition to all test series. All series achieved similar COD removal (Figure 5.6B), and similar nitrite oxidation rate (Figure 5.6C). The extent of COD removal at the end of incubation ranged from 97.5 to 98% among all five series. The specific nitrite removal rate (NRR) was 18.2, 18.0, 17.2, 16.1 and 18.2 mg N/g VSS-d in series amended with 0, 5, 10, 20 and 40 mg/L PAA, respectively. Nitrate measured at the end of the incubation was 101, 108, 116, 102 and 104 mg N/L in series amended with 0, 5, 10, 20 and 40 mg/L PAA, respectively, while the VSS at the end of incubation was 2.06±0.04, 1.97±0.11, 1.96±0.1, 2.04±0.02 and 2.1±0.15 g/L. The series amended with 10 mg/L PAA had the highest nitrate concentration and lowest VSS at the end of incubation, which suggests more cell lysis occurred in this series and correspondingly resulted in more nitrate production. Compared to the results of the effect of PAA solution on nitrite oxidation (Section 5.3.1), the observed negligible effect of H_2O_2 on nitrite oxidation demonstrates that the inhibitory effect of the PAA solution was dominated by PAA rather than H_2O_2.
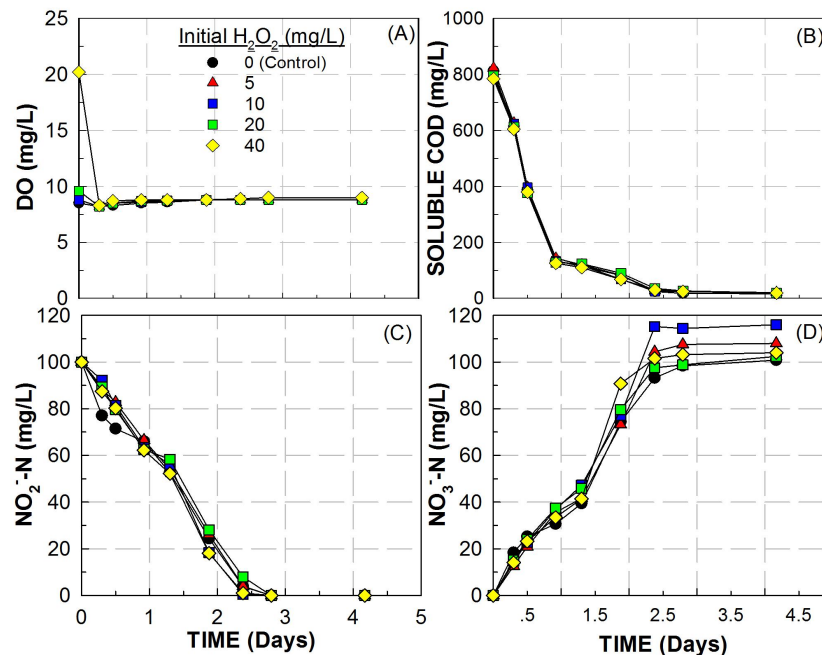
Figure 5.6. Time trend of DO (A), soluble COD (B), nitrite (C), and nitrate (D) concentration in Bioassay 7.

5.3.3 Effect of PAA on Denitrification

The objective of the first denitrification batch bioassay was to evaluate the effect of direct PAA addition on denitrification. PAA decayed completely within minutes upon addition to all test series. After 3.2 d of incubation, the extent of COD removal was 57, 55, 51, 37 and 23 % corresponding to 0, 5, 10, 20 and 40 mg/L initial PAA, respectively. Cell lysis resulting from the PAA addition contributed to the observed decreased COD removal with increasing initial PAA concentration. Complete removal of nitrate was achieved by all culture series within 30 h of incubation (Figure 5.7A). The initial specific nitrate removal rate (SNRR) was 254, 233, 86, 89 and 84 mg N/g VSS-d at an initial PAA of 0, 5, 10, 20 and 40 mg/L, respectively, resulting in 50% inhibition (i.e., IC_{50} value) for nitrate removal of 8 mg/L PAA (Figure 5.7D). Transient nitrite levels from 20 to 30 mg N/L were observed in the series with an initial PAA concentration of 0 and 5 mg/L. Nitrite reached a level of 57 mg N/L in the series with an initial PAA of 40 mg/L

and required 3.2 d for its complete removal (Figure 5.7B). The specific N_2 production

rate (SNPR) was 88.8, 60, 50.4, 45.6 and 36 mg N/g VSS-d at an initial PAA of 0, 5, 10,

20 and 40 mg/L, respectively, resulting in an IC_{50} value for N_2 production of 22 mg/L

PAA (Figure 5.7E). Compared to the control (i.e., PAA free) series, biomass loss was not

observed in the 5 mg/L initial PAA series over the 30-h incubation, while biomass

decrease by 6, 11, and 39% was observed in the 10, 20 and 40 mg/L initial PAA series,

respectively. The soluble organic N at the end of the incubation was 1.4, 9.8, 7.7, 26.9

and 59.3 mg N/L in the 0, 5, 10, 20 and 40 mg/L initial PAA series, respectively. The

total N balance at the end of the incubation was 99.6, 100.9, 101.0, 104.0 and 105.8% for

the series with 0, 5, 10, 20 and 40 mg/L initial PAA dose, respectively.

Table 5.4. pH, VSS and nitrate removal rates as a function of initial PAA concentration in the first denitrification bioassay.

PAA	pH		Final VSS	NRR	SNRR	Relative
(mg/L)	Initial[a]	Final	(g/L)	(mg N/L-d)	(mg N/g VSS-d)	NRR
0	8.6	8.6	1.18±0.04[b]	235±36[c]	199±31	1.00
5	8.4	8.5	1.18±0.05	232±24	198±21	0.99
10	8.3	8.4	1.10±0.03	96±5	88±4	0.41
20	8.3	8.4	1.04±0.05	102±9	98±9	0.43
40	8.3	8.3	0.71±0.03	72±21	102±29	0.56

[a] After PAA addition; [b] Mean ± standard deviation; [c] Mean ± standard error
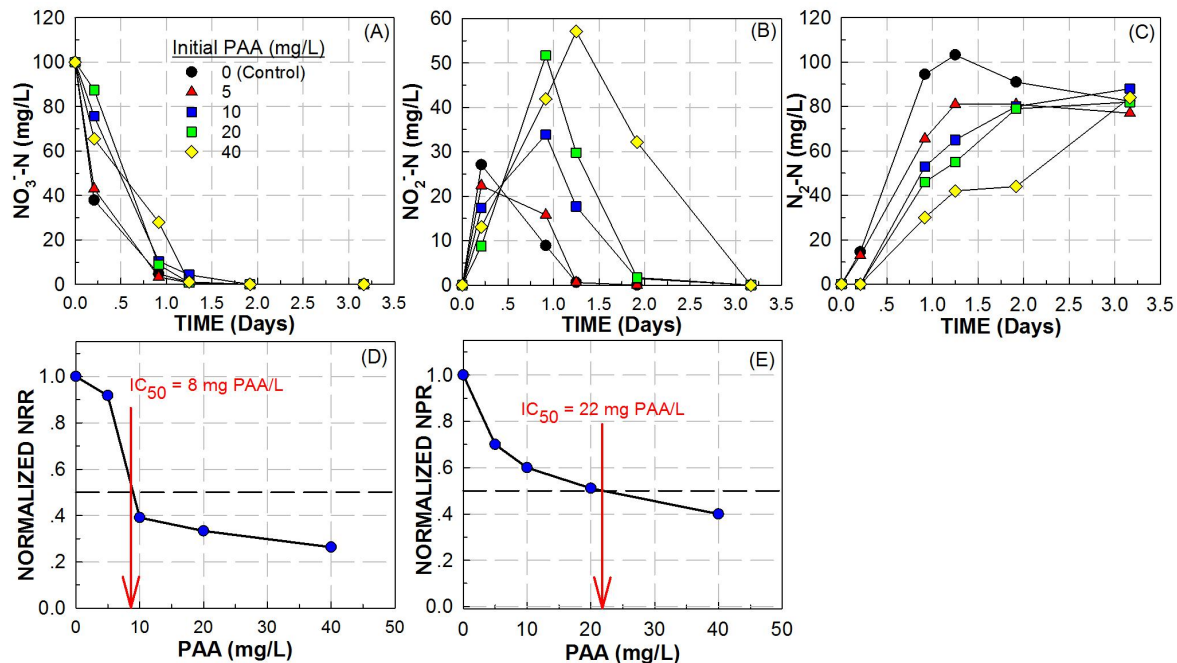
Figure 5.7. Time trend of nitrate (A), nitrite (B) concentration and production of N₂-N (C) in Bioassay 4. Normalized nitrate removal rate (NRR) in each series vs. PAA (mg/L) (D). Normalized nitrogen (N₂) production rate (NPR) in each series vs. PAA (mg/L) (E).

The objective of the second denitrification batch bioassay was to evaluate the effect of direct and indirect PAA addition at 20 mg/L on denitrification. PAA decayed completely within 5 min when pre-decomposed in DAF effluent and within minutes when directly added to the culture. At the end of the 2.8-d incubation, the extent of COD removal was 62, 54, and 46% by the control, indirect and direct PAA addition series, respectively. The net ammonium release by the end of the incubation was 3.5, 8.4 and 21 mg N/L in the control, indirect and direct PAA addition series, respectively. The increased ammonium release in the two PAA-amended culture series is the direct result of cell lysis. Complete removal of nitrate was achieved in all series, with specific nitrate removal rate (SNRR) of 132, 122 and 96 mg N/g VSS-d by the control, indirect and direct PAA addition series, respectively. Low nitrite levels (< 2 mg N/L) were observed in the control and indirect series, while nitrite reached a level of 19 mg N/L in the series

with direct 20 mg/L PAA addition, requiring 1.8 d for its complete removal (Figure 5.8B).

The specific N_2 production rate (SNPR) was 110, 106 and 83 mg N/g VSS-d in the

control, indirect and direct series, respectively. Compared to the control (i.e., PAA free)

series, biomass decrease by 2 and 14% was observed in the series amended with 20 mg/L

PAA indirectly and directly, respectively. The soluble organic N at the end of the

incubation was 1.7, 3.2 and 9 mg N/L in the control, indirect and direct series,

respectively. The total N balance at the end of the incubation was 101.9, 98.8, and 99.5%

for the control, indirect and direct series, respectively.

Table 5.5. pH, VSS and nitrate removal rates as a function of direct vs. indirect initial PAA addition in the second denitrification bioassay.

PAA	pH		Final VSS	NRR	SNRR	Relative
(mg/L)	Initial[a]	Final	(g/L)	(mg N/L-d)	(mg N/g VSS-d)	ARR
0	7.5	7.5	1.1±0.04[b]	131±4[c]	119±4	1.00
20 direct	7.2	7.4	0.95±0.09	95±7	100±8	0.73
20 indirect	7.2	7.3	1.08±0.09	121±2	113±2	0.93

[a] After PAA addition; [b] Mean ± standard deviation; [c] Mean ± standard error
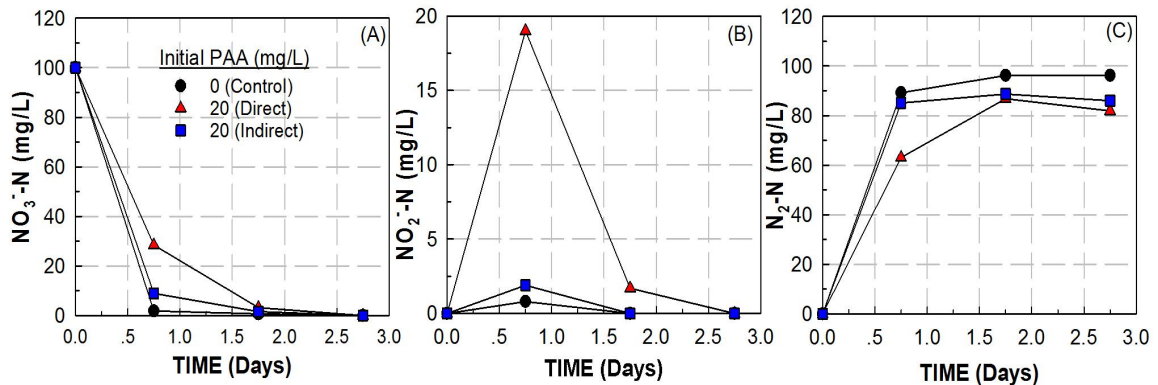
Figure 5.8. Time trend of nitrate (A), nitrite (B) concentration and production of N_2-N (C) in Bioassay 5.

5.4 Summary

Overall, the inhibition of PAA solution on aerobic degradation, nitrification and denitrification was dose-dependent, with negligible to mild inhibition at a low PAA dose (i.e., 5 to 20 mg/L) and significant inhibition at a higher PAA dose (i.e., 40 mg/L). H_2O_2 inhibited the first step of nitrification, i.e., ammonia oxidation to nitrite, whereas it did not inhibit the second step of nitrification, i.e., nitrite oxidation to nitrate. By comparing the inhibitory effect of the PAA solution and H_2O_2 on nitrification, and by also considering the low H_2O_2 concentration (≤ 5 mg/L) in the PAA solution, the effect of the PAA solution on nitrification is dominated by PAA rather than H_2O_2. Minor inhibition, resulting in less than 10% decrease of SARR and SNPR, was caused by indirect addition of PAA solution, which is the direct result of fast PAA decomposition in the complex, organic feed.

CHAPTER 6. LONG-TERM EFFECT OF PAA ON A MIXED AEROBIC CULTURE

6.1 Introduction

As discussed in Chapter 4, Section 4.3.1, PAA concentrations in excess of 1,000 and 75 mg/L were detected in the main chiller tank and chiller overflow, respectively, while PAA was not detected in DAF influent and underflow wastewater during the normal plant operation (Ch. 4, section 4.3.1). However, 25 to 30 mg/L PAA was detected in the DAF underflow wastewater at the end of the poultry processing plant daily operational shift, which coincided with the emptying of chiller tanks. Information related to the potential inhibitory effect of PAA solutions on biological wastewater treatment processes commonly used by the poultry processing industry is extremely limited. Thus, evaluation of the effect of PAA on biological wastewater treatment processes typically used by the poultry processing industry is urgently needed.

The overall goal of this study was to assess the long-term effect of PAA solution on aerobic organic matter degradation and nitrification, biological processes commonly used for the treatment of poultry processing wastewater. The following questions needed to be answered: a) Do PAA solutions and associated H_2O_2 inhibit aerobic degradation and nitrification in the treatment of poultry processing wastewater, and if they do, what are PAA and H_2O_2 inhibitory levels? b) Is the impact of PAA solution on aerobic degradation and nitrification associated with enzyme inhibition and/or decreased microbial culture viability? c) Is the impact of PAA and H_2O_2 reversible and does microbial acclimation

take place over the long-term operation with addition of PAA and H_2O_2? To address these questions, the following tasks were carried out. Aerobic bioreactors, semi-continuously fed with poultry processing wastewater, amended with PAA solution and H_2O_2 at increasing concentrations, were operated for 166 d. The effect of PAA and H_2O_2 on aerobic degradation and nitrification was evaluated, quantified in terms of chemical oxygen demand (COD) removal and nitrification rates. Microbial responses to PAA solution, such as culture viability and intracellular reactive oxygen species (ROS), were also evaluated. Complementary aerobic batch assays were conducted with single, direct PAA addition to determine potential acclimation taking place over the long-term operation with addition of PAA solution. Finally, the microbial community diversity and composition over the long-term operation with PAA and H_2O_2 addition were evaluated.

6.2 Materials and Methods

6.2.1 Chemicals and Wastewater

Chemicals are described in Chapter 3 Section 3.2.1.

DAF underflow wastewater was collected twice over a 6-month period at a poultry processing plant in the Southeast US, at mid plant operation shift. The DAF wastewater was stored at 4^oC in completely filled plastic containers with zero headspace. Table 6.1 summarizes the characteristics of the DAF underflow wastewater collected twice from a poultry processing facility during mid plant operation shift. Neither PAA nor H_2O_2 was detected, which is consistent with data reported in Chapter 4, Section 4.3.1, in which PAA was detected in the DAF influent and underflow wastewater only at the

end of the operation shift as a result of emptying the chiller tanks before equipment

cleaning and sanitation. The DAF underflow wastewater was slightly acidic, which is

typical for this and other poultry processing facilities (Hajaya and Pavlostathis, 2012).

The total COD concentration of the DAF underflow wastewater varied between 955 and

1240 mg/L; the soluble COD concentration was between 82 and 94% of total COD

(Table 6.1). Among the organic macromolecular constituents of the DAF underflow

wastewater, crude protein was the major one (over 40% of total COD), whereas lipids

and total carbohydrates represented 5 and 2% of the total COD, respectively (Table 6.1).

VFAs accounted for 63 to 76% of soluble COD. Ammonia-N was between 14 and 27%

of organic N. However, along with the COD decrease during storage, the ammonia-N

concentration increased by as much as 100%, the result of low microbial activity even at

4°C. During storage at 4°C, the DAF wastewater COD concentration decreased by as

much as 35% and its ammonium-N concentration increased by as much as 100%, the

result of low microbial activity even at 4°C.

Table 6.1 Characteristics of DAF wastewater collected twice at the study poultry processing plant.

Parameter	Value
pH	5.6 (5.3-5.8)[a]
PAA (mg/L)	ND[b]
H_2O_2 (mg/L)	ND
TSS (mg/L)	70 (60-80)
VSS (mg/L)	37 (34-40)
Total COD (mg/L)	1098 (955-1240)
Soluble COD (mg/L)	954 (895-1013)
VFAs (mg COD/L)	654 (564-774)
Total N (mg N/L)[c]	118 (83-153)
Ammonia (mg N/L)	18.5 (18-19)
Organic N (mg N/L)	100 (65-134)
Crude protein (mg/L)	623 (408-837)
Total P (mg P/L)	28 (27-29)
Orthophosphate (mg P/L)	16 (14-18)
Lipids (mg/L)	40 (37-63)
Carbohydrates (mg/L)[d]	25 (24-25)

[a] Mean value (range); [b] ND, not detected; [c] Total nitrogen, i.e., sum of organic, ammonia, nitrite, and nitrate nitrogen; [d] Expressed as glucose

6.2.2 Setup and Operation of Bioreactors

Three semi-continuously fed aerobic bioreactors (R1, R2, and R3) were set up and maintained at room temperature (22±1°C). The reactors started with stock culture from a lab-scale reactor, fed with DAF wastewater over 2.5 years. Details of the stock culture are presented in Chapter 5, Section 5.2.1. The reactors were 2.8 L Spinner cell flasks (Bellco Glass, Inc., Vineland, NJ) with a total culture volume of 1.5 L, mixed with externally driven magnetic impeller assemblies. Aeration was achieved with pre-humidified compressed air at a flow rate of 1.0 standard cubic feet per hour (SCFH). The three reactors were fed as follows: R1, DAF wastewater only; R2, DAF wastewater and H_2O_2 added either in the feed (indirect addition), or directly in the reactor (direct addition); and R3, DAF wastewater and PAA solution (indirect or direct addition).

Indirect PAA and H_2O_2 addition simulated treatment of wastewater devoid of residual PAA and/or H_2O_2, whereas direct addition simulated treatment of residual PAA- and H_2O_2-barring wastewater. The reactors were fed every 2 d after settling for 1 h and removing 1 L supernatant; 0.5 L mixed liquor was removed every 6 d. The resulting hydraulic retention time (HRT) and solids retention time (SRT) was 3 and 18 d, respectively. Preliminary nitrification tests showed that for the stock culture used in this study and the levels of ammonium resulting from the aerobic degradation of DAF wastewater, the pH dropped below 6.5, which adversely affected the nitrification rate. As a result, at each feeding, $NaHCO_3$ was added at an initial concentration of 500 mg/L to provide inorganic carbon to nitrifying bacteria and sufficient alkalinity to maintain a pH above 7.0.

The long-term operation of the reactors consisted of four phases (Fig. 6.1). In Phase I (control), the reactors were fed for 40 d with PAA- and H_2O_2-free DAF wastewater. Operation of R1 was the same throughout the four phases. In Phase II (indirect H_2O_2 and PAA solution addition), before feeding, the wastewater feed to R2 was amended with H_2O_2 at gradually increasing concentrations corresponding to the H_2O_2 concentrations in the PAA solution-amended feed to R3. Aliquots of H_2O_2 and PAA working solutions were added to the R2 and R3 wastewater feed, respectively, 40 min before feeding. Under these conditions, H_2O_2 and PAA were completely decomposed in the wastewater feed (pH 6.5 to 7.0). The resulting, nominal reactor H_2O_2 and PAA initial concentrations were increased stepwise over time from 0.7 to 8.4 mg/L H_2O_2 in R2 and from 5/0.7 to 60/8.4 mg/L PAA/H_2O_2 in R3 (Fig. 6.1). It should be noted that to above-mentioned, nominal reactor H_2O_2 and PAA concentrations correspond to feed H_2O_2 and

PAA concentrations 1.5-fold higher (equal to the ratio of culture and feed volume, 1.5/1.0). Thus, the range of equivalent feed concentrations was 1.05 to 13.65 mg H_2O_2 /L and 7.5 to 90 mg PAA/L. In Phase III (direct H_2O_2 and PAA solution addition), both R2 and R3 were fed as in Phase II, but with direct addition of H_2O_2 and PAA working solutions to the reactors immediately after adding the DAF wastewater. It should be noted that preliminary tests conducted with either direct or indirect followed by direct addition of PAA/H_2O_2 did not result in any significant difference relative to COD removal and nitrification inhibition.

As noted in Chapter 3, Section 3.2.2, the equivalent weight of PAA and H_2O_2 is equal to their molecular weight (PAA, 76 g/mole; H_2O_2, 34 g/mole). Thus, in terms of equivalents, one mole of H_2O_2 is 2.235-fold stronger oxidant than one mole of PAA. Based on the above, towards the end of Phase III, and in order to match the oxidation capacity of PAA in R3, after the last feeding of R2 with 8.4 mg/L H_2O_2, 27 mg/L H_2O_2 were added directly to R2, which is equivalent to 60 mg/L PAA in terms of electron transfer during decomposition. It should be noted that a nominal reactor concentration of 27 mg H_2O_2/L is equivalent to 40.5 mg H_2O_2/L in the feed. In Phase IV (recovery phase), all three reactors were maintained as in Phase I, fed with H_2O_2- and PAA-free DAF wastewater. The following parameters were monitored over the long-term operation: pH, DO, soluble COD (sCOD), ammonium, nitrite, nitrate, total and volatile suspended solids (TSS, VSS), culture viability and intracellular ROS.
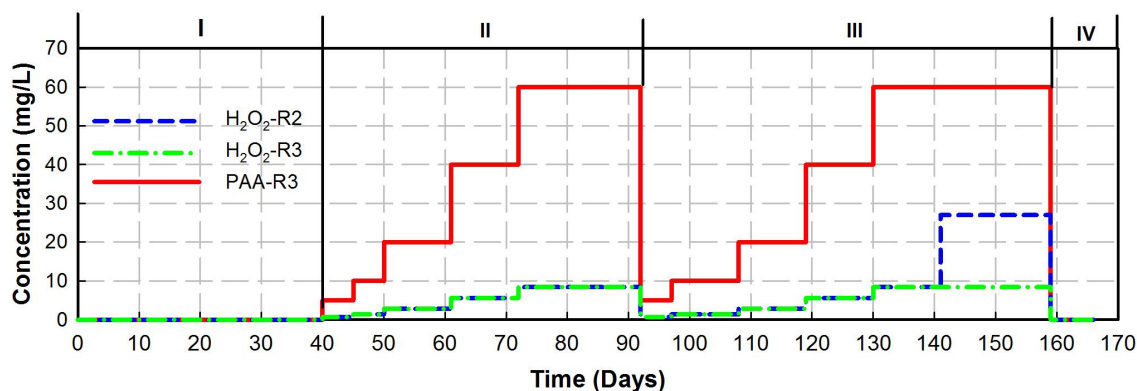
Figure 6.1. Initial, nominal reactor H₂O₂ and PAA concentration in Phase I (control), II (indirect H₂O₂ and PAA solution addition), III (direct H₂O₂ and PAA solution addition), and IV (recovery) in R2 and R3 during the 166-d operation.

6.2.3 Short-term Batch Assays

The purpose of these aerobic batch assays was to evaluate possible increased inhibitory effect of the PAA solution on aerobic degradation and nitrification in R3 (direct addition of PAA solution) and culture acclimation at different stages during the long-term operation. The batch assays were carried out in 580-mL glass aspirator bottles. At the end of several feeding cycles during the long-term operation of R1, 450 mL of R1 mixed liquor was transferred to the bottle, allowed to settle for 1 h and then 300 mL supernatant was replaced with an equal volume of DAF wastewater, along with 500 mg/L NaHCO₃. PAA solution was directly added to the bottle, resulting in initial PAA/H₂O₂ concentrations from 0/0 to 60/8.4 mg/L. The bottle contents were aerated with pre-humidified compressed air. Incubation was carried at room temperature (22±1°C). The following parameters were monitored over the incubation time: pH, DO, sCOD, ammonium, nitrite, and nitrate. Initial and final TSS and VSS were also measured for all batch series.

94

6.2.4 Microbial Community Analysis

Bacterial DNA extraction, quantification, and sequencing were performed following standard protocols as described in Chapter 3, Section 3.3.

6.2.5 Analytical Methods

pH, COD, N species, total solids (TS) and volatile solids (VS), total suspended solids (TSS) and volatile suspended solids (VSS), gas production and composition, VFAs, DO, total carbohydrates, total lipids, culture viability, and intracellular ROS were measured as described in Chapter 3, Section 3.1. PAA and H_2O_2 were measured by the DPD method as described in Chapter 3, Section 3.2.3. The fraction of heterotrophic bacteria, ammonia-oxidizing bacteria (AOB), nitrite-oxidizing bacteria (NOB) in the stock mixed heterotrophic/autotrophic culture was determined by using sodium azide (NaN_3) and allylthiourea (ATU) to inhibit AOB and NOB, respectively, and then measuring oxygen uptake rates as previously described (Surmacz-Gorska et al., 1996).

6.3 Results and Discussion

6.3.1 Bioreactors Performance

Operation of the three reactors (R1, R2, and R3) lasted for 166 d (Figure 6.1), divided into four phases (Section 6.2.2). Throughout the entire operation, all three reactors were fed with DAF wastewater every 2 d, while R2 and R3 received H_2O_2 or PAA solution, respectively, added to the feed 40 min ahead of feeding (Phase II), or directly added to the reactors after feeding with DAF wastewater (Phase III).

6.3.1.1 Phase I

During Phase I (40 d; twenty 2-d feeding cycles), all three reactors reached stable and similar performance. The mean pH and DO in the three reactors ranged from 8.1 to 8.4 and from 8.0 to 8.2 mg/L, respectively. At 40 d of operation (end of Phase I), the VSS concentration was comparable across the three reactors, ranging from 2.00 to 2.08 g/L (Figure 6.2). The mean extent of soluble COD removal was not significantly different among all three reactors (93.2±1.5%; $p > 0.05$) (Table 6.2). The initial ammonium removal rate (ARR) was also not significantly different among all three reactors (28.3±0.8 mg N/L-d; $p > 0.05$) at the end of Phase I (Table 6.3). It should be noted that the reported ARR is the net result of three simultaneous processes: organic matter degradation leading to ammonification, ammonium uptake due to microbial growth, and ammonium oxidation to nitrite. Nitrite levels in all three reactors were always below 0.5 mg N/L during Phase I. Because nitrite was simultaneously produced from ammonium and oxidized to nitrate, the rate of nitrate production indirectly reflects the nitrite oxidation rate. The mean nitrate production rate (NPR) across all three reactors was 62.1±3.3 mg N/L-d during Phase I. Overall, the performance of the three reactors was stable and similar during Phase I.

6.3.1.2 Phase II

During Phase II (day 40 to 94; twenty seven 2-d feeding cycles), the performance of the three reactors was evaluated at five, gradually increased H_2O_2 and PAA levels (0.7 to 8.4 mg H_2O_2/L; 5 to 60 mg PAA/L), both added to the DAF wastewater prior to feeding (indirect addition). The mean pH and DO concentration in the three reactors were

8 - 8.2 and 7.8 - 8.1 mg/L, respectively. At the end of Phase II, the VSS concentration in R1, R2, and R3 was 2.13±0.13, 2.02±0.04, and 1.79±0.11 g/L. Compared to the end of Phase I, the VSS concentration in both R1 and R2 was similar, but decreased by ca. 14% in R3.

The extent of sCOD removal and the initial, net ARR ranged from 92 to 97% and from 30 to 35 mg N/L-d across all three reactors during Phase II, respectively; the ARR was not significantly different ($p > 0.05$) (Tables 6.2 and 6.3). Nitrite concentrations were below 0.5 mg N/L in all three reactors throughout Phase II. Along with the decrease in ammonium, nitrate increased almost linearly (Figure 6.3B). The NPR ranged from 58.8 to 63.9 mg N/L-d across all three reactors and was not significantly different ($p > 0.05$) (Table 6.3). Taken all together, indirect addition of H_2O_2 and/or PAA solution at the above-stated concentration range did not significantly affect organic matter degradation and nitrification.

6.3.1.3 Phase III

During Phase III (day 94 to 160; twenty five to twenty seven feeding cycles), H_2O_2 and PAA/H_2O_2 were added directly to R2 and R3, respectively, after feeding with DAF wastewater (Figure 6.4A). H_2O_2 and PAA were not detected in R2 and R3 after feeding, a result of fast decomposition in the complex matrix of the reactors' feed and contents. The pH in R2 immediately upon H_2O_2 addition ranged from 7.5 to 7.8 as the H_2O_2 dose increased from 0.7 to 27 mg/L. The pH in R3 immediately upon PAA addition varied from 7.5 to 6.8 as the PAA/H_2O_2 dose increased from 5/0.7 to 60/8.4 mg/L. It should be noted that the above-mentioned pH values are over an order of magnitude

lower than the PAA pK_a value of 8.2 (Luukkonen and Pehkonen, 2017). Thus, for the short time PAA lasted in the culture (less than 15 min at a dose of 60 mg PAA/L), PAA existed in its un-dissociated form (CH_3COOOH), which is considered to be the most effective form in terms of its biocidal activity (Luukkonen and Pehkonen, 2017; McFadden et al., 2017). The DO was maintained at 7.8 to 8.1 mg/L in both R2 and R3. The sCOD removal in R1 (control) ranged from 92.3 to 96.7%, comparable to that during Phase I and II (Table 6.2). The sCOD removal in R2 varied from 92.6 to 99.6% up to 8.4 mg H_2O_2/L, then decreased to between 86.9 and 87.5% at 27 mg H_2O_2/L. The sCOD removal in R3 varied from 92.2 to 98.8% up to 40/5.6 mg /L PAA/H_2O_2, then decreased to as low as 88.0% at 60/8.4 mg/L PAA/H_2O_2 (4th feeding cycle; Table 6.2). Thus, given sCOD removal in R2 was not impacted by 8.4 mg/L H_2O_2, the lower sCOD removal in R3 at 60/8.4 mg /L PAA/H_2O_2 is attributed to PAA or PAA in combination with H_2O_2 rather than to H_2O_2. In a previous study, wet oxidation of a high strength pharmaceutical wastewater using H_2O_2 resulted in decreased COD as the H_2O_2 concentration increased (Zeng et al., 2017).

Table 6.3 summarizes the initial ARR at different stages of Phase III. The relative ARR (RARR; i.e., ARR rates in R2 and R3 normalized to that in R1) are shown in Fig. 1B. The RARR in R2 varied from 0.98 to 1.12 up to 8.4 mg H_2O_2/L and gradually decreased to as low as 0.43 by the end of the 4th feeding cycle with 27 mg H_2O_2/L. The RARR in R3 varied between 0.82 and 1.12 up to the first feeding with 40/5.6 mg/L PAA/H_2O_2, but declined to ca. 0.36 by the end of the 4th feeding cycle with 60/8.4 mg/L PAA/H_2O_2. Given that H_2O_2 up to 8.4 mg/L did not negatively affect the ARR in R2, the observed decrease of ARR in R3 at 40/5.6 and even more at 60/8.4 mg/L PAA/H_2O_2 is

predominantly attributed to PAA or the combination of PAA and H_2O_2. Therefore, directly added PAA solution negatively affected ARR and the impact is predominantly attributed to PAA. Pedersen et al. (2009) reported that the ARR in recirculating aquaculture systems was not affected by 1 mg PAA/L, but decreased significantly at 2 and 3 mg PAA/L. In addition, Pedersen et al. (2012) reported that 64 mg H_2O_2/L significantly decreased the ARR from 0.60 to 0.13 g N/m^2-d by a biofilter in a commercial recirculating aquaculture system.

Nitrite in R1 was below 0.5 mg N/L throughout Phase III (Table 6.3). In contrast, the nitrite concentration in R2 increased with increased concentration of directly added H_2O_2, reaching ca. 23 mg N/L after the 4th direct addition of 27 mg H_2O_2/L (Figure 6.3H; Table 6.3), which represents ca. 50% of the feed ammonium-N concentration. The nitrite concentration in R3 increased dramatically with increased concentration of direct addition of PAA solution, reaching ca. 42 mg N/L after the 4th direct addition with 60/8.4 mg/L PAA/H_2O_2 (Figure 6.3G; Table 6.3), which represents ca. 90% of the feed ammonium-N concentration. Therefore, although 8.4 mg/L H_2O_2 did not affect ammonium removal, it affected nitrite removal. However, the effect of PAA on nitrite oxidation was much more pronounced than that of H_2O_2. Although in the study of Pedersen et al. (2012) 64 mg/L of H_2O_2 only marginally affected nitrite oxidation, it resulted in significant sCOD release in the biofilter as a result of organic matter degradation/solubilization. Given that H_2O_2 reacts with organic matter, which quenches its oxidative effect, combined with the fact that the biofilter biomass was attached as opposed to suspended, the negative impact of H_2O_2 on biofilter nitrification was minimal compared to that observed in the present study. Suurnakki et al. (2020) also reported that

the nitrite oxidation rate in a biofilter at recirculating aquaculture systems was not affected by 1.1 mg PAA/L applied once per week, but decreased significantly when PAA was applied two and four times per week, concluding that the impact of PAA on nitrite oxidation was greater as the PAA application frequency increased.

The relative NPR (RNPR; i.e., NPR rates in R2 and R3 normalized to that in R1) are shown in Fig. 6.4D. Similar to the effect of H_2O_2 on RARR in R2, the RNPR in R2 varied from 0.9 to 1.1 up to 8.4 mg H_2O_2/L and gradually decreased to as low as 0.3 by the end of the 4th feeding cycle with 27 mg H_2O_2/L. The RNPR in R3 varied between 1.0 and 1.1 up to the first feeding with 40/5.6 mg/L PAA/H_2O_2 and then declined to ca. 0.2 by the end of the 4th feeding cycle with 60/8.4 mg/L PAA/H_2O_2. Given that H_2O_2 up to 8.4 mg/L did not inhibit the NPR in R2, the observed decrease of NPR in R3 at 40/5.6 and even more at 60/8.4 mg/L PAA/H_2O_2 is predominantly attributed to PAA or the combination of PAA and H_2O_2.

At the end of direct addition of 5.6 mg/L H_2O_2 in R2 and 40/5.6 mg/L PAA/H_2O_2 in R3 during Phase III, the concentration of TSS and VSS in all three reactors was close to that at the end of Phase II (Figure 6.2). Thus, direct addition of H_2O_2 to R2 up to 5.6 mg/L and PAA solution to R3 up to 40/5.6 mg/L PAA/H_2O_2 did not affect the biomass concentration. However, by the end of Phase III, the VSS concentration decreased by ca. 6, 7 and 20% in R1, R2 and R3, respectively, compared to the VSS at the mid of Phase III. The higher VSS loss in R3 is attributed to solids solubilization as well as bacteria lysis, primarily caused by PAA. In the study of Shang and Hou (2009), when municipal sludge was pretreated with PAA before anaerobic digestion, the TSS concentration decreased by 20 to 28% at a PAA dose between 127 and 3059 mg/L, respectively.

Suurnakki et al. (2020) reported that the TSS concentration of biofilters in recirculating aquaculture systems decreased by ca. 33 to 45% after 1.1 mg PAA/L was directly applied four times a week.

6.3.1.4 Phase IV

During Phase IV (i.e., recovery phase feeding DAF wastewater only; day 160 to 166), sCOD removal in R2 and R3 increased from the first to the third feeding and reached a value comparable to that of R1 (Table 6.2). The RARR in both R2 and R3 gradually increased and reached 1.02 and 1.01, respectively, by the end of the 3rd feeding cycle (Table 6.3; Figure 4B). Nitrite concentration in both R2 and R3 decreased to below 0.5 mg N/L after the 3rd feeding cycle with H_2O_2- and PAA-free feed (Figure 6.3I). The RNPR in both R2 and R3 gradually increased and reached 1.0 and 1.1, respectively, by the end of the 3rd feeding cycle (Figure 6.4D). Thus, fast recovery of organic matter degradation and complete nitrification was restored in both R2 and R3 when direct addition of H_2O_2 and PAA solution ended.

Table 6.2. Extent of soluble COD removal (%) by the three aerobic reactors in Phase I through IV.

Phase	Feeding Cycle[a]	Initial H_2O_2/PAA-H_2O_2 (mg/L)	R1	R2	R3
I[b]	1-20	--/--[b]	93.1±0.1[c]	93.3±1.4	93.3±0.8
II[d]	1	0.7/5-0.7	91.7±1.2	94.1±0.0	90.9±0.9
	1	1.4/10-1.4	90.5±0.4	93.6±0.4	91.9±0.3
	1	2.8/20-2.8	93.5±1.1	93.3±1.2	92.6±0.7
	1	5.6/40-5.6	93.6±0.5	93.4±1.2	92.1±0.9
	1	8.4/60-8.4	95.1±0.9	95.0±0.7	94.6±0.7
III[e]	2	0.7/5-0.7	92.3±0.5	93.8±0.4	94.3±0.2
	3	0.7/5-0.7	93.8±0.4	94.6±0.7	94.6±0.5
	1	1.4/10-1.4	92.8±0.9	92.6±0.4	92.2±0.6
	6	1.4/10-1.4	93.3±0.2	94.4±0.3	94.4±0.6
	1	2.8/20-2.8	95.5±0.4	98.7±0.3	98.3±0.4
	6	2.8/20-2.8	95.6±0.4	99.1±0.2	98.8±0.3
	1	5.6/40-5.6	94.5±0.2	96.7±0.4	97.3±0.6
	6	5.6/40-5.6	95.2±0.4	99.6±0.0	97.1±0.2
	1	8.4/60-8.4	96.4±0.4	99.4±0.2	95.0±0.2
	6	8.4/--	96.3±0.1	99.4±0.0	--
	1	27/--	95.6±0.1	91.4±0.3	--
	2	27/--	96.7±0.2	86.9±1.1	--
	3	27/--	--	87.2±1.0	--
	4	27/--	--	87.5±1.8	--
	2	--/60-8.4	--	--	89.1±0.1
	3	--/60-8.4	--	--	88.8±0.3
	4	--/60-8.4	--	--	88.0±0.2
IV[f]	1	--	96.0±0.1	91.2±0.6	89.9±0.4
	2	--	95.6±0.2	92.3±0.9	92.9±0.5
	3	--	96.7±0.1	95.3±0.3	95.1±0.1

[a] Feeding cycle at corresponding H_2O_2 and/or PAA concentration; [b] Control phase without H_2O_2 and/or PAA solution addition (duration, 40 d); [c] Mean ± standard deviation; [d] Indirect addition of H_2O_2 and/or PAA solution (duration, 54 d); [e] Direct addition of H_2O_2 and/or PAA solution (duration, 90 d); [f] Recovery phase without H_2O_2 and/or PAA solution addition (duration, 6 d).

Table 6.3. Initial ammonia removal rates (ARR), observed maximum nitrite levels, and nitrate production rates (NPR) in the three aerobic reactors in Phase I through IV.

Phase	Feeding Cycle[a]	Initial H_2O_2/ PAA-H_2O_2 (mg/L)	ARR (mg N/L-d)			Maximum Nitrite Level (mg N/L)		
			R1	R2	R3	R1	R2	R3
I[b]	1-20	--[b]	27.8±0.3[c]	29.0±0.3	28.2±0.5	ND[d]	ND	ND
II[e]	1	0.7/5-0.7	29.4±0.1	29.8±0.1	28.8±0.1	ND	ND	ND
	1	1.4/10-1.4	29.4±0.2	29.9±0.3	28.3±0.2	ND	ND	ND
	1	2.8/20-2.8	28.0±0.6	34.3±0.2	34.1±0.4	ND	ND	ND
	1	5.6/40-5.6	27.6±0.6	31.3±0.1	32.3±0.1	ND	ND	ND
	1	8.4/60-8.4	33.0±0.3	35.9±0.1	35.8±0.6	ND	ND	ND
III[f]	2	0.7/5-0.7	33.0±0.2	37.2±0.3	37.1±0.2	ND	ND	ND
	3	0.7/5-0.7	33.8±0.4	34.2±0.2	36.4±0.5	ND	ND	ND
	1	1.4/10-1.4	40.8±0.4	40.0±0.1	44.0±0.1	ND	ND	2.8
	6	1.4/10-1.4	41.3±0.2	41.0±1.4	41.3±0.9	ND	ND	2.3
	1	2.8/20-2.8	39.8±0.7	46.6±0.3	44.3±0.2	ND	3.4	3.7
	6	2.8/20-2.8	44.5±0.7	44.2±1.0	42.5±0.3	ND	4.3	3.8
	1	5.6/40-5.6	45.8±0.3	51.9±2.4	42.4±0.4	ND	5.7	33,3
	6	5.6/40-5.6	50.4±0.3	43.8±0.1	28.6±0.3	ND	9.1	32.4
	1	8.4/60-8.4	47.5±0.4	38.8±0.7	26.7±0.1	ND	15.8	32.3
	6	8.4/--	43.1±0.1	41.1±0.1	--	ND	9.7	--
	1	27/--	43.3±0.1	24.7±0.3	--	ND	20.9	--
	2	27/--	46.7±0.1	18.0±0.0	--	ND	22.3	--
	3	27/--	--	17.2±0.0	--	--	20.3	--
	4	27/--	--	17.1±0.3	--	--	23.2	--
	2	--/60-8.4	--	--	16.1±0.1	--	--	40.7
	3	--/60-8.4	--	--	14.7±0.0	--	--	43.1
	4	--/60-8.4	--	--	14.2±0.1	--	--	41.6
IV[g]	1	--	42.7±0.2	36.6±0.1	31.3±0.1	ND	9.5	14.6
	2	--	42.0±0.2	39.7±0.1	38.9±0.1	ND	3.3	4.2
	3	--	41.0±0.2	41.9±0.2	41.4±0.1	ND	ND	ND

[a] Feeding cycle at corresponding H_2O_2 and/or PAA concentration; [b] Control phase without H_2O_2 and/or PAA solution addition (duration, 40 d); [c] Mean ± standard deviation; [d] ND, not detected; [e] Indirect addition of H_2O_2 and/or PAA solution (duration, 54 d); [f] Direct addition of H_2O_2 and/or PAA solution (duration, 90 d); [g] Recovery phase without H_2O_2 and/or PAA solution addition (duration, 6 d).

Table 6.3 (Continued). Initial ammonia removal rates (ARR), observed maximum nitrite levels, and nitrate production rates (NPR) in the three aerobic reactors in Phase I through IV.

Phase	Feeding Cycle[a]	Initial H_2O_2/ PAA-H_2O_2 (mg/L)	NPR (mg N/L-d)		
			R1	R2	R3
I[b]	1-20	--[b]	63.0±0.9	59.8±1.0	63.6±1.7
II[e]	1	0.7/5-0.7	63.4±0.7	65.9±1.4	63.9±1.4
	1	1.4/10-1.4	60.5±0.7	60.0±1.5	62.1±1.5
	1	2.8/20-2.8	58.8±1.7	61.1±0.4	62.7±1.9
	1	5.6/40-5.6	63.2±1.1	62.2±2.5	61.8±0.9
	1	8.4/60-8.4	62.0±2.8	60.3±4.4	61.2±0.0
III[f]	2	0.7/5-0.7	63.8±1.4	65.2±0.6	68.4±1.7
	3	0.7/5-0.7	60.9±1.3	68.4±1.7	66.0±1.7
	1	1.4/10-1.4	58.3±1.9	66.0±5.1	64.8±3.4
	6	1.4/10-1.4	61.9±2.1	67.5±2.1	60.0±0.7
	1	2.8/20-2.8	62.2±1.0	61.2±0.3	60.9±1.3
	6	2.8/20-2.8	57.6±0.5	69.4±1.4	60.0±2.7
	1	5.6/40-5.6	63.0±1.7	65.0±0.3	60.8±3.4
	6	5.6/40-5.6	61.8±1.0	58.3±0.4	39.6±0.0
	1	8.4/60-8.4	61.4±0.9	64.1±1.0	21.7±0.8
	6	8.4/--	60.9±0.9	63.0±0.1	--
	1	27/--	60.9±0.5	39.0±0.2	--
	2	27/--	62.6±2.7	28.5±0.0	--
	3	27/--	--	20.3±0.3	--
	4	27/--	--	25.8±0.9	--
	2	--/60-8.4	--	--	14.7±0.1
	3	--/60-8.4	--	--	13.4±0.5
	4	--/60-8.4	--	--	14.1±0.2
IV[g]	1	--	96.0±	55.2±0.0	24.5±1.1
	2	--	95.6±	63.8±2.3	56.4±2.8
	3	--	96.7±	63.3±2.7	67.7±0.7

[a] Feeding cycle at corresponding H_2O_2 and/or PAA concentration; [b] Control phase without H_2O_2 and/or PAA solution addition (duration, 40 d); [c] Mean ± standard deviation; [d] ND, not detected; [e] Indirect addition of H_2O_2 and/or PAA solution (duration, 54 d); [f] Direct addition of H_2O_2 and/or PAA solution (duration, 90 d); [g] Recovery phase without H_2O_2 and/or PAA solution addition (duration, 6 d).
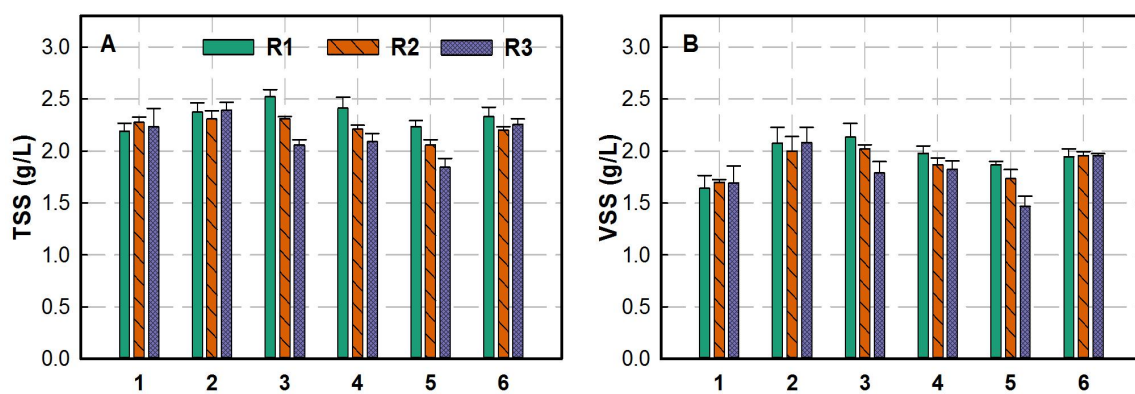
Figure 6.2. TSS (A) and VSS (B) concentration in the three aerobic reactors at different stages during the long-term operation (Phase I through IV). Condition: 1, Initial; 2, End of Phase I; 3, End of Phase II; 4, Phase III, end of 5.6/40 mg/L H_2O_2/PAA; 5, Phase III, end of 27/60 mg/L H_2O_2/PAA; 6, End of Phase IV (recovery). Error bars are standard deviations.
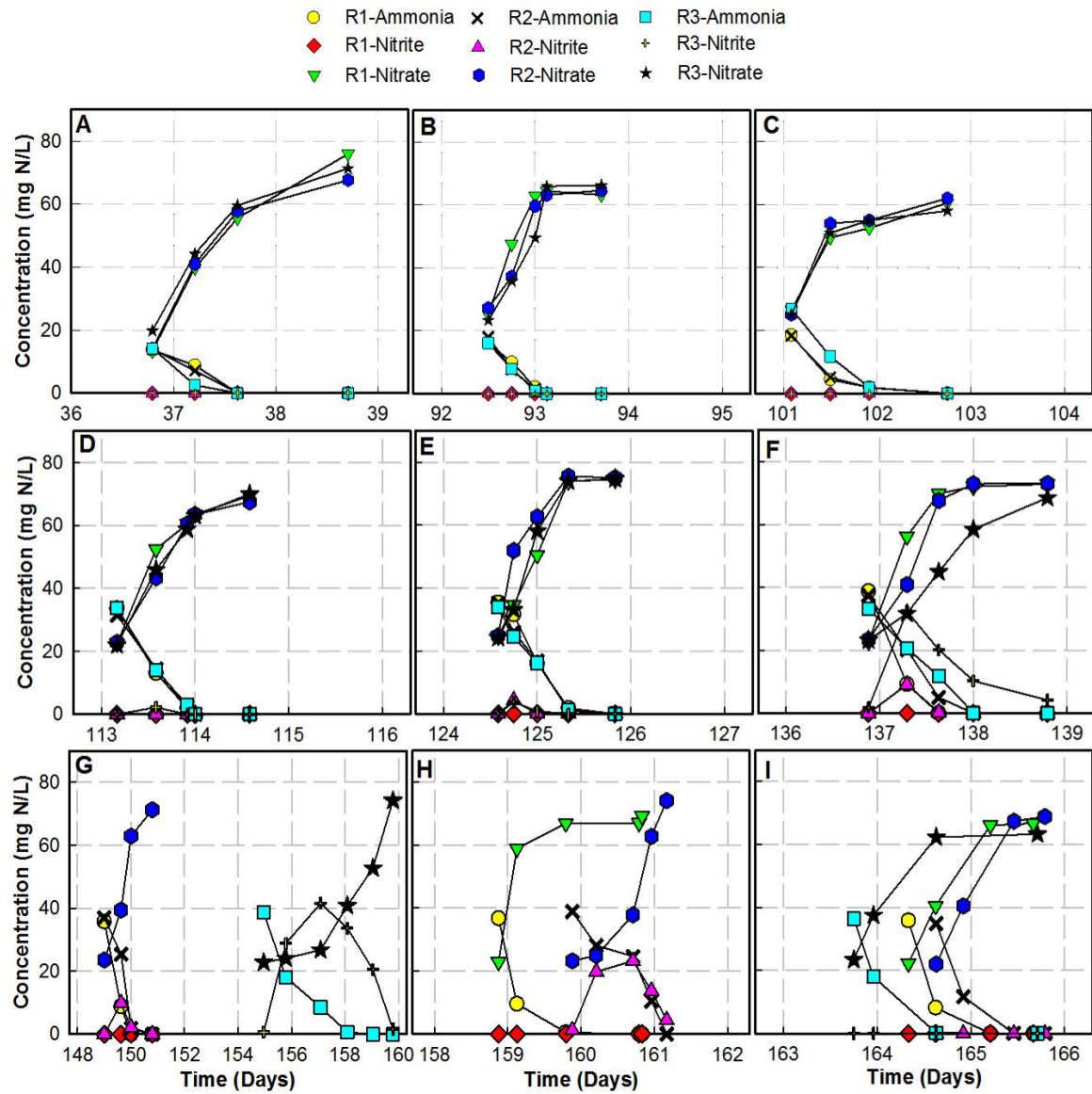
Figure 6.3. Time-trend of ammonium-N, nitrite-N, and nitrate-N in the three reactors at the end of Phase I (A), Phase II (B), Phase III last 5/0.7 (C), 10/1.4 (D), 20/2.8 (E), 40/5.6 (F), and 60/8.4 (G) mg/L PAA/H$_2$O$_2$ addition; last 27 mg/L H$_2$O$_2$ (H) addition; and Phase IV (I).
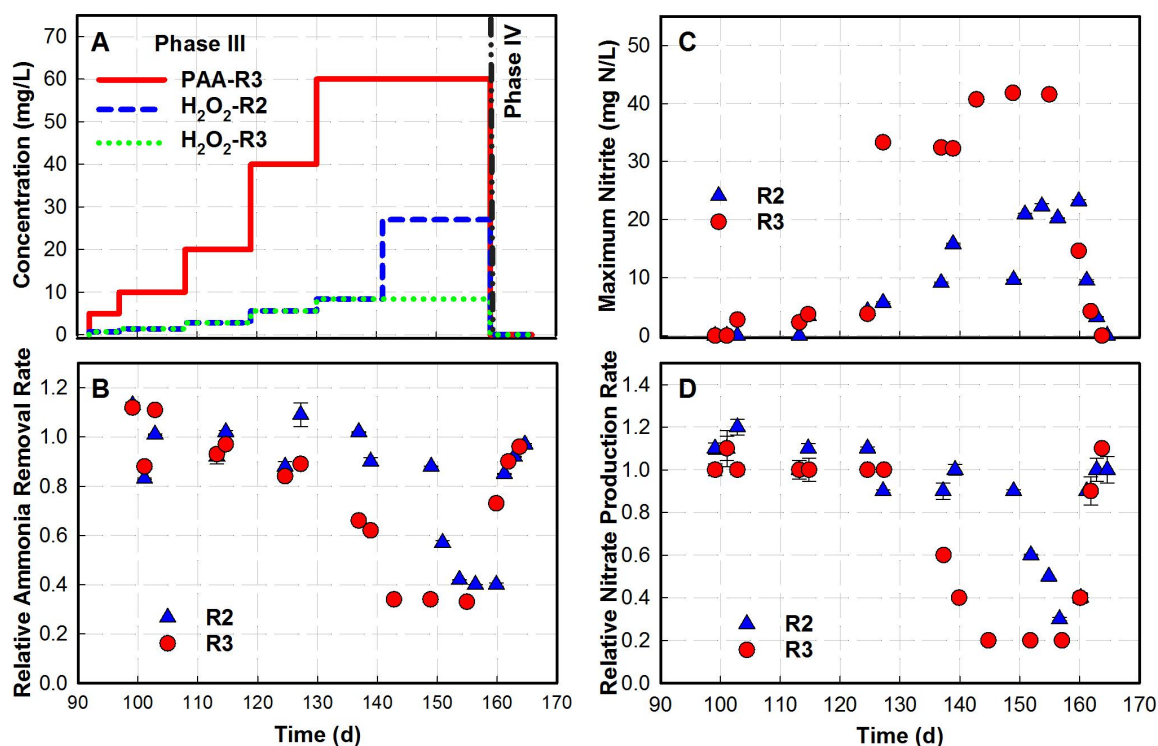
Figure 6. 4. Initial, nominal reactor H₂O₂ and PAA concentration in Phase III (direct H₂O₂ and PAA solution addition) and IV (recovery) in R2 and R3 during the long-term operation (A); Relative ammonium removal rate (B); Maximum observed nitrite concentration (C); and Relative nitrate production rate (D). Error bars are standard deviations.

6.3.2 Short-term Aerobic Batch Assays

Table 6.4 summarizes the extent of sCOD removal, initial ARR, maximum observed nitrite level, and NPR during the short-term batch assays conducted over time with mixed liquor from the long-term R1 reactor, then directly amended with PAA solution up to 60/8.4 mg/L PAA/H_2O_2. The pH, DO, soluble COD, and nitrogen species trend during the short-term batch assays is shown in Figure 6.5. The DO level immediately after feeding was low as the DO concentration in the DAF feed over the storage was low, but increased with increased PAA solution dose as a result of DO released due to PAA and H_2O_2 decomposition; then, the DO level rapidly increased as a result of aeration with compressed air (Figure 6.5B). The time-trend of sCOD (Figure 6.5C) and sCOD removal (Table 6.4) were comparable among all batch series and similar to those achieved by the long-term R3 reactor upon the first direct addition of 60/8.4 mg/L PAA/H_2O_2. However, slightly lower sCOD removal (88%; Table 6.2) was observed during the last (fourth) feeding cycle of R3 with 60/8.4 mg/L PAA/H_2O_2, which is attributed to the long-term operation of R3 with addition of the PAA solution. The TSS and VSS in the batch series with 5/0.7 and 10/1.4 mg/L initial PAA/H_2O_2 were comparable to those in the control, while the VSS in series with 20/2.8, 40/5.6 and 60/8.4 mg/L initial PAA/H_2O_2 direct addition was 10, 18 and 29% lower than in the control, respectively, suggesting that PAA/$H_2O_2 \geq$ 20/2.8 mg/L caused cell lysis (Figure 6.6).

Complete ammonium removal was achieved within 30 h of incubation in all test series (Figure 6.5D) and the ARR ranged from 33.4 to 46.4 mg N/L-d without any particular trend relative to the added PAA solution level (Table 6.4). The specific ARR (ARR normalized to the mean VSS of each series) ranged from 18.1 to 26.3 mg N/g

VSS-d. In contrast, the specific ARR in the long-term R3 gradually decreased from 20.1 to 8.6 mg N/g VSS-d with direct addition of 5/0.7 to 60/8.4 mg/L PAA/H_2O_2. It is noteworthy that although the VSS in both the batch assay series and the long-term R3 decreased as the directly added PAA solution level increased (Figure 6.6), the observed decrease in the specific ARR in the long-term R3 was more than the decrease in its VSS concentration. Thus, over the long-term operation of R3 with directly added, increased PAA and H_2O_2 levels, its ammonium oxidation rate decreased, showing an increasingly negative effect of the PAA solution on the reactor's performance.

Transient nitrite concentrations below 0.5 mg N/L were observed in all batch series with initial $PAA/H_2O_2 \leq 20/2.8$ mg/L, while nitrite reached ca. 20 and 28 mg N/L in the series amended with 40/5.6 and 60/8.4 mg/L initial PAA/H_2O_2, respectively (Figure 6.5E; Table 6.4). Complete nitrite removal was achieved in all batch series within 50 h of incubation (Fig. 2E). In contrast, the maximum observed nitrite levels in the long-term R3 after the first feeding with 40/5.6 and 60/8.4 mg/L PAA/H_2O_2 were ca. 60% and 30% higher, respectively, than in the batch series at the same initial PAA/H_2O_2 concentrations (Tables 6.3 and 6.4). The NPR ranged from 63 to 74 mg N/L-d in series with PAA/H_2O_2 up to 40/5.6 mg/L, without any particular trend relative to the initial PAA solution level, while was ca. 39 mg N/L-d in series with 60/8.4 mg/L PAA/H_2O_2, a decrease by 38 to 47% compared to the other batch series (Table 6.4). As discussed in Section 6.3.1, the NPR in the long-term R3 gradually decreased from 66.0 to 14.1 mg N/L-d with direct addition of 5/0.7 to 60/8.4 mg/L PAA/H_2O_2 (Table 6.3). Thus, over the long-term operation of R3 with directly added, increased PAA and H_2O_2 levels, NPR increasingly decreased. Similar to the specific ARR, the decrease in the specific NPR in

the long-term R3 by the end of Phase III was much higher than that observed with the

batch series with direct addition of 60/8.4 mg/L PAA/H_2O_2, suggesting that the observed

decrease of the NPR in R3 over its long-term operation was higher than the decrease in

its VSS concentration. Therefore, the nitrification activity of the bioreactors declined

over time during the long-term operation with addition of PAA solution, indicating that

acclimation of the microbial community to the PAA solution did not take place. In

contrast to this observation, rapid microbial acclimation to benzalkonium chlorides

(BACs), common components in quaternary ammonium compounds (QACs) used as

sanitizers in poultry processing plants, was observed in a continuous-flow biological

nitrogen removal system while treating poultry processing DAF wastewater amended

with a mixture of BACs (Hajaya and Pavlostathis, 2012; 2013).

Table 6.4. Extent of soluble COD removal, initial ammonia removal rate (ARR), maximum observed nitrite level, and nitrate production rate (NPR) in batch assays conducted at a range of PAA solution levels using R1 mixed liquor.[a]

PAA/H_2O_2 (mg/L)	COD Removal (%)	ARR (mg N/L-d)	Maximum Nitrite Level (mg N/L)	NPR (mg N/L-d)
0/0	93.5±0.7[b]	33.4±0.3	ND[e]	69.2±2.8
5/0.7	93.5±0.3	33.4±0.9	ND	74.0±2.8
10/1.4	96.0±0.4	46.4±0.6	1.9	72.2±1.4
20/2.8	97.9±0.1	44.9±0.1	3.0	73.4±0.9
40/5.6	97.9±0.3	45.6±1.1	20.4	63.4±1.4
60/8.4	95.1±0.4	37.0±0.3	28.2	39.4±2.0

[a] Long-term R1 mixed liquor removed at the end of several feeding cycles, amended with PAA solution corresponding to PAA/H_2O_2 initial concentrations directly added to long-term R3 at different feeding cycles (Phase III).
[b] Mean ± standard deviation; [c] ND, not detected.
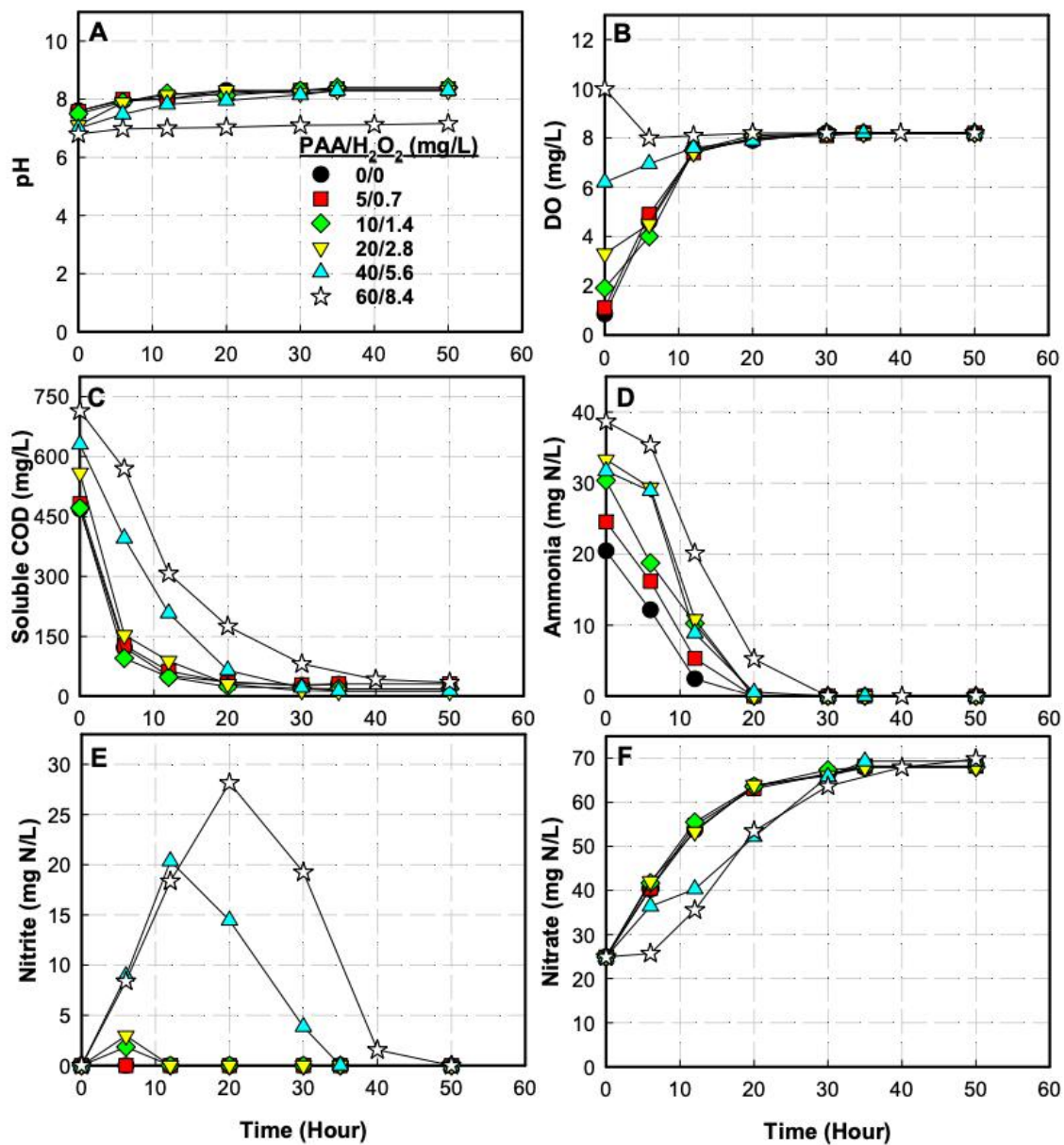
Figure 6.5. Time-trend of pH (A), dissolved oxygen (DO) (B), soluble COD (C), ammonia (D), nitrite (E), and nitrate (F) during the incubation of the batch assays conducted with R1 mixed liquor.
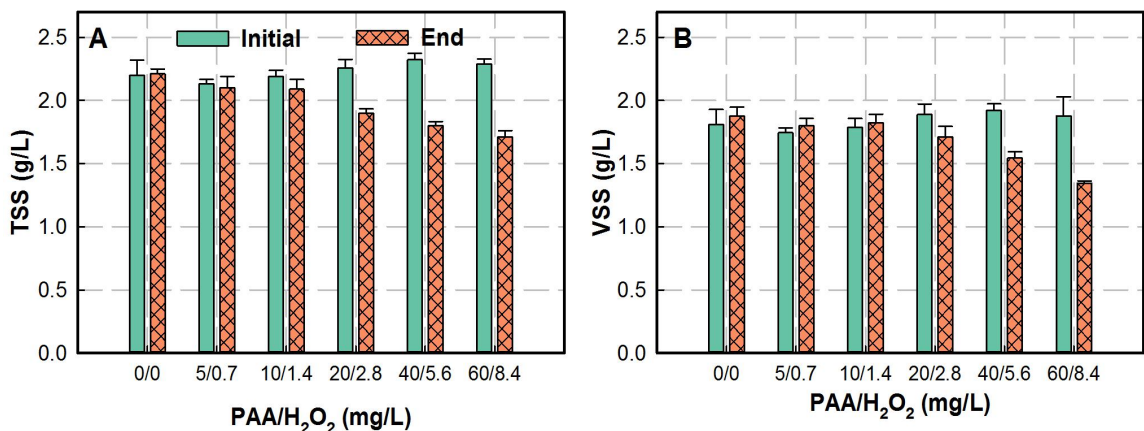
Figure 6.6. Initial and end of incubation TSS (A) and VSS (B) of batch assays conducted with R1 mixed culture amended with a range of initial PAA solution levels. Error bars are standard deviations.

6.3.3 Culture Viability

The viability (i.e., fraction of live cells) of the microbial communities in the three, long-term operated bioreactors was evaluated at the end of Phase II, III, and IV with results shown in Figure 6.7A. Culture viability in R1 (control) was relatively the same across the three phases, ranging from 85 to 87%. At the end of Phase II, culture viability in the three bioreactors was comparable, ranging from 86 to 88%. Thus, indirect addition of solutions up to 60/8.4 mg/L PAA/H_2O_2 and 8.4 mg H_2O_2/L did not impact culture viability. In contrast, viability in R2 and R3 at the end of Phase III was 8 and 22% lower than in R1, respectively. Thus, direct addition of PAA and/or H_2O_2 decreased culture viability; the PAA effect was much greater than that of H_2O_2. It should be emphasized that reported culture viability values refer to the entire mixed bacterial communities. Given that the fraction of the heterotrophic bacterial population was over 90% (Chapter 5, Section 5.2.1), the impact of PAA and/or H_2O_2 specifically on the nitrifier population size is difficult to determine. By the end of Phase III, the ARR, NPR, and culture viability in

112

R2 decreased by 60, 58, and 8% and in R3 decreased by 67, 77, and 22%, respectively. Thus, the long-term impact of H_2O_2 in R2 and PAA solution in R3 on nitrification is predominantly attributed to enzyme inhibition rather than loss of cell viability. At the end of Phase IV, culture viability in both R2 and R3 increased by 8 and 20 %, respectively, both reaching a level comparable to the mean value in R1 (ca. 86%), indicating that the impact on culture viability was fast reversed after direct addition of PAA and/or H_2O_2 ended. Thus, given that the ARR and NPR in both R2 and R3 increased rapidly during Phase IV and the increase was much more significant than the increase of culture viability, it is concluded that the impact of H_2O_2 and PAA on nitrification is predominantly attributed to their inhibitory effect on enzymes, such as ammonia monooxygenase and nitrite oxidoreductase, and secondarily on the loss of cell viability over the long-term operation.

In order to further evaluate culture viability in response to directly added PAA and H_2O_2, culture viability was measured by conducting a batch assay with R1 mixed liquor amended with a range of initial PAA solution or H_2O_2 levels, with results shown in Figure 6.7B. Compared to the control, culture viability slightly increased in the culture series amended with PAA solution at 5/0.7 to 20/2.8 mg/L PAA/H_2O_2, attributed to the positive effect of acetic acid in the PAA solution as well as that produced as a result of PAA decomposition. Thus, acetate compensated for the negative effect of PAA and H_2O_2 on culture viability. Compared to the control, culture viability in series directly amended with PAA solution at 40/5.6 and 60/8.4 mg/L PAA/H_2O_2 was lower by ca. 10 and 30%, respectively. Therefore, as the PAA/H_2O_2 concentration increased above 40/5.6 mg/L, the negative effect of PAA on culture viability could not be offset by the positive effect of

acetic acid. Culture viability in series amended with 5 to 60 mg/L H_2O_2 decreased by 2 to 20% compared to the control. Thus, direct addition of H_2O_2 also decreased culture viability, but the decrease was lower compared to PAA, especially at 60 mg/L. Lee et al. (2016) demonstrated that cell membrane integrity was significantly and increasingly compromised by 5,000 mg/L PAA for contact time from 15 to 120 s. Wang et al. (2020) demonstrated that cell membrane integrity of *Morganella psychrotolerans* was increasingly compromised by 20 to 80 mg/L PAA for a 5-min contact time. Zhang et al. (2019) showed holes formed in the center of *E. coli* TOP10p cells with 8 to 60 mg/L PAA treatment for 15 min contact time.

Direct addition of 60/8.4 mg/L PAA/H_2O_2 resulted in comparable decrease of culture viability in the long-term R3 and in the batch series (22% vs. 30%), but ARR and NPR decreased more in the long-term R3 than in the batch series (64% vs. 18% and 80% vs. 45%, respectively). Thus, inhibition of nitrification-related enzymes worsened over the long-term operation of R3 with direct addition of PAA solution.
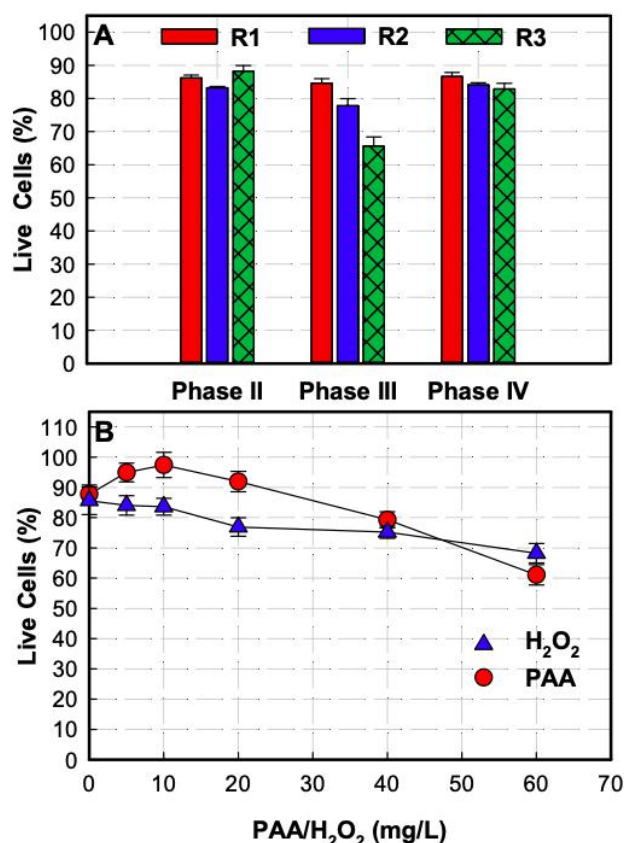
Figure 6.7. Fraction of live cells in the three long-term operated aerobic reactors measured at the end of Phase II, III, and IV (A); Fraction of live cells in R1 mixed liquor amended directly with PAA solution or H$_2$O$_2$ at an initial concentration range from 0 to 60 mg/L (B). Error bars are standard deviations.

6.3.4 Intracellular ROS

Intracellular ROS of the microbial communities in the three, long-term operated bioreactors was evaluated at the end of Phase II, III, and IV with results shown in Figure 6.8A. At the end of Phase II, intracellular ROS in R2 and R3 cultures was 6 and 19% lower than in R1 (control), respectively, suggesting indirect addition of PAA and/or H$_2$O$_2$ either inhibited intracellular ROS production or induced production of ROS quenching enzymes (e.g., catalase and superoxidase) (Imlay, 2008), or both. At the end of Phase III, the intracellular ROS in R2 and R3 cultures was 13% lower and 8% higher than in R1,

respectively, suggesting that direct addition of 27 mg H_2O_2/L did not cause excess cell oxidative stress to the R2 microbial community, but direct addition of 60 mg PAA/L caused a slight increase in cell oxidative stress to the R3 microbial community (Fig. 6.8A). Overall, H_2O_2 and PAA did not significantly affect the intracellular ROS of the H_2O_2-exposed (R2) and PAA/H_2O_2-exposed (R3) communities over the long-term operation of these reactors. In contrast, nitrification was affected by the long-term addition of H_2O_2 and even more by the addition of PAA (Section 6.3.2) to a higher extent than intracellular ROS. Thus, intracellular ROS did not affect nitrification rates. As discussed in Section 6.3.3, the decrease in nitrification rates over the long-term operation with addition of H_2O_2 and PAA/H_2O_2 to R2 and R3 was predominantly the result of enzyme inhibition.

In order to further evaluate intracellular ROS in response to added PAA and H_2O_2, intracellular ROS was measured in a batch assay conducted with R1 mixed liquor and direct addition of PAA or H_2O_2 up to 60 mg/L each with results shown in Figure 6.8.B. The relative intracellular ROS of the long-term R1 culture directly exposed to H_2O_2 decreased as the H_2O_2 concentration increased reaching the lowest value of 0.13 at 20 mg/L H_2O_2, then gradually increased to 0.94 at 60 mg/L H_2O_2. In contrast, the relative intracellular ROS of the long-term R1 culture directly exposed to PAA solution decreased as the PAA concentration increased, reaching the lowest value of 0.60 at 10/1.4 mg/L PAA/H_2O_2, then sharply increased to 2.2 at 60/8.4 mg/L PAA/H_2O_2. Overall, the R1 culture intracellular ROS was much higher in response to the PAA solution than to H_2O_2.

The decrease of intracellular ROS in R1 culture upon addition of low concentrations of H_2O_2 and PAA solution is attributed to two factors: a) increased activity

of intracellular enzymes (e.g., catalase, peroxides, and superoxidase); and b) no or minor extracellular ROS diffusion into the cells. The increase in intracellular ROS with increased concentration of H_2O_2 or PAA solution is attributed to extracellular PAA and H_2O_2 diffusion into the cells as well as other ROS produced intracellularly by them, such as $OH^{\bullet}$, a higher extent of cell membrane damage or both, while ROS-degrading enzymes could not quench them. Most ROS have very short half-life (10^{-6} s for $O_2^{\bullet-}$ and 10^{-9} s for $OH^{\bullet}$; Dickinson and Change, 2012); thus, when formed extracellularly will not last long enough to diffuse into the cell. However, the half-life of H_2O_2 and PAA in the culture used in this study was 4 to 5 min. H_2O_2 diffuses into cells across cell membrane as previously demonstrated (Seaver and Imlay, 2001). PAA may also diffuse into cells. Fast PAA diffusion into Gram-negative *Escherichia coli* and Gram-positive *Enterococcus durans* and *Staphylococcus epidermidis*, resulting in intracellular oxidative stress, was recently demonstrated by Zhang et al. (2020). It is noteworthy that although the intracellular ROS in the batch series of R1 culture directly amended with 60/8.4 mg/L PAA/H_2O_2 increased by 2.2-fold compared to the control, the ARR was comparable to that of the control; thus, the increased intracellular ROS did not result in a decrease of ARR. The relative intracellular ROS of the R1 culture exposed to 60/8.4 mg/L PAA/H_2O_2 was much higher than that of the long-term R3 culture at the end of Phase III (2.2 vs. 1.08), suggesting that the capacity of the long-term R3 culture to manage cell oxidative stress increased during the long-term operation with PAA addition. Thus, the observed significant decrease in nitrification rates (both ARR and NPR) over the long-term operation of R3 with addition of PAA solution was not related to intracellular ROS.
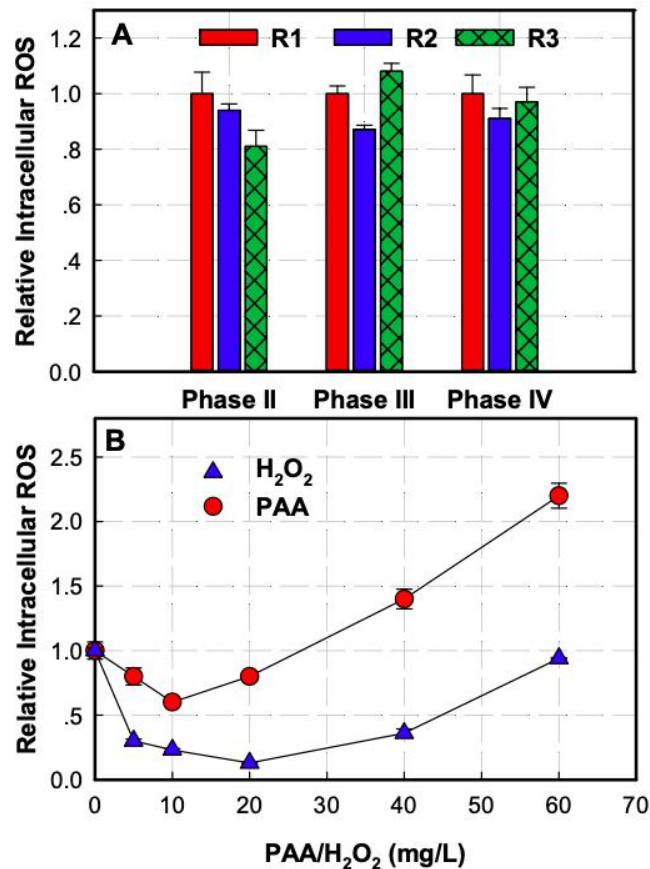
Figure 6.8. Intracellular reactive oxygen species (ROS) relative to R1 (control) in the three aerobic reactors at the end of Phase II, III and IV during the long-term operation (A); Relative intracellular ROS in R1 culture directly amended with PAA or H_2O_2 solution at an initial concentration range from 0 to 60 mg/L (B). Error bars are standard deviations.

6.3.5 Microbial Community Structure

Based on the Shannon index, the microbial community diversity in R1 (control) remained relatively constant throughout the 166-d of operation. Compared to R1, the diversity of the R2 and R3 communities was slightly higher at the end of Phase II (indirect addition of H_2O_2 and PAA solution), but decreased at the end of Phase III (direct addition of H_2O_2 and PAA solution); the decrease was significantly higher in the PAA/H_2O_2 amended reactor (R3) than the H_2O_2 amended reactor (R2) (Table 6.5). Based on Principle Component Analysis (PCA) at order level, from the end of Phase II to the

118

end of Phase III (94 to 160 d), the microbial communities shifted significantly in the three reactors (Figure 6.9). On PC1 (57.42%), the communities shifted from the end of Phase II to the end of Phase III, especially in R1, indicating that the shifts on PC1 were attributed to the long-term operation of the reactors under completely aerobic conditions compared to the stock mixed culture which was subjected to alternating aerobic/anoxic/aerobic phases weekly. On PC2 (35.72%), at the end of Phase II, the R2 and R3 communities were clustered closely and away from the R1 community, indicating that indirect addition of H_2O_2 and PAA solutions resulted in a similar shift of the R2 and R3 communities, respectively, compared to the R1 community. Furthermore, on PC2 (35.72%), the R1 community did not shift from the end of Phase II to the end of Phase III; however, the R2 and R3 communities shifted significantly, especially in R3 (Figure 6.9), suggesting that direct addition of PAA solution to R3 led to a greater change of the microbial community composition than the direct addition of H_2O_2 in R2.

Table 6.6 summarizes the relative abundance of the top 30 abundant orders in the communities of the three reactors at the end of Phase II, III and IV. Figure 6.10 and 6.11 shows the relative abundance of the communities at order level. Across the three reactors, the most abundant orders were *Flavobacteriales* (9 to 41%), *Rhodocyclales* (5 to 11%), *Rhizobiales* (5 to 11%), *Rhodobacterales* (3 to 10%), unclassified *α-Proteobacteria* (4 to 10%), and unclassified *Acidobacteria-Gp4* (1 to 9%). From the end of Phase II to the end of Phase III, the relative abundance of *Flavobacteriales,* whose main function is organic matter degradation*,* in R1, R2 and R3 decreased by 50, 53, and 81%, respectively; the highest decrease in R3 suggests that *Flavobacteriales* were negatively impacted by the long-term operation with direct addition of PAA solution. By the end of Phase III, the

119

relative abundance of *Bdellovibrionales* in R3 increased from < 0.1% to 1.4% suggesting

enrichment in response to PAA solution addition. From the end of Phase II to the end of

Phase III, the relative abundance of *Rhodocyclales,* whose main function is fatty acids

degradation, increased by 7% in R1 and 17% in R2, but decreased by 53% in R3,

suggesting that *Rhodocyclales* were negatively affected by PAA addition.

By the end of Phase II, the relative abundance of *Nitrosomonadales*, whose main function

is ammonium oxidation, was 1.93, 2.27, and 1.55% in R1, R2, R3, respectively; the

relative abundance of *Nitrospirales*, whose main function is nitrite oxidation, was 2.22,

2.55, and 1.79% in R1, R2, R3, respectively (Table 6.6). It should be noted that the

relative abundance of both *Nitrosomonadales* and *Nitrospirales* was very low throughout

the entire long-term operation. From the end of Phase II to the end of Phase III, there was

no significant time-trend change in the relative abundance of *Nitrosomonadales* and

Nitrospirales in the three reactors; however, the relative abundance of both orders

followed the series R2 > R1 > R3. Thus, as mentioned above, the observed significant

decrease in nitrification rates in R2 and R3 during Phase III was not associated with loss

of nitrifiers. Table 6.7 summarizes the relative abundance of the top 30 abundant genera

of the microbial communities in the three reactors at the end of Phase II, III and IV and

Figure 6.12 presents the TreeBar plot of their relative abundance at genus level. Across

the three reactors, the most abundant were unclassified *Flavoacteriaceae* (7 to 39%),

unclassified *Bacteria* (1 to 37%), *Thauera* (4 to 14%), α-*Proteobacteria* (4 to 10%),

Thermomonas (1 to 5%), *Paracoccus* (1 to 5%) and *Amaricoccus* (0 to 4%). From the

end of Phase II to the end of Phase III and IV, the relative abundance of unclassified

Flavobacteriaeae decreased by ca. 1-, 1- and 2-fold in R1, R2 and R3, respectively,

suggesting that the unclassified *Flavobacteriaeae* were negatively affected in R3 by direct addition of PAA solution and their recovery was limited. Similarly, from the end of Phase II to the end of Phase III and IV, the relative abundance of *Thauera* remained stable in R1 and R2, but decreased by ca. 1-fold in R3, suggesting *Thauera* was negatively impacted in R3 by direct addition of PAA solution. In contrast to unclassified *Flavobacteriaeae* and *Thauera*, from Phase II end to Phase III and IV end the relative abundance of *Thermomonas* remained stable in R1 and R2, while increased up to 4-fold in R3, suggesting that *Thermomonas* was not inhibited, but was enriched when PAA in combination with H_2O_2 but not H_2O_2 alone was directly added. From Phase II end to Phase III end, the relative abundance of unclassified α-*Proteobacteria* decreased by ca. 1-fold in R1, but increased by ca. 0.7-fold in both R2 and R3, suggesting that the unclassified α-*Proteobacteria* were not inhibited but rather were enriched by the directly added H_2O_2 or PAA or both.

Table 6.5. Number of reads, OTUs and alpha diversity indices of the microbial communities in the three aerobic bioreactors over their long-term operation.

Sample	Reads	OTUs	Alpha Diversity Index				
			Shannon	Shannon Even	Chao	Ace	Simpson
AE1P2	102794	482	3.774	0.611	580.1	554.3	0.049
AE2P2	84331	444	3.389	0.556	497.6	504.1	0.097
AE3P2	87377	470	3.370	0.548	555.7	541.2	0.120
AE1P3	97520	496	3.368	0.543	576.1	572.6	0.120
AE2P3	114163	517	3.759	0.602	594.5	594.3	0.053
AE3P3	83149	495	4.256	0.686	554.6	555.2	0.027
AE1P4	98740	514	3.323	0.532	578.8	593.7	0.115
AE2P4	102416	508	3.766	0.604	607.0	602.5	0.051
AE3P4	86237	516	4.299	0.688	603.0	584.1	0.027

Abbreviations: AE1, AE2, and AE3 correspond to reactors R1, R2, and R3; P2, P3, and P4 correspond to end of Phase II, III, and IV.

Table 6.6. Relative abundance at order level (top 30 orders) of the microbial communities in the three aerobic bioreactors over their long-term operation.

Order	AE1P2	AE2P2	AE3P2	AE1P3	AE2P3	AE3P3
Actinomycetales	1.64	1.04	0.99	0.67	0.88	4.63
Aeromonadales	T	T	T	T	T	0.49
Bdellovibrionales	TT	T	T	T	T	1.35
Burkholderiales	3.39	2.80	4.61	2.71	4.11	4.80
Caldilineales	0.36	0.23	0.22	0.47	0.50	0.57
Caulobacterales	0.66	4.84	1.60	1.37	0.59	2.56
Cytophagales	1.96	1.50	1.12	3.06	3.30	2.95
Flavobacteriales	17.41	34.03	40.77	8.67	15.92	7.77
Gemmatimonadales	0.30	0.15	0.12	0.26	0.19	T
Legionellales	0.10	0.21	0.08	0.21	0.44	0.20
Myxococcales	T	T	T	T	0.30	T
Nitrosomonadales	1.93	2.77	1.55	1.07	1.74	1.37
Nitrospirales	2.22	2.55	1.79	0.67	1.28	0.48
Opitutales	0.19	0.14	0.15	T	0.14	T
Planctomycetales	2.93	1.96	2.14	4.11	4.86	5.96
Pseudomonadales	0.34	0.17	0.26	1.04	0.73	5.16
Rhizobiales	10.91	7.26	7.83	5.43	6.68	9.68
Rhodobacterales	9.72	7.75	8.78	3.26	4.96	4.26
Rhodocyclales	11.33	11.15	9.75	12.15	13.45	4.56
Rhodospirillales	1.27	1.12	1.20	1.33	0.89	1.67
Sphingobacteriales	1.30	1.28	1.87	1.22	1.20	2.59
Sphingomonadales	0.39	0.36	0.33	0.29	0.31	2.22
Xanthomonadales	3.58	2.18	3.56	2.09	2.24	23.22
Unclassified						
Acidobacteria-Gp3	0.37	0.22	0.22	0.32	0.23	0.14
Acidobacteria-Gp4	8.60	5.63	1.85	1.00	2.49	1.44
α-Proteobacteria	9.34	5.59	3.58	5.70	8.78	6.53
Bacteria	4.73	1.30	1.87	37.24	18.59	2.47
Bacteroidetes	0.36	0.41	0.50	0.78	0.72	0.44
β-Proteobacteria	3.62	2.60	2.51	2.88	3.15	1.20
γ-Proteobacteria	0.22	0.19	0.18	0.60	0.41	0.29

Abbreviations: AE1, AE2, and AE3 correspond to reactors R1, R2, and R3; P2 and P3 correspond to end of Phase II and III. T and TT, relative abundance below 0.1% and 0.01%, respectively.

Table 6.6 (Continued). Relative abundance at order level (top 30 orders) of the microbial communities in the three aerobic bioreactors over their long-term operation.

Order	AE1P4	AE2P4	AE3P4	Role[a]	Ref.
Actinomycetales	0.53	0.94	2.23		
Aeromonadales	T	TT	0.84		
Bdellovibrionales	T	TT	1.49	TM, ARB	(1)
Burkholderiales	3.23	4.27	8.93	OAD	(2)
Caldilineales	0.31	0.50	0.34		
Caulobacterales	0.48	0.47	1.78		
Cytophagales	2.84	3.42	2.66		
Flavobacteriales	12.61	18.05	9.10	OD, PD	(3)
Gemmatimonadales	0.28	0.23	T		
Legionellales	0.18	0.35	0.12		
Myxococcales	T	0.11	T	IOD	(4)
Nitrosomonadales	0.93	1.75	0.77	AO	(5)
Nitrospirales	0.89	1.79	0.26	NO	(6)
Opitutales	T	0.14	T		
Planctomycetales	3.68	4.96	4.90	SS	(7)
Pseudomonadales	0.86	0.28	6.29		
Rhizobiales	4.51	6.25	7.17	NF	(8)
Rhodobacterales	3.28	5.49	5.55	PR	(9)
Rhodocyclales	14.31	12.41	7.21	FAD	(10)
Rhodospirillales	1.02	0.89	1.12		
Sphingobacteriales	1.23	0.97	2.35		
Sphingomonadales	0.33	0.35	2.02		
Xanthomonadales	2.26	2.30	21.36	NR	(11)
Unclassified					
Acidobacteria-Gp3	0.17	0.23	T		
Acidobacteria-Gp4	0.97	3.22	0.65		
α-Proteobacteria	4.69	9.89	5.42		
Bacteria	34.69	15.81	2.08		
Bacteroidetes	0.94	0.56	0.76		
β-Proteobacteria	3.28	2.92	1.23		
γ-Proteobacteria	0.39	0.45	0.23		

Abbreviations: AE1, AE2, and AE3 correspond to reactors R1, R2, and R3; P4 correspond to end of IV. T and TT, relative abundance below 0.1% and 0.01%.

Role: AO, ammonia oxidation; NO, nitrite oxidation; OD, organics degradation; IOD, insoluble organics degradation; PD, phenol degradation; TPR, P removal; NR, nitrite reduction; NF, nitrogen fixation; FAD, fatty acids degradation; OAD, oxalic acid degradation; SS, sterols synthesis; TM, thiamine synthesis; ARB, adenine ribonucleotide biosynthesis.

References: (1) Hespell and Odelson, 1978; (2) Garrity, 2005; (3) Enke et al., 2018; (4) Shimkets et al., 2006; (5) Garrity, 2005; (6) Koch et al., 2005; (7) Pearson et al., 2003; (8) Young et al., 2001; (9) Maszenan et al., 1997; (10) Boden et al., 2017; (11) Finkman et al., 2000

Table 6.7. Relative abundance at genus level (top 30 genera) of the microbial communities in the three aerobic bioreactors over their long-term operation.

Genus	AE1P2	AE2P2	AE3P2	AE1P3	AE2P3	AE3P3
Amaricoccus	3.67	2.09	2.82	1.05	1.41	0.34
Bosea	0.15	0.14	0.16	0.16	0.22	1.06
Brevundimonas	0.62	4.81	1.55	1.35	0.57	2.51
Chryseobacterium	0.75	1.06	2.02	0.39	0.45	0.70
Comamonas	0.21	0.17	1.65	0.18	0.15	1.23
Hydrogenophaga	0.30	0.30	0.36	0.16	0.22	1.10
Luteimonas	1.37	0.58	1.58	0.47	0.72	2.23
Mycobacterium	1.44	0.95	0.85	0.61	0.79	4.25
Niabella	0.50	0.43	0.68	0.09	0.22	0.50
Nitrospira	2.22	2.55	1.79	0.67	1.28	0.48
Paracoccus	4.57	4.54	4.70	1.36	2.43	2.73
Persicitalea	0.54	0.64	0.45	2.76	2.32	2.80
Pseudomonas	0.25	0.11	0.18	0.90	0.18	1.15
Pseudoxanthomonas	0.50	0.35	0.44	0.28	0.26	5.52
Sphingopyxis	0.06	0.06	0.06	0.06	0.08	1.58
Thauera	11.17	10.98	9.53	12.03	13.34	4.43
Thermomonas	1.15	0.89	1.14	0.87	0.89	4.69
Unclassified						
α-Proteobacteria	9.34	5.59	3.58	5.70	8.78	6.53
Bacteria	4.73	1.30	1.87	37.24	18.59	2.47
β-Proteobacteria	3.62	2.60	2.51	2.88	3.15	1.20
Bradyrhizobiaceae	0.13	0.10	0.11	0.06	0.08	0.25
Burkholderiales	0.75	0.81	0.77	0.96	2.18	0.57
Chitinophagaceae	0.51	0.52	0.81	0.46	0.48	1.01
Comamonadaceae	1.49	1.29	1.63	1.01	1.31	1.51
Flavobacteriaceae	16.61	32.85	38.64	8.25	15.44	6.93
Phyllobacteriaceae	2.63	1.71	1.54	2.58	2.89	1.09
Planctomycetaceae	2.71	1.79	1.97	3.58	3.95	5.01
Rhizobiales	2.85	2.31	3.30	1.66	2.14	4.26
Rhodobacteraceae	1.48	1.12	1.26	0.84	1.12	1.20
Xanthomonadaceae	0.46	0.31	0.33	0.31	0.30	9.31

Abbreviations: AE1, AE2, and AE3 correspond to reactors R1, R2, and R3; P2, P3, and P4 correspond to end of Phase II, III, and IV.

Table 6.7 (Continued). Relative abundance at genus level (top 30 genera) of the microbial communities in the three aerobic bioreactors over their long-term operation.

Genus	AE1P4	AE2P4	AE3P4
Amaricoccus	1.02	1.57	0.30
Bosea	0.19	0.22	0.76
Brevundimonas	0.47	0.45	1.74
Chryseobacterium	0.44	0.54	1.06
Comamonas	0.16	0.17	3.44
Hydrogenophaga	0.16	0.22	2.04
Luteimonas	0.42	0.75	1.85
Mycobacterium	0.49	0.85	1.92
Niabella	0.10	0.25	0.43
Nitrospira	0.89	1.79	0.26
Paracoccus	1.43	2.68	3.93
Persicitalea	2.62	2.30	2.53
Pseudomonas	0.76	0.12	1.41
Pseudoxanthomonas	0.31	0.26	4.82
Sphingopyxis	0.07	0.08	1.43
Thauera	14.12	12.31	6.33
Thermomonas	0.97	0.90	4.22
Unclassified			
α-Proteobacteria	4.69	9.89	5.42
Bacteria	34.69	15.81	2.08
β-Proteobacteria	3.28	2.92	1.23
Bradyrhizobiaceae	0.05	0.07	0.22
Burkholderiales	1.25	2.33	0.63
Chitinophagaceae	0.52	0.46	0.72
Comamonadaceae	1.08	1.27	2.16
Flavobacteriaceae	12.13	17.47	7.82
Phyllobacteriaceae	1.87	2.50	0.67
Planctomycetaceae	3.21	4.11	4.10
Rhizobiales	1.53	2.14	3.14
Rhodobacteraceae	0.83	1.24	1.32
Xanthomonadaceae	0.32	0.30	9.09

<u>Abbreviations</u>: AE1, AE2, and AE3 correspond to reactors R1, R2, and R3; P2, P3, and P4 correspond to end of Phase II, III, and IV.
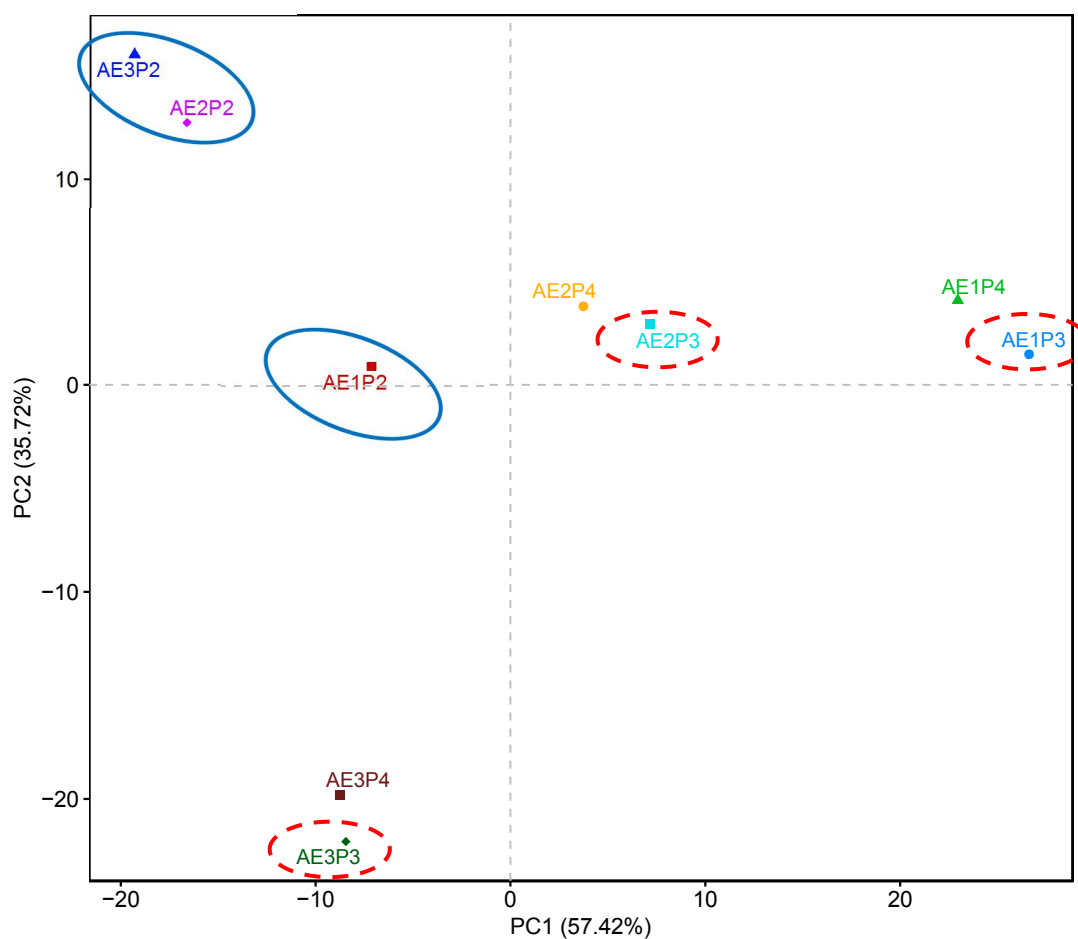
Figure 6.9. Principal component analysis at order level of the microbial communities in the three long-term bioreactors at the end of Phase II (solid blue circle), III (broken red circle) and IV.

Abbreviations: AE1, AE2, and AE3 correspond to reactors R1, R2, and R3; P2, P3, and P4 correspond to end of Phase II, III, and IV.
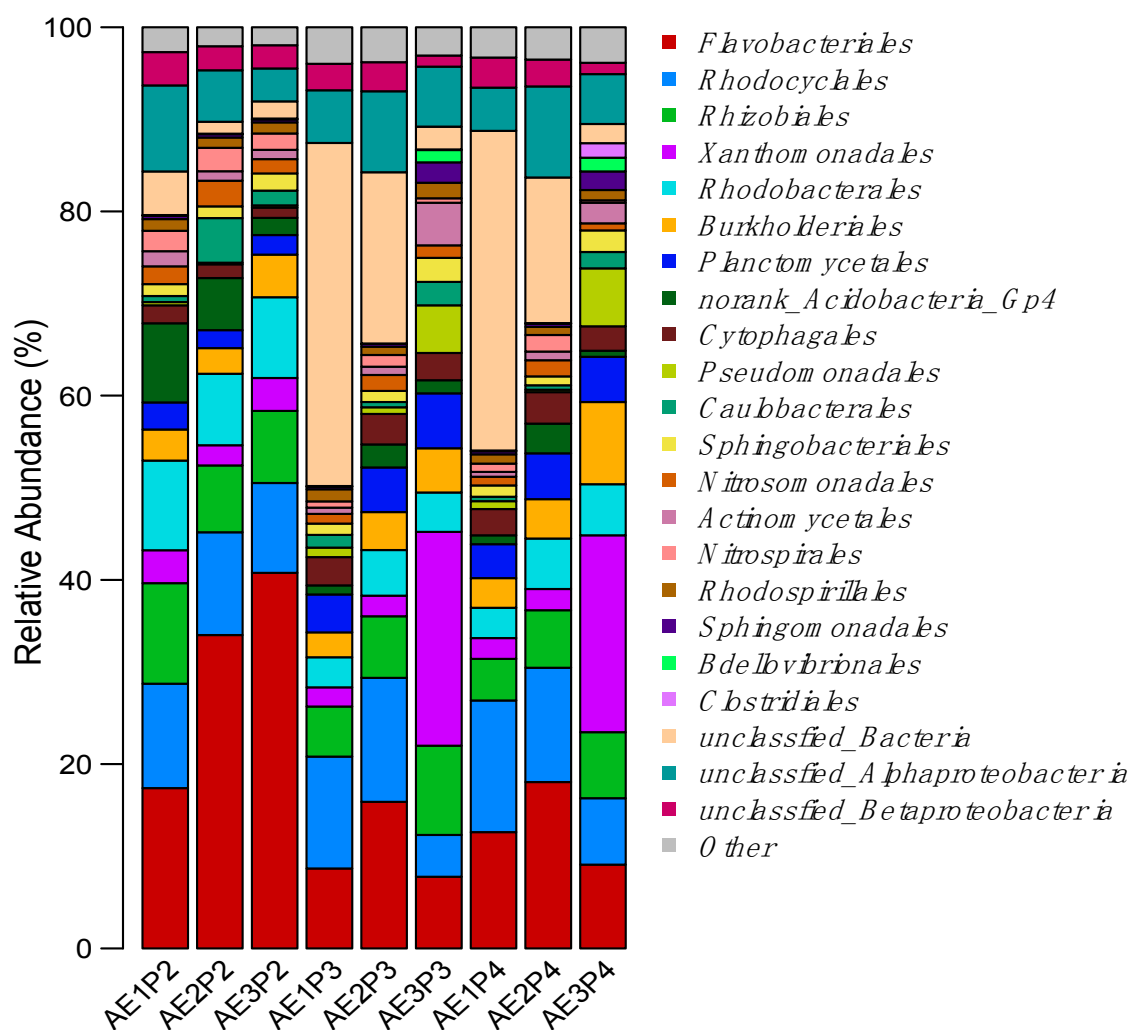
Figure 6.10. Relative abundance at order level of the communities in the three aerobic long-term bioreactors at the end of Phase II, III and IV.

Abbreviations: AE1, AE2, and AE3 correspond to reactors R1, R2, and R3; P2, P3, and P4 correspond to end of Phase II, III, and IV.

.
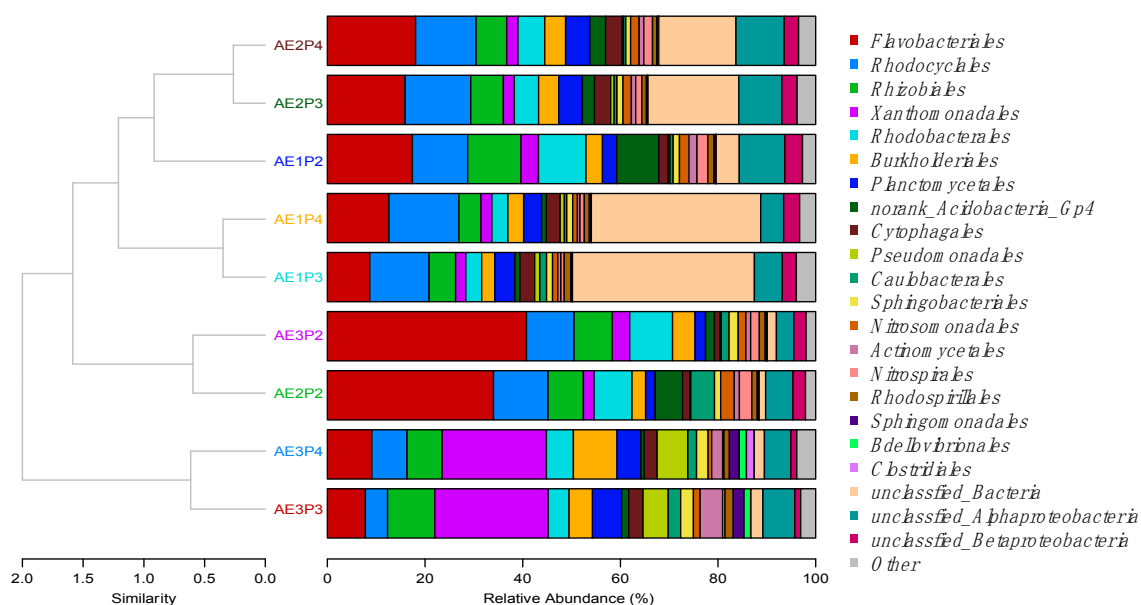
Figure 6.11. Relative abundance TreeBar plot at order level of the microbial communities in the three long-term bioreactors at the end of Phase II, III and IV.

Abbreviations: AE1, AE2, and AE3 correspond to reactors R1, R2, and R3; P2, P3, and P4 correspond to end of Phase II, III, and IV.
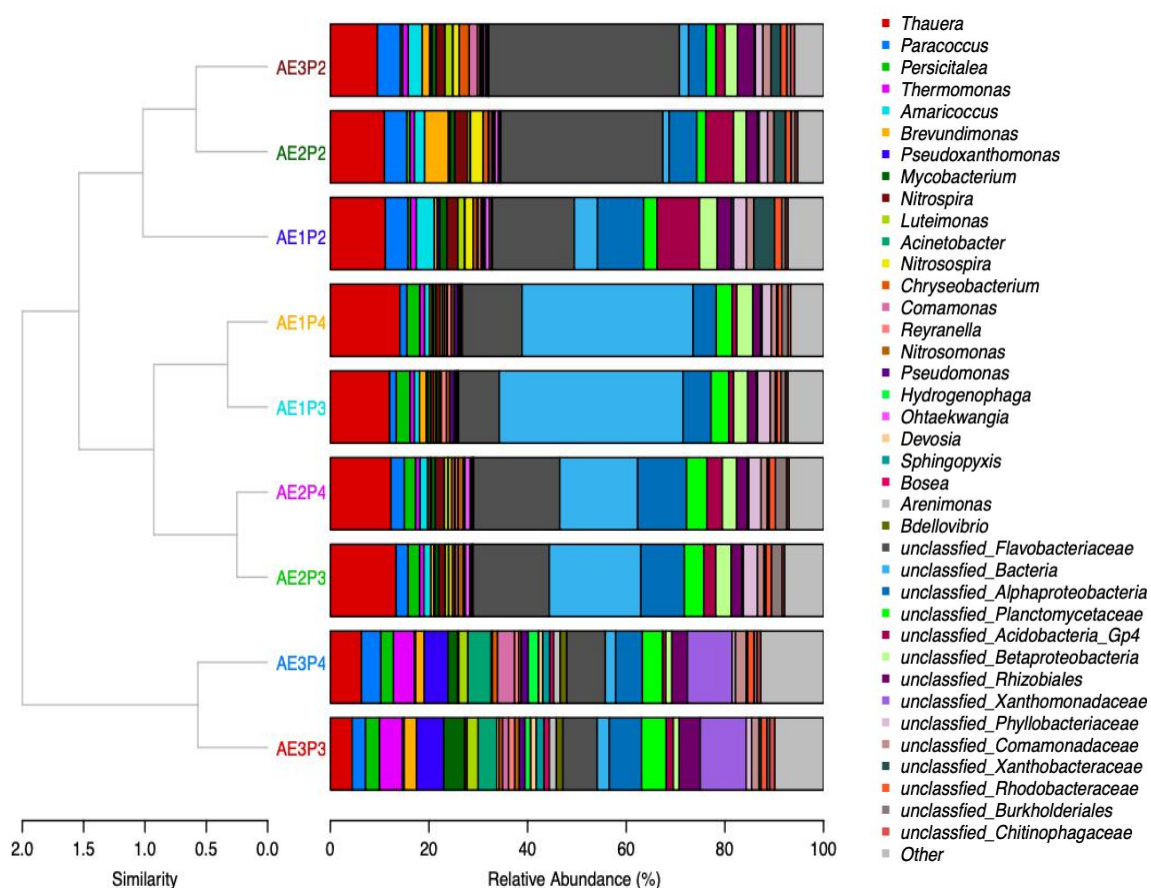
Figure 6.12. Relative abundance TreeBar plot at genus level of the microbial communities in the three long-term bioreactors at the end of Phase II, III and IV.

Abbreviations: AE1, AE2, and AE3 correspond to reactors R1, R2, and R3; P2, P3, and P4 correspond to end of Phase II, III, and IV.

6.4 Summary

Peracetic acid (PAA) has been widely used as a disinfectant in many industries; its use in poultry processing is steadily increasing. However, information related to the potential inhibitory effect of PAA solutions (PAA and H_2O_2) on biological wastewater treatment processes used by the poultry processing industry is extremely limited. The work reported here assessed the long-term effect of PAA solution on aerobic degradation and nitrification in three bioreactors fed with poultry processing wastewater by

129

quantifying the extent of COD removal and nitrification rates. Changes in culture viability, intracellular reactive oxygen species (ROS), and microbial community structure were also evaluated. Indirect and direct addition of H_2O_2 and PAA at gradually increased concentrations up to 60 mg PAA/L and up to 27 mg H_2O_2/L did not significantly affect the aerobic degradation of poultry processing DAF wastewater, quantified as the extent of sCOD removal. Although H_2O_2 alone mildly affected nitrite oxidation to nitrate, the effect of PAA solution on nitrification was predominantly attributed to PAA alone or in combination with H_2O_2. The impact of the PAA solution on nitrification worsened and microbial acclimation did not take place over the long-term operation. Both aerobic organic matter degradation and nitrification recovered fast after PAA and/or H_2O_2 direct addition ended. The observed decrease in nitrification rates is predominantly attributed to enzyme inhibition than to loss of nitrifiers. Intracellular ROS was not the cause of the observed deterioration of nitrification over the long-term operation with addition of H_2O_2 and/or PAA/H_2O_2; the capacity of the microbial community to manage PAA-induced cell oxidative stress increased over the long-term operation with addition of PAA solution, though microbial diversity decreased significantly. The microbial community composition shifted over the long-term operation with addition of H_2O_2 and even more with addition of PAA solution. Overall, the results of this study suggest that aerobic organic matter degradation and nitrification of poultry processing wastewater will not be affected during the normal plant operation when residual PAA and H_2O_2 are not present in the wastewater. However, nitrification will be affected when wastewater streams with high residual PAA concentrations are expected at the end of the plant operation shift due to emptying of chiller tanks, or in the case of accidental PAA solution spills.

CHAPTER 7. LONG-TERM EFFECT OF PAA ON A MIXED ANOXIC CULTURE

7.1 Introduction

As discussed in Chapter 5, Section 5.3.1, 25 to 30 mg/L PAA was detected in the DAF underflow wastewater at the end of the poultry processing plant daily operational shift, which coincided with the emptying of chiller tanks. However, information related to the potential inhibitory effect of PAA solutions on biological wastewater treatment processes commonly used by the poultry processing industry is extremely limited. The long-term effect of PAA on nitrification and aerobic organic degradation was evaluated in Chapter 6, Thus, long-term evaluation of the effect of PAA denitrification and organics degradation in anoxic reactors was urgently needed.

The overall goal of the work reported in this chapter was to assess the long-term effect of PAA solution on anoxic organic matter degradation and denitrification, biological processes commonly used for the treatment of poultry processing wastewater. The following questions needed to be answered: a) Do PAA solutions and associated H_2O_2 inhibit anoxic organic matter degradation and denitrification in the treatment of poultry processing wastewater, and if they do, what are PAA and H_2O_2 inhibitory levels? b) Is the impact of PAA and H_2O_2 on anoxic organic matter degradation and denitrification associated with enzyme inhibition and/or decreased microbial culture viability? c) Is the impact of PAA and H_2O_2 reversible and does microbial acclimation take place over the long-term operation with addition of PAA and H_2O_2? To address these questions, the following tasks were carried out. Anoxic bioreactors, semi-

continuously fed with poultry processing wastewater, amended with PAA solution and H_2O_2 at gradually increased concentrations, were operated for 166 d. The effect of PAA and H_2O_2 on anoxic organic matter degradation and denitrification was evaluated, quantified in terms of chemical oxygen demand (COD) removal and denitrification rates. Microbial responses to PAA solution, such as culture viability and intracellular reactive oxygen species (ROS), were also evaluated. Complementary anoxic batch assays were conducted with single, direct PAA addition to determine potential acclimation taking place over the long-term operation with addition of PAA solution. Finally, the microbial community diversity and composition over the long-term operation with PAA and H_2O_2 addition were evaluated.

7.2 Materials and Methods

7.2.1 Chemicals and Wastewater

Chemicals are described in Chapter 3, Section 3.2.1. Wastewater is described in Chapter 6, Section 6.2.1.

7.2.2 Setup and Operation of Bioreactors

Three semi-continuously fed anoxic bioreactors (R1, R2, and R3) were set up and maintained at room temperature (22 ± 1°C). The reactors started with stock culture from a lab-scale reactor, fed with DAF wastewater over 2.5 years. Details of the stock culture are presented in Section 5.2.1, above. The reactors were 2.8 L glass bottles with a total culture volume of 1.5 L, sealed with rubber stoppers and mixed with magnetic stirrers. The three reactors were fed as follows: R1, DAF wastewater only; R2, DAF wastewater

and H_2O_2 added either in the feed (indirect addition), or directly in the reactor (direct addition); and R3, DAF wastewater and PAA solution (indirect or direct addition). Indirect PAA and H_2O_2 addition simulated treatment of wastewater devoid of residual PAA and/or H_2O_2, whereas direct addition simulated treatment of residual PAA- and H_2O_2-bearing wastewater. The reactors were fed every 2 d after settling for 1 h and removing 1 L supernatant; 0.5 L mixed liquor was removed every 6 d. The resulting hydraulic retention time (HRT) and solids retention time (SRT) was 3 and 18 d, respectively. At each feeding, 150 to 250 mg N/L initial $NaNO_3$ was added to provide excess nitrate to prevent development of anaerobic conditions due to excess residual organic carbon. Thus, the initial $NaNO_3$ concentration was increased as the initial organic carbon load increased in R3 resulting from increased PAA/acetic acid load. Therefore, on an electron equivalent basis, the ratio of initial nitrate to total COD ranged from 0.93 to 1.05. For consistency, all three reactors received the same initial $NaNO_3$ concentration, which was increased over the long-term operation.

The long-term operation of the reactors consisted of four phases (Figure 7.1). In Phase I (control), the reactors were fed for 40 d with PAA- and H_2O_2-free DAF wastewater. Operation of R1 was the same throughout the four phases. In Phase II (indirect H_2O_2 and PAA solution addition), before feeding, the wastewater feed to R2 was amended with H_2O_2 at gradually increased concentrations corresponding to the H_2O_2 concentrations in the PAA solution-amended feed to R3. Aliquots of H_2O_2 and PAA working solutions were added to the R2 and R3 wastewater feed, respectively, 40 min before feeding. Under these conditions, H_2O_2 and PAA were completely decomposed in the wastewater feed (pH 6.5 to 7.0). The resulting, nominal reactor H_2O_2 and PAA initial

133

concentrations were increased stepwise over time from 0.7 to 8.4 mg/L H_2O_2 in R2 and

from 5/0.7 to 60/8.4 mg/L PAA/H_2O_2 in R3 (Figure 7.1). In Phase III (direct H_2O_2 and

PAA solution addition), both R2 and R3 were fed as in Phase II, but with direct addition

of H_2O_2 and PAA working solutions to the reactors immediately after adding the DAF

wastewater. Towards the end of Phase III, and in order to match the oxidation capacity of

H_2O_2 in R2 to that of PAA in R3, after the last feeding of R2 with 8.4 mg/L H_2O_2, 27

mg/L H_2O_2 were added directly to R2, which is equivalent to 60 mg/L PAA in terms of

electron transfer during decomposition. In Phase IV (recovery phase), all three reactors

were maintained as in Phase I, fed with H_2O_2- and PAA-free DAF wastewater. The

following parameters were monitored over the long-term operation: pH, soluble COD

(sCOD), ammonia, nitrite, nitrate, headspace pressure, gas composition (N_2, N_2O and

CO_2), total and volatile suspended solids (TSS, VSS), culture viability, and intracellular

ROS.
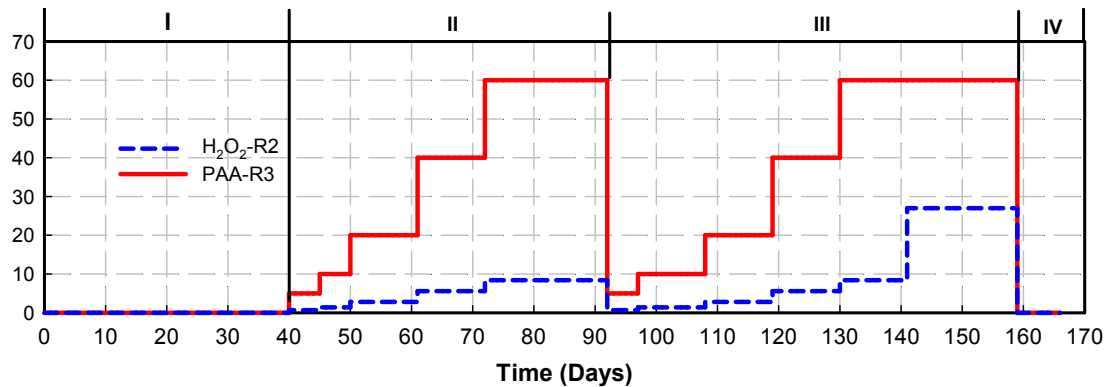
Figure 7.1. Initial, nominal reactor H_2O_2 and PAA concentration in Phase I (control), II (indirect H_2O_2 and PAA solution addition), III (direct H_2O_2 and PAA solution addition), and IV (recovery) in R2 and R3 during the 166-d operation.

7.2.3 Short-term Batch Assays

The purpose of the anoxic batch assay was to evaluate possible increased inhibitory effect of the PAA solution on anoxic organic matter degradation and denitrification in R3 (direct addition of PAA solution) and culture acclimation at different stages during the long-term operation. The batch assay was carried out in 580-mL glass aspirator bottles, sealed with rubber stoppers. At the end of several feeding cycles during the long-term operation of R1, 450 mL of R1 mixed liquor was transferred to the bottle pre-flushed with He, allowed to settle for 1 h and then 300 mL supernatant was replaced with an equal volume of DAF wastewater, along with 150 to 250 mg N/L $NaNO_3$. PAA solution was directly added to the bottle, resulting in initial PAA/H_2O_2 concentrations from 0/0 to 60/8.4 mg/L. Incubation was carried at room temperature ($22\pm1^\circ$C). The following parameters were monitored over the incubation time: pH, sCOD, ammonia, nitrite, and nitrate, headspace pressure, and gas composition (N_2, N_2O, CO_2). Initial and final TSS and VSS were also measured for all batch series.

7.2.4 Microbial Community Analysis

Bacterial DNA extraction, quantification, and sequencing were performed following standard protocols as described in Chapter 3, Section 3.3.

7.2.5 Analytical Methods

pH, COD, N species, total solids (TS) and volatile solids (VS), total suspended solids (TSS) and volatile suspended solids (VSS), gas production and composition, VFAs, DO, total carbohydrates, total lipids, culture viability, and intracellular ROS were

measured as described in Chapter 3, Section 3.1. PAA and H_2O_2 were measured by DPD method as described in Chapter 3, Section 3.2.3. The fraction of heterotrophic bacteria, ammonia-oxidizing bacteria (AOB), nitrite-oxidizing bacteria (NOB) in the stock mixed heterotrophic/autotrophic culture was determined by using sodium azide (NaN_3) and allylthiourea (ATU) to inhibit AOB and NOB, respectively, and then measuring oxygen uptake rates as previously described (Surmacz-Gorska et al., 1996).

7.3 Results and Discussion

7.3.1 Bioreactors Performance

Operation of the three reactors (R1, R2, and R3) lasted for 166 d (Figure 7.1), divided into four phases (Section 7.2.2). Throughout the entire operation, the three reactors were fed with DAF wastewater every 2 d, while R2 and R3 also received H_2O_2 or PAA solution, respectively, added to the DAF wastewater feed 40 min ahead of feeding (Phase II), or directly to the reactors after feeding with DAF wastewater (Phase III).

7.3.1.1 Phase I

During Phase I (40 d; twenty 2-d feeding cycles), the three reactors reached stable and similar performance. The mean pH in the three reactors ranged from 8.3 to 8.5 mg/L. At 40 d of operation (end of Phase I), the VSS concentration was comparable across the three reactors, ranging from 2.05 to 2.18 g/L (Figure 7.2). The mean extent of sCOD removal after 2-d incubation was not significantly different among the three reactors (93.9±1.8%; $p > 0.05$) (Table 7.1). The initial nitrate removal rate (NRR) and observed

maximum nitrite levels were also not significantly different among the three reactors

(313.3±17.9 mg N/L-d, $p > 0.05$; 16.7±2.0 mg N/L, $p > 0.05$) at the end of Phase I (Table

7.2). N_2 was the only gas detected in the headspace of the three reactors.

7.3.1.2 Phase II

During Phase II (day 40 to 94; twenty seven 2-d feeding cycles), the performance

of the three reactors was evaluated at five, gradually increased H_2O_2 and PAA levels (0.7

to 8.4 mg H_2O_2/L; 5 to 60 mg PAA/L), both added to the DAF wastewater prior to

feeding (indirect addition). The mean pH in the three reactors was 8.3 - 8.6. N_2 was the

only gas detected in the headspace of the three reactors. At the end of Phase II, the VSS

concentration in R1, R2, and R3 was 1.91±0.14, 1.72±0.15, and 1.59±0.10 g/L (Figure

7.2). Compared to the end of Phase I, the VSS concentration in R2 and R3 decreased by

ca. 18 and 27%, respectively.

The extent of sCOD removal and the initial NRR ranged from 93 to 94% and

from 404 to 452 mg N/L-d across the three reactors at the end of Phase II, respectively

(both not significantly different among the three reactors; $p > 0.05$) (Tables 7.1 and 7.2).

At the end of Phase II, the observed maximum nitrite concentrations in R1 and R3 were

comparable, but were lower in R2 by 29% compared to the mean maximum nitrite

concentration in R1 and R3. Given that the NRR was comparable across the three

reactors at the end of Phase II, the lower maximum nitrite concentration in R2 suggests

that nitrite reduction in R2 was faster than in R1 and R3 at the end of Phase II. Taken all

together, indirect addition of H_2O_2 and/or PAA solution at the above-stated concentration

range did not significantly affect anoxic organic matter degradation and denitrification.

7.3.1.3 Phase III

During Phase III (day 94 to 160; twenty five to twenty seven feeding cycles), H_2O_2 and PAA/H_2O_2 were added directly to R2 and R3, respectively, after feeding with DAF wastewater (Figure 7.1). H_2O_2 and PAA were not detected in R2 and R3 after feeding, a result of fast PAA decomposition in the complex matrix of the reactors' feed and contents (Chen and Pavlostathis, 2019). The sCOD removal in R1 (control) ranged from 93.9 to 96.5%, comparable to that during Phase I and II (Table 7.1). The sCOD removal in R2 varied from 93.7 to 99.4% up to 8.4 mg H_2O_2/L, then decreased to as low as 80.1% at 27 mg H_2O_2/L (4th feeding cycle; Table 7.1). The sCOD removal in R3 varied from 95.4 to 99.6% up to 40/5.6 mg/L PAA/H_2O_2, then decreased to as low as 88.0% at 60/8.4 mg/L PAA/H_2O_2 (4th feeding cycle; Table 7.1). Thus, given the sCOD removal in R2 was not impacted by 8.4 mg/L H_2O_2, the lower sCOD removal in R3 at 60/8.4 mg/L PAA/H_2O_2 is attributed to PAA alone or PAA in combination with H_2O_2 rather than to H_2O_2. In a previous study, wet oxidation of a high strength pharmaceutical wastewater using H_2O_2 resulted in decreased COD as the H_2O_2 concentration increased (Zeng et al., 2017).

Table 7.2 summarizes the initial NRR at different stages of Phase III. The relative NRR (RNRR; i.e., NRR rates in R2 and R3 normalized to that in R1) are shown in Fig. 1B. The RNRR in R2 varied from 0.83 to 1.04 up to 8.4 mg H_2O_2/L and gradually decreased to as low as 0.45 by the end of the 4th feeding cycle with 27 mg H_2O_2/L. The RNRR in R3 varied between 0.86 and 1.13 up to 20/2.8 mg/L PAA/H_2O_2, but declined to ca. 0.48 by the end of the 4th feeding cycle with 60/8.4 mg/L PAA/H_2O_2. Given that the

138

RNRR was not significantly affected by 8.4 mg/L H_2O_2 in R2, the observed decrease of NRR in R3 at 40/5.6 and even more at 60/8.4 mg/L PAA/H_2O_2 is predominantly attributed to PAA or the combination of PAA and H_2O_2. Therefore, directly added PAA solution negatively affected NRR and the impact is predominantly attributed to PAA.

Maximum nitrite concentrations in R1 ranged from 33.8 to 49.0 mg N/L throughout Phase III (Table 7.2). In contrast, the nitrite concentration in R2 increased with increased concentration of directly added H_2O_2, reaching ca. 90 mg N/L after the 4th direct addition of 27 mg H_2O_2/L (Figure 7.3C; Figure 7.4H; Table 7.2) which represents ca. 39% of the initially added nitrate-N concentration. The nitrite concentration in R3 increased dramatically with increased concentration of direct addition of PAA solution, reaching ca. 151 mg N/L after the 4th direct addition with 60/8.4 mg/L PAA/H_2O_2 (Figure 7.3C; Figure 7.4G; Table 7.2), which represents ca. 60% of the initially added nitrate-N concentration. The maximum nitrite concentration in R2 was 58.5 mg N/L after the 4th addition of 8.4 mg/L H_2O_2 (ca. 39% higher than in R1), while in R3 was 150.4 mg N/L (ca. 250% higher than in R1) after the 4th addition of 60/8.4 mg/L PAA/H_2O_2. Therefore, H_2O_2 alone at 8.4 mg/L negatively affected nitrite removal, but the major impact on nitrite removal at 60/8.4 mg/L PAA/H_2O_2 in R3 is attributed to PAA or its combination with H_2O_2 rather than H_2O_2 alone.

Up to the first addition of 27 mg/L H_2O_2, the headspace of R2 was 100% N_2. N_2O was detected in the headspace of R2 since the second feeding with 27 mg/L H_2O_2, ranging from 1.5 to 7.9% (Figure 7.5), representing ca. 10 to 52 mg N/L N_2O with reference to the reactor mixed liquor volume. Based on Henry's Law and the Henry's constant of N_2O, 0.025 mol/L-atm (Sander, 2015), assuming ideal gas and equilibrium

139

conditions, and no ionic effect in the aqueous phase, there was 6 to 31 mg N/L N_2O partitioning in R2 mixed liquor. Thus, the total N_2O produced ranged from 16 to 83 mg/L, representing ca. 7 to 36% of the initially added nitrate-N concentration. Up to the last addition of 40/5.6 mg/L PAA/H_2O_2, the headspace of R3 was 100% N_2. N_2O and CO_2 were detected in the headspace of R3 since the first addition of 40/5.6 mg/L PAA/H_2O_2, ranging from 3.1 to 9.6% and 1.4 to 10.8%, respectively (Figure 7.5). It should be noted that nitric oxide (NO) was not detected under any of the conditions examined in this study. CO_2 was not detected in either R1 or R2, suggesting that the observed CO_2 in R3 resulted from the degradation of acetic acid supplied by the PAA solution and produced as a result of PAA decomposition. The N_2O detected in R3 headspace represented 20 and 64 mg N/L N_2O with reference to R3 mixed liquor volume. Based on Henry's Law, N_2O in the aqueous phase of R3 was 12 to 37 mg N/L. Thus, in total, 32 to 101 mg N/L N_2O was produced in R3, representing ca. 15 to 46% of the initially added nitrate-N concentration. Given N_2O was not detected in R2 headspace at an initial H_2O_2 of 8.4 mg/L, the negative impact on the complete nitrate reduction by 60/8.4 mg/L PAA/H_2O_2 is predominantly attributed to PAA or its combination with H_2O_2.

Based on the PAA and H_2O_2 decomposition reactions, the theoretical O_2 production is 0.211 mg O_2/mg PAA and 0.471 mg O_2/mg H_2O_2. Thus, the theoretically produced O_2 is 1.4 mg/L for a dose of 5/0.7 mg/L PAA/H_2O_2 and 16.6 mg/L for 60/8.4 mg/L PAA/H_2O_2. For a range of initial nitrate (150 to 250 mg N/L), on an electron equivalent basis, the theoretically produced O_2 amounts for 0.32 to 2.34% of the initially added nitrate. Thus, the competition for electron donor between the two electron acceptors, i.e., O_2 and nitrate, was minimal. The measured total O_2 (i.e., the sum of O_2 in

gas phase and dissolved O_2) normalized to the liquid volume at the highest PAA/H_2O_2 dose to R3, i.e., 60/8.4 mg/L PAA/H_2O_2, was 19 mg/L, which decreased to undetectable level within 30 h of incubation. Thus, mainly anoxic conditions were maintained within the 2-d feeding cycles of the reactors.

At the end of direct addition of 5.6 mg/L H_2O_2 in R2 and 40/5.6 mg/L PAA/H_2O_2 in R3 during Phase III, the concentration of TSS and VSS in the three reactors was close to that at the end of Phase II (Figure 7.2). Thus, direct addition of H_2O_2 to R2 up to 5.6 mg/L and PAA solution to R3 up to 40/5.6 mg/L PAA/H_2O_2 did not affect the biomass concentration. By the end of Phase III, the VSS concentration remained unchanged in R1, but decreased slightly by ca. 7 and 18% in R2 and R3, respectively, compared to the VSS at the mid of Phase III. The higher VSS loss in R3 is attributed to solids solubilization as well as bacteria lysis, primarily caused by PAA. At the end of Phase III, the VSS in R2 and R3 was 15 and 25% lower than in R1, respectively; however, the NRR in R2 and R3 was 55 and 52% lower than in R1, respectively. Therefore, in both R2 and R3, the negative impact of H_2O_2 and PAA solution on nitrate removal was attributed more to enzyme inhibition than the loss of biomass.

7.3.1.4 Phase IV

During Phase IV (i.e., recovery phase feeding DAF wastewater only; day 160 to 166) (Figure 7.1), sCOD removal increased and nitrite levels decreased in R2 and R3 from the first to the third feeding and reached values comparable to that of R1 (Table 7.1; Table 7.2 and Figure 7.3C). The RNRR in both R2 and R3 gradually increased and reached 0.99 and 1.04, respectively, by the end of the third feeding cycle (Table 7.2;

Figure 7.3B). Thus, fast recovery of organic matter degradation and complete

denitrification were restored in both R2 and R3 when direct addition of H_2O_2 and PAA

solution ended.

Table 7.1. Extent of soluble COD removal (%) by the three anoxic reactors in Phase I through IV (end of 2-d incubation).

Phase	No. Feeding Cycles[a]	Initial H_2O_2/PAA-H_2O_2 (mg/L)	R1	R2	R3
I[b]	1-20	--/--[b]	93.9±0.1[c]	94.6±0.3	93.1±1.0
II[d]	1	0.7/5-0.7	95.1±0.6	94.4±0.5	93.0±0.5
	1	1.4/10-1.4	94.9±0.8	96.1±0.4	93.6±0.5
	1	2.8/20-2.8	94.4±0.4	95.6±0.4	92.4±0.6
	1	5.6/40-5.6	94.7±0.0	94.7±0.9	91.0±0.8
	1	8.4/60-8.4	92.5±1.4	93.7±0.8	93.5±1.3
III[e]	2	0.7/5-0.7	96.5±0.8	95.3±0.2	97.4±0.2
	3	0.7/5-0.7	96.0±0.4	96.5±0.5	96.2±0.3
	1	1.4/10-1.4	94.2±0.4	95.4±0.4	96.2±0.2
	6	1.4/10-1.4	95.5±0.6	94.7±0.3	95.4±0.5
	1	2.8/20-2.8	95.1±0.4	93.7±0.1	96.4±0.3
	6	2.8/20-2.8	96.4±0.3	95.6±0.7	98.0±0.1
	1	5.6/40-5.6	95.7±0.3	98.6±0.1	99.6±0.1
	6	5.6/40-5.6	93.8±0.4	98.8±0.3	98.5±0.4
	1	8.4/60-8.4	93.9±0.5	99.4±0.3	97.8±0.3
	6	8.4/--	94.9±0.8	98.9±0.2	--
	1	27/--	94.6±0.1	89.3±0.2	--
	2	27/--	94.9±0.1	80.1±0.3	--
	3	27/--	--	86.6±0.2	--
	4	27/--	--	83.6±0.4	--
	2	--/60-8.4	--	--	88.9±0.6
	3	--/60-8.4	--	--	86.0±0.5
	4	--/60-8.4	--	--	83.8±1.5
IV[f]	1	--	94.9±0.1	91.1±0.3	89.7±0.3
	2	--	94.5±0.4	94.8±0.3	91.5±0.4
	3	--	94.9±0.2	97.0±0.3	91.6±0.9

[a] Feeding cycle at corresponding H_2O_2 and/or PAA concentration; [b] Control phase without H_2O_2 and/or PAA solution addition (duration, 40 d); [c] Mean ± standard deviation; [d] Indirect addition of H_2O_2 and/or PAA solution (duration, 54 d); [e] Direct addition of H_2O_2 and/or PAA solution (duration, 90 d); [f] Recovery phase without H_2O_2 and/or PAA solution addition (duration, 6 d).

Table 7.2. Initial nitrate removal rates (NRR) and observed maximum nitrite levels in the three anoxic reactors in Phase I through IV.

Phase	No. Feeding Cycles[a]	Initial H_2O_2/ PAA-H_2O_2 (mg/L)	NRR (mg N/L-d)		
			R1	R2	R3
I[b]	1-20	--[b]	328.0±3.8[c]	314.7±3.8	297.3±1.9
II[e]	1	0.7/5-0.7	302.6±3.6	311.1±1.2	295.3±3.0
	1	1.4/10-1.4	350.0±2.8	309.5±0.7	327.5±3.5
	1	2.8/20-2.8	405.6±3.4	364.8±6.8	393.6±13.6
	1	5.6/40-5.6	415.5±3.4	412.1±7.3	386.2±9.8
	1	8.4/60-8.4	418.2±1.7	404.4±2.6	451.5±2.1
III[f]	2	0.7/5-0.7	452.8±2.8	423.9±1.4	510.8±1.4
	3	0.7/5-0.7	518.2±2.3	508.6±6.8	487.7±4.5
	1	1.4/10-1.4	527.7±2.5	519.4±2.7	495.0±0.0
	6	1.4/10-1.4	534.0±8.5	494.6±2.3	484.9±2.3
	1	2.8/20-2.8	484.0±0.0	526.0±2.8	534.0±2.8
	6	2.8/20-2.8	452.0±5.7	434.0±2.8	388.0±11.3
	1	5.6/40-5.6	516.0±3.4	445.2±3.4	450.0±3.4
	6	5.6/40-5.6	478.5±2.1	402.2±3.1	365.2±6.2
	1	8.4/60-8.4	482.4±5.6	410.4±3.4	349.5±6.4
	6	8.4/--	478.5±2.0	413.1±7.3	--
	1	27/--	492.0±5.7	276.0±4.2	--
	2	27/--	493.7±4.9	246.0±2.8	--
	3	27/--	--	269.1±2.4	--
	4	27/--	--	219.4±4.9	--
	2	--/60-8.4	--	--	295.5±6.4
	3	--/60-8.4	--	--	231.6±1.7
	4	--/60-8.4	--	--	235.2±3.4
IV[g]	1	--	472.7±2.2	328.0±5.7	306.0±8.5
	2	--	455.0±0.9	477.2±1.7	486.0±2.8
	3	--	471.0±5.2	484.0±5.7	508.8±6.8

[a] Feeding cycle at corresponding H_2O_2 and/or PAA concentration; [b] Control phase without H_2O_2 and/or PAA solution addition (duration, 40 d); [c] Mean ± standard deviation; [d] ND, not detected; [e] Indirect addition of H_2O_2 and/or PAA solution (duration, 54 d); [f] Direct addition of H_2O_2 and/or PAA solution (duration, 90 d); [g] Recovery phase without H_2O_2 and/or PAA solution addition (duration, 6 d).

144

Table 7.2 (Continued). Initial nitrate removal rates (NRR) and observed maximum nitrite levels in the three anoxic reactors in Phase I through IV.

Phase	No. Feeding Cycles[a]	Initial H_2O_2/ PAA-H_2O_2 (mg/L)	Maximum Nitrite Level (mg N/L)		
			R1	R2	R3
I[b]	1-20	--[b]	15.3±0.4[c]	16.3±0.1	18.4±0.3
II[e]	1	0.7/5-0.7	15.4±0.3	17.4±0.2	23.0±0.1
	1	1.4/10-1.4	17.3±0.1	18.9±0.1	26.2±0.3
	1	2.8/20-2.8	15.1±0.1	15.4±0.1	22.3±0.4
	1	5.6/40-5.6	25.4±0.1	19.3±1.1	25.2±0.2
	1	8.4/60-8.4	29.5±0.7	21.2±1.2	30.2±0.3
III[f]	2	0.7/5-0.7	34.0±1.4	30.7±0.4	43.7±0.5
	3	0.7/5-0.7	33.8±1.1	37.7±1.0	48.5±0.7
	1	1.4/10-1.4	45.1±0.1	37.4±0.9	54.0±1.4
	6	1.4/10-1.4	46.8±0.3	39.5±0.8	50.1±0.1
	1	2.8/20-2.8	49.0±1.3	40.5±0.7	55.2±0.3
	6	2.8/20-2.8	45.6±0.9	48.6±0.9	57.4±0.9
	1	5.6/40-5.6	44.8±1.1	48.7±0.5	59.6±0.6
	6	5.6/40-5.6	47.5±0.7	32.5±0.7	62.5±0.7
	1	8.4/60-8.4	43.4±1.4	41.1±0.1	102.5±2.1
	6	8.4/--	42.5±2.0	58.5±0.1	--
	1	27/--	42.0±0.7	75.4±0.2	--
	2	27/--	43.1±0.4	87.5±0.3	--
	3	27/--	--	92.4±0.1	--
	4	27/--	--	90.4±0.6	--
	2	--/60-8.4	--	--	128.8±1.1
	3	--/60-8.4	--	--	156.0±0.3
	4	--/60-8.4	--	--	150.4±0.2
IV[g]	1	--	30.4±0.2	60.6±0.6	76.8±0.1
	2	--	32.4±0.1	34.5±0.4	52.6±0.1
	3	--	32.1±0.5	30.7±0.1	33.4±0.2

[a] Feeding cycle at corresponding H_2O_2 and/or PAA concentration; [b] Control phase without H_2O_2 and/or PAA solution addition (duration, 40 d); [c] Mean ± standard deviation; [d] ND, not detected; [e] Indirect addition of H_2O_2 and/or PAA solution (duration, 54 d); [f] Direct addition of H_2O_2 and/or PAA solution (duration, 90 d); [g] Recovery phase without H_2O_2 and/or PAA solution addition (duration, 6 d).
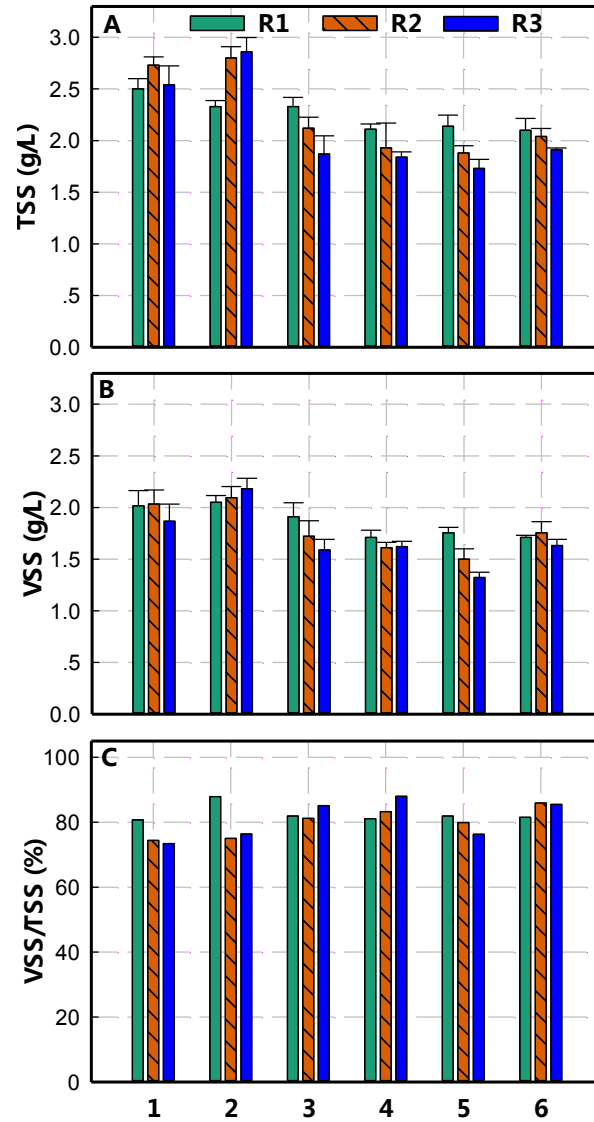
Figure 7.2. TSS (A) and VSS (B) concentration and VSS/TSS (%) (C) in the three anoxic reactors at different stages during the long-term operation (Phase I through IV). Condition: 1, Initial; 2, End of Phase I; 3, End of Phase II; 4, Phase III, end of 5.6/40 mg/L H_2O_2/PAA; 5, Phase III, end of 27/60 mg/L H_2O_2/PAA; 6, End of Phase IV (recovery) (Error bars are standard deviations).
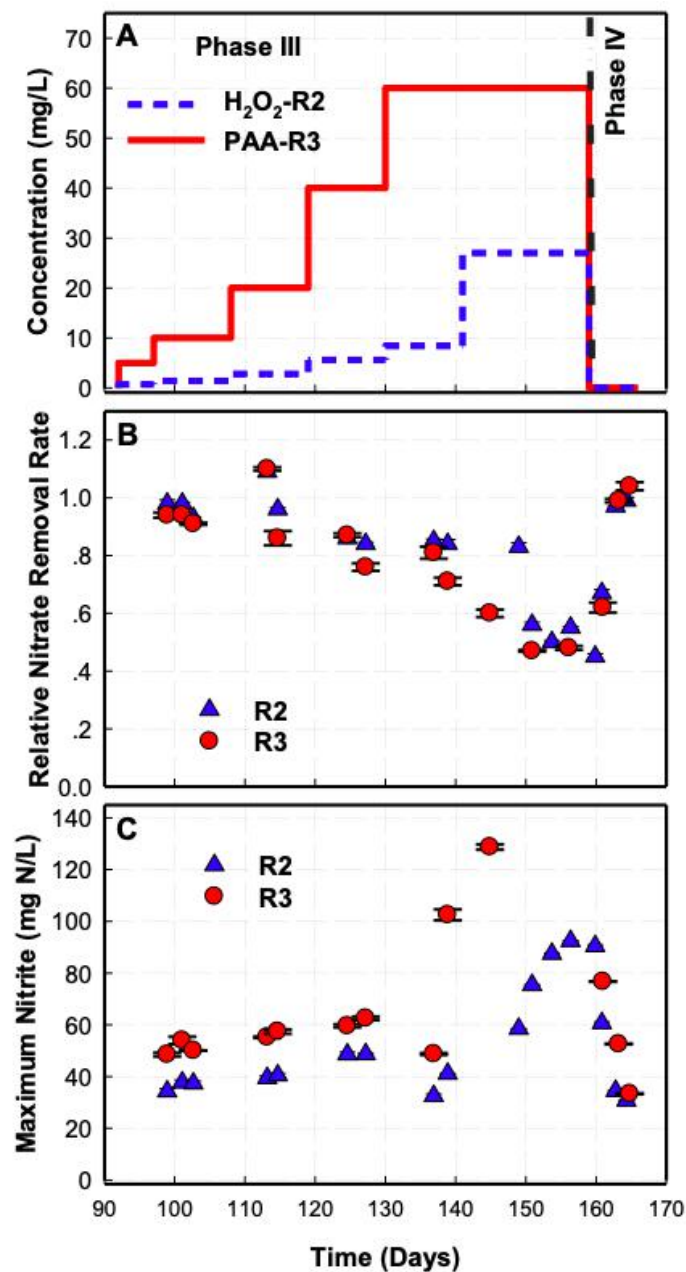
Figure 7.3. Initial, nominal reactor H₂O₂ and PAA concentration in Phase III (direct H₂O₂ and PAA solution addition) and IV (recovery) in R2 and R3 during the long-term operation (A); Relative nitrate removal rate (B); and Maximum observed nitrite concentration (C). Error bars are standard deviations.
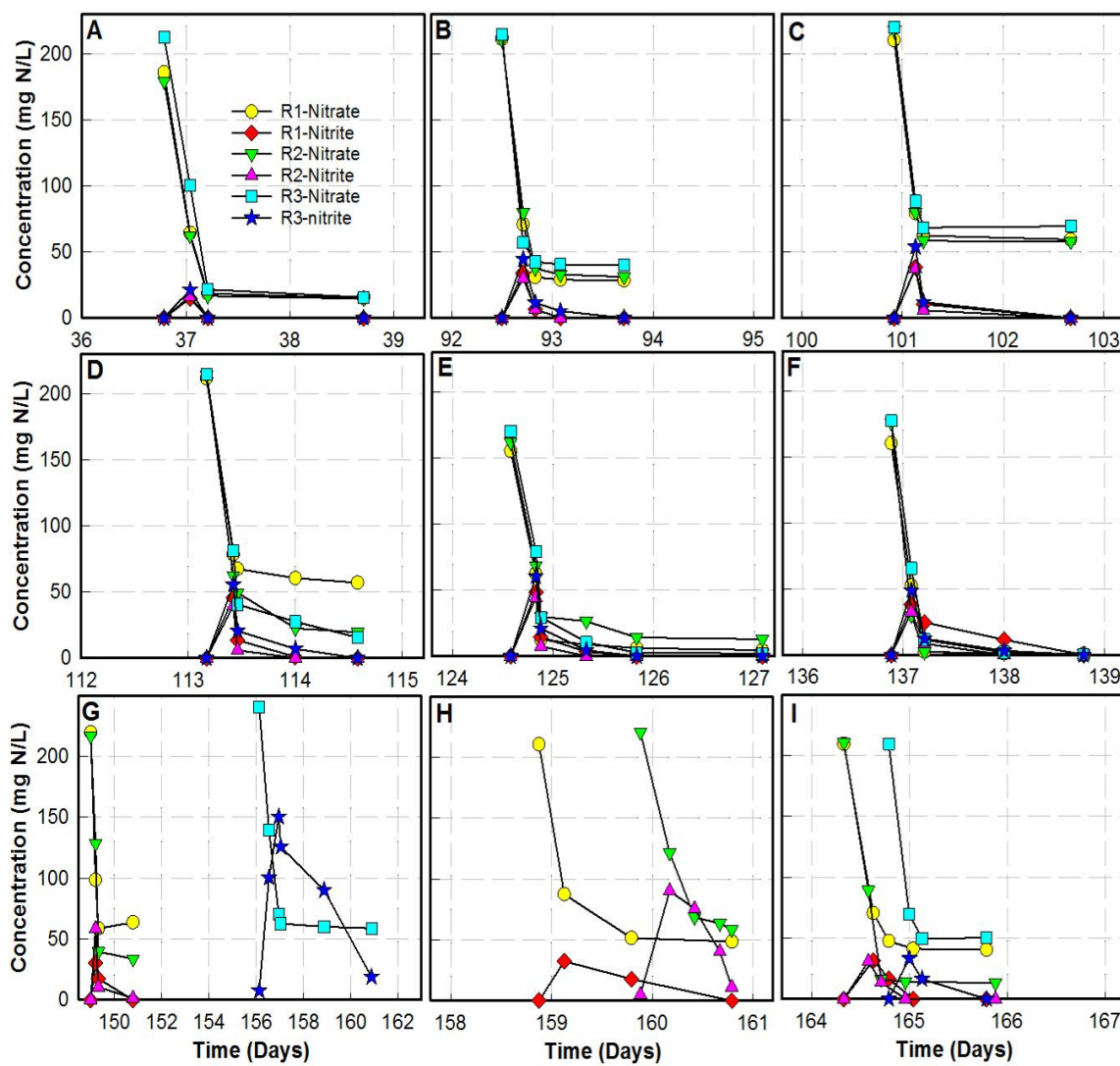
Figure 7.4. Time-trend of nitrate-N and nitrite-N in the three reactors at the end of Phase I (A), Phase II (B), Phase III last 5/0.7 (C), 10/1.4 (D), 20/2.8 (E), 40/5.6 (F), and 60/8.4 (G) mg/L PAA/H₂O₂ addition; last 27 mg/L H₂O₂ (H) addition; and Phase IV (I).

148
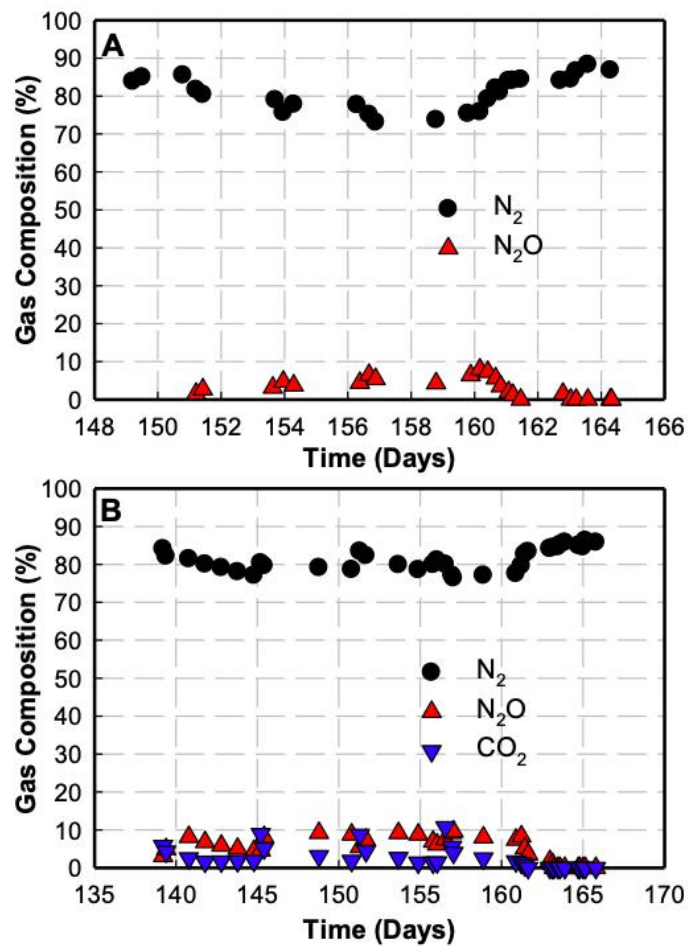
Figure 7.5. Headspace gas composition (%): N_2 and N_2O in R2 (A), N_2, N_2O, and CO_2 in R3 (B). (100% N_2 in R1 headspace not shown).

7.3.2 Short-term Anoxic Batch Assay

Table 7.3 summarizes the extent of sCOD removal, initial NRR and maximum observed nitrite level during the short-term batch assay conducted over time with mixed liquor from the long-term R1 reactor, then directly amended with PAA solution up to 60/8.4 mg/L PAA/H_2O_2. The time-trend of sCOD (Figure 7.6B) and sCOD removal extent (Table 7.3) were comparable among all batch series and similar to those achieved by the long-term R3 reactor upon the first direct addition of 60/8.4 mg/L PAA/H_2O_2. The TSS and VSS in the batch series with 5/0.7 and 10/1.4 mg/L initial PAA/H_2O_2 were comparable to those in the control, while the VSS in series with 20/2.8, 40/5.6, and 60/8.4 mg/L initial PAA/H_2O_2 direct addition was 18, 29 and 41% lower than in the control, respectively, suggesting that PAA/H_2O_2 $\geq$ 20/2.8 mg/L caused cell lysis (Figure 7.7).

Fast denitrification was completed within 30 h of incubation in all test series (Figure 7.6E). The NRR in the control and the series with 5/0.7 mg/L PAA/H_2O_2 were comparable, while the NRR decreased from ca. 513 to 229 mg N/L-d as the PAA/H_2O_2 concentration increased (Table 7.3). The specific NRR (NRR normalized to the mean VSS of each series) decreased from ca. 271 to 152 mg N/g VSS-d in series amended with PAA/H_2O_2 from 5/0.7 to 60/8.4 mg/L, respectively. The specific NRR in the long-term R3 gradually decreased from ca. 304 to 237 mg N/g VSS-d with direct addition of first 5/0.7 to first 60/8.4 mg/L PAA/H_2O_2, respectively. Therefore, the long-term R3 had a higher nitrate removal rate than the short-term batch assay in response to the same PAA solution dose. It is noteworthy that the decrease of VSS concentration, NRR, and RNRR were all higher in the batch series amended with 60/8.4 mg/L PAA/H_2O_2 than the long-term R3 at the end of Phase III; therefore, a certain degree of acclimation of the R3

150

microbial community to PAA solution took place over the long-term operation with PAA solution. It is also noteworthy that in the batch assay series with 60/8.4 mg/L PAA/H_2O_2, the decrease of VSS concentration (ca. 41%) was relatively close to the decrease of NRR (ca. 54%) (Figure 7.7); however, in the long-term R3 the VSS decrease (ca. 25%) was much lower than the NRR decrease (ca. 52%) (discussed in Section 7.3.1). Therefore, in the short-term batch assay, the negative impact on nitrate reduction is mainly attributed to the loss of biomass than enzyme inhibition, opposite of what was observed with the long-term R3.

The maximum nitrite concentration in the batch assay increased from 30 to 130 mg N/L as the initial PAA/H_2O_2 concentration increased from 0/0 to 60/8.4 mg/L (Figure 7.6F; Table 7.3). Complete nitrite removal was achieved in all batch series within 40 h of incubation, except the one amended with 60/8.4 mg/L PAA/H_2O_2 (Figure 7.6F). In contrast, the maximum observed nitrite levels in the long-term R3 after the first feeding with 20/2.8, 40/5.6 and 60/8.4 mg/L PAA/H_2O_2 were ca. 21%, 24% and 21% lower, respectively, than in the batch series at the same initial PAA/H_2O_2 concentrations (Tables 7.2 and 7.3). Overall, the denitrification performance of the long-term R3 was better than in the short-term batch assay, indicating that acclimation of the microbial community to PAA solution took place during the long-term operation. Similar to this observation, rapid microbial acclimation to fluctuating redox potential was observed in soil microbial communities (DeAngelis et al., 2010). Also, bacterial acclimation to ozone-produced oxidants (OPOs) was observed in a study which evaluated the impact of OPOs on nitrification in moving-bed biofilters in marine recirculating aquaculture systems (Schroeder et al., 2015).

Table 7.3. Extent of soluble COD removal, initial nitrate removal rate (NRR) and maximum observed nitrite level in batch assays conducted at a range of PAA solution levels using R1 mixed liquor.[a]

PAA/H$_2$O$_2$ (mg/L)	COD Removal (%)	NRR (mg N/L-d)	Maximum Nitrite Level (mg N/L)
0/0	94.5±0.3[b]	496.8±0.5	30.3±0.4
5/0.7	94.6±0.3	513.3±1.5	40.3±0.4
10/1.4	94.8±0.3	440.6±2.4	51.5±0.7
20/2.8	95.4±0.8	332.4±1.7	69.7±0.2
40/5.6	95.3±0.2	305.8±1.4	78.3±0.4
60/8.4	95.7±0.1	228.6±0.9	130.0±1.4

[a] Long-term R1 mixed liquor removed at the end of several feeding cycles, amended with PAA solution corresponding to PAA/H$_2$O$_2$ initial concentrations directly added to long-term R3 at different feeding cycles (Phase III).

[b] Mean ± standard deviation; [c] ND, not detected.
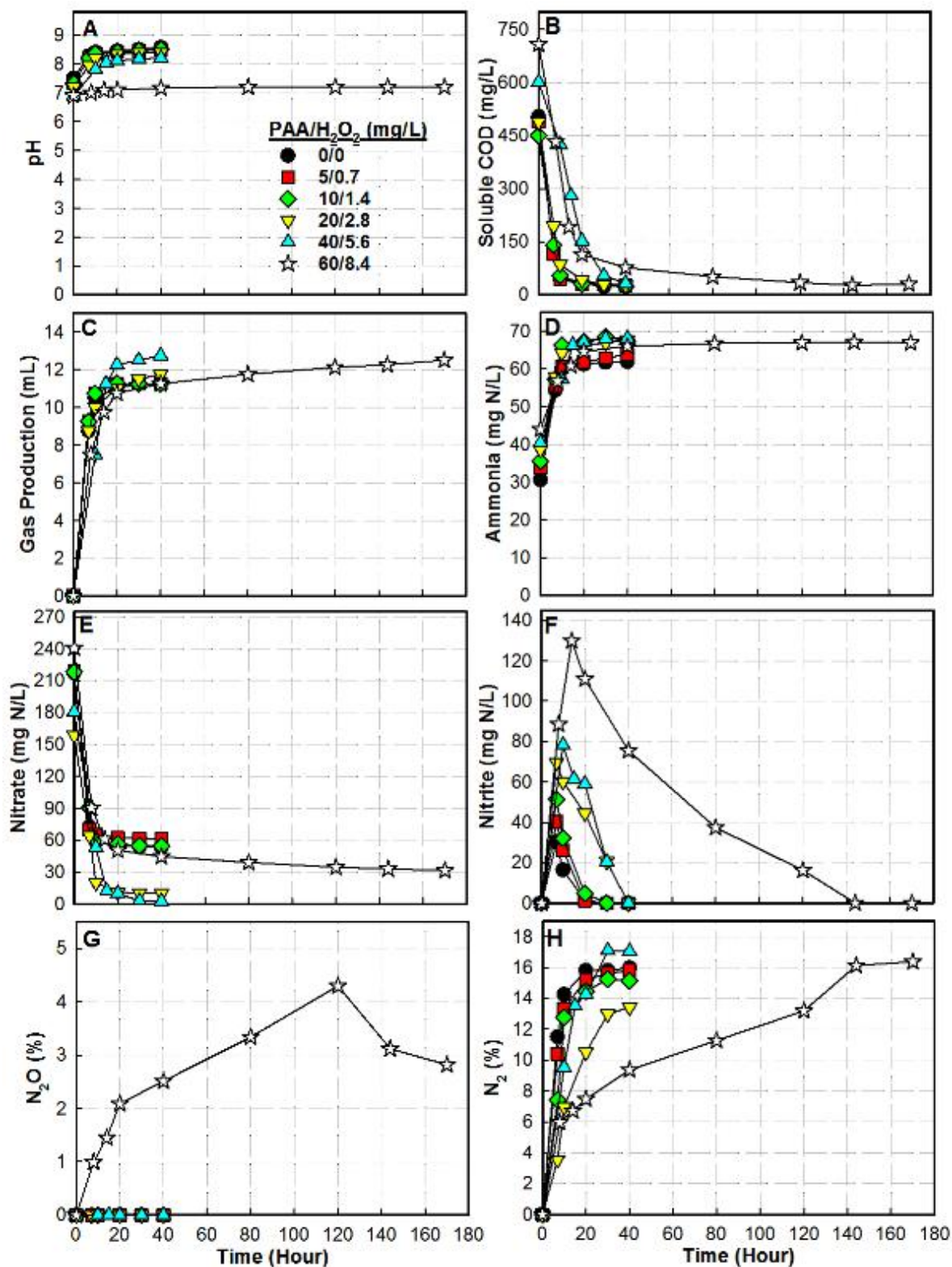
Figure 7.6. Time-trend of pH (A), soluble COD (B), gas production (C), ammonia (D), nitrate (E), nitrite (F), headspace N₂O (G), and headspace N₂ (H) during the incubation of the batch assays conducted with R1 mixed liquor.
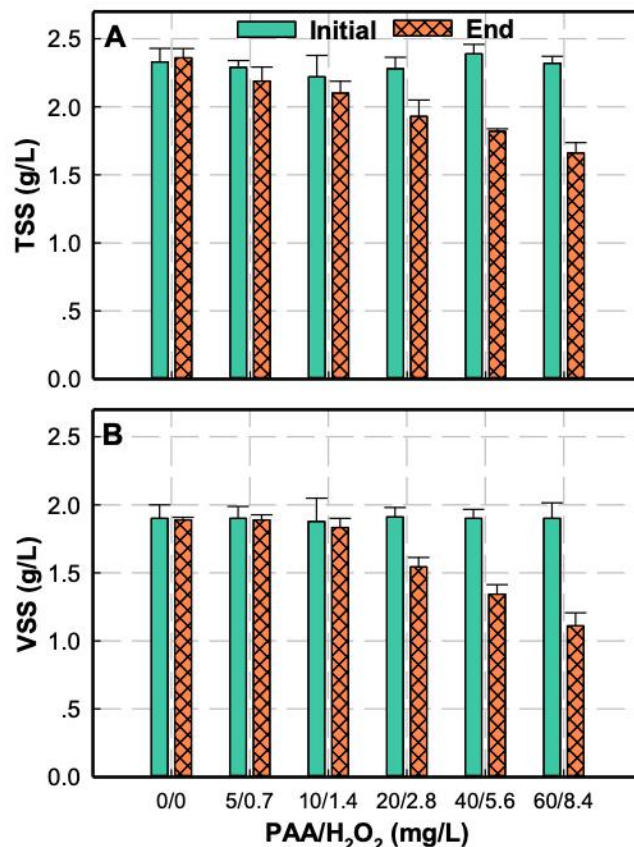
Figure 7.7. Initial and end of incubation TSS (A) and VSS (B) of batch assays conducted with R1 mixed culture amended with a range of initial PAA solution levels (Error bars are standard deviations).

7.3.3 Culture viability

The viability (i.e., fraction of live cells) of the microbial communities in the three, long-term operated bioreactors was evaluated at the end of Phase II, III, and IV with results shown in Figure 7.8A. Culture viability in R1 (control) was relatively the same across the three phases, ranging from 80 to 83%. At the end of Phase II, culture viability in the three bioreactors was comparable, ranging from 83 to 84%. Thus, indirect addition of solutions up to 8.4 mg H_2O_2/L and 60/8.4 mg/L PAA/H_2O_2 did not impact culture viability. In contrast, cell viability in R2 and R3 at the end of Phase III was ca. 15 and 27% lower than in R1, respectively. Thus, direct addition of PAA and/or H_2O_2 decreased

culture viability; the PAA effect was much greater than that of H_2O_2. By the end of Phase III, the NRR in R2 and R3 was 55 and 52% lower than in R1, respectively (Section 7.3.1), which is much higher than the decrease of cell viability in R2 (ca. 15%) and R3 (ca. 27%), suggesting the long-term negative impact of H_2O_2 in R2 on denitrification is predominantly attributed to enzyme inhibition while the impact of PAA solution on denitrification in R3 is attributed to both enzyme inhibition and loss of cell viability. At the end of Phase IV, culture viability in both R2 and R3 increased by 12 and 23%, respectively, both reaching a level comparable to the mean value in R1 (ca. 82%), indicating that the impact on culture viability was fast reversed after direct addition of PAA and/or H_2O_2 ended. Thus, given that during Phase IV the NRR increased by 54% and 56% in R2 and R3, respectively, further supports the above-stated conclusion relative to the long-term negative impact of H_2O_2 and PAA solution on denitrification.

In order to further evaluate culture viability in response to directly added PAA and H_2O_2, culture viability was measured by conducting a batch assay with R1 mixed liquor amended with a range of initial PAA solution or H_2O_2 levels, with results shown in Figure 7.8B. The cell viability in the batch assay decreased from 82.4 to 47.7% as PAA/H_2O_2 concentration increased from 0/0 to 60/8.4 mg/L and decreased from 84.7 to 52.8% as H_2O_2 concentration increased from 0 to 60 mg/L. Thus, direct addition of PAA and/or H_2O_2 decreased culture viability, and the degree of decrease was comparable at the same PAA and H_2O_2 concentration. However, on a molar concentration basis, 60 mg/L PAA is equal to 0.79 mM PAA while 60 mg/L H_2O_2 is equal to 1.76 mM H_2O_2. Also, 60 mg/L PAA is equal to 27 mg/L H_2O_2 on equivalent weight basis. Thus, H_2O_2 is weaker at reducing cell viability than PAA on an equivalent weight basis. It is noteworthy that

155

direct addition of 60/8.4 mg/L PAA/H$_2$O$_2$ in the batch series resulted in decreased cell

viability by ca. 42%, while it only decreased by ca. 27% in the long-term R3 at the end of

Phase III. Therefore, partial microbial community acclimation to PAA solution took

place during the long-term anoxic operation with addition of PAA solution.
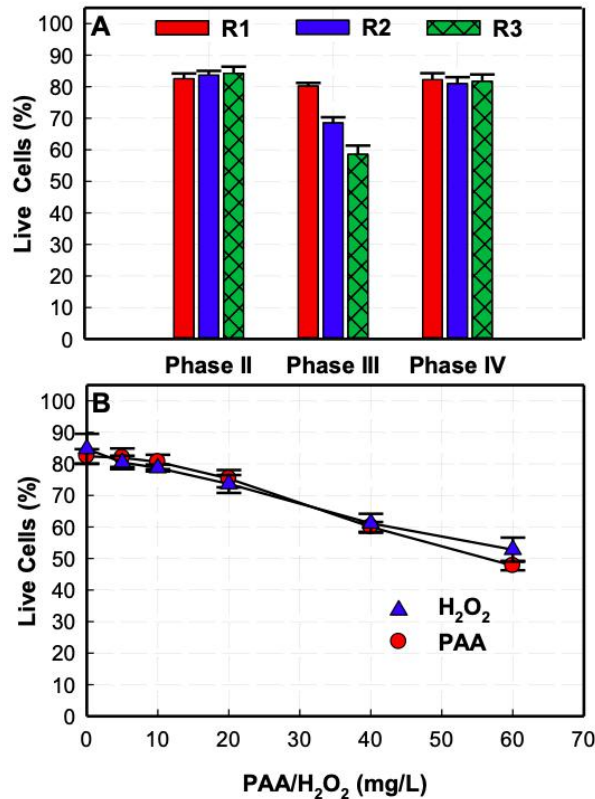
Figure 7.8. Fraction of live cells in the three long-term operated anoxic reactors measured at the end of Phase II, III, and IV (A); Fraction of live cells in R1 mixed liquor amended directly with PAA solution or H$_2$O$_2$ at an initial concentration range from 0 to 60 mg/L (B). Error bars are standard deviations.

7.3.4 Intracellular ROS

Intracellular ROS of the microbial communities in the three, long-term operated

bioreactors was evaluated at the end of Phase II, III, and IV with results shown in Figure

7.9A. At the end of Phase II, intracellular ROS in R2 and R3 cultures was 6 and 22%

lower than in R1 (control), respectively, suggesting indirect addition of PAA and/or H$_2$O$_2$

either inhibited intracellular ROS production or increased the levels of antioxidative

156

defense enzymes (e.g., catalase and superoxide dismutase) (Imlay, 2008), or both. Up-regulation of superoxide dismutase was induced in the halophilic, denitrifying bacterium *Pannonibacter* sp. strain DN in response to 3.5 mM hydroxyethane-(1,1-bisphosphonic acid; HEDP) (Koju et al., 2020). At the end of Phase III, the intracellular ROS in R2 and R3 cultures was 82% and 94% higher than in R1, respectively, suggesting that direct addition of H_2O_2 in R2 and PAA solution in R3 both caused cell oxidative stress to the anoxic cultures (Figure 7.9A). In a previous study, in response to 100 μM H_2O_2, production of intracellular ROS by *Pseudomonas stutzeri* under denitrifying conditions was more than 6-fold higher compared to the nitrifier *Nitrosomonas europaea* under aerobic conditions (Yang et al., 2012). Exposure to silver nanoparticles resulted in intracellular ROS production by *Pseudomonas stutzeri* under denitrifying conditions leading to decreased nitrate and nitrite reduction along with considerable decrease in the level of the requisite denitrification related gene expression (Wu et al., 2020).

At the end of Phase IV, the relative intracellular ROS in R2 and R3 cultures decreased to ca. 1.0, suggesting the previously caused oxidative stress during Phase III was removed during the recovery phase. Overall, H_2O_2 and PAA significantly affected the intracellular ROS of the H_2O_2-amended (R2) and PAA/H_2O_2-amended (R3) communities over the long-term operation of these reactors. Thus, oxidative stress caused by PAA and/or H_2O_2 may be another reason for the lower denitrification activity observed in both R2 and R3 in Phase III. Therefore, in addition to the reason for the observed decreased denitrification activity discussed in Section 7.3.1, above, the decrease in denitrification activity over the long-term operation with addition of H_2O_2 to R2 and

PAA/H_2O_2 to R3 was the combined effect of enzyme inhibition, loss of cell viability, and cell oxidative stress.

In order to further evaluate intracellular ROS in response to added PAA and H_2O_2, intracellular ROS was measured in a batch assay conducted with R1 mixed liquor and direct addition of PAA or H_2O_2 solutions up to 60 mg/L each with results shown in Figure 7.9B. The relative intracellular ROS of the long-term R1 culture with direct addition of H_2O_2 was ca. 1.0 at $H_2O_2 \leq 10$ mg/L and increased as the H_2O_2 concentration increased reaching the highest value of 2.8 at 60 mg/L H_2O_2. Likewise, the relative intracellular ROS of the long-term R1 culture with direct addition of PAA solution was ca. 1.0 at PAA/$H_2O_2 \leq 20/2.8$ mg/L and increased as the PAA solution dose increased, reaching the highest value of 3.6 at 60/8.4 mg/L PAA/H_2O_2. Overall, the R1 culture intracellular ROS was higher in response to the PAA solution than to H_2O_2.

The increase in intracellular ROS with increased concentration of H_2O_2 or PAA solution is attributed to extracellular ROS (PAA, H_2O_2, or other ROS produced by them) diffusion into the cells as a result of a high extracellular ROS concentration gradient, a high extent of cell membrane damage or both, while antioxidative defense enzymes could not completely quench the ROS.

Overall, high relative intracellular ROS was observed when these anoxic cultures were exposed to strong oxidants (i.e., H_2O_2, PAA). It is noteworthy that the increase of intracellular ROS was correlated with decreased NRR and cell viability, suggesting that the observed decrease of denitrification activity was related to the increased intracellular ROS and decreased cell viability. Similar to our results, a negative correlation between the production of intracellular ROS, denitrification activity and the expression level of

denitrification related genes was observed upon exposure of *Pseudomonas stutzeri* to silver nanoparticles (Wu et al., 2020). It is also noteworthy that the relative intracellular ROS of the R1 culture batch series at 60/8.4 mg/L PAA/H_2O_2 was much higher than that of the long-term R3 culture at the end of Phase III (3.6 vs. 1.2), suggesting that in addition to a higher denitrification activity, the capacity of the long-term R3 culture to overcome the effect of strong oxidants (i.e., H_2O_2, PAA) and cell oxidative stress increased during the long-term operation with addition of PAA solution.
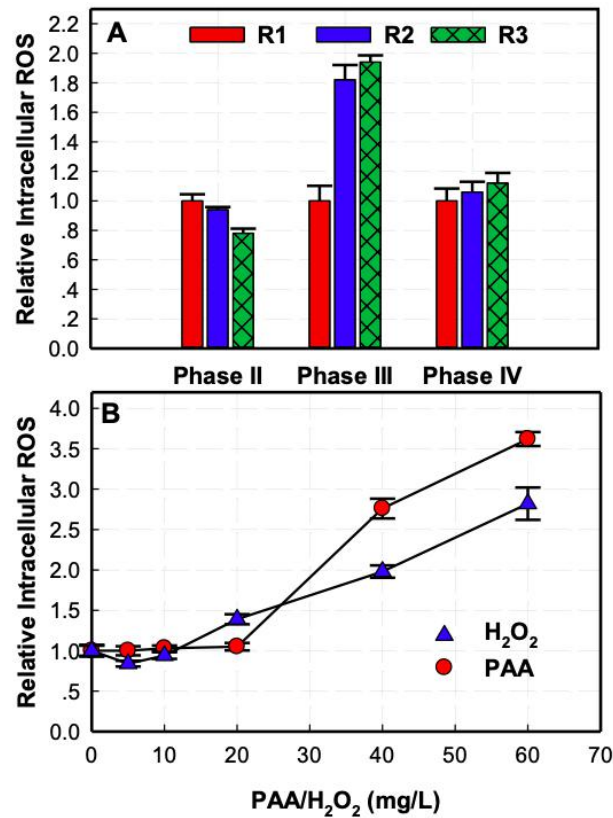
Figure 7.9. Intracellular reactive oxygen species (ROS) relative to R1 (control) in the three anoxic reactors at the end of Phase II, III and IV during the long-term operation (A); Relative intracellular ROS in R1 culture directly amended with PAA or H_2O_2 solution at an initial concentration range from 0 to 60 mg/L (B). Error bars are standard deviations.

7.3.5 Microbial community structure

Table 7.4 summarizes the total number of OTUs and microbial community diversity indices of the nine samples, including Shannon, Shannon Even, Chao, Ace and Simpson index. The total number of OTUs in the three reactors ranged from 417 to 472 from Phase II to Phase IV. Thus, the richness of the three reactors was comparable during the three phases of the long-term operation. Based on the Shannon index, the microbial community diversity in R1 (control) remained relatively constant throughout the 166-d of operation. The Shannon index of the three reactors was comparable at the end of Phase II (indirect addition of H_2O_2 and PAA solution), but at the end of Phase III (direct addition of H_2O_2 and PAA solution) the Shannon index of R3 was ca. 12% lower than the mean index of R1 and R2, indicating R3 had a higher diversity than R1 and R2 at the end of Phase III (Table 7.4).

Principle Component Analysis (PCA) results at order and genus level are comparable (Figure 7.10 and 7.11). At order level, from the end of Phase II to the end of Phase III (94 to 160 d), the microbial communities shifted significantly in the three reactors. On PC1 (89.71%), the communities in R1 and R2 shifted from the end of Phase II to the end of Phase III, indicating that the shifts on PC1 are attributed to the long-term operation of the reactors under anoxic conditions compared to the stock mixed culture which was subjected to alternating aerobic/anoxic/aerobic phases weekly. However, from the end of Phase II to the end of Phase III, the microbial community in R3 did not shift on PC1, which is more likely attributed to the strong oxidizing effect of PAA, added periodically, resulted in alternating anoxic/microaerobic conditions immediately after the addition of PAA, similar to the alternating aerobic/anoxic conditions of the stock mixed

160

culture. On PC2 (8.04%), at the end of Phase II, the microbial communities in the three reactors were clustered closely, indicating that indirect addition of H_2O_2 and PAA solutions did not result in a significant shift of the R2 and R3 communities, compared to the R1 community. However, at the end of Phase III, the R3 community had shifted far away from the closely clustered R1 and R2 on PC2 (Figure 7.10), indicating that direct addition of PAA solution changed the R3 microbial community composition significantly.

Table 7.5 summarizes the relative abundance of the top 25 orders in the communities of the three reactors at the end of Phase II, III and IV. Across the three reactors, the most abundant orders were *Flavobacteriales* (4 to 46%), *Rhodocyclales* (5 to 30%), *Xanthomonadales* (7 to 27%), *Sphingobacteriales* (3 to 17 %), *Rhodobacterales* (8 to 12%), and unclassified *Bacteroidetes* (1 to 11%), and *Burkholderiales* (5 to 9%). The following discussion on the relative abundance at order level in the communities of the three reactors refers to changes from the end of Phase II to the end of Phase III. In both R1 and R2, *Flavobacteriales* relative abundance decreased by ca. 7-fold while *Rhodocyclales* relative abundance increased by ca. 1.5-fold. However, *Flavobacteriales* relative abundance in R3 remained almost the same and *Rhodocyclales* relative abundance decreased by ca. 0.35-fold. Thus, direct addition of PAA alone or in combination with H_2O_2 did not affect *Flavobacteriales* but affected *Rhodocyclales*. In both R1 and R2 *Sphingobacteriales* relative abundance increased by ca. 2-fold while in R3 decreased by ca. 0.35-fold. Thus, PAA alone or in combination with H_2O_2 negatively affected *Sphingobacteriales*. *Xanthomonadales* relative abundance in R1 and R2 remained almost the same while in R3 increased by ca. 1.5-fold, suggesting that direct addition of PAA solution resulted in the enrichment of *Xanthomonadales*.

Burkholderiales in R1 and R2 increased by ca. 1.5- and 1.7-fold, respectively, while remained nearly unchanged in R3, suggesting that direct addition of PAA solution negatively affected *Burkholderiales.*

Table 7.6 summarizes the relative abundance at genus level in the communities of the three reactors at the end of Phase II, III and IV. Figure 7.12 and 7.13 show the relative abundance of the communities at genus level. The major denitrifying genera were *Thauera, Thermomonas,* and *Chryseobacterium,* and the unclassified families *Chitinophagaceae* and *Enterobacteriaceae*. The following discussion on the change of relative abundance at genus level in the communities of the three reactors refers to changes from the end of Phase II to the end of Phase III. The composition of the R1 and R2 communities at genus level was very close, while that of R3 was significantly different. *Thauera* increased from a mean 9% to 22% in R1 and R2, while decreased from 8% to 5% in R3. Similarly, *Chitinophagaceae* increased from a mean 5% to 13% in R1 and R2, while decreased from 5% to 2% in R3. In contrast, *Thermomonas* remained at a mean 9% in R1 and R2, while increased from 9% to 24% in R3. Therefore, among the three denitrifying genera, *Thauera* and unclassified *Chitinophagaceae* were negatively impacted by the PAA solution while *Thermomonas* was enriched. *Chryseobacterium* remained below 2% in both R1 and R2, but increased from 1% to 25% in R3, suggesting that *Chryseobacterium* was not negatively impacted during the long-term operation with addition of PAA solution, but instead was enriched. Fontoura et al. (2019) reported that when *Chryseobactrium* sp. kr6 was grown in a chicken feather medium for feather hydrolysate production, a novel antioxidant peptide was produced; its antioxidant activity was evaluated using the 2,2′-azino- bis-(3-ethylbenzothiazoline)-6-sulfonic acid (ABTS)

162

radical scavenging method. Kundu et al. (2014) reported that *Chryseobacterium* sp. R31 are able to perform denitrification under aerobic conditions. The results of these two studies may explain the observed increase of *Chryseobactrium* in R3 during Phase III. First, *Chryseobacterium* produces an antioxidant peptide which might react with PAA; second, it is able to perform denitrification under aerobic conditions, which matches the conditions in R3 where O_2 was produced by both PAA and H_2O_2 as discussed in Section 3.1.3, above. Similarly, unclassified *Enterobacteriaceae* was always below 0.1% in R1 and R2, while increased from <0.1% to 1.4% in R3 from the end of Phase II to the end of Phase III, suggesting that *Enterobacteriaceae* was not negatively impacted by the PAA solution. Hmidet et al. (2019) reported antioxidant lipopeptides were produced by *Enterobacter cloacae*. *Enterobacteriaceae* have also been reported to perform aerobic denitrification (Guo et al., 2016). Thus, similar to the case of *Chryseobacterium*, these two studies also provide potential reasons of the observed increase of *Enterobacteriaceae* in R3 during Phase III.

Table 7.4. Number of reads, OTUs and alpha diversity indices of the microbial communities in the three anoxic bioreactors over their long-term operation.

Sample	Reads	OTUs	Alpha Diversity Index				
			Shannon	Shannon Even	Chao	Ace	Simpson
AN1P2	119363	461	2.945	0.480	564.056	562.620	0.149
AN2P2	106824	425	2.797	0.462	546.727	533.450	0.175
AN3P2	110889	428	2.889	0.477	529.019	539.530	0.155
AN1P3	87766	472	3.358	0.545	674.784	610.990	0.080
AN2P3	98089	451	3.380	0.553	514.851	539.647	0.070
AN3P3	100106	417	2.946	0.488	485.357	498.765	0.116
AN1P4	83952	454	3.251	0.531	528.417	539.202	0.099
AN2P4	74308	432	3.379	0.557	522.000	537.746	0.074
AN3P4	93608	424	3.023	0.500	515.122	516.648	0.105

Abbreviations: AN1, AN2, and AN3 correspond to reactors R1, R2, and R3; P2, P3, and P4 correspond to end of Phase II, III, and IV.

Table 7.5. Relative abundance at order level (top 25 orders) of the microbial communities in the three anoxic bioreactors over their long-term operation.

Order	AN1P2	AN2P2	AN3P2	AN1P3	AN2P3	AN3P3
Actinomycetales	0.18	0.16	0.11	0.23	0.18	0.16
Bacteroidales	0.31	0.11	0.06	0.48	0.25	0.16
Burkholderiales	5.17	4.78	5.23	7.60	8.31	5.93
Caulobacterales	0.16	0.15	0.13	0.15	0.14	0.13
Cytophagales	0.40	0.35	0.35	0.45	0.50	0.32
Enterobacteriales	0.09	0.07	0.05	0.08	0.06	1.44
Flavobacteriales	42.36	45.96	42.63	5.75	5.94	38.98
Nitrosomonadales	0.26	0.25	0.25	0.49	0.48	0.24
Planctomycetales	0.26	0.26	0.26	0.44	0.44	0.24
Pseudomonadales	0.24	0.16	0.17	0.24	0.16	0.22
Rhizobiales	0.99	0.97	0.93	1.53	1.45	1.25
Rhodobacterales	8.53	8.26	8.86	9.47	12.46	8.78
Rhodocyclales	10.13	8.69	8.16	24.59	20.21	5.38
Rhodospirillales	0.23	0.20	0.21	0.24	0.24	0.12
Selenomonadales	0.14	0.08	0.04	0.10	0.09	0.04
Sphingobacteriales	7.52	6.92	7.61	13.39	15.12	2.83
Sphingomonadales	0.26	0.26	0.22	0.27	0.30	0.28
Xanthomonadales	11.44	11.07	11.88	12.50	10.43	27.27
norank Acidobacteria Gp3	0.18	0.15	0.14	0.25	0.28	0.03
norank Acidobacteria Gp4	0.79	0.63	0.67	1.15	1.55	0.24
Unclassified						
α-*Proteobacteria*	0.81	0.77	0.70	0.67	0.81	0.61
Bacteria	1.25	1.32	1.56	3.21	3.48	1.36
Bacteroidetes	3.81	4.44	5.87	8.03	11.10	1.34
β-*Proteobacteria*	2.74	2.71	2.42	5.76	3.73	1.56
γ-*Proteobacteria*	0.25	0.20	0.19	0.67	0.47	0.16

Abbreviations: AN1, AN2, and AN3 correspond to reactors R1, R2, and R3; P2, P3, and P4 correspond to end of Phase II, III, and IV.

Role: AO, ammonia oxidation; OD, organics degradation; PR, P removal; NR, nitrite reduction; NF, nitrogen fixation; FAD, fatty acids degradation; OAD, oxalic acid degradation; SS, sterols synthesis.

References: (1) Garrity, 2005; (2) Enke et al., 2018; (3) Garrity, 2005; (4) Pearson et al., 2003; (5) Young et al., 2001; (6) Maszenan et al., 1997; (7) Boden et al., 2017; (8) Finkman et al., 2000.

Table 7.5 (Continued). Relative abundance at order level (top 25 orders) of the microbial communities in the three anoxic bioreactors over their long-term operation.

Order	AN1P4	AN2P4	AN3P4	Role[a]	Ref.
Actinomycetales	0.22	0.17	0.16		
Bacteroidales	0.34	0.25	0.18		
Burkholderiales	8.42	8.84	6.06	OAD	(1)
Caulobacterales	0.15	0.14	0.13		
Cytophagales	0.43	0.61	0.32		
Enterobacteriales	0.09	0.09	1.21		
Flavobacteriales	4.28	5.53	39.00	OD	(2)
Nitrosomonadales	0.62	0.47	0.23	AO	(3)
Planctomycetales	0.35	0.44	0.27	SS	(4)
Pseudomonadales	0.23	0.17	0.20		
Rhizobiales	1.48	1.51	1.40	NF	(5)
Rhodobacterales	8.28	12.40	10.18	PR	(6)
Rhodocyclales	30.36	21.99	5.63	FAD	(7)
Rhodospirillales	0.21	0.24	0.11		
Selenomonadales	0.09	0.11	0.06		
Sphingobacteriales	12.69	16.93	3.05		
Sphingomonadales	0.22	0.22	0.30		
Xanthomonadales	11.33	6.68	24.71	NR	(8)
norank_Acidobacteria_Gp3	0.15	0.35	0.05		
norank_Acidobacteria_Gp4	0.99	1.58	0.28		
Unclassified					
α-Proteobacteria	0.67	0.80	0.66		
Bacteria	2.60	3.37	1.23		
Bacteroidetes	7.18	11.10	1.24		
β-Proteobacteria	6.14	3.63	1.53		
γ-Proteobacteria	0.55	0.43	0.16		

Abbreviations: AN1, AN2, and AN3 correspond to reactors R1, R2, and R3; P2, P3, and P4 correspond to end of Phase II, III, and IV.

Role: AO, ammonia oxidation; OD, organics degradation; PR, P removal; NR, nitrite reduction; NF, nitrogen fixation; FAD, fatty acids degradation; OAD, oxalic acid degradation; SS, sterols synthesis.

References: (1) Garrity, 2005; (2) Enke et al., 2018; (3) Garrity, 2005; (4) Pearson et al., 2003; (5) Young et al., 2001; (6) Maszenan et al., 1997; (7) Boden et al., 2017; (8) Finkman et al., 2000

Table 7.6. Relative abundance at genus level of the microbial communities in the three anoxic bioreactors over their long-term operation.

Genus	AN1P2	AN2P2	AN3P2	AN1P3	AN2P3	AN3P3
Thauera	10.02	8.59	8.06	24.34	20.05	5.26
Thermomonas	8.33	9.61	9.44	10.63	8.46	23.53
Chryseobacterium	1.94	1.48	1.34	0.48	0.59	25.09
Paracoccus	3.76	3.48	4.22	4.25	5.97	5.64
Niabella	1.38	1.90	1.92	0.27	0.48	0.40
Taibaiella	0.25	0.37	0.30	0.91	1.20	0.40
Unclassified Bacteria						
Flavobacteriaceae	40.13	44.17	41.17	5.03	5.19	13.58
Chitinophagaceae	5.83	4.56	5.30	12.14	13.38	1.95
Bacteroidetes	3.81	4.44	5.87	8.03	11.10	1.34
Rhodobacteraceae	4.51	4.53	4.40	5.00	6.19	2.92
Comamonadaceae	2.92	2.59	2.94	4.29	5.04	4.22
β-proteobacteria	2.74	2.71	2.42	5.76	3.73	1.56
Bacteria	1.25	1.32	1.56	3.21	3.48	1.36
Xanthomonadaceae	2.47	0.92	1.89	1.27	1.43	2.93
Burkholderiales	1.53	1.55	1.67	2.00	1.85	0.48
Acidobacteria_Gp4	0.79	0.63	0.67	1.15	1.55	0.23
Enterobacteriaceae	0.08	0.06	0.05	0.08	0.05	1.44
Other	8.25	7.08	6.78	11.15	10.26	7.67

Abbreviations: AN1, AN2, and AN3 correspond to reactors R1, R2, and R3; P2, P3, and P4 correspond to end of Phase II, III, and IV.

Role: DN, denitrification; ATO, anti-oxidizing.

References: (9) Shinoda et al., 2004; (10) Mergaert et al., 2003; (11) Fontoura et al., 2019; (12) Kundu et al., 2014; (13) Torrentó et al., 2011; (14) Hmidet et al., 2019; (15) Fu et al., 2020.

Table 7.6 (Continued). Relative abundance at genus level of the microbial communities in the three anoxic bioreactors over their long-term operation.

Genus	AN1P4	AN2P4	AN3P4	Role	Ref.
Thauera	30.08	21.82	5.52	DN	(9)
Thermomonas	9.50	5.06	21.32	DN	(10)
Chryseobacterium	0.42	0.57	23.34	ATO, DN	(11), (12)
Paracoccus	3.72	6.13	7.11		
Niabella	0.25	0.52	0.39		
Taibaiella	0.54	0.99	0.45		
Unclassified Bacteria					
Flavobacteriaceae	3.64	4.73	15.42		
Chitinophagaceae	11.85	15.36	2.16	DN	(13)
Bacteroidetes	7.18	11.10	1.24		
Rhodobacteraceae	4.30	5.97	2.84		
Comamonadaceae	4.29	5.20	4.31		
β-proteobacteria	6.14	3.63	1.53		
Bacteria	2.60	3.37	1.23		
Xanthomonadaceae	1.24	1.19	2.62		
Burkholderiales	2.69	2.24	0.55		
Acidobacteria_Gp4	0.99	1.58	0.28		
Enterobacteriaceae	0.09	0.09	1.21	ATO, DN	(14), (15)
Other	10.48	10.45	8.47		

Abbreviations: AN1, AN2, and AN3 correspond to reactors R1, R2, and R3; P2, P3, and P4 correspond to end of Phase II, III, and IV.

Role: DN, denitrification; ATO, anti-oxidizing.

References: (9) Shinoda et al., 2004; (10) Mergaert et al., 2003; (11) Fontoura et al., 2019; (12) Kundu et al., 2014; (13) Torrentó et al., 2011; (14) Hmidet et al., 2019; (15) Fu et al., 2020.
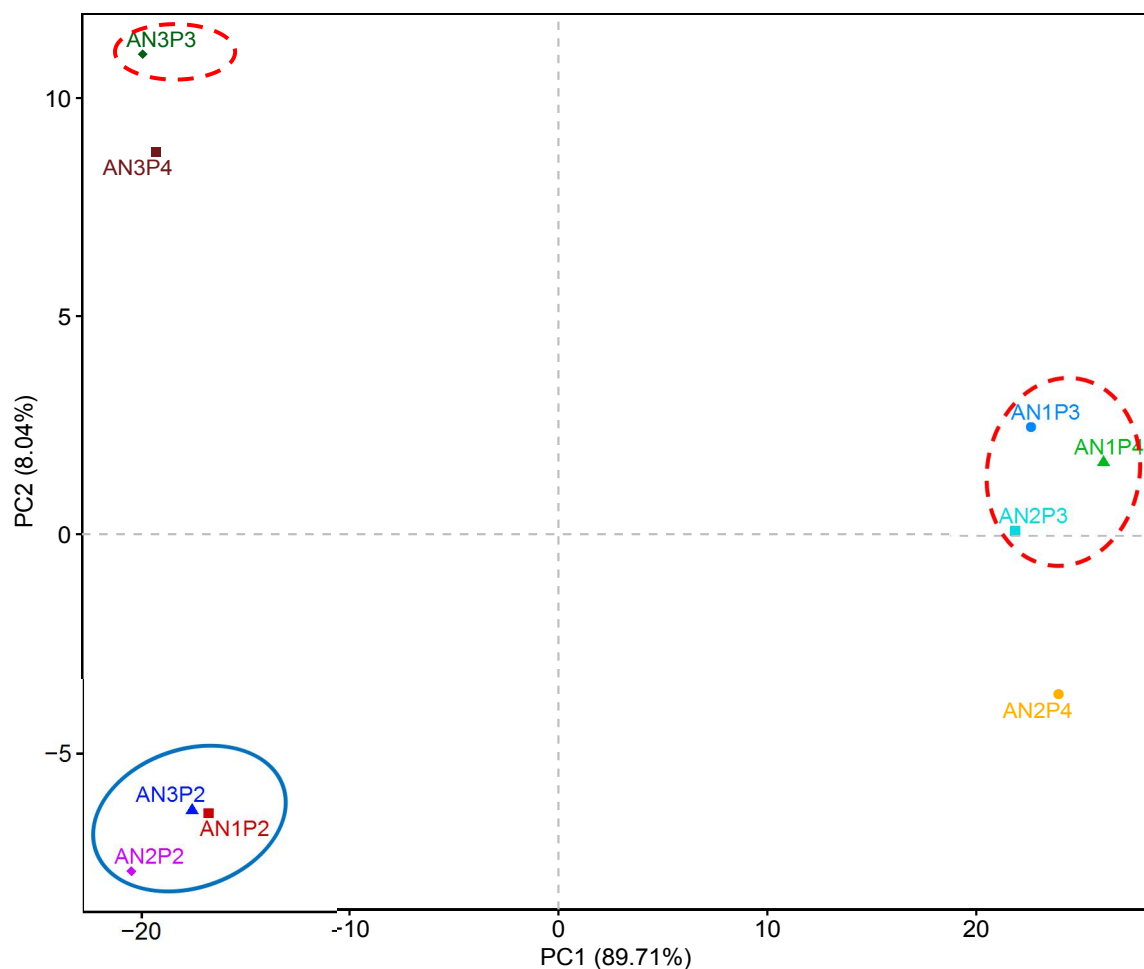
Figure 7.10. Principal component analysis at order level of the microbial communities in the three long-term bioreactors at the end of Phase II (solid blue circle), III (broken red circle) and IV.

Abbreviations: AN1, AN2, and AN3 correspond to reactors R1, R2, and R3; P2, P3, and P4 correspond to end of Phase II, III, and IV.
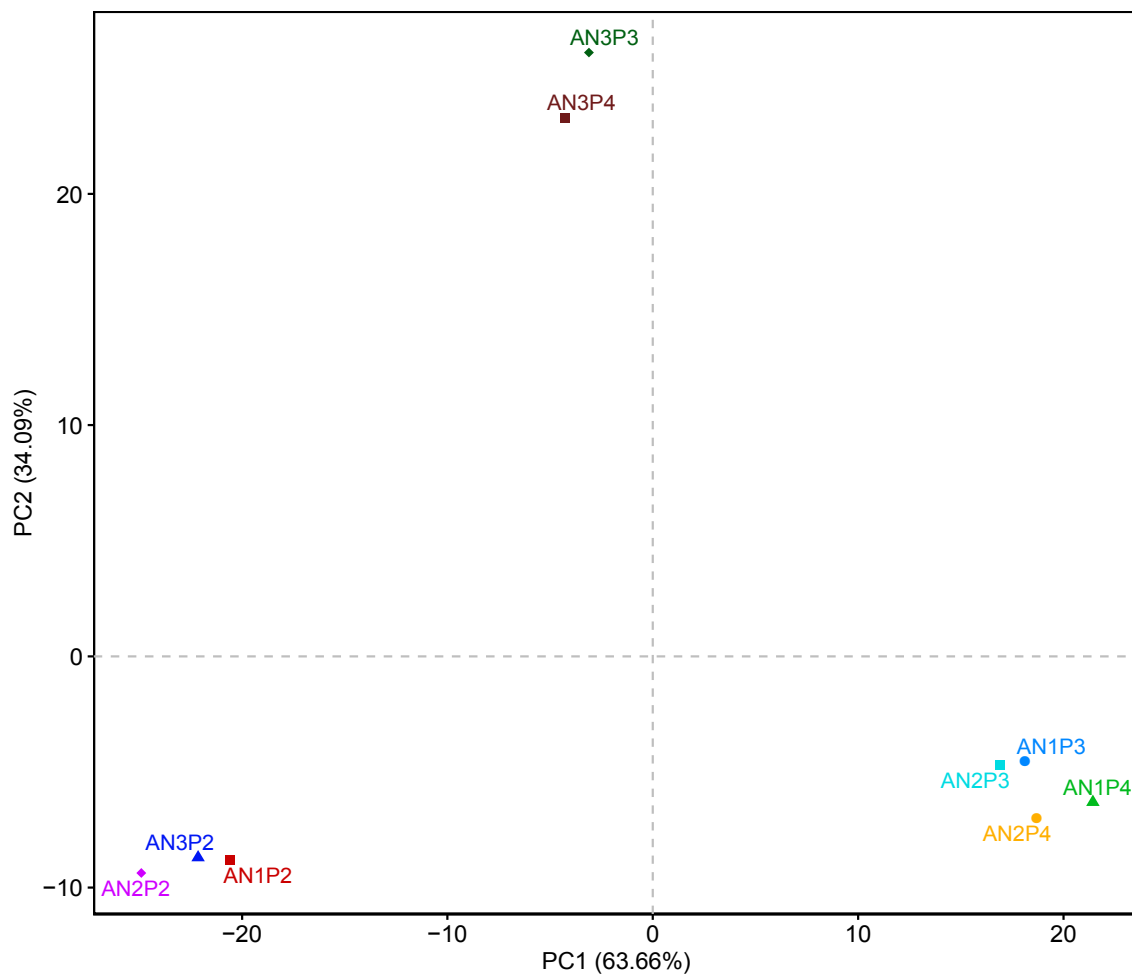
Figure 7.11. Principal component analysis at genus level of the microbial communities in the three long-term bioreactors at the end of Phase II, III and IV.

Abbreviations: AE1, AE2, and AE3 correspond to reactors R1, R2, and R3; P2, P3, and P4 correspond to end of Phase II, III, and IV.
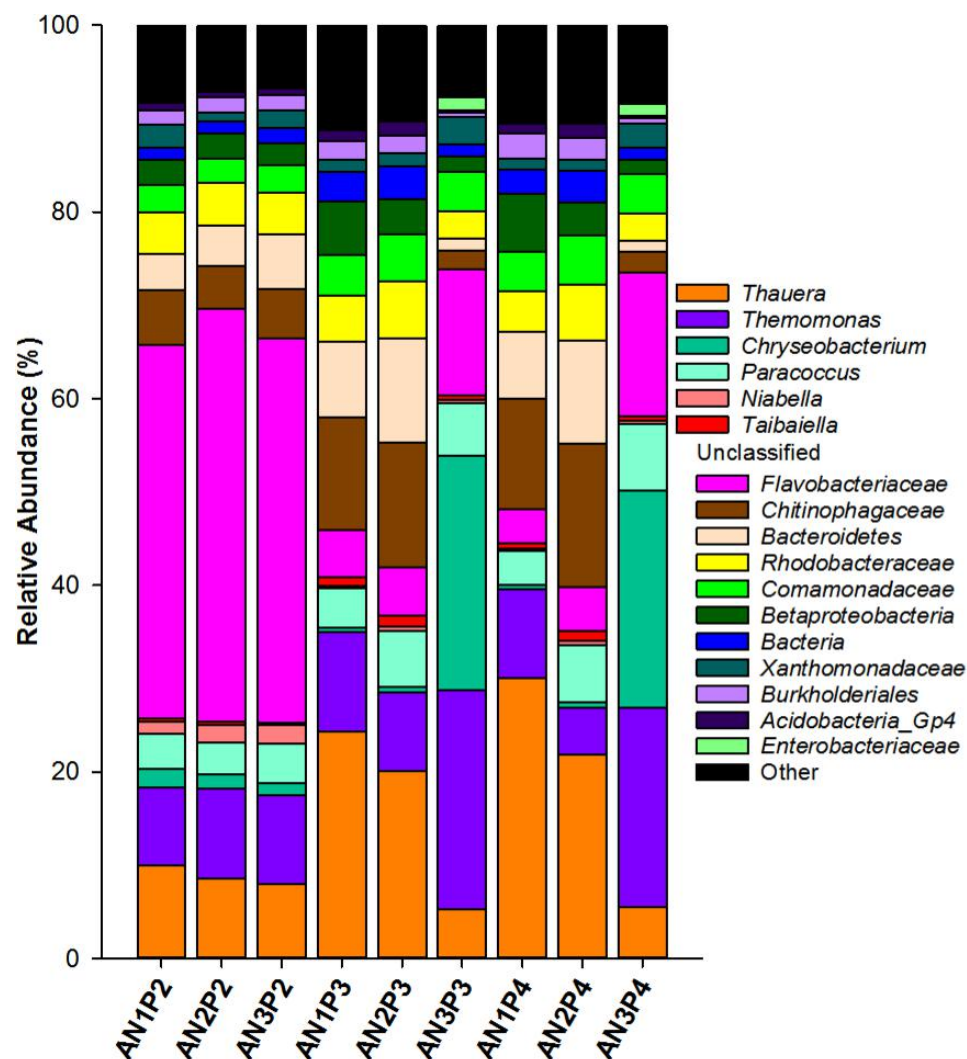
Figure 7.12. Relative abundance at genus level of the microbial communities in the three anoxic long-term bioreactors at the end of Phase II, III and IV.

Abbreviations: AN1, AN2, and AN3 correspond to reactors R1, R2, and R3; P2, P3, and P4 correspond to end of Phase II, III, and IV.
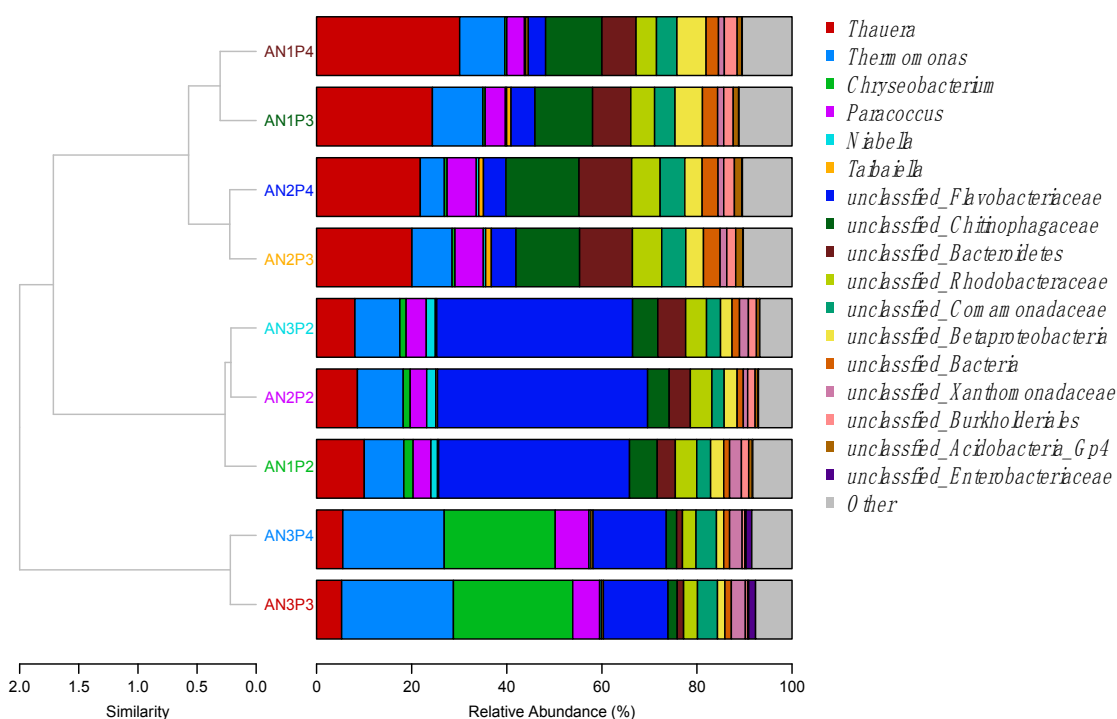
Figure 7.13. Relative abundance TreeBar plot at genus level of the microbial communities in the three long-term bioreactors at the end of Phase II, III and IV.

Abbreviations: AN1, AN2, and AN3 correspond to reactors R1, R2, and R3; P2, P3, and P4 correspond to end of Phase II, III, and IV.

7.4 Summary

Peracetic acid (PAA) has been extensively used as a sanitizer in many industries; its use in poultry processing is steadily increasing. However, information related to the potential inhibitory effect of PAA solutions (PAA and H_2O_2) on biological wastewater treatment processes used by the poultry processing industry is extremely limited. The work reported here assessed the long-term effect of PAA solution on anoxic organic matter degradation and denitrification in three bioreactors fed with poultry processing wastewater by quantifying the extent of COD removal and nitrate removal rate. Changes in culture viability, intracellular reactive oxygen species (ROS), and microbial

172

community structure were also evaluated. Indirect and direct addition of H_2O_2 and PAA at gradually increased concentrations up to 60 mg PAA/L and up to 27 mg H_2O_2/L did not significantly affect the anoxic organic matter degradation in the poultry processing DAF wastewater, quantified as the extent of sCOD removal. However, the PAA solution negatively affected denitrification at 60/8.4 mg/L PAA/H_2O_2. The effect of PAA solution on denitrification was predominantly attributed to PAA alone or in combination with H_2O_2. Microbial acclimation to PAA solution took place over the long-term operation. Both anoxic organic matter degradation and denitrification recovered fast after PAA and/or H_2O_2 direct addition ended. The observed decrease in NRR, transient high nitrite level, and N_2O production are attributed to both enzyme inhibition and loss of cell viability. The increase of intracellular ROS in response to PAA and/or H_2O_2 is related to the observed decrease in denitrification activity, but the capacity of the microbial community to manage PAA/H_2O_2-induced cell oxidative stress increased over the long-term operation with addition of PAA solution. The microbial community composition in R3 shifted significantly over the long-term operation with addition of PAA solution, but in R2 (H_2O_2-amended) remained close to the control (R1). The denitrifying genera *Thauera* and unclassified *Chitinophagaceae* were negatively impacted by PAA solution, whereas *Chryseobacterium* and *Enterobacteriaceae* were enriched over the long-term operation with addition of PAA solution, more likely the result of antioxidants production and their ability to perform aerobic denitrification. Overall, the results of this study suggest that anoxic organic matter degradation and denitrification of poultry processing wastewater will not be affected during the normal plant operation when residual PAA and H_2O_2 are not present in the wastewater. However, denitrification will be affected when

wastewater with high residual PAA concentrations is expected at the end of plant

operational shifts due to emptying of chiller tanks, or in the case of accidental PAA

solution spills.

CHAPTER 8. LONG-TERM EFFECT OF PAA SOLUTION ON A BIOLOGICAL NITROGEN REMOVAL (BNR) SYSTEM

8.1 Introduction

Wastewater generated during sanitation practices in poultry processing facilities is combined with other wastewater streams and typically treated in dissolved air floatation (DAF) units, followed by biological nitrogen removal (BNR) systems comprised of a combination of fermentation, nitrification and denitrification along with aerobic/anoxic degradation of organic matter. Achieving efficient BNR is only possible by sustaining the biological processes involved and their microbial populations at their optimum physiological and environmental conditions. However, industry reports refer to PAA in poultry processing wastewater as part of the regular disinfection process and/or because of accidental spills, suspected of leading to severe upsets of biological wastewater treatment processes, especially BNR, thus making it difficult to meet effluent discharge requirements. In spite of the negative impact on the effluent quality in the case of upset biological treatment processes, to the best of our knowledge no information is available relative to the fate and effect of PAA solutions on poultry processing wastewater biological treatment processes. Our study has documented PAA carryover into various poultry processing waste streams and its decomposition in such streams (see Chapter 4, Section 4.3). Previous tests related to the effect of PAA solution on BNR processes, such as nitrification, denitrification, and organic matter degradation were conducted on individual biological processes within the confine of a single environmental condition

175

(aerobic or anoxic) and did not assess the effect of PAA solution on multiple processes in series (e.g., sequence of nitrification/denitrification) (see Chapter 6 and 7).

The objectives of the study described in this chapter were to a) systematically assess the fate and long-term effect of a PAA solution on a continuous-flow, bench-scale BNR system (anaerobic-anoxic-aerobic reactors in series with internal recycle) for an in-depth assessment of the three sub-processes (i.e., organic matter removal, nitrification, denitrification); b) evaluate the diversity and stability of microbial communities in the BNR system upon exposure to the PAA solution.

8.2 Materials and Methods

8.2.1 Chemicals and Wastewater

Chemicals are as described in Chapter 3, Section 3.2.1. Wastewater is described in Chapter 6, Section 6.2.1.

8.2.2 Setup and Operation of the Continuous-flow BNR System

The BNR system consisted of three reactors: an anaerobic fermentation reactor (R1, 8 L) used to provide readily degradable organic carbon to be used in subsequent denitrification, an anoxic reactor (R2, 4 L) for denitrification, and an aerobic reactor (R3, 5 L reactor, plus a 1.5 L internal settler for biomass recycle) for nitrification (Figure. 8.1). The BNR system was maintained at room temperature ($22\pm1^{o}C$). Mixed liquor was recycled between R3 and R2 to provide nitrate formed in R3 to the anoxic reactor, R2. R1

and R2 were both sealed glass bottles mixed with magnetic stirrers. R3 and its internal settler were made from Plexiglas; R3 contents were mixed occasionally by a magnetic stirrer and constantly by an overhead mechanical mixer equipped with an impeller. Aeration in R3 was achieved with pre-humidified compressed air at a flow rate between 0.5 to 1 standard cubic feet per minute (scfm) through a fine pore stone diffuser, insuring DO concentration between 4 to 7 mg/L. Feeding and wasting of R1, recycle from R3 to R2 and back to R3 was achieved with three Masterflex® peristaltic pumps (Cole-Parmer, Vernon Hills, IL., USA) controlled by a Model XT, table top, electronic timer (Chrontrol Corp., San Diego, CA, USA). The clarified effluent was discharged from the top of the internal settler by gravity. The seed used for the three reactors was mixed liquor withdrawn from an aerobic/anoxic autotrophic/heterotrophic stock culture that had been maintained in the laboratory for 2.5 years with original seed collected from a poultry processing wastewater treatment plant (see Chapter 5, Section 5.2.1). To provide a continuous wastewater source, a 9-L glass bottle, filled with poultry processing DAF underflow wastewater was kept in a refrigerator at 4ºC, its contents continuously mixed with a stirring bar and magnetic stirrer. In order to prevent aerobic degradation of the feed wastewater while kept refrigerated, its headspace was flashed with He, and then connected to a 10-L Tedlar bag filled with He.
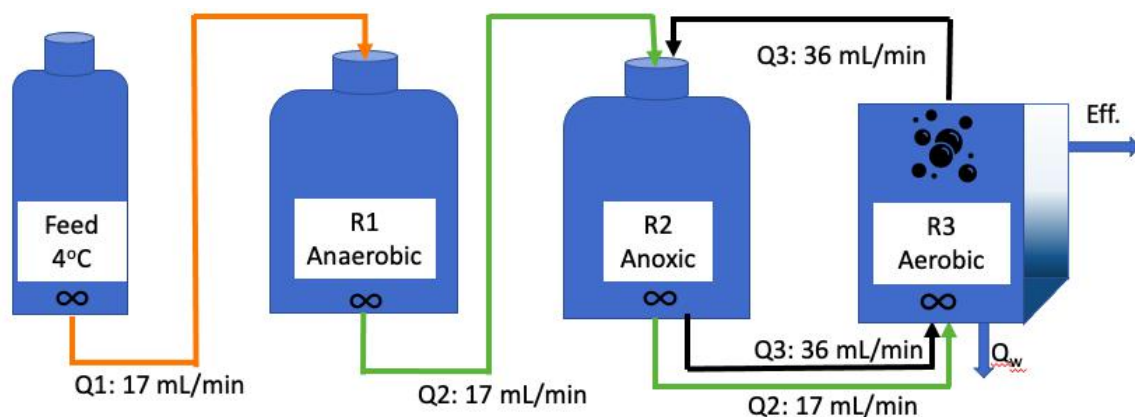
Figure 8.1. Three-reactor BNR system. An internal clarifier continuously returned settled biomass to R3. Q1, influent to R1; Q2, simultaneous feed from R1 to R2 and R3; Q3, internal recycle between R2 and R3; Q_w, intermittent wastage of R3 mixed liquor.

In order to establish continuous-flow conditions for system operation, the electronic timer was used to activate and deactivate the three pumps for a specific duration every hour. The sequence of events was as follows: pump A (dual heads) was turned on for 10 min per hour at a flow rate of 36 mL/min to recycle mixed liquor between the anoxic (R2) and the aerobic reactor (R3) providing nitrate for the anoxic reactor and ammonia to the aerobic reactor. Pump B (dual heads) was then turned on for 5 min per hour at a flow rate of 19 mL/min and anaerobic reactor (R1) mixed liquor was pumped to the anoxic reactor (R2) to supply the organic carbon/electron donor required for denitrification (first pump head). At the same time, an equal volume of anoxic reactor mixed liquor was pumped from R2 to the aerobic reactor, R3 (second pump head), thus maintaining a constant anoxic reactor liquid volume, and overfilling the aerobic reactor to trigger gravity effluent discharge. Finally, pump C (single head) was turned on for 5 min per hour at a flow rate of 19 mL/min to pump feed from the refrigerated feed reservoir to the anaerobic reactor, R1. Based on the above-stated flow rates and pumping durations, the R3-R2 recycle ratio compared to the overall BNR system flow rate of 2 L/d was 4.0.

Waste biomass was manually removed directly from the aerobic reactor daily, after the settler baffle was lifted and the contents of both the reactor and the settler were completely mixed for 10 min. The flow rate of the entire BNR system was 2 L/d, resulting in 4, 2, and 3.25 d hydraulic retention time (HRT) in R1, R2, and R3 plus settler, respectively. Except during the system upset (see Section 3.1), ca. 400 mL mixed liquor was manually wasted daily from R3, resulting in 16 d nominal solids retention time (SRT) for the entire BNR system. Based on the daily biomass removed from R3 along with biomass removed through the effluent from the settler overflow (VS in R3 and R3 effluent ca. 1.6 and 0.01 g/L, respectively; see Section 3.1), the effective SRT was 15.6 d. TS/VS measurements were used to evaluate biomass concentration rather than TSS/VSS, considering potential very slow filtration in the event of very poor mixed liquor bio-flocculation during the long-term operation. As a result, it should be noted that VS values reported here reflect organic soluble substances in addition to the biomass.

Tracer analysis of the clean BNR system was conducted using a stock NaCl solution (ca. 2 g/L; 4 mS/cm) at a flow rate of 2 L/d. Conductivity was measured with a HACH HQ40D portable multi meter (HACH, Loveland, CO, USA). The first test was run with the three reactors (R1, 8 L; R2, 4 L; and R3 plus internal settler, 6.5 L) in series, while the second test was run with the two reactors (R2, R3 plus internal settler). Figure 8.2A and 8.2B shows the conductivity over time in the three- and two-reactor system, respectively. For the three-reactor system, it took ca. 10.4 d, i.e., ca. 2.6 HRTs (1 HRT = 4 d) for the R1 conductivity to reach 95% of the influent conductivity, whereas it took ca. 18.4 and 19.4 d for the same conductivity to be reached in R2 and R3, respectively. For the two-reactor system, it took ca. 14.1 d, i.e., ca. 7.1 HRTs (1 HRT = 2 d) for the R2

179

conductivity to reach 95% of the influent conductivity, whereas it took ca. 15.1 d for the

same conductivity to be reached in R3.
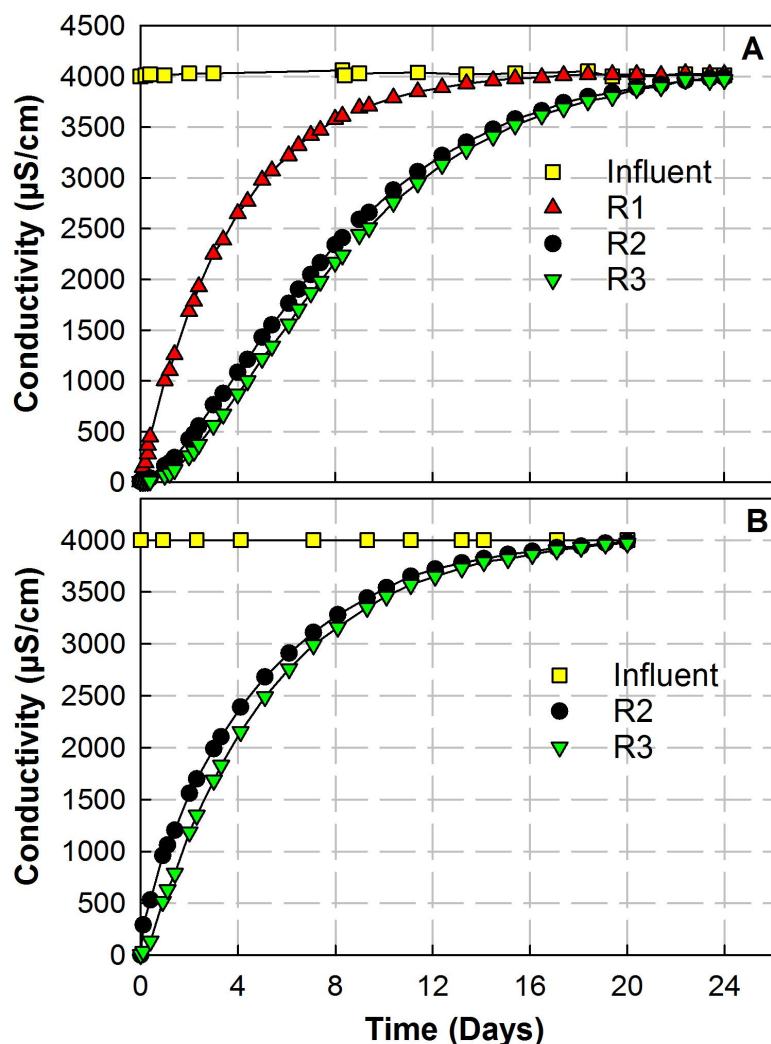
Figure 8.2. Conductivity time trend in the three-reactor BNR system (A) and in the two-reactor system (B) during the tracer tests.

Operation of the BNR system lasted for 168 d, divided in six phases (Figure 8.3), as follows. In Phase I (control phase), the system was operated for 20 d, fed with PAA/H_2O_2-free DAF underflow wastewater. In Phase II, the system was operated for 80 d, fed with PAA/H_2O_2-free DAF wastewater, while PAA working solution was directly

added to R1 for 1 min per hour by a syringe pump (Cole-Parmer, Vernon Hills, Illinois,

USA) at a flowrate of 2 mL/min, resulting in PAA/H_2O_2 concentration (normalized to the

feed wastewater) stepwise increased from 80/11.4 to 200/28.6 mg/L. In Phase III, the

system was operated for 20 d, fed with DAF wastewater that had been amended with

PAA solution resulting in stable, residual PAA, stepwise increased from 40 to 200 mg/L.

The feed with stable residual PAA was prepared by directly adding stock PAA solution in

the feed at an initial concentration of 600/86, 800/115, and 950/136 mg/L PAA/H_2O_2

resulting in final, stable 40/0, 80/0, and 200/0 mg/L PAA/H_2O_2 after 1 day. The acetic

acid concentration in the PAA/H_2O_2-free feed ranged from ca. 310 to 370 mg/L, and ca.

2400 to 3470 mg/L in the feed with final 40 to 200 mg/L residual PAA. The increased

acetic acid concentration in the PAA solution-amended feed was acetic acid in the stock

PAA solution, plus that resulting from PAA decomposition (Table 8.1). The ratio of final,

calculated to final, measured acetic acid in the PAA solution-amended feed was between

98% and 104%. Thus, as previously discussed (Chapter 4, Section 4.3.3), PAA

decomposition resulted in equimolar concentration of acetic acid. In Phase IV (long

recovery phase), the system was operated for 12 d, fed with PAA/H_2O_2-free DAF

wastewater at a flow rate of 0.5 L/d for another 25 d. In Phase V, R1 was removed from

the BNR system and the DAF underflow wastewater was directly fed to R2 at a flow rate

of 2 L/d. All operations were the same as in Phase III, i.e., system fed with DAF

wastewater with residual PAA gradually increased from 40 to 80 mg/L. A higher residual

PAA concentration in the feed during Phase V was not possible as system upset occurred

(see Section 8.3.1.5). NaOH (1 or 2 N) was directly added to R2 intermittently by a

syringe pump to keep the pH in R2 between 7.0 and 7.4 during Phase V. In Phase VI

(second recovery phase), the system was operated for 6 d (3 HRT for R2), fed with

PAA/H_2O_2-free DAF wastewater.

Table 8.1. Acetic acid (AA) production and balance in DAF underflow wastewater amended with stock PAA solution.

Initial PAA (mg/L)	Final Stable PAA (mg/L)	DAF AA (mg/L)	AA in PAA Solution (mg/L)	AA Produced by PAA (mg/L)	Final Calculated AA (mg/L)	Final Measured AA (mg/L)	AA Balance[a] (%)
600	40	374	1560	442	2376	2402	98.9
800	80	345	2080	568	2993	2883	103.8
960	200	312	2496	600	3408	3466	98.3

[a] Ratio of final, calculated to final, measured AA (expressed as %).
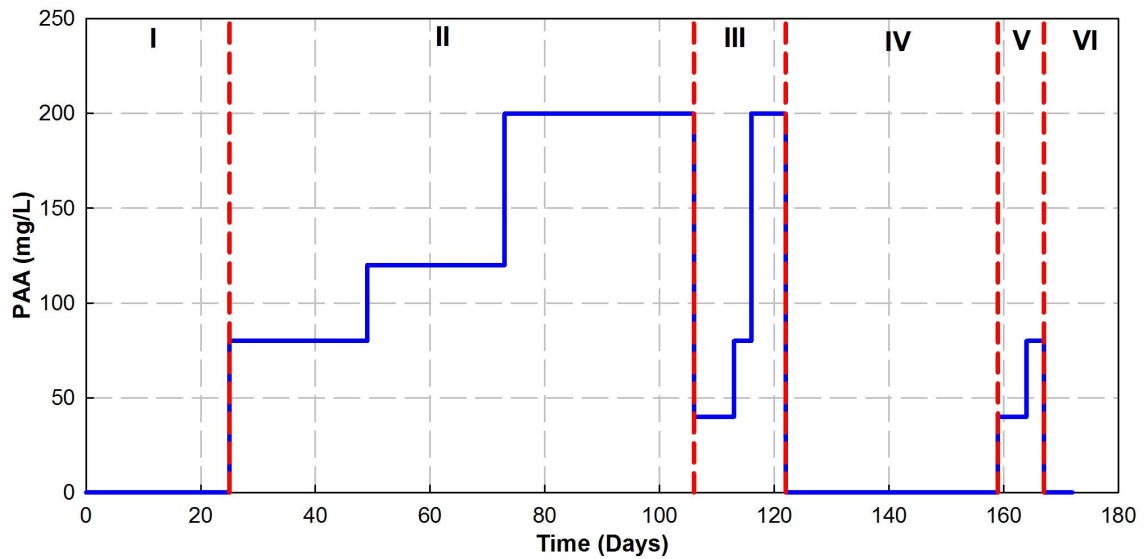
Figure 8.3. Six operational phases of the BNR system.

Phase I, control phase; Phase II, PAA solution direct addition to R1 at 80/11, 120/17 and 200/29 mg/L PAA/H_2O_2 normalized to the feed; Phase III, stable residual PAA at 40, 80 and 200 mg/L in the feed; Phase IV, first recovery phase; Phase V, stable residual PAA at 40 and 80 mg/L in the feed directly added to R2; Phase VI, second recovery phase.

8.2.3 Batch Assays

Batch assays were performed at different stages during the operation of the BNR system to assess the effect of PAA solution on the fermentation in R1, denitrification in

R2, and organic matter degradation as well as nitrification in R3 at each phase during the BNR system operation.

8.2.3.1 Batch anaerobic fermentation assays

Batch assays with R1 mixed liquor were performed to assess the effect of PAA solution on the DAF wastewater feed hydrolysis, volatile fatty acids (VFAs) production, and ammonia release from the feed organic nitrogen (ammonification). The assays were conducted in 160 mL serum bottles (120 mL liquid volume) sealed with rubber stoppers and aluminum crimps, and flushed with He gas for 15 min before any addition. An aliquot of 60 mL R1 mixed liquor was added to one bottle, followed by addition of 60 mL of feed. Another bottle with 120 mL R1 mixed liquor, without feed addition, served as the control, was set up once, in order to evaluate fermentation of R1 mixed liquor without feed addition. Incubation was carried at room temperature ($22\pm1^{\circ}C$) and the mixed liquor contents were mixed magnetically. Soluble COD, VFAs, pH, ammonia, and gas production and composition were measured periodically throughout the incubation period.

8.2.3.2 Batch anoxic denitrification assays

Batch assays with R2 mixed liquor were performed to assess the effect of PAA solution on the denitrification activity of the mixed liquor in the anoxic reactor (R2). The assays were conducted in 160 mL serum bottles (120 mL liquid volume) sealed with rubber stoppers and aluminum crimps, and flushed with He gas for 15 min before any addition. An aliquot of 119 mL R2 mixed liquor was added to one bottle, followed by the addition of $NaNO_3$ and glucose, resulting in initial concentrations of 100 mg N/L and 640 mg COD/L, respectively. Another bottle with 120 mL R2 mixed liquor, but without

NaNO$_3$ or glucose addition, served as the control, was set up once to elevate

denitrification activity of R2 mixed liquor without external nitrate and glucose addition.

Incubation was carried at room temperature (22±1°C) and the mixed liquor contents were

mixed magnetically. Soluble COD, pH, ammonia, nitrite, nitrate, and gas production and

composition were measured periodically throughout the incubation period. The initial

nitrate removal rate (NRR) was calculated by linear regression of the initial nitrate

concentration data over time.

8.2.3.3 Batch aerobic assays

Batch assays with R3 mixed liquor were performed to assess the effect of PAA

solution on organic matter degradation as well as the nitrification activity of the mixed

liquor in the aerobic reactor (R3). The batch assays were conducted in 250 mL

Erlenmeyer flasks (120 mL liquid volume). An aliquot of 117 mL R3 mixed liquor was

added to each flask, followed by the addition of NH$_4$Cl, NaHCO$_3$ and glucose, resulting

in initial concentrations of 100 mg N/L, 1200 mg/L, and 640 mg COD/L, respectively.

Another flask with R3 mixed liquor, but without glucose addition, served as the control,

was set up once to evaluate nitrification without external carbon (i.e., glucose) addition.

Incubation was carried out at room temperature (22±1°C) and the mixed liquor contents

were mixed magnetically. Soluble COD, pH, ammonia, nitrite, and nitrate were measured

periodically throughout the incubation period. The initial ammonia removal rate (ARR)

was calculated by linear regression of the initial ammonia concentration data over time.

8.2.4 Microbial Community Analysis

Bacterial DNA extraction, quantification, and sequencing were performed

following standard protocols as described in Chapter 3, Section 3.3.

8.2.5 Analytical Methods

pH, COD, N species, total solids (TS) and volatile solids (VS), total suspended solids (TSS) and volatile suspended solids (VSS), gas production and composition, VFAs, DO, total carbohydrates, and total lipids were measured as described in Chapter 3, Section 3.1. PAA and H_2O_2 were measured by the DPD method as described in Chapter 3, Section 3.2.3. The fraction of heterotrophic bacteria, ammonia-oxidizing bacteria (AOB), and nitrite-oxidizing bacteria (NOB) in the stock mixed heterotrophic/autotrophic culture was determined by using sodium azide (NaN_3) and allylthiourea (ATU) to inhibit AOB and NOB, respectively, and then measuring oxygen uptake rates as previously described (Surmacz-Gorska et al., 1996).

8.3 Results and Discussion

8.3.1 Bioreactors performance

8.3.1.1 Phase I

During Phase I (day 0 to 20), the pH varied from 5.0 to 5.6 in the feed and gradually decreased from 7.2 to 5.9 in R1 as a result of fermentation and VFAs production in R1. The pH varied from 7.4 to 8.0 in R2 and from 7.8 to 8.3 in R3 (Figure 8.4A). Dissolved oxygen (DO) was always at or above 4.0 mg/L in both R3 and the internal settler. The soluble COD varied from 758 to 943 mg/L in the feed and gradually increased from 665 to 994 mg/L in R1 as a result of hydrolysis of the feed particulate organic matter (Figure 8.4B). The soluble COD varied from 105 to 154 mg/L in R2 and from 35 to 68 mg/L in R3. The total COD was 1066±67 and 989±107 mg/L in the feed and R1, respectively. Therefore, the extent of soluble COD removal of the entire BNR

system varied from 93.2 to 94.7% during Phase I. The total VFAs varied from 584 to 794 mg COD/L in the feed and from 642 to 776 mg COD/L in R1 (Figure 8.5). During Phase I, the predominant VFAs in the feed were n-butyrate (50 to 60%), acetate (30 to 40%), and propionate (5 to 10%, COD basis). The predominant VFAs in R1 were acetate (50 to 60%), propionate (10 to 20%) and n-butyrate (10 to 20%). Although no significant VFAs production took place in R1 compared to the feed, the major VFAs changed from n-butyrate to acetate from the feed to R1. VFAs were not detected in R2 or R3 during Phase I.

Ammonia varied from 13 to 19 mg N/L in the feed and gradually increased from 38 to 63 mg N/L in R1 as a result of ammonification (Figure 8.4C). Ammonia varied from 6 to 12 mg N/L in R2 while was below the detection limit (< 0.1 mg N/L) in R3. Nitrite was not detected in the BNR system throughout Phase I. Nitrate was below the detection limit (< 0.1 mg N/L) in the feed and R1 (Figure 8.4D), while gradually decreased from 17 mg N/L to below the detection limit in R2 and varied from 11 to 27 mg/L in R3 during Phase I. The total N varied from 215 to 227 mg/L and 18 to 26 mg/L in the feed and the R3 effluent, respectively, resulting in 90 to 92% extent of N removal for the entire BNR system. The mean TS and VS concentrations in the three reactors were 0.91/0.34, 1.87/1.33, and 2.06/1.43 g/L in R1, R2, and R3, respectively (Table 8.2). The absorbance at 650 nm of the R3 effluent ranged from 0.007 to 0.015 throughout all the phases, corresponding to a VS concentration of 0.042 to 0.09 g/L. Thus, loss of solids through the effluent was minor and was not affected by PAA.

The gas headspace in both R1 and R2 was ca. 100% N_2 (Figure 8.7). The mean gas production in R1 and R2 was ca. 100 and 130 mL/d, respectively, equal to ca. 116

and 150 mg N/d as N_2 production, respectively. Table 8.4 summarizes the total N (mg

N/d) in the influent, waste biomass, and N_2 production in R1 and R2, resulting in a mean

N balance of 106%. In order to optimize the overall extent of N removal of the BNR

system, the R2-R3 recycle ratio was gradually increased from 4 to 8 and operated at 8 for

4 d. The extent of sCOD removal at a R2-R3 recycle ratio of 8 remained at a mean of

95%, similar to that at a recycle ratio of 4. The mean ammonia concentration in the

effluent increased from below detection limit to ca. 2 mg N/L while the mean nitrate

concentration in the effluent decreased from 18 to 12 mg N/L, as a result of increasing

the recycle ratio. The resulted extent of N removal at the R2-R3 recycle ratio of 8

remained at 92%, similar to that at recycle ratio 4. Thus, the extent of COD and N

removal was not significantly affected by increasing the R2-R3 recycle ratio above 4. As

a result, a R2-R3 recycle ratio of 4 was used in all phases. Overall, the BNR system

reached steady state during Phase I. In a previous study with a similar BNR system fed

with poultry processing DAF effluent, the mean nitrate concentration in R3 decreased

from ca. 20 to 13 mg N/L as the R2-R3 recycle ratio increased from 4 to 6, while the

ammonia concentration in R3 was not affected by the increased recycle ratio (Hajaya,

2012).

8.3.1.2 Phase II

During Phase II (day 21 to 101), PAA working solution was directly added to R1

at three, stepwise increased PAA/H_2O_2 levels (80/11.4, 120/17.1, 200/28.6 mg/L

PAA/H_2O_2 (normalized to the feed) and the performance of the BNR system was

evaluated at every PAA level. Throughout Phase II, PAA or H_2O_2 was not detected in any

of the three reactors. The pH varied from 5.5 to 6.3 and from 5.0 to 5.6 in the feed and R1,

respectively, indicating the buffer capacity of R1 was enough to tolerate the acidity

caused by the addition of the PAA solution at the above stated levels. The pH in R2 and

R3 varied from 6.5 to 7.4 and from 6.9 to 7.9, respectively (Figure 8.4A). The soluble

and total COD of the feed, varied from 777 to 943 and from 988 to 1126, respectively,

similar to values observed in Phase I. The soluble COD in R1 increased stepwise from a

mean value of 900 mg/L to 1400 mg/L as the PAA level increased stepwise from 80 to

200 mg/L (normalized in the feed), which was attributed to the acetic acid in the PAA

solution and that produced by PAA decomposition. The soluble COD varied from 111 to

302 and from 56 to 135 mg/L in R2 and R3, respectively (Figure 8.4B). Considering the

soluble COD attributed to the addition of PAA solution, the extent of COD removal of

the entire BNR system varied from 90.4 to 96% throughout Phase II, indicating organic

matter degradation was not affected by the direct addition of PAA solution to R1 at the

above stated levels. The total VFAs in the feed varied from 540 to 810 mg COD/L; the

major species were acetate (20 to 30%) and n-butyrate (25 to 50%), similar to the

observed VFAs in Phase I. The total VFAs in R1 increased stepwise from a mean value

of 750 to 1250 mg COD/L, attributed to the acetic acid introduced to R1 by the addition

of the PAA solution as well as by PAA decomposition (Figure 8.5). However, in Phase II,

VFAs were not detected in R2 or R3, as it was the case in Phase I, suggesting the BNR

system was capable of degrading the additional acetic acid resulting from the addition of

the PAA solution.

Ammonia gradually increased from ca. 16 to 52 mg N/L in the feed during Phase

II, a result of ammonification during feed storage. Ammonia in R1 varied from 43 to 72

mg N/L, 24 to 30 mg N/L higher than in the feed, attributed to the ammonification taking

place in R1. Ammonia varied from ca. 9 to 19 mg N/L in R2 and was below the detection limit (<0.1 mg N/L) in R3 throughout Phase II (Figure 8.4C). Nitrate in R3 varied from 14 to 19 mg N/L and was not detected in the feed, R1, or R2 (Figure 8.4D). Nitrite was not detected in the feed or in any of the three reactors during Phase II. The BNR system reached 82 to 93% extent of N removal during Phase II, which was close and slightly higher than the extent of N removal during Phase I. Therefore, the overall system N removal was not affected by the direct addition of PAA solution to R1 at the above stated levels. Throughout Phase II, the VS concentration varied from 0.32 to 0.70, 0.90 to 1.56, and 1.09 to 1.71 g/L in R1, R2, and R3, respectively (Table 8.2), without any particular trend related to the addition of the PAA solution at gradually increased PAA/H_2O_2 levels.

8.3.1.3 Phase III

During Phase III (day 102 to 122), the feed was pre-amended with PAA solution to reach stable, target residual PAA concentrations, which simulated residual PAA-bearing wastewater carried to biological treatment systems. The feed was amended with 600, 800 and 1000 mg/L PAA one day before use to obtain feed with relatively stable, residual PAA concentration at ca. 40, 80 and 200 mg/L, respectively. PAA was not detected in any of the three reactors when the feed residual PAA was 40 mg/L. As the feed residual PAA was increased to 80 and 200 mg/L, PAA was detected in R1, increasing gradually from ca. 2 mg/L at day 112 to 181 mg/L at day 122 (Figure 8.8). PAA was also detected in R2 as high as 7 mg/L from day 120 to 122 when system upset occurred, as discussed below (Figure 8.8). The pH in the feed dropped to between 4.0 and 4.2 as a result of PAA solution addition, mainly attributed to the acetic acid (pK_a 4.76) introduced by the PAA solution as well as produced by the decomposition of PAA. Thus,

most of the acetic acid in the feed was in the protonated form rather than acetate. During Phase III, the pH of R1 was maintained at ca. 5.0 by addition of NaOH intermittently added via a syringe pump, in order to eliminate any potential, detrimental effect of pH on the system performance. The pH in R2 and R3 varied from 6.9 to 7.2 and from 7.7 to 8.3, respectively (Figure 8.4A). The feed soluble COD increased from a mean value of 900 to 4000 mg/L, attributed to the stepwise increased PAA level in the feed. Correspondingly, the soluble COD in R1 increased from a mean value of 1400 to 3900 mg/L (Figure 8.4B). During Phase III, the soluble COD increased from ca. 150 to 1550 mg/L in R2 and from ca. 80 to 940 mg/L in R3, resulting in a lower extent of overall system COD removal at ca. 76% by the end of Phase III. Similar to soluble COD, VFAs in the feed increased from ca. 600 to 3800 mg COD/L (Figure 8.5 &8.6), predominantly attributed to the acetic acid (86 to 90%) brought and produced by addition of the PAA solution. Similar to the feed, VFAs in R1 increased from ca. 1200 to 3900 mg COD/L. It is noteworthy that VFAs were never detected in R2 in Phase I or II as mentioned above, while total VFAs, as high as ca. 1400 mg COD/L, were detected in R2 by the end of Phase III. Therefore, organic matter degradation in the entire BNR system was negatively affected while the system was fed with DAF wastewater carrying residual PAA during Phase III.

The ammonia concentration was very close in the feed and R1, ranging from 56 to 67 mg N/L (Figure 8.4C), suggesting ammonification in R1 ceased during Phase III. The ammonia concentration varied from ca. 14 to 21 mg N/L in R2 while increased to as high as ca. 13 mg N/L in R3, suggesting that nitrification in R3 was negatively affected while the system was fed with DAF wastewater carrying residual PAA during Phase III. Nitrate was not detected in the feed, R1 or R2 before Phase III, while during Phase III nitrate

gradually increased to 18.3, 8.7, and 2.9 mg N/L in the feed, R1, and R2, respectively

(Figure 8.4D). The increase of nitrate in the feed and R1 was possibly attributed to the

oxidation of ammonia to nitrate by the high dosage of PAA solution as mentioned above.

In order to evaluate the effect of PAA addition on N species in DAF underflow

wastewater, 1 L DAF underflow wastewater was amended with PAA solution at an initial

PAA/H_2O_2 concentration of 900/130 mg/L, and N species, as well as PAA and H_2O_2

were monitored for 24 h (Table 8.5). This test showed that the ammonia concentration

remained at ca. 20 mg N/L and nitrite was not detected, while nitrate increased from ca. 1

to 15 mg N/L, suggesting that some N species were oxidized to nitrate under the effect of

the high PAA concentration. It is possible that ammonia was produced by the degradation

of organic matter under the effect of PAA and the produced ammonia was further

oxidized to nitrate without an apparent change of the ammonia concentration. Residual

nitrate detected in R2 indicates that denitrification in R2 was negatively affected by the

use of DAF wastewater with residual PAA during Phase III. Correspondingly, the nitrate

concentration in R3 decreased to as low as ca. 1.0 mg N/L (Figure 8.4D) as a result of

nitrification inhibition. The VS concentration in R1 was close (mean: 0.76 and 0.51 g/L)

at the end of system operation with 40 and 80 mg/L residual feed PAA, while

significantly increased to 1.22 g/L at the end of feeding with 200 mg/L residual feed PAA

(Table 8.2), mainly attributed to the increased acetic acid introduced to R1. Excessive

foaming at the top of R3 was observed, along with biomass loss due to overflowing foam.

The foaming was mainly attributed to protein released from excessive cell lysis. The VS

concentration in R2 increased from 1.39 to 1.57 g/L and then decreased to 1.10 g/L at the

end of feeding with residual feed PAA from 40 to 80 and then 200 mg/L; similarly, the

VS concentration in R3 increased from 1.58 to 1.64 g/L and then decreased to 1.01 g/L at the end of feeding with residual feed PAA from 40 to 80 and then 200 mg/L, suggesting that a high residual feed PAA level (i.e., 200 mg/L) led to biomass loss in both R2 and R3. Overall, the extent of COD and N removal of the BNR system decreased to ca. 77 and 75%, respectively, at the end of Phase III.

8.3.1.4 Phase IV-

During Phase IV (i.e., recovery phase, feeding PAA/H_2O_2-free DAF wastewater; day 123 to 134 at full organic loading, day 135 to 159 at a quarter of organic loading) (Figure 8.3), the pH in the feed and R1 varied from 6.5 to 6.8 and from 5.1 to 5.9, respectively. Correspondingly, the pH in R2 varied from 6.8 to 7.8 and was ca. 8.5 in R3 (Figure 8.4A). The PAA in R1 decreased from a high concentration (ca. 180 mg/L) to below the detection limit (0.1 mg/L) at the end of 2-d recovery operation and decreased from ca. 7 mg/L to below the detection limit in R2 at the end of 1-d recovery operation (Figure 8.8). The soluble COD decreased from ca. 3900 to 1000, 1500 to 130, and 940 to 100 mg/L in R1, R2, and R3, respectively, at the end of the 12-d recovery operation (Figure 8.4B), suggesting the capacity of the BNR system to degrade organic matter was recovered by the end of Phase IV. Similar to the trend of soluble COD, the total VFAs decreased significantly from 4000 to 900 mg COD/L and from 1400 to 88 mg COD/L in R1 and R2, respectively, by the end of Phase IV (Figure 8.5). VFAs were not detected in R3. After the 12-d recovery operation, the ammonia concentration varied from 62 to 64 mg N/L in the feed, while increased from 60 to 71 mg N/L in R1 (Figure 8.4C), suggesting ammonification was partially restored in R1 by the end of Phase IV. The ammonia concentration in R2 increased from 11 to 23 mg N/L and decreased from 13 mg

N/L to non-detectable levels in R3 after 4-d recovery operation, suggesting that nitrification recovered fast during Phase IV (Figure 8.4C). By the end of the 4-d recovery operation, the R1 nitrate concentration decreased significantly from 9 and 3 mg N/L and from 3 mg N/L to non-detectable levels in R2, suggesting that denitrification also recovered fast during Phase IV. The nitrate concentration gradually increased from 1 to 16 mg N/L in R3, further showing that the nitrification had also recovered by the end of the 4-d recovery operation (Figure 8.4D).

8.3.1.5 Phase V

After the recovery of the BNR system in Phase IV, R1 was removed from the system and DAF wastewater with a stable, residual PAA concentration stepwise increased from 40 to 80 mg/L was fed directly to R2 during Phase V (day 160 to 167). PAA was not detected in R2 or R3 during Phase V. The pH in the feed varied from 4.0 to 4.2 as a result of PAA solution addition, which introduced and produced acetic acid. During Phase V, the pH of R2 was maintained between 7.0 to 7.5 by intermittent addition of 1N or 2N NaOH to R2 via a syringe pump, in order to eliminate any potential pH effect on the system performance. The pH varied from 8.3 to 8.6 in R3 during Phase V (Figure 8.4A). The feed soluble COD increased from a mean value of 900 to 3200 mg/L, attributed to the increased residual PAA level from 40 to 80 mg/L in the feed and its associated acetic acid as discussed above. Correspondingly, the soluble COD increased from ca.130 to 1450 and from 100 to 1400 mg/L in R2 and R3, respectively (Figure 8.4B). Thus, the extent of system soluble COD removal decreased to as low as 56% by the end of Phase V. Similar to soluble COD, VFAs in the feed increased from ca. 700 to 3130 mg COD/L (Figure 8.5) during Phase V, predominantly attributed to acetic acid (80

to 88% on a COD basis) introduced by addition of the PAA solution and produced by PAA decomposition. During Phase V, the total VFAs concentration in R2 increased gradually from ca. 90 to 1390 mg COD/L, attributed to the increased total VFAs concentration in the feed. Therefore, organic matter degradation in the BNR system was negatively affected by operation with residual PAA during Phase V. The feed ammonia concentration varied from 16 to 19 mg N/L (Figure 8.4C), much lower than what was in previous phases as a result of using newly collected DAF wastewater from the poultry processing plant. The ammonia concentration in R2 decreased from 16 to 9 mg N/L, while increased from a mean value of 1.0 to as high as 8.7 mg N/L in R3 as residual PAA concentration increased stepwise from 40 to 80 mg/L, suggesting nitrification in R3 was negatively affected with operation with residual PAA during Phase V. The nitrate concentration gradually increased from non-detected to 10.7 and 3.2 mg N/L in the feed and R2, respectively, as residual PAA concentration increased stepwise from 40 to 80 mg/L (Figure 8.4D). As mentioned above, the increase of the nitrate concentration in the feed may be due to oxidation of ammonia to nitrate by the high PAA levels. Residual nitrate detected in R2 indicates that denitrification in R2 was negatively affected with residual PAA during Phase V. Correspondingly, the nitrate concentration decreased from a mean value of 10 to as low as 1.0 mg N/L in R3 as residual PAA concentration increased stepwise from 40 to 80 mg/L (Figure 8.4D), due to the fact that nitrification in R3 was also negatively affected. By the end of Phase V, the VS concentration decreased to 1.19 and 1.38 g/L in R2 and R3, respectively, suggesting that high, residual PAA levels in the feed (i.e., 80 mg/L) led to biomass loss in both R2 and R3.

8.3.1.6 Phase VI-

During Phase VI (i.e., second recovery phase feeding PAA/H_2O_2-free DAF wastewater; day 168 to 173) (Figure 8.3), the feed pH increased from 5.4 to 5.8 due to omission of PAA solution. Correspondingly, the pH varied from 7.2 to 7.6 in R2 without any external pH adjustment and was ca. 8.5 in R3 (Figure 8.4A). At the end of the 6-d (3 HRT) recovery operation, the soluble COD decreased from 1450 to 200 and from 1400 to 130 mg/L in R2 and R3, respectively (Figure 8.4B), suggesting that organic matter degradation in the BNR system had recovered by the end of Phase VI, similarly to the recovery in Phase IV. Similar to the trend of soluble COD, the total VFAs concentration significantly decreased from 1400 to 120 mg COD/L in R2 by the end of Phase VI (Figure 8.5). After the 6-d recovery operation, the ammonia concentration increased from 9 to 25 mg N/L in R2 (Figure 8.4C), while decreased from 9 to 2 mg N/L in R3, suggesting that nitrification recovered fast during Phase VI (Figure 8.4C). The nitrate concentration in R2 decreased from 3 mg N/L to non-detectable by the end of the 6-d recovery operation, suggesting that denitrification also recovered during Phase VI. The nitrate concentration in R3 gradually increased from 2 to 10 mg N/L, resulting from the recovered nitrification (Figure 8.4D).

Throughout the six phases, the R3 mixed liquor settling was assessed by measuring the sludge volume index (SVI); data are summarized in Table 8.3. The SVI value varied from 52 to 82 mL/g. For normal, non-bulking mixed liquor, typical SVI values for aerobic, suspended growth systems are between 50 and 100 mL/g (Metcalf and Eddy, 5th edition, 2014). Thus, the R3 mixed liquor settling was not significantly affected

by the BNR system operation with PAA solution addition, either direct or as residual

PAA at concentration ≤ 200 mg/L.

Table 8.2. TS, VS (g/L), and VS/TS ratio (%) in the three reactors during the BNR system operation (Phase I to VI).

Reactor	Phase	Stage	TS (g/L)	VS (g/L)	VS/TS (%)
R1	I	Initial	0.75 ± 0.05[a]	0.58 ± 0.06[a]	77.1
		End	0.68 ± 0.02	0.53 ± 0.03	78.7
	II	80 PAA	0.99 ± 0.04	0.32 ± 0.03	32.8
		120 PAA	1.08 ± 0.06	0.70 ± 0.02	64.6
		200 PAA	1.05 ± 0.06	0.58 ± 0.03	55.0
	III	R40 PAA	1.91 ± 0.06	0.76 ± 0.06	39.7
		R80 PAA	1.99 ± 0.03	0.51 ± 0.04	25.4
		R200 PAA	2.01 ± 0.18	1.22 ± 0.09	60.7
	IV	Recovery	1.41 ± 0.09	0.83 ± 0.03	58.9
R2	I	Initial	1.35 ± 0.08	1.08 ± 0.09	80.0
		End	1.73 ± 0.00	1.53 ± 0.03	88.3
	II	80 PAA	1.50 ± 0.08	0.90 ± 0.04	60.0
		120 PAA	2.18 ± 0.09	1.56 ± 0.07	71.4
		200 PAA	2.25 ± 0.18	1.30 ± 0.09	57.8
	III	R40 PAA	2.56 ± 0.08	1.39 ± 0.05	54.3
		R80 PAA	3.03 ± 0.12	1.57 ± 0.07	51.7
		R200 PAA	3.02 ± 0.06	1.10 ± 0.04	36.5
	IV	Recovery	3.10 ± 0.06	1.68 ± 0.06	54.3
	V	R80 PAA	2.54 ± 0.12	1.19 ± 0.02	47.0
	VI	Recovery	3.23 ± 0.11	1.91 ± 0.11	59.0
R3	I	Initial	1.71 ± 0.06	1.43 ± 0.08	83.7
		End	1.77 ± 0.02	1.55 ± 0.04	87.3
	II	80 PAA	1.76 ± 0.04	1.09 ± 0.01	62.1
		120 PAA	2.64 ± 0.12	1.71 ± 0.03	64.5
		200 PAA	2.41 ± 0.05	1.39 ± 0.01	57.7
	III	R40 PAA	2.66 ± 0.09	1.58 ± 0.06	59.5
		R80 PAA	3.17 ± 0.05	1.64 ± 0.09	51.7
		R200 PAA	2.83 ± 0.06	1.01 ± 0.05[a]	35.7
	IV	Recovery	2.97 ± 0.04	1.89 ± 0.08	63.7
	V	R80 PAA	2.73 ± 0.10	1.38 ± 0.09	50.7
	VI	Recovery	3.43 ± 0.08	2.07 ± 0.06	60.5

[a] Mean ± standard deviation ($n = 3$)

Table 8.3. Sludge volume index (SVI, mL/g) of R3 mixed liquor during the BNR system operation (Phase I to VI).

Phase	Stage	SVI (mL/g)
I	Initial	73
	End	69
II	80 PAA	61
	120 PAA	54
	200 PAA	82
III	R40 PAA	72
	R80 PAA	75
	R200 PAA	80
IV	Recovery	68
V	R80 PAA	52
VI	Recovery	69

Table 8.4. Nitrogen balance of the BNR system during Phase I.

Total N (mg/d)					
Influent	Effluent	Waste Biomass	R1 N_2 Production	R2 N_2 Production	N Balance (%) [a]
420±20	20±4	160±14	116±8	150±16	106±9

[a] Sum of N in the effluent, waste biomass, and N_2 produced in R1 and R2 divided by the influent total N; [b] Mean ± standard deviation ($n = 3$)

Table 8.5. Concentration of nitrogen species (mg N/L), PAA and H_2O_2 (mg/L) during the preparation of DAF underflow wastewater with residual PAA.

Time (h)	Ammonia	Nitrite	Nitrate	Total N	PAA	H_2O_2
0	20.7	ND[a]	1.1	225.0	900.0	135.0
10	20.1	ND	14.1	220.0	298.0	10.2
24	20.0	ND	14.7	221.0	204.0	ND

[a] ND, not detected
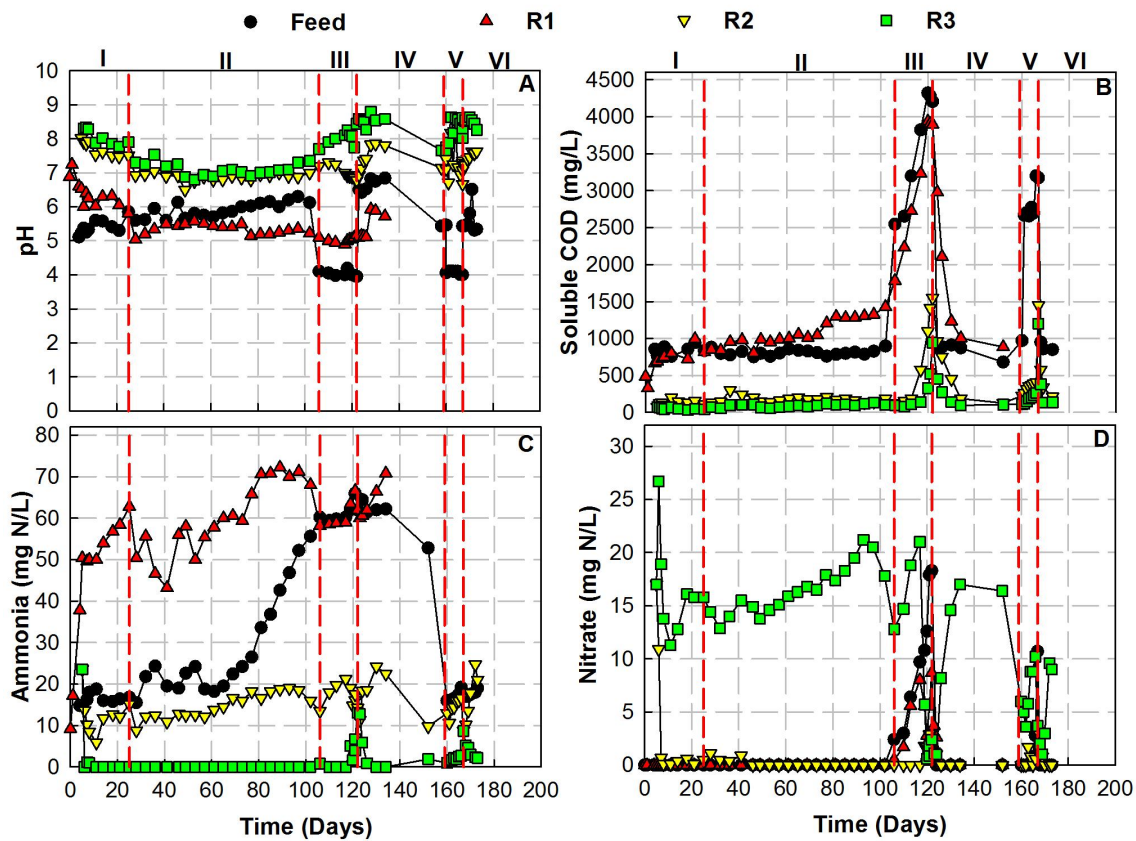
Figure 8.4. Time trend of pH (A), soluble COD (B), ammonia-N (C), and nitrate-N (D) in the feed and three reactors during the BNR system operation (Phase I to VI).
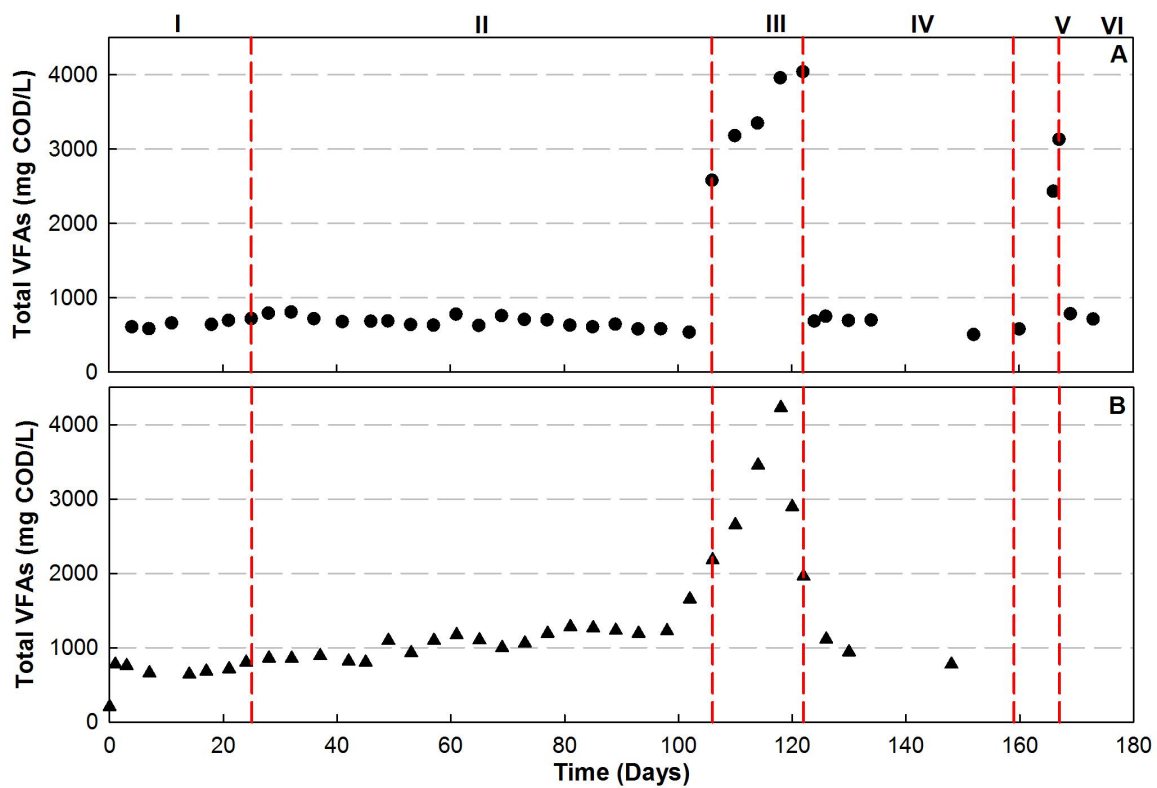
Figure 8.5. Time trend of total VFAs in the feed (A) and R1 (B) (Phase I to VI).
(VFAs were not detected in R2 and R3).
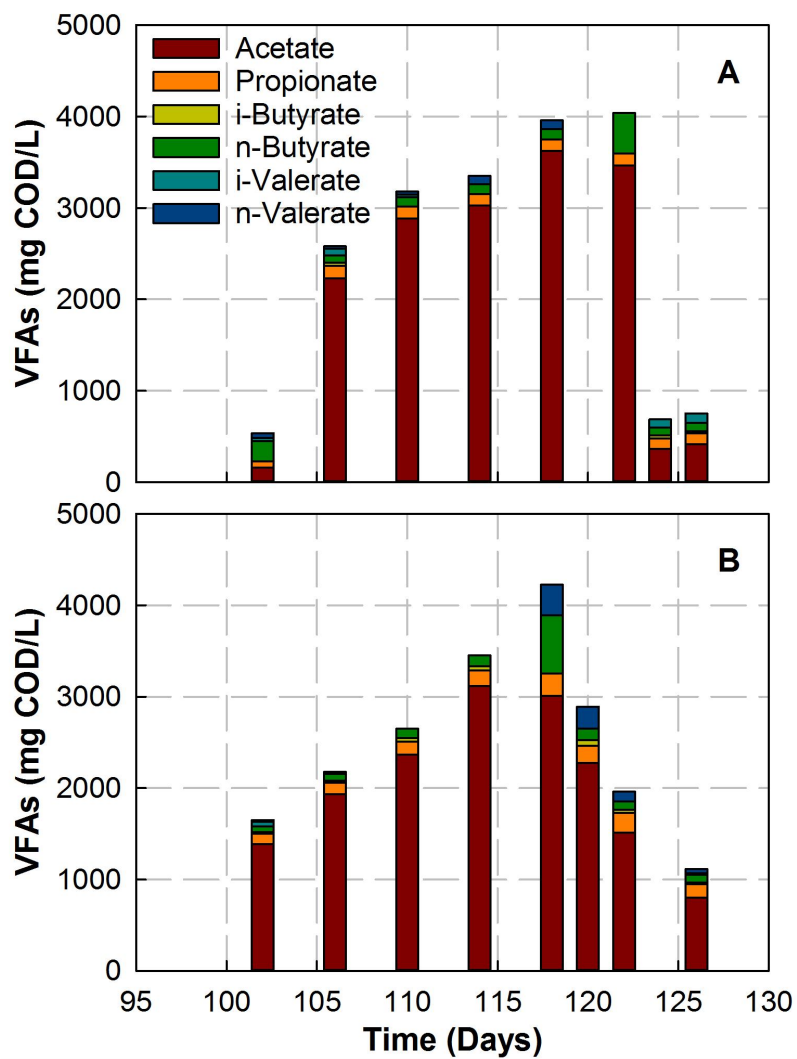
Figure 8.6. Time trend of VFAs in the feed (A) and R1 (B) from the end of Phase II to the beginning of Phase IV (day 102 to 126).
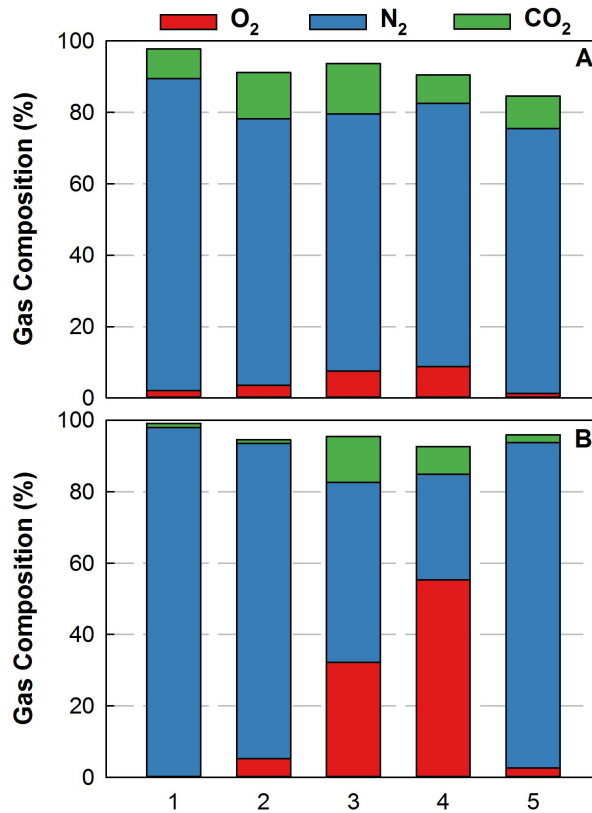
Figure 8.7. Gas composition in the headspace of R1 (A) and R2 (B).

Condition: 1, end of Phase I; 2, end of Phase II; 3, end of feeding 80 mg/L residual PAA in Phase III; 4, end of feeding 200 mg/L residual PAA in Phase III; 5, end of Phase IV.
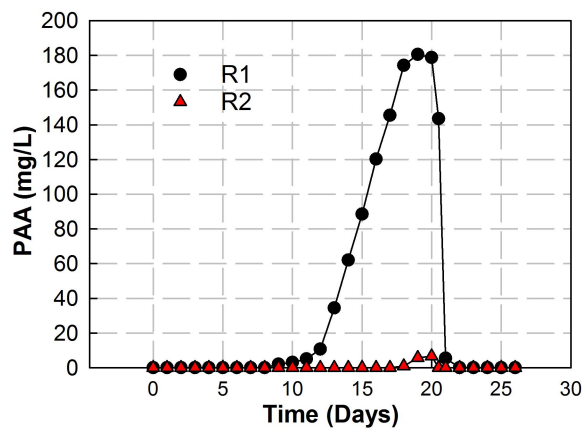
Figure 8.8. PAA concentration in R1 and R2 during Phase III (day 102 to 122) (feeding with DAF wastewater with 80 and 200 mg/L residual PAA; 4 and 9 days, respectively).

8.3.2 Batch assays

8.3.2.1 Batch anaerobic assays

Table 8.6 summarizes the ammonia concentration and N_2 produced in batch anaerobic assays conducted with 50% volume of mixed liquor from R1 and 50% feed, during the operation of the BNR system. The concentration of ammonia produced varied from 21 to 27 and from 24 to 38 mg N/L during Phase I and Phase II, respectively. However, the ammonia production in R1 decreased to 0.6 mg N/L during Phase III, which was 2.6 mg N/L less than the initial ammonia concentration, indicating that ammonia release from organic N was negatively impacted by directly feeding with 40 to 200 mg/L residual PAA. Ammonia production in the anaerobic assay recovered and increased to 8 mg N/L at the end of Phase IV. Similar to the time trend of ammonia production, N_2 production in R1 also decreased in Phase III and recovered in Phase IV (Table 8.6). However, the mechanism of N_2 production in R1 during Phase I and II is not clear, as neither nitrite nor nitrate were detected in R1 or in the anaerobic batch assays during Phase I and II. In order to better understand the possible pathway of N_2 production in R1 and the anaerobic batch assays, another batch assay using R1 mixed liquor was set up at the end of Phase II, consisting of three series: R1 mixed liquor (control), R1 mixed liquor amended with 100 mg N/L nitrite, and R1 mixed liquor amended with 100 mg N/L nitrate. Table 8.7 summarizes the N species in this batch assay. The nitrite-amended series had similar N_2 production and residual ammonia as the nitrate-amended series, suggesting that there was no significant anaerobic ammonia oxidation (Anammox) taking place in R1. Microbial community analysis (Section 3.0, below) further supports absence of Anammox in R1.

8.3.2.2 Batch anoxic assays

Table 8.8 summarizes the nitrate removal rate (NRR) and the extent of soluble COD removal in batch anoxic assays conducted with R2 mixed liquor at different phases of the BNR system operation. The NRR varied from 160 to 186 mg N/L-d during Phase I, II, and III while feeding with 40 to 80 mg/L PAA, and decreased to 150, 71, and 37 mg N/L-d at the end of one, two, and three HRT with feeding 200 mg/L PAA, respectively. Then, the NRR increased to 210 mg N/L-d within 3 HRT in Phase IV, suggesting that the denitrification activity of the R2 mixed liquor was not negatively impacted by direct PAA addition to R1 at the above stated concentrations. However, feeding R1 with residual PAA drastically decreased the NRR. This impact was fast reversed by feeding PAA/H_2O_2-free DAF wastewater for three HRTs. After the complete recovery of the BNR system, during Phase V, the NRR again decreased to 153 mg N/L-d after feeding for three HRTs with 40 mg/L residual PAA wastewater and further decreased to 63 mg N/L-d within one HRT of feeding with 80 mg/L residual PAA wastewater, indicating that the denitrification activity in R2 was again negatively impacted by residual PAA. Thus, for the BNR system without the anaerobic/fermentation reactor R1, the impact of residual PAA was more pronounced at a lower level than in the case of the three-reactors BNR system (Phase III).

Similar to the NRR, the extent of soluble COD removal in the anoxic batch assays varied from 82 to 89% during Phase I, II and III while feeding with 40 to 80 mg/L residual PAA wastewater, and decreased to 77, 61, and 29% at the end of 1, 2, and 3 HRT while feeding with 200 mg/L residual PAA wastewater, respectively. The extent of soluble COD removal increased to 91% within three HRTs in Phase IV. During Phase V,

the extent of soluble COD removal again decreased to 78% after three HRTs feeding with 40 mg/L residual PAA wastewater and further decreased to 34% within one HRT feeding with 80 mg/L residual PAA wastewater. The extent of soluble COD removal increased to 85% at the end of the 3-HRT recovery (Phase VI). Thus, the extent of soluble COD removal was negatively affected by PAA, but its impact was fast reversed after feeding with PAA/H_2O_2-free DAF wastewater. Again, the impact of lower residual PAA levels on soluble COD removal was more pronounced in the two-reactor BNR system compared to the three-reactor system.

8.3.2.3 Batch aerobic assays

Table 8.9 summarizes the ammonia removal rate (ARR) and the extent of soluble COD removal in batch aerobic assays conducted with R3 mixed liquor at different phases of BNR system operation. The ARR varied from 168 to 206 mg N/L-d during Phase I, II, and III while feeding with 40 to 80 mg/L PAA, and decreased to 156, 57, and 35 mg N/L-d at the end of one, two, and three HRT, respectively, with feeding wastewater with residual 200 mg/L PAA. In Phase IV (recovery), the ARR increased to 167 and 194 mg N/L-d at the end of one and three HRT, respectively, suggesting that the nitrification activity of the R3 mixed liquor was not negatively impacted by direct PAA addition to R1 at the above stated concentrations. However, feeding R1 with wastewater with residual PAA drastically decreased the ARR. This impact was fast reversed with three HRT feeding with PAA/H_2O_2-free DAF wastewater. After the complete recovery of the BNR system, during Phase V, the ARR again decreased to 158 mg N/L-d after feeding for three HRTs with 40 mg/L residual PAA wastewater and further decreased to 54 mg N/L-d within one HRT feeding with 80 mg/L residual PAA wastewater, indicating that

the nitrification activity in R3 was again negatively impacted by PAA. Thus, for the BNR system without R1, the impact of residual PAA was more pronounced at a lower level than in the case of the three-reactors system (Phase III). Furthermore, the nitrification activity in R3 recovered from the second system upset as fast as it recovered from the first system upset, suggesting that the negative impact of feeding with residual PAA wastewater was not persistent.

The extent of soluble COD removal in the aerobic batch assays gradually decreased from 88 to 69% from Phase I to II, attributed to the low organic loading to R3 resulting from the high extent of COD removal achieved by R2. During Phase III, the extent of soluble COD removal decreased from 67 to 29%, suggesting that the aerobic organic matter degradation in R3 was negatively affected by feeding with residual PAA at 80 to 200 mg/L (normalized to the feed wastewater). In Phase IV (recovery), the extent of soluble COD removal increased to 59 and 78% at the end of one and three HRT, respectively, indicating that the aerobic degradation in R3 completely recovered by the end of Phase IV. During Phase V, the extent of soluble COD removal again decreased to 62% after three HRTs feeding with 40 mg/L residual PAA wastewater and further decreased to 56% within one HRT feeding with 80 mg/L residual PAA wastewater. Again, the extent of soluble COD removal increased to 75% by the end of three HRT in Phase VI (recovery). Thus, the extent of soluble COD removal was negatively affected by PAA, but its impact was fast reversed after feeding with PAA/H_2O_2-free DAF wastewater. The impact of lower residual PAA levels on soluble COD removal was more pronounced in the two-reactor BNR system compared to the three-reactor system.

Table 8.6. Ammonia and N₂ produced in batch anaerobic assays conducted with R1 mixed liquor during the BNR system operation.

Phase	Stage	NH₄-N Produced (mg/L)	N₂ Produced (mg/L) [a]
I	Initial	26.5 ± 0.2[b]	24.6 ± 0.9
	End	20.6 ± 0.7	28.1 ± 0.2
II	80 PAA	24.3 ± 0.2	35.5 ± 1.3
	120 PAA	37.7 ± 0.4	27.7 ± 1.1
	200 PAA	25.8 ± 0.1	14.7 ± 0.5
III	R40 PAA	-2.6 ± 0.1[c]	9.2 ± 0.2
	R80 PAA	0.2 ± 0.1	5.9 ± 0.1
	R200 PAA-1 HRT	0.2 ± 0.2	5.1 ± 0.8
	R200 PAA-2 HRT	0.6 ± 0.2	4.6 ± 0.2
	R200 PAA-3 HRT	0.4 ± 0.2	4 ± 0.3
IV	Recovery -1 HRT	2.8 ± 0.1	13.1 ± 0.7
	Recovery -3 HRT	8 ± 0.5	16.9 ± 1.0

[a] Normalized to the batch assay liquid volume; [b] Mean ± standard deviation ($n = 3$); [c] A decrease in ammonia concentration was observed

Table 8.7. Nitrogen balance in the anaerobic assay conducted with R1mixed liquor (control), R1 mixed liquor amended with nitrite, and R2 mixed liquor amended with nitrate.

N Species	Series		
	Control	Nitrite-amended	Nitrate-amended
Initial N (mg/L)			
Ammonia-N	70.2±0.2[a]	70.2±0.2	70.2±0.5
Nitrite-N	ND[b]	100±0.1	ND
Nitrate-N	ND	ND	100±0.5
N_2-N	ND	ND	ND
Measured Total N	106.5±5.0	205.0±11.0	203.0±8.0
Organic N	36.3±3.6	34.8±4.9	32.8±8.2
Total N	106.5±5.0	205.0±11.0	203.0±8.0
Final N (mg/L)			
Ammonia-N	63.6±0.6	62.6±0.2	64.0±1.0
Nitrite-N	ND	79.1±1.5	ND
Nitrate-N	ND	ND	79.0±1.2
N_2-N	6.9±0.5	13.3±1.3	10.8±0.7
Measured Total N	96.0±6.0	178.5±6.0	174.5±4.0
Organic N	32.4±6.9	36.8±8.0	31.5±6.3
Total N	102.9±6.5	191.8±7.3	185.3±4.7

[a] Mean ± standard deviation (n = 3); [b] ND, not detected

Table 8.8. Initial nitrate removal rate (NRR) and extent of soluble COD removal in batch anoxic assays conducted with R2 mixed liquor at different phases of the BNR system operation (Phase I to VI).

Phase	Stage	NRR (mg N/L-d)	COD Removal (%)
I	Initial	186±12[a]	75.8±2.5
	End	171±7	89.2±3.0
II	80 PAA	160±5	83.4±2.2
	120 PAA	186±11	84.5±2.8
	200 PAA	180±9	82.3±2.5
III	R40 PAA	183±7	86.2±2.2
	R80 PAA	177±10	83±4.0
	R200 PAA-1 HRT	150±3	76.9±2.6
	R200 PAA-2 HRT	71±3	60.9±2.0
	R200 PAA-3 HRT	37±1	29.3±2.2
IV	Recovery -1HRT	201±4	75.4±3.0
	Recovery -3HRT	210±9	91.5±2.0
V	R40 PAA	153±5	78.2±2.4
	R80 PAA	63±5	34.3±3.0
VI	Recovery -1HRT	154±11	81.1±3.6
	Recovery -3HRT	206±10	85.8±2.6

[a] Mean ± standard deviation (n = 3)

Table 8.9. Initial ammonia removal rate (ARR) and extent of soluble COD removal in batch aerobic assays conducted with R3 mixed liquor at different phases of the BNR system operation (Phase I to VI).

Phase	Stage	ARR (mg N/L-d)	COD Removal (%)
I	Initial	203±4[a]	89.5±4.0
	End	168±6	87.6±4.2
II	80 PAA	192±11	82.8±1.2
	120 PAA	204±2	79.3±1.6
	200 PAA	200±5	69.2±1,0
III	R40 PAA	206±7	62.2±1.0
	R80 PAA	197±3	67±1.8
	R200 PAA-1 HRT	156±8	56.5±0.8
	R200 PAA-2 HRT	57±2	47.2±1.2
	R200 PAA-3 HRT	35±3	29.3±1.0
IV	Recovery -1 HRT	167±5	59.4±1.8
	Recovery -3 HRT	194±8	78.1±2.4
V	R40 PAA	158±4	62.1±3.0
	R80 PAA	54±4	55.6±2.0
VI	Recovery -1 HRT	151±6	72.2±2.6
	Recovery -3 HRT	193±9	75.2±2.0

[a] Mean ± standard deviation ($n = 3$)

8.3.3 Microbial community analysis

Table 8.10 summarizes the number of operational taxonomic units (OTUs) and the microbial community diversity indices of the seventeen culture samples of the BNR system. Overall, the number of OTUs in R1, R2, and R3 increased from the end of Phase I to the end of Phase II, then decreased twice during Phase III, and then increased again at the end of Phase IV. Thus, the richness of the BNR system increased by the direct addition of PAA to R1 during Phase II, while decreased by feeding with PAA directly to R1. The Shannon index of R1 gradually increased from ca. 5.2 to 6.4 from the end of Phase I to the end of Phase IV, suggesting the microbial diversity in R1 slowly decreased during the whole BNR system operation. The Shannon indices of R2 and R3 were close, varying from 5.3 to 5.9 from the end of Phase I to the end of feeding at 80 mg/L PAA in Phase III, while significantly decreased to a mean value of 3.2 at the end of feeding at 200 mg/L PAA in Phase III; then it increased again to a mean value of 6.5 at the end of Phase IV. Thus, the microbial diversity in R2 and R3 reached its maximum at the end of Phase III when system upset occurred.

Principal coordinates analysis (PCoA) based on weighted UniFrac is shown in Figure 8.9. Feed and feed amended with PAA shifted mainly on PC1 (44.62%). Similarly, R1 also shifted mainly on PC1 (44.62%). The R1 community at the end of feeding with 200 mg/L residual PAA wastewater in Phase III shifted farthest from R1 community at the end of Phase I, while R1 community at end of Phase II and IV located between them. Thus, PC1 is likely representing the total amount of PAA solution added to the system. The microbial communities in R2 and R3 were very close in all phases of the BNR system operation, which is attributed to the fact that R2 and R3 mixed liquor was

212

continuously cycled back and forth during the operation. From Phase I to feeding with 80 mg/L residual PAA wastewater in Phase III, the communities in R2 and R3 shifted slightly on PC2 (21.38%). The major shift of R2 and R3 communities on PC2 was from feeding 80 to 200 mg/L PAA in Phase III. Due to the fact that PAA was not detected in R2 or R3, except during the system upset at the end of Phase III, suggests that PC2 does not represent PAA but a factor that may be related to PAA, such as acetic acid concentration. As discussed in Section 8.3.1, VFAs were never detected in R2 during Phase I or II but more than 1000 mg/L acetic acid was measured in R2 during the system upset at the end of Phase III, which further indicates that PC2 may represent the acetic acid concentration. At the end of Phase IV, the communities in both R2 and R3 shifted back and were closer to those at the end of Phase I and II, possibly a result of VFAs removal during Phase IV.

The microbial relative abundance at order level of the BNR system is shown in Figure 8.10. The major orders in the feed and the feed amended with PAA were *Lactobacillales* (ca. 53 and 43%, respectively) and *Pseudomonadales* (ca. 33 and 23%, respectively), suggesting that both of these two major orders were negatively affected by PAA. However, as the feed was amended with 1000 mg/L initial PAA resulting in ca. 200 mg/L residual PAA, it lost bioactivity as a result of the PAA strong biocidal efficacy. Thus, the measured change of microbial composition was a result of change in dead cell DNA. *Lactobacillales* are Gram-positive, catalase-negative, rod-shaped bacteria that produce lactic acid as the major end product of fermentation (Angelis and Gobbetti, 2011). *Pseudomonadales* belong to the class γ-Proteobacteria which utilize lactic acid to produce acetic and propionic acid (Yamada and Yukphan, 2008). As stated in Section

8.3.1, above, the sum of acetic and propionic acid accounted for ca. 50% of the total

VFAs in the feed.

At the end of Phase I, the major orders in R1 were *Lactobacillales* (ca. 22%)*,*

Synergistales (ca. 19%), *Bacteroidales* (ca. 15%)*, and Pseudomonadales* (ca. 8%)*.*

However, *Lactobacillales* and *Synergistales* in R1 decreased to ca. 1 and 0.7%,

respectively, at the end of Phase II, suggesting that these two orders were significantly

and negatively affected by PAA during Phase II when PAA solution was directly added

to R1. Similar to *Lactobacillales* and *Synergistales, Bacteroidales* in R1 decreased to ca.

9% at the end of Phase II, suggesting that this order was also negatively affected by

directly added PAA during Phase II. At the end of Phase II, the major orders in R1 were

Campylobacterales (ca. 25%) and *Pseudomonadales* (ca. 24%), suggesting that these two

orders were not negatively affected by PAA. Kim et al. (2015) reported that

Campylobacter jejuni can modulate the expression of genes involved in oxidative stress

resistance mainly via the peroxide resistance regulator and *Campylobacter* oxidative

stress regulator. Thus, it supports that *Campylobacterales* was unimpacted by PAA but

got enriched instead. During Phase III, at the end of feeding 80 mg/L residual PAA

wastewater, the major orders in R1 were *Lactobacillales* (ca. 20%)*, Synergistales* (ca.

18%), *Bacteroidales* (ca. 14%)*, and Pseudomonadales* (ca. 7%), which is very similar to

the microbial structure in R1 at the end of Phase I. Thus, the significantly and negatively

impacted *Lactobacillales* and *Synergistales* recovered after the direct PAA addition to R1

was ceased. However, as the residual PAA in the feed increased to 200 mg/L during

Phase III, *Lactobacillales, Synergistales* and *Bacteroidales* in R1 decreased again to 0.4,

0.2 and 0.2%, respectively, while *Betaproteobacteriales* (ca. 18.4%), *Sphingomonadales*

(ca. 8.8%), *Rhodospirillales* (ca. 8.7%), and *Chitinophagales* (ca. 8.3%) became the

major orders in R1, indicating that these four orders were enriched when the BNR

systems was fed with residual PAA wastewater. At the end of Phase IV, *Synergistales* (ca.

22%) and *Bacteroidales* (ca. 12%) became the major orders in R1, similar to the

composition in R1 at the end of Phase I. However, at the end of Phase IV, *Lactobacillales*

(ca. 0.1%) and *Pseudomonadales* (ca. 0.5%) were not increased back to levels observed

in Phase I. Thus, the negative impact of feeding with wastewater with a high

concentration of residual PAA (i.e., 200 mg/L) was reversed for *Synergistales* and

Bacteroidales while was not reversed for *Lactobacillales* and *Pseudomonadales.*

As shown in Figure 8.10, the microbial composition of R2 and R3 was extremely

similar throughout the BNR system operation, which is also reflected by the above

discussed PCoA data. Thus, the relative abundance of major orders in R2 and R3 are

discussed below together. At the end of Phase I, the major orders in R2/R3 were

Betaproteobacteriales (ca. 26%)*, Sphingobacteriales* (ca. 19%), *Rhodobacterales* (ca.

13%), and *Rhizobiales* (ca. 6%). However, at the end of Phase II, *Betaproteobacteriales,*

Sphingobacteriales and *Rhodobacterales* in R2/R3 decreased to ca. 11, 10, and 5%,

respectively, suggesting that *Betaproteobacteriales* and *Sphingobacteriales* were

significantly and negatively affected by PAA during Phase II when PAA solution was

directly added to R1. The observed decrease of *Sphingobacteriales* under the effect of

PAA agrees with the findings that *Sphingobacteriales* was negatively affected by PAA or

in combination with H_2O_2 in anoxic denitrification bioreactors (Chapter 7, Section 7.3.5).

Rhizobiales in R2/R3 decreased to ca. 3% at the end of Phase II, suggesting that this

215

order was also mildly impacted by the direct addition of PAA to R1 during Phase II. From the end of Phase I to the end of Phase II, *Rhodospirillales* increased from ca. 0.9 to 24% and *Chitinophagales* increased from 0.9 to 7.9% in R2/R3, suggesting that these two orders were enriched by the addition of PAA solution to R1. However, the observed increase of *Chitinophagales* under the effect of PAA is contradictory to the findings that PAA solutions negatively impacted *Chitinophagales* in anoxic denitrifying bioreactors in our previous study (Chapter 7, Section 7.3.5). From the end of Phase II to the end of feeding 80 mg/L residual PAA wastewater in Phase III, *Betaproteobacteriales* increased from ca. 11 to 21%, *Chitinophagales* increased from ca. 8 to 15%, and *Pirellulales* increased from ca. 6 to 12%, becoming the major orders in R2/R3. The abundance of *Betaproteobacteriales, Chitinophagales,* and *Pirellulales* was lower in R1 than in R2/R3; none of these three orders increased in R1 from the end of Phase II to the end of feeding 80 mg/L residual PAA wastewater in Phase III, suggesting that these three orders were enriched in R2/R3. However, *Rhodospirillales* and *Sphingobacteriales* in R2/R3 decreased from ca. 24 to 6% and from 10 to 4% from the end of Phase II to the end of feeding 80 mg/L residual PAA wastewater in Phase III, suggesting these two orders were negatively impacted by PAA. Expectedly, *Rhodospirillales* and *Sphingobacteriales* in R2/R3 further decreased to 1.4 and 0.2%, respectively, as the residual PAA concentration increased to 200 mg/L in the feed. Nevertheless, as the feed residual PAA increased to 200 mg/L, *Sphingomonadales* and *Pseudomonadales* in R2/R3 increased from ca. 0.3 to 61% and 0.1 to 6.8%, respectively, indicating that they were resistant to the strong oxidants like PAA and were enriched under the effect of PAA. The detected *Sphingomonadales* consisted of ca. 100% *Novosphingobium* (Table 8.11).

216

Novosphingobium sp. PP1Y has been reported as a potential source of novel metabolites with antioxidant activity, preventing ROS accumulation (Petruk et al., 2019). This agrees with our finding that *Sphingomonadales* significantly increased (i.e., 0.3 to 61%) during the BNR system operation with the highest PAA level (i.e., 200 mg/L residual PAA in the feed). At the end of Phase IV, *Betaproteobacteriales, Rhodobacterales,* and *Rhizobiales* increased back to ca. 20, 8, and 7%, respectively, becoming the major orders in R2/R3 again as was the case in Phase II, suggesting the PAA impact on these orders was fast reversed. However, at the end of Phase IV, *Sphingomonadales* and *Pseudomonadales* in R2/R3 decreased to 1.9 and 0.2%, respectively, suggesting that they were not favored in the PAA-free system.

The most abundant denitrifying genera in R2 were *Defluviicoccus, Paracoccus, Pseudomonas, Pseudoxanthomonas* and *Pirellula* (Table 8.11). With the exception of *Pseudomonas* and *Pseudoxanthomonas,* all other genera were negatively impacted by feeding with 200 mg/L residual PAA wastewater. The denitrifying capability of one *Defluviicoccus* species (Cluster 1 DvGAOs) was evaluated and reported by Wang et al. (2007). *Paracoccus denitrificans,* has been found as a putative denitrifying species (Carlson, 1983). *Pseudomonas stutzeri* and *Pseudomonas aeruginosa* are also major denitrifying species (Carlson, 1983). *Pseudomonas* and *Pseudoxanthomonas* were identified as major denitrifiers in ammonia and nitride oxidizing bacterial enrichments (Baskaran et al., 2020). The unimpacted genera, *Pseudomonas,* was the major nitrifiers in R3. Six *Pseudomonas* strains, capable of heterotrophic nitrification, were isolated and showed a complete oxidation of 100 mg/L NH_4Cl during a 96-h cultivation (Tran et al., 2019).

Table 8.10. OTU numbers and alpha diversity indices of the microbial communities in the BNR system over the four-phase operation.

Group	Sample[a]	OTUs	Ace	Chao1	Simpson	Shannon
1	FEED	432	599.7	568.4	0.741	3.099
	FEEDPAA	647	804.1	778.7	0.859	4.822
2	R1.I	492	761.6	731.6	0.934	5.258
	R1.II	631	799.1	812.3	0.909	5.190
	R1.III80	590	719.1	708.9	0.948	5.726
	R1.III200	547	623.0	603.9	0.967	6.105
	R1.IV	690	888.3	892.4	0.970	6.422
3	R2.I	555	681.0	703.3	0.938	5.719
	R2.II	655	815.0	800.4	0.954	5.935
	R2.III80	474	638.3	623.7	0.962	5.828
	R2.III200	402	538.9	505.3	0.630	3.266
	R2.IV	638	779.9	752.0	0.980	6.732
4	R3.I	501	584.5	583.8	0.943	5.674
	R3.II	657	828.7	809.5	0.948	5.790
	R3.III80	377	407.0	390.4	0.935	5.322
	R3.III200	360	508.3	503.3	0.614	3.153
	R3.IV	573	723.1	710.8	0.974	6.417

[a] Abbreviations:
FEED: feed;
FEEDPAA: feed amended with PAA at an initial concentration of 1000 mg/L;
R1.I, R2.I, and R3.I: R1, R2, and R3 mixed liquor at the end of Phase I;
R1.II, R2.II, and R3.II: R1, R2, and R3 mixed liquor at the end of Phase II;
R1.III80, R2.III80, and R3.III80: R1, R2, and R3 mixed liquor at the end of feeding 80 mg/L residual PAA wastewater (Phase III);
R1.III200, R2.III200, and R3III200: R1, R2, and R3 mixed liquor at the end of feeding 200 mg/L residual PAA wastewater (Phase III);
R1.IV, R2.IV, and R3.IV: R1, R2, and R3 mixed liquor at the end of Phase I.

Table 8.11. Relative abundance (%) at genus level (top 12 genera) of the microbial communities in BNR system samples [a].

Genus	FEED	FEED PAA	R1.I	R1.II	R1.III80	R1.III 200	R1.IV
Novosphingobium	0.0	0.5	0.0	0.1	0.0	8.3	2.9
Lactococcus	48.5	36.5	20.3	0.7	17.7	0.2	0.0
Defluviicoccus	0.0	0.2	0.0	0.2	0.7	8.7	0.4
Arcobacter	0.0	0.0	0.0	24.6	0.1	0.1	0.6
Pseudomonas	21.8	15.4	1.0	3.1	1.0	0.4	0.2
Acinetobacter	11.7	7.4	7.0	20.8	6.4	0.2	0.1
Dinghuibacter	0.0	0.2	0.0	0.0	0.1	6.2	0.3
Paracoccus	0.0	0.1	0.0	1.7	0.2	1.3	0.1
Pirellula	0.0	0.7	0.0	0.2	0.1	4.9	0.2
Bacteroides	0.2	0.1	0.6	6.9	0.8	0.0	0.4
Lactobacillus	6.5	5.6	1.2	0.1	1.3	0.0	0.0
Pseudoxanthomonas	0.2	1.4	0.0	0.0	0.0	0.4	0.4

[a] For sample abbreviations, see Table 8.10 footnotes

Table 8.11 (Continued). Relative abundance (%) at genus level (top 12 genera) of the microbial communities in BNR system samples [a].

Genus	R2. I	R2. II	R2. III80	R2. III 200	R2. IV	R3. I	R3. II	R3. III80	R3. III 200	R3. IV
Novosphingobi-um	0.0	0.0	0.0	60.3	0.7	0.0	0.1	0.0	61.7	0.4
Lactococcus	0.6	0.1	0.0	0.0	3.2	0.3	0.1	0.0	0.0	1.6
Defluviicoccus	0.9	23.9	5.8	1.4	0.2	1.0	25.9	3.3	1.3	0.1
Arcobacter	0.0	0.5	0.0	0.0	0.0	0.0	0.3	0.0	0.0	0.0
Pseudomonas	0.0	0.1	0.1	1.9	0.2	0.0	0.1	0.0	2.1	0.1
Acinetobacter	0.1	0.6	0.0	0.6	0.0	0.1	0.3	0.0	0.6	0.1
Dinghuibacter	0.0	5.4	11.1	0.8	0.1	0.0	5.0	14.3	0.7	0.0
Paracoccus	7.8	3.2	1.1	0.1	0.2	9.0	3.1	0.2	0.1	0.2
Pirellula	0.9	2.6	7.2	0.8	2.0	0.7	2.7	4.3	0.6	2.4
Bacteroides	0.0	0.3	0.0	0.0	0.1	0.0	0.2	0.1	0.1	0.3
Lactobacillus	0.0	0.0	0.0	0.0	0.1	0.0	0.0	0.0	0.0	0.1
Pseudoxantho-monas	0.1	0.0	0.2	1.8	4.1	0.1	0.0	0.7	4.7	5.5

[a] For sample abbreviations, see Table 8.10 footnotes
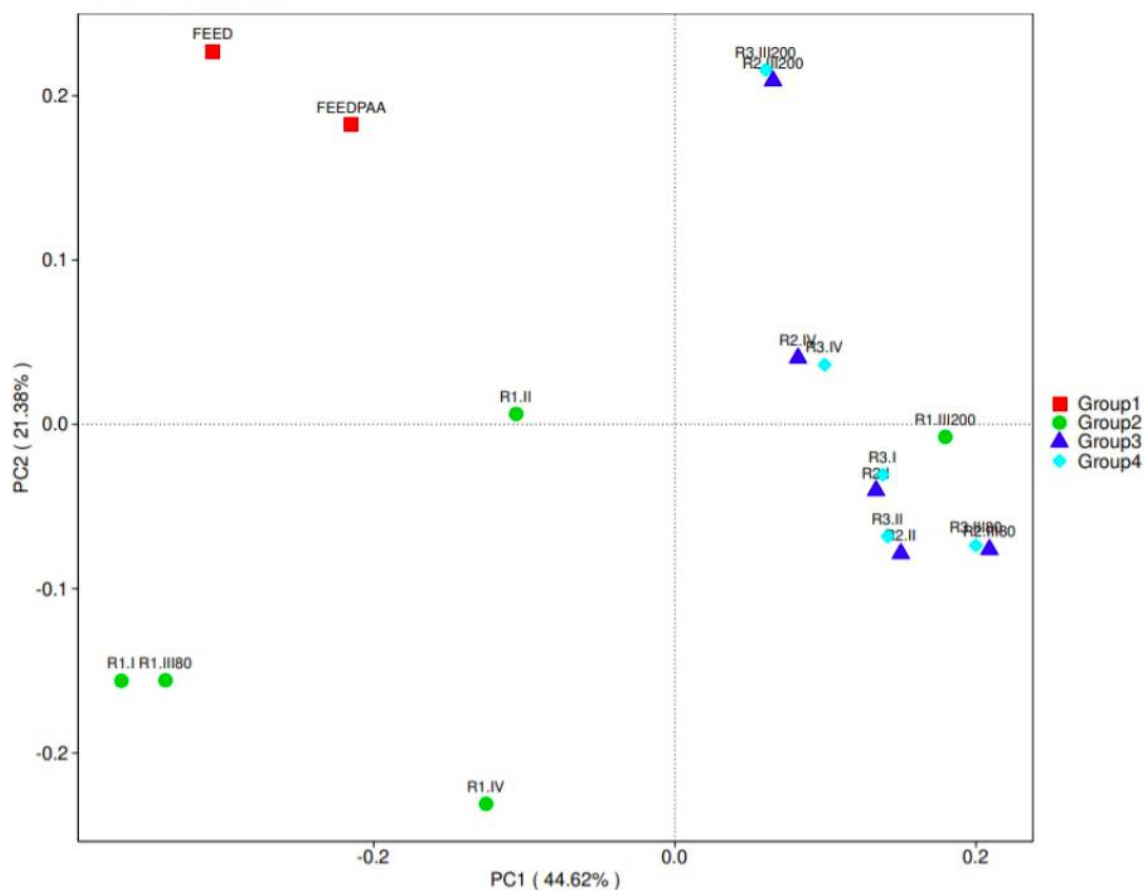
Figure 8.9. Principal coordinates analysis based on weighted UniFrac of the microbial communities in the BNR system at order level.

Group 1 (red square), 2 (green circle), 3 (blue triangle), and 4 (light blue diamond) are samples from feed and feed+PAA, R1, R2, and R3, respectively (see Table 8.10).
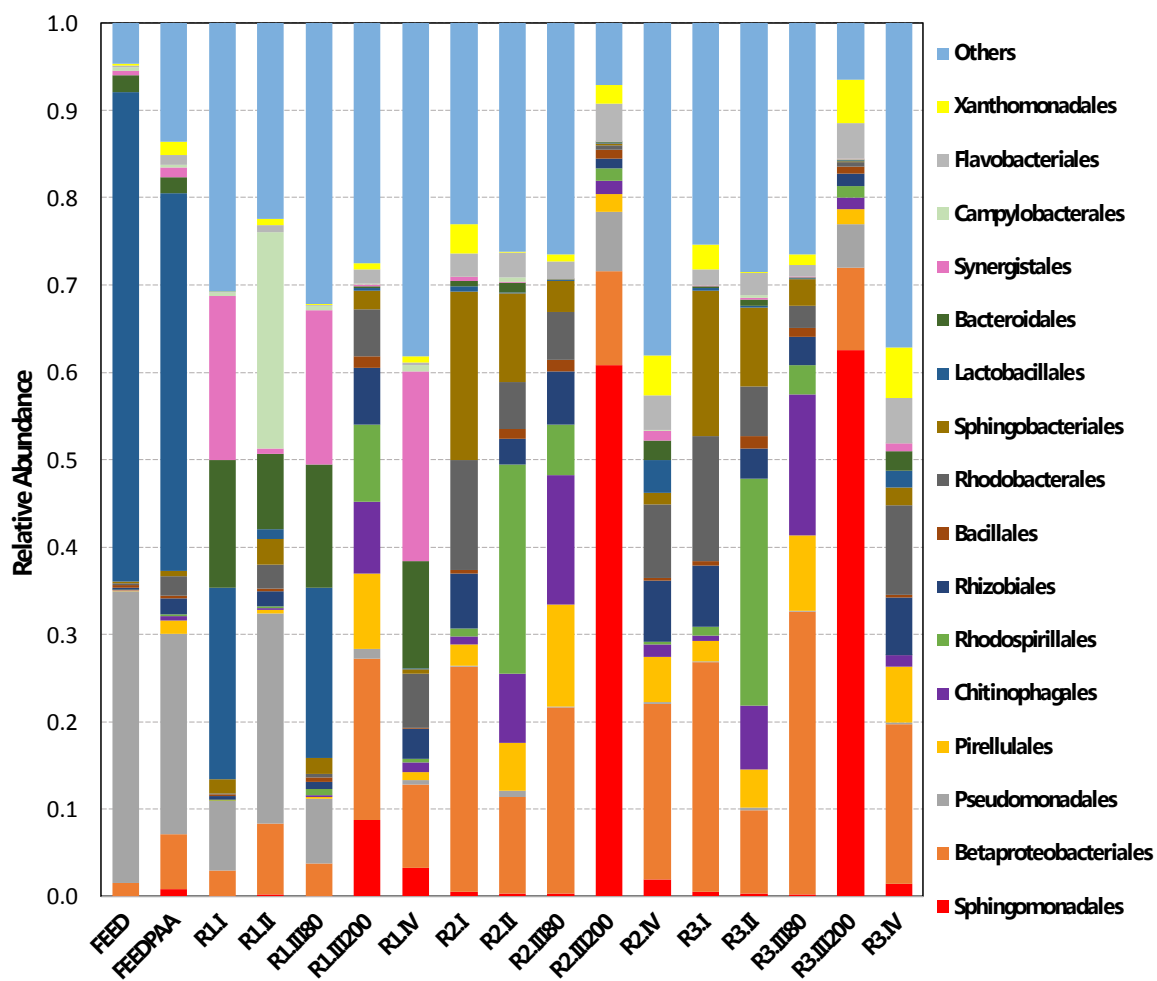
Figure 8.10. Order level relative abundance bar plot of the microbial communities in the BNR system.

For sample abbreviations, see Table 8.10 footnotes

8.4 Summary

Continuous, direct addition of PAA at stepwise increased concentrations from 80 to 200 mg/L in the anaerobic reactor (R1) did not affect the performance of the three-reactor BNR system in terms of organic matter degradation and N removal, quantified as the extent of both soluble COD and N removal. However, both organic matter degradation and N removal were negatively affected by continuous feeding with wastewater carrying residual PAA, especially at 80 and 200 mg/L residual PAA. Fast recovery of organic matter degradation and N removal was achieved within three HRTs feeding with PAA/H_2O_2-free DAF wastewater. The BNR system was more susceptible to residual PAA without the R1, i.e., two-reactor system, as system upset occurred at a lower residual PAA level than when R1 was used (i.e., three-reactor system). The BNR system recovered from the second system upset as fast as it recovered from the first system upset, indicating that the system was able to completely recover from the impact of PAA; the effect of PAA on system performance was not lasting. Microbial community analysis showed that the major orders *Lactobacillales, Synergistales, Bacteroidales*, and *Pseudomonadales* in R1 were all negatively impacted by PAA; the PAA impact on *Synergistales* and *Bacteroidales* was reversed while was not on *Lactobacillales* and *Pseudomonadales* after operation with PAA solution free DAF wastewater. In contrast, *Campylobacterales* and *Sphingomonadales* were enriched, attributed to their antioxidizing ability reported previously by other studies. However, both *Campylobacterales* and *Sphingomonadales* were not favored during the PAA-free system operation. The microbial communities in R2 and R3 were very similar, due to the continuous mixed liquor cycling between them. All major orders in R2 and R3,

Betaproteobacteriales, Sphingobacteriales and *Rhodobacterales*, were negatively affected by PAA.

CHAPTER 9. EFFECT OF PAA ON AN ENRICHED NITRIFYING CULTURE

9.1 Introduction

Nitrification plays an important role in wastewater treatment systems for the purpose of N removal. Nitrification mainly consists of two steps: ammonia oxidation to nitrite by ammonia oxidizing bacteria (AOB) and nitrite oxidization to nitrate by nitrite oxidizing bacteria (NOB) (Rittmann and McCarty, 2001). Although it has been applied extensively, nitrification is a very sensitive process easily affected by external factors such as pH, dissolved oxygen (DO) levels, temperature, microbial density, and inhibitory compounds (Anthonisen et al., 1976). However, information related to the effect of PAA solution on AOB and NOB is not available. As discussed in Chapter 5 and 6, both PAA and H_2O_2 negatively affected nitrification in mixed heterotrophic cultures; however, the inhibitory effect on nitrifiers was not elucidated. Therefore, the objective of this chapter was to evaluate the effect of PAA and H_2O_2 solution on nitrification, microbial community structure and gene expression.

9.2 Materials and Methods

9.2.1 Chemicals

Chemicals are as described in Chapter 3, Section 3.2.1.

9.2.2 Enriched Nitrifying Culture

A 4-L aerobic nitrifying culture was developed using inoculum mixed liquor obtained from the activated sludge reactor of a poultry processing plant in the Southeastern US. The culture was enriched and maintained in a 5-L glass bottle at room

temperature (22 ± 1ºC), aerated with pre-humidified compressed air, mixed magnetically, and fed with 30 g N/L NH$_4$Cl every 3 h using a periplasmic pump controlled with an electronic timer. The resulting ammonia loading rate was 120 mg N/L-d. The pH of the culture was maintained at ca. 7.3 by a HD-pH/P pH controller (Etatron, Italy) connected to a 1 N NaHCO$_3$ solution. For the purpose of enriching slowly growing nitrifying bacteria, every 3 d, the culture was settled for 1 h and then 3 L of culture supernatant was wasted and replaced with fresh culture medium. Every 6 d, 1 L mixed liquor was wasted. Based on the above-described culture maintenance, the hydraulic and solids retention times were 4 and 24 d, respectively. The composition of the culture medium is shown in Table 9.1. The enriched nitrifying culture was maintained for 10 months before used in batch bioassays described below. pH, DO, total suspended solids (TSS), volatile suspended solids (VSS), ammonia, nitrite, and nitrate were periodically measured. The time-trend N species of a batch reactor conducted using the control enriched nitrifying culture is shown in Figure 9.1. Initial ammonia removal rates (ARR) were calculated by linear regression of ammonia concentration vs. time data. As nitrite is an intermediate, produced and then oxidized to nitrate at 1:1 molar ratio, initial nitrite removal rates (NRR) were calculated as the initial nitrate production rates (NPR) by linear regression of time-trend nitrate concentration data. Under steady state, the pH was 7.3$\pm$0.1, the DO was 7.5$\pm$0.4 mg/L, TSS/VSS was 432$\pm$15/170$\pm$20 mg/L. Ammonia or nitrite was not detected at the end of every 3 h feeding with NH$_4$Cl. The relative abundance of viable AOB, NOB, and heterotrophs was ca. 86, 11, and 3%, respectively, based on oxygen uptake rate measurements (Surmacz-Gorska et al., 1996).
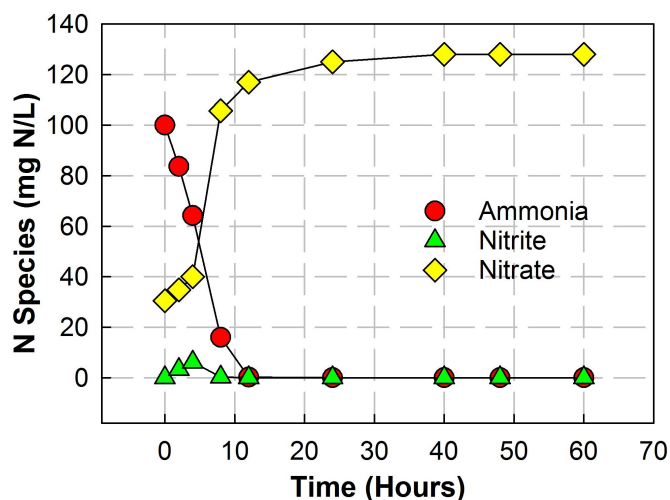
Figure 9.1. Time-trend of N species concentration (mg/L) in a batch reactor conducted with the enriched nitrifying culture.

Table 9.1. Composition of the nitrifying culture medium and trace metal solution.

Medium components	Concentration (mg/L)
1. K_2HPO_4	600
2. KH_2PO_4	335
3. $CaCl_2 \cdot 2H_2O$	67.5
4. $MgCl_2 \cdot 6H_2O$	135
5. $MgSO_4 \cdot 7H_2O$	267.5
6. $FeCl_2 \cdot 4H_2O$	67.5
7. Trace metal solution[a]	1

Trace metal solution components	Concentration (mg/L)
1. $ZnCl_2$	25
2. $MnCl_2 \cdot 4H_2O$	15
3. H_3BO_3	150
4. $CoCl_2 \cdot 6H_2O$	100
5. $CuCl_2 \cdot 2H_2O$	5
6. $NiSO_4 \cdot 6H_2O$	10
7. $NaMoO_4 \cdot 2H_2O$	15

[a] 1 mL trace metal solution per 9 L of culture medium

9.2.3 Batch Assays

9.2.3.1 Batch abiotic assay

In order to assess possible, abiotic oxidation of ammonia by the PAA solution, i.e., PAA and H_2O_2, a batch assay was conducted with three test series, set up in 0.5-L glass aspiration bottles with 400 mL sterilized nitrifying culture medium, amended with PAA solution or H_2O_2, resulting in an initial PAA/H_2O_2 concentration of 0/0, 3/0.42, and 0/3 mg/L, respectively. All three series were amended with 100 mg N/L NH_4Cl and 1200 mg/L $NaHCO_3$ at the beginning of the incubation. The bottle contents were aerated with pre-humidified compressed air, mixed magnetically, and incubated at room temperature (22±1°C). Ammonia, nitrite and nitrate were measured at 0, 24, 48, and 60 h of incubation. Ammonia was not degraded in any of the series throughout the incubation, indicating ammonia oxidation did not take place abiotically by either PAA or H_2O_2.

9.2.3.2 Batch nitrification assays

Two aerobic nitrification batch assays were conducted using mixed liquor from the enriched nitrifying culture right before feeding with NH_4Cl (Section 1.2, above). One assay, consisting of six 500-mL glass aspiration bottles, was set up with an initial PAA/H_2O_2 concentration of 0/0, 0.2/0.03, 0.5/0.07, 1/0.14, 2/0.28, and 3/0.42 mg/L, respectively. In order to distinguish and compare the effect of PAA from that of H_2O_2, another assay, consisting of six 500-mL glass aspiration bottles, was set up with an initial H_2O_2 concentration of 0, 0.2, 0.5, 1, 2, and 3 mg/L, respectively. All series in both assays were set up with 390 mL of enriched nitrifying culture (400 mL total liquid volume), amended with 100 mg N/L NH_4Cl and 1200 mg/L $NaHCO_3$ at the beginning of the incubation. The bottle contents were aerated with pre-humidified compressed air, mixed magnetically, and incubated at room temperature (22±1°C). The DO, pH, ammonia,

nitrite and nitrate were measured at 0, 2, 4, 8, 12, 24, 40, 48, and 60 h of incubation. TSS, VSS and live cell fraction of the test series in both assays were measured at 2-h and 60-h of incubation, representing the initial and final biomass concentration and cell viability, respectively. Intracellular ROS was measured after 2-h incubation. OUR measurements, including overall culture activity (OUR_{All}), ammonia oxidation (OUR_{NH4}), nitrite oxidation (OUR_{NO2}), and heterotrophic activity (OUR_{Heter}) for both assays were conducted at 2-h of incubation. Bacterial DNA extraction, quantification, sequencing, as well as bioinformatic analysis were performed for samples withdrawn from all test series amended with PAA/H_2O_2 at the end of 60-h incubation (See Section 1.5, below). Total bacteria mRNA was extracted, purified, and analyzed for samples withdrawn from all test series amended with PAA/H_2O_2 at 24-h incubation (See Section 1.6, below).

9.2.4 Transcriptomic Analysis

Transcriptomic analysis followed the procedures described in Chapter 3, Section 3.4.

9.2.5 Analytical Methods

pH, N species, TSS and VSS, DO, culture viability, and intracellular ROS were measured as described in Chapter 3, Section 3.1. PAA and H_2O_2 were measured by the DPD method as described in Chapter 3, Section 3.2.3. The fraction of heterotrophic bacteria, AOB, and NOB in the stock enriched nitrifying culture was determined by using sodium azide (NaN_3) and allylthiourea (ATU) to inhibit AOB and NOB, respectively, and

then measuring oxygen uptake rates (OURs) as previously described (Surmacz-Gorska et al., 1996).

9.3 Results and Discussion

Nitrification is a two-step process: ammonia oxidation to nitrite, followed by nitrite oxidation to nitrate (Rittmann and McCarty, 2001; Tchobanoglous et al., 2014). Autotrophic nitrifiers utilize ammonia and nitrite as the only limiting substrates for microbial growth, and Monod kinetics are used to describe the substrate utilization rates. The substrate (S, i.e., ammonia or nitrite) utilization rate is as follows:

$$\frac{dS}{dt} = \frac{k\,X\,S}{K_s + S}\,\frac{DO}{K_{DO} + DO} \qquad (9.1)$$

where k is the maximum specific substrate utilization rate (mg N/mg VSS-h), X is the biomass concentration (mg VSS/L), S is the substrate (i.e., ammonia or nitrite) concentration (mg N/L), K_s is the half-saturation constant for S (mg N/L), DO is the DO concentration (mg DO/L), K_{DO} is the half-saturation constant for DO (mg DO/L), and t is time (h). Under no oxygen limitations (i.e., DO $\geq$ 7 mg/L), and assuming no ammonia or nitrite inhibition, constant neutral pH, and negligible biomass growth during the relatively short duration of the batch assays, Equation 9.1 is reduced to the following equation:

$$\frac{dS}{dt} = \frac{k'\,S}{K_s + S} \qquad (9.2)$$

where, $k' = k\,X$, is the maximum substrate utilization rate (mg N/L-h). The k' and K_S values were obtained by nonlinear regression of the initial ammonia removal rate (ARR) vs. ammonia concentration and the initial nitrite removal rate (NRR) vs. nitrite concentration (Figure 9.2) using SigmaPlot 14.0. The estimated k' values were

9.5±0.2and 6.3±0.1 mg N/L-h for ammonia and nitrite removal, respectively. The estimated K_S values were 3.8±0.8 mg NH_4^+-N/L and 13.1±0.7 mg NO_2^--N/L. K_S values ranging from 0.14 to 5.0 mg NH_4^+-N/L have been reported for ammonia oxidation to nitrite (Sin et al., 2008) and values between 0.30 and 0.70 mg NH_4^+-N/L have been reported based on full scale plant performance (Tchobanoglous et al., 2014). Lower K_S values, ranging from 0.05 to 0.30 mg NO_2^--N/L, have been reported for the oxidation of nitrite to nitrate (Sin et al., 2008).
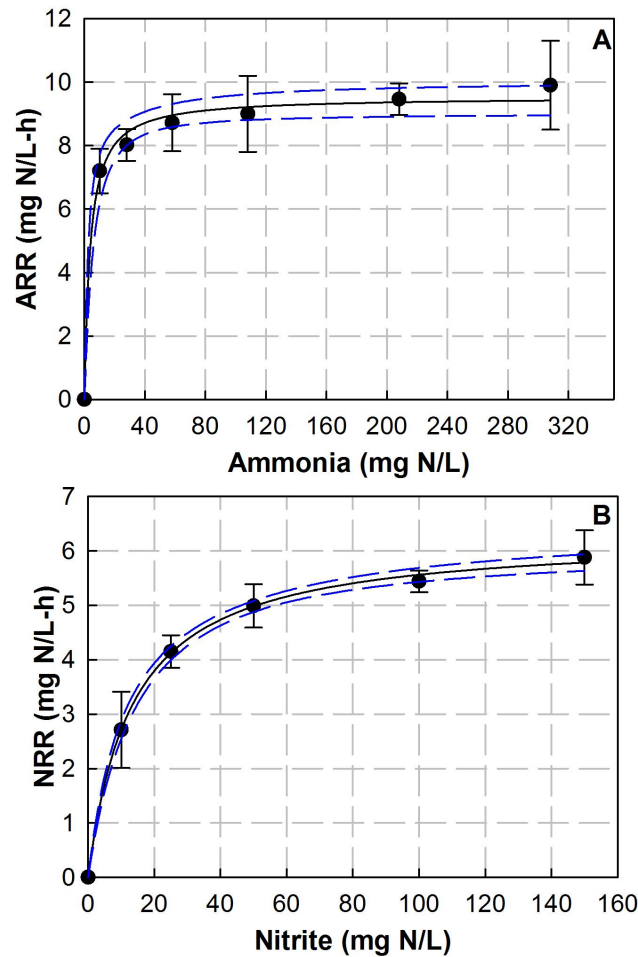
Figure 9.2. Initial ARR vs. initial ammonia concentration (A); initial NRR vs. initial nitrite concentration (B). Black solid line is regression curve and blue broken lines are 95% confidence band. Error bars are standard deviations.

230

9.3.1 Effect of PAA and H_2O_2 on Nitrification

9.3.1.1 Effect of H_2O_2 on nitrification

The pH in all test series of the batch assay was 8.4/8.8 and 7.6/7.8 initially and at the end of the 60-h incubation, respectively. The DO concentration varied from 7.4 to 7.8 mg/L in all six series. H_2O_2 was not detected in any of the six series due to its fast decomposition. Table 9.2 summarizes the initial ARR, SARR, NPR and SNPR of the batch assay six series. The initial ARR varied from ca. 10.4 to 10.5 mg N/L-h among all series, suggesting that ammonia oxidation was not affected by H_2O_2 at the above stated initial concentrations. Likewise, the initial NPR varied from 15.5 to 17.3 without any clear trend among all series, suggesting that nitrite oxidation was not affected by H_2O_2 at the above stated initial concentrations.

Table 9.2. Initial ammonia removal rate (ARR), specific ammonia removal rate (SARR), nitrate production rate (NPR), and specific nitrate production rate (SNPR) in a batch assay conducted with the enriched nitrifying culture at a range of initial H_2O_2 concentrations.

H_2O_2 (mg/L)	ARR (mg N/L-h)	SARR (mg N/g VSS-h)	NPR (mg N/L-h)	SNPR (mg N/g VSS-h)
0	10.4±0.8[a]	64.8±5.3	16.0±0.6	100.0±3.8
0.2	10.4±0.8	63.8±4.8	16.8±1.0	102.9±6.1
0.5	10.5±0.8	65.6±5.0	16.9±1.4	105.6±8.7
1	10.5±0.8	67.2±4.9	17.3±0.8	110.4±5.1
2	10.4±0.7	68.0±4.8	17.3±0.8	112.8±5.2
3	10.4±0.8	66.2±5.1	15.5±1.5	98.9±9.6

[a] Mean ± standard deviation ($n = 3$)

9.3.1.2 Effect of PAA solution on nitrification

The pH in all test series of the batch assay was 8.3/8.4 and 7.5/7.6 initially and at the end of the 60-h incubation, respectively. The DO concentration varied from 7.4 to 7.8 mg/L in all six series. PAA or H_2O_2 was not detected in any of the six series due to their fast

decomposition (Chapter 4, Section 4.3.2). Figure 9.3 and Table 9.3 show the time-trend ammonia concentration and the initial ammonia removal rate (ARR) in the six batch assay series. The initial ARR values in the series amended with 0, 0.2, and 0.5 mg/L PAA were very close and ranged from 10.2 to 10.8 mg N/L-h, but decreased to as low as 3.8 mg N/L-h as the initial PAA concentration was increased to 3 mg/L, representing a decrease by ca. 64% of the initial ARR compared to the control series. Thus, PAA $\geq$ 1 mg/L negatively affected ammonia removal. Figure 9.4 and Table 9.3 show the time-trend nitrate concentration and the initial NPR in the six batch assay series. The initial nitrate production rate (NPR), and thus nitrite removal rate (NRR), in the series amended with 0 and 0.2 mg/L PAA were very close and ranged from 16.4 to 15.6 mg N/L-h, but decreased to as low as 3.7 mg N/L-h as the initial PAA concentration increased to 3 mg/L, representing a decrease by ca. 42% of the initial NPR compared to the control series. Therefore, PAA $\geq$ 0.5 mg/L negatively affected nitrite oxidation to nitrate. Therefore, based on the negligible H_2O_2 effect discussed in Section 9.3.1.1, above, the negative effect of the PAA solution on nitrification was predominantly attributed to PAA alone. Assuming a constant nitrifying biomass concentration during the relatively short duration of the batch assays conducted in this study, and non-competitive inhibition, the relationship between the initial ARR or NPR and the concentration of the inhibitor (i.e., PAA) can be described by the Michaelis-Menten based noncompetitive enzyme inhibition, as follows (Rittmann and McCarty, 2001):

$$\frac{dS}{dt} = \frac{k' \, S \, K_I}{(K_S + S)(K_I + I)} \qquad (9.3)$$

where, V_{max} is the maximum rate (mg N/L-h), S is the substrate (i.e., ammonia or nitrite) concentration (mg N/L), K_M is the Michaelis-Menten coefficient (mg N/L), I is the

232

inhibitor concentration (mg PAA/L), and K_I is the inhibition coefficient (mg PAA/L), i.e.,

the PAA concentration at which the substrate utilization rate is half its maximum value.

In the case of high substrate (i.e., ammonia or nitrite) concentration relative to K_M values,

Equation 9.3 is simplified as follows:

$$\frac{dS}{dt} \approx \frac{k' K_I}{K_I + I}$$

The determination of the V_{max} and K_I values was done using nonlinear regression in

SigmaPlot 14.0. The V_{max} value was 11.4±0.7 for ARR and 17.1±1.4 for NPR. The K_I

value of PAA for both ARR and NPR was relatively low, 2.3±0.6 and 1.6±0.5 (estimate ±

standard error) mg/L PAA, respectively. Compared to the K_I value of other inhibitors to

nitrification, the PAA inhibition values suggest a high susceptibility of the nitrifying

bacteria to PAA. For example, the K_I value of 2-propanone, aniline, chromium,

formaldehyde and methanol on nitrifiers was 804, 3, 50, 61 and 116 mg/L, respectively

(Gheewala et al., 2004; Beg et al., 1982; Oslislo and Lewandowski, 1985). The K_I value

of benzalkonium chloride on nitrifiers was 1.5±0.9 mg BAC/L, which suggests a high

susceptibility of nitrifying bacteria (mainly ammonia oxidizers) to BAC (Yang et al.,

2015).

PAA below 20 mg/L had a minor inhibitory effect on nitrification in a mixed

heterotrophic culture (Chapter 6, Section 6.3), predominantly attributed to the fact that

PAA was fast decomposed by the high organic content of the wastewater fed to the

heterotrophic culture, as well as the higher biomass concentration of the heterotrophs in

the mixed culture, combined with their high antioxidant capacity.

Table 9.3. Initial ammonia removal rate (ARR), specific ammonia removal rate (SARR), nitrate production rate (NPR), and specific nitrate production rate (SNPR) in a batch assay conducted with the enriched nitrifying culture at a range of initial PAA/H₂O₂ concentrations.

PAA/H$_2$O$_2$ (mg/L)	ARR (mg N/L-h)	SARR (mg N/g VSS-h)	NPR (mg N/L-h)	SNPR (mg N/g VSS-h)
0/0	10.6±0.7[a]	70.7±4.4	16.4±0.8	109.3±5.3
0.2/0.03	10.8±0.7	65.8±4.2	15.6±0.2	95.5±1.2
0.5/0.07	10.2±1.0	59.8±5.8	13.4±1.1	78.8±6.5
1/0.14	7.8±0.5	46.9±3.2	10.9±0.4	65.4±2.4
2/0.28	6.7±0.4	42.9±2.7	9.6±0.5	61.3±2.9
3/0.42	3.8±0.2	25.1±1.3	3.7±0.1	20.7±0.9

[a] Mean ± standard deviation ($n = 3$)
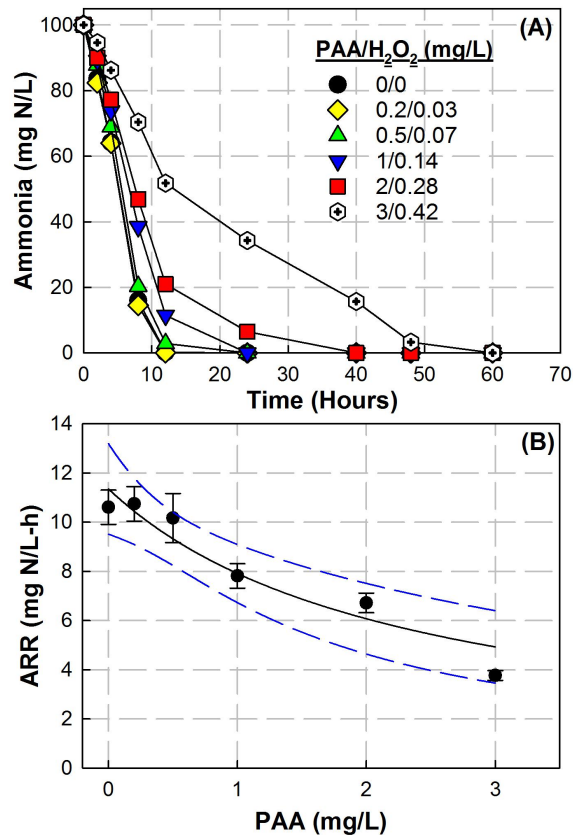
Figure 9.3. Time-trend of ammonia concentration in the batch assay conducted with the enriched nitrifying culture; series amended with PAA/H₂O₂ 0/0 to 3/0.42 mg/L, respectively (A); initial ARR vs. initial PAA concentration, with regression curve (black solid line) and 95% confidence band (blue broken lines) (B). Error bars are standard deviations.
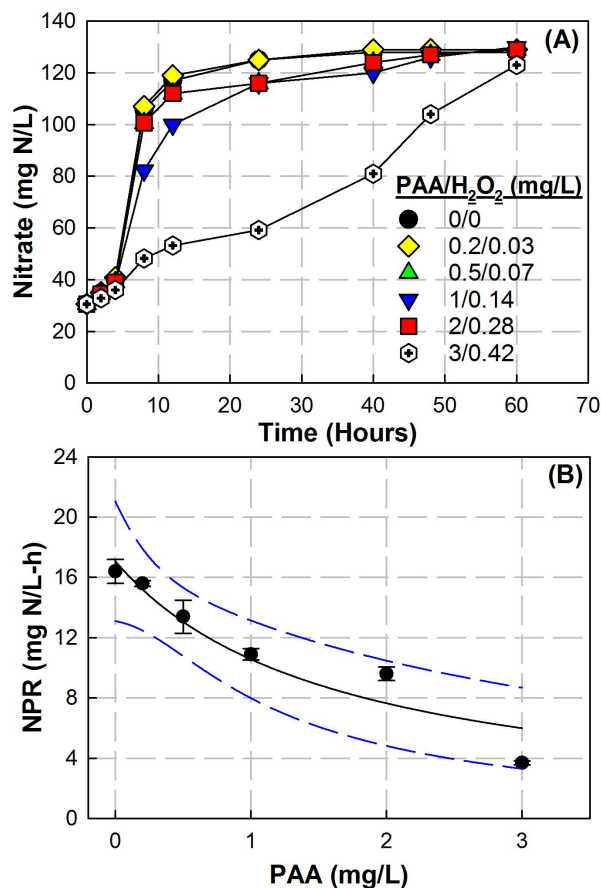
Figure 9.4. Time-trend of nitrate concentration in the batch assay conducted with the enriched nitrifying culture; series amended with PAA/H₂O₂ 0/0 to 3/0.42 mg/L, respectively (A); NPR vs. initial PAA concentration, with regression curve (black solid line) and 95% confidence band (blue broken lines) (B). Error bars are standard deviations.

9.3.2 Effect of PAA and H_2O_2 on Cell Viability and Intracellular ROS

9.3.2.1 Effect of H_2O_2 on cell viability and intracellular ROS

Table 9.4 summarizes the TSS, VSS, and cell viability data of the six batch assay series. The mean TSS and VSS values varied from 390 to 420 mg/L and from 150 to 160 mg/L, respectively, suggesting that direct addition of H_2O_2 at an initial concentration from 0 to 3 mg/L did not cause significant cell lysis. At 2 h of incubation, the cell viability varied from ca. 72 to 78% without any particular trend among all culture series.

235

Likewise, at the end of the 60-h incubation, the cell viability varied from ca. 82 to 87% (Figure 9.5A). At 2 h of incubation, the relative intracellular ROS of the six test culture series varied from 0.9 to 1.0 without any particular trend among all series (Table 9.5 and Figure 9.5B). Thus, direct addition of H_2O_2 at the above stated initial concentrations did not affect cell viability or intracellular ROS, in agreement with the non-impacted nitrification rates as discussed in Section 9.3.1, above.

Table 9.4. TSS, VSS and cell viability of the test series in the batch assay conducted with the enriched nitrifying culture amended with a range of initial H_2O_2 concentration at 2 and 60 h of incubation.

Incubation Time (h)	Initial H_2O_2 (mg/L)	TSS (mg/L)	VSS (mg/L)	VSS/TSS (%)	Cell Viability (%)
2	0	397±12 [a]	160±10	40.3	72.3±3.2
	0.2	417±12	163±15	39.2	71.6±4.4
	0.5	413±6	160±26	38.7	74.2±3.5
	1	393±12	157±6	39.8	77.5±2.7
	2	397±25	153±21	38.7	78.4±2.5
	3	390±17	157±12	40.2	72.1±3.3
60	0	483±25	203±12	42.1	84.7±2.1
	0.2	473±25	210±10	44.4	85.1±0.5
	0.5	483±35	223±15	46.2	87.4±0.9
	1	473±38	207±6	43.7	81.8±2.6
	2	490±44	207±21	42.2	84.7±2.1
	3	483±6	203±12	42.1	84.8±1.7

[a] Mean ± standard deviation (n = 3)

Table 9.5. Relative intracellular ROS of the batch assay series amended with a range of initial H_2O_2 concentration at 2 h of incubation.

H_2O_2 (mg/L)	Relative Intracellular ROS[a]
0 (Control)	1.00±0.13 [b]
0.2	0.91±0.14
0.5	0.90±0.10
1	1.00±0.07
2	0.99±0.09
3	0.92±0.05

[a] Normalized to the H_2O_2-free control. [b] Mean ± standard deviation (n = 3).

Figure 9.5. Cell viability vs. H_2O_2 concentration during the nitrification batch assay conducted with the enriched nitrifying culture, measured at 2 and 60 h of incubation (A); Relative intracellular ROS vs. initial H_2O_2 concentration during the nitrification batch assay conducted with the enriched nitrifying culture measured at 2 h of incubation (B). Error bars are standard deviations.

9.3.2.2 Effect of PAA solution on cell viability and intracellular

Table 9.6 summarizes the TSS, VSS, and cell viability data of the six batch assay test series. The mean initial and final VSS concentrations at 2 and 60 h of incubation varied from ca. 150 to 170 mg/L and 190 to 210 mg/L, respectively, without any clear trend among the six series, indicating that direct addition of PAA solution at an initial concentration from 0/0 to 3.0/0.42 mg/L PAA/H_2O_2 did not cause any cell lysis during the batch assay. At 2 h of incubation, the cell viability increased from ca. 73 to 95% as the initial PAA concentration increased from 0 to 1 mg/L, while it decreased to ca. 89 and 73% as the initial PAA concentration was further increased to 2 and 3 mg/L, respectively (Figure 9.6A). The increase of cell viability was attributed to the positive effect of acetic acid to the fast-growing heterotrophs as discussed in Chapter 6 Section 6.3. At the end of the 60-h incubation, the cell viability had increased from ca. 86 to 94% as the initial PAA concentration was increased from 0 to 0.5 mg/L, while it decreased to ca. 83, 74 and 66% as the initial PAA concentration was further increased to 1, 2, and 3 mg/L, respectively. Although the acetic acid positive effect concealed the negative effect of PAA on cell viability, the net viability increase in each series from the 2-h to the 60-h incubation indicates that the control had a significantly higher net increase of cell viability (ca. 13%) than all the other PAA-amended series (ca. 15% net decrease to 1% net increase of cell viability). Thus, assuming acetic acid had no negative impact on the net cell viability increase throughout the incubation, it is reasonable to assume that the observed decrease of net cell viability was attributed to the impact of PAA. The significantly net decrease of cell viability in the series with 1, 2, and 3 mg/L initial PAA concentration also

238

corresponds to the decreased ARR and NPR in these series as discussed in Section 2.1.2, above.

At 2 h of incubation, the relative intracellular ROS in the six batch assay series decreased to 0.84 and 0.87 as the initial PAA concentration was increased to 0.5 and 1 mg/L, while it increased to 1.01 and 1.16 as the PAA concentration was further increased to 1 and 2 mg/L (Table 9.7 and Figure 9.6B). The level of intracellular ROS in the nitrifying culture upon the addition of PAA solution is attributed to two factors: a) the activity of intracellular enzymes (e.g., catalase, peroxides, and superoxidase); and b) extracellular ROS diffusion into the cells. The increase in intracellular ROS with increased concentration of the PAA solution was predominantly attributed to extracellular PAA diffusion into the cells as well as other ROS produced intracellularly by them, such as OH$^{\bullet}$. Most ROS have very short half-life (10^{-6} s for $O_2^{\bullet-}$ and 10^{-9} s for OH$^{\bullet}$; Dickinson and Change, 2012); thus, when ROS are formed extracellularly will not last long enough to diffuse into the cell. However, PAA diffuses into cells. Fast PAA diffusion into Gram-negative *Escherichia coli* and Gram-positive *Enterococcus durans* and *Staphylococcus epidermidis*, resulting in intracellular oxidative stress, was recently demonstrated by Zhang et al. (2020). However, in the present studyPAA completely decomposed immediately after addition to the culture, even at the highest concentration of 3 mg/L. Thus, the change of intracellular ROS was very minor in this study.

Table 9.6. TSS, VSS and cell viability of the six series in the batch assay conducted with the enriched nitrifying culture amended with a range of initial PAA/H$_2$O$_2$ concentration at 2 and 60 h of incubation.

Incubation Time (h)	Initial PAA/H$_2$O$_2$ (mg/L)	TSS (mg/L)	VSS (mg/L)	VSS/TSS (%)	Cell Viability (%)
2	0/0	407±6 [a]	150±17	36.9	72.8±3.8
	0.2/0.03	397±15	163±15	41.2	95.7±1.3
	0.5/0.07	413±15	170±26	41.1	92.9±3.7
	1/0.14	410±17	167±15	40.7	95.4±0.5
	2/0.28	403±25	157±12	38.8	88.8±4.0
	3/0.42	390±10	150±10	38.5	72.7±1.0
60	0/0	490±10	193±15	39.5	86.1±3.5
	0.2/0.03	477±6	207±12	43.4	92.7±2.4
	0.5/0.07	493±15	203±12	41.2	94.3±0.9
	1/0.14	503±12	213±12	42.4	82.8±2.8
	2/0.28	480±10	210±10	43.7	73.5±1.8
	3/0.42	467±12	203±6	43.6	66.0±1.9

[a] Mean ± standard deviation (n = 3)

Table 9.7. Relative intracellular ROS of the six batch assay series amended with a range of initial PAA/H$_2$O$_2$ concentration at 2 h of incubation.

PAA/H$_2$O$_2$ (mg/L)	Relative Intracellular ROS[a]
0/0 (Control)	1.00±0.14 [b]
0.2/0.03	0.95±0.02
0.5/0.07	0.84±0.05
1/0.14	0.87±0.15
2/0.28	1.01±0.06
3/0.42	1.16±0.18

[a] Normalized to the PAA/H$_2$O$_2$-free control. [b] Mean ± standard deviation (n = 3).
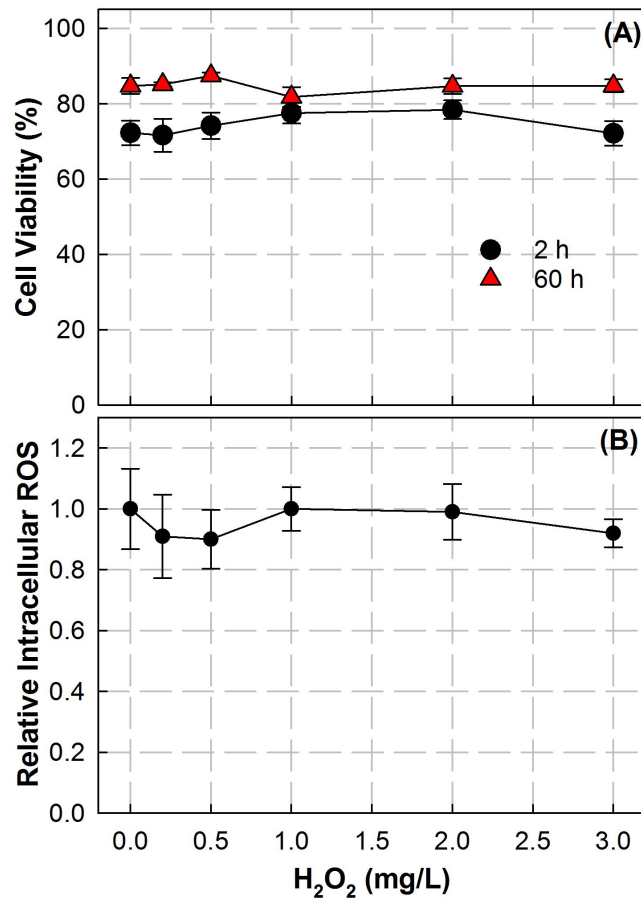
Figure 9.6. Cell viability vs. initial PAA concentration during the nitrification batch assay conducted with the enriched nitrifying culture, measured at 2 and 60 h of incubation (A); Relative intracellular ROS vs. initial PAA concentration during the nitrification batch assay conducted with the enriched nitrifying culture measured at 2 h of incubation (B). Error bars are standard deviations.

9.3.3 Effect of PAA and H_2O_2 on Culture Oxygen Uptake Rate (OUR)

9.3.3.1 Effect of H_2O_2 on OUR

Table 9.8 summarizes the control normalized, relative OUR values (i.e., OUR_{All}, OUR_{NH4}, OUR_{NO2}, and OUR_{Heter}) by all batch assay series amended with initial H_2O_2 concentration up to 3 mg/L. Overall, all relative OUR values were very close to 1; thus, direct addition of H_2O_2 up to 3 mg/L did not affect the respiratory activity of the nitrifying bacteria.

Table 9.8. Control normalized, relative oxygen uptake rates (OUR) of batch assay series amended with a range of initial H_2O_2 concentration at 2 h of incubation[a].

H_2O_2 (mg/L)	OUR_{NH4}	OUR_{NO2}	OUR_{Heter}	OUR_{All}
0 (Control)	1	1	1	1
0.2	1.01	0.98	0.91	0.95
0.5	0.96	1.02	0.97	0.99
1	0.99	1.01	0.93	0.98
2	1.03	1.00	0.99	1.00
3	1.10	1.07	1.01	1.02

[a] OUR coefficient of variation $\leq 5\%$

9.3.3.2 Effect of PAA Solution on OUR

Figure 9.7 and Table 9.9 show the control normalized, relative OUR values (i.e., OUR_{All}, OUR_{NH4}, OUR_{NO2}, and OUR_{Heter}) by the batch assay series amended with initial PAA/H_2O_2 concentrations up to 3/0.42 mg/L. The relative OUR_{All} decreased to as low as 0.11 as the initial PAA concentration was increased to 3 mg/L. Similarly, the relative OUR_{NH4} and OUR_{NO2} decreased to as low as 0.04 and 0.41, respectively, as the initial PAA concentration was increased to 3 mg/L. Thus, direct addition of PAA solution had a profound negative effect on the respiratory activity of the nitrifying bacteria. The impact

was greater on ammonia oxidation than on nitrite oxidation. However, the relative

OUR_{Heter} was always higher than 1, and varied from 1.01 to 1.20, suggesting that directly

added PAA solution did not negatively affect the respiratory activity of the heterotrophic

bacteria, but instead had a positive effect attributed to acetic acid contained in the PAA

solution as well as that produced by the decomposition of PAA (0.7 to 10.5 mg/L total

acetic acid). Based on the negligible H_2O_2 effect discussed in Section 9.3.3.1, above, the

negative effect of the PAA solution on nitrification was predominantly attributed to PAA

alone.

Table 9.9. Control normalized, relative oxygen uptake rates (OUR) of batch assay series amended with a range of initial PAA/H_2O_2 concentration at 2 h of incubation[a].

PAA/H_2O_2 (mg/L)	OUR_{NH4}	OUR_{NO2}	OUR_{Heter}	OUR_{All}
0/0 (Control)	1	1	1	1
0.2/0.03	0.75	0.98	1.19	0.79
0.5/0.07	0.36	0.93	1.05	0.45
1/0.14	0.24	0.95	1.08	0.34
2/0.28	0.06	0.66	1.18	0.15
3/0.42	0.04	0.41	1.14	0.11

[a] OUR coefficient of variation ≤ 5%

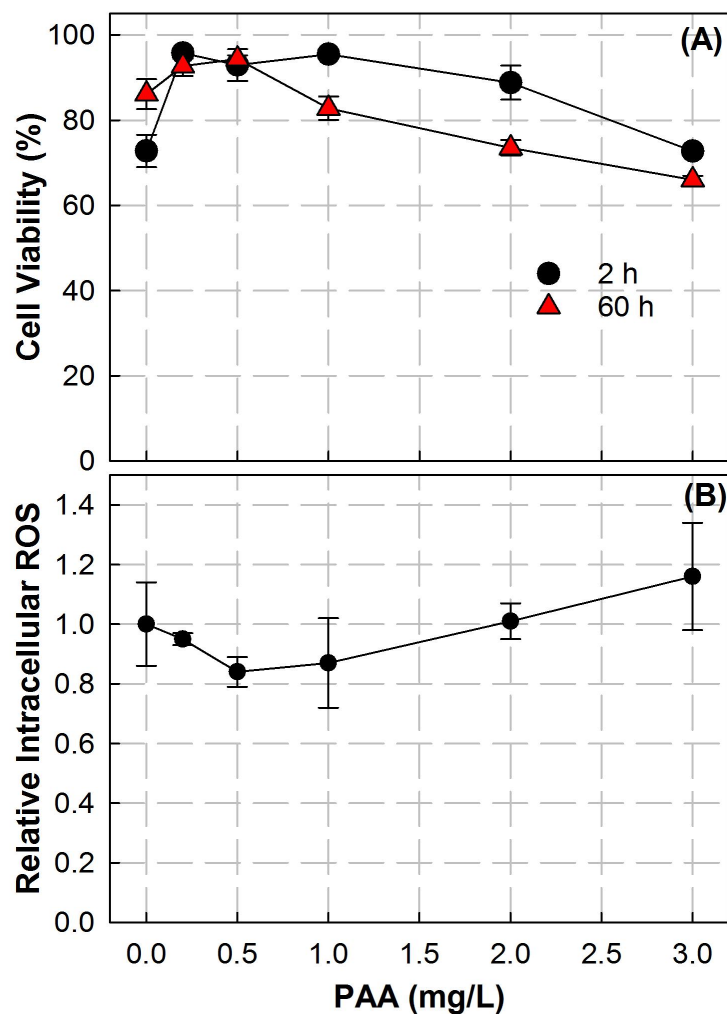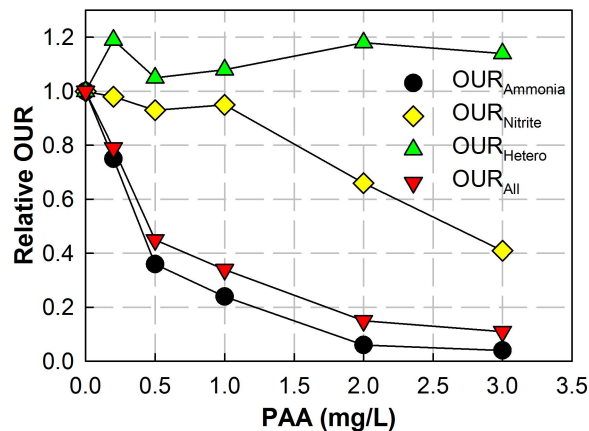**Figure 9.7. Relative oxygen uptake rates (OUR) vs. initial PAA concentration during the nitrification batch assay conducted with the enriched nitrifying culture measured at 2 h of incubation.**

9.3.4 Effect of PAA and H_2O_2 on Microbial Community Structure and Gene Expression

The major genera in five nitrifying culture samples were *Nitrosospira* and *Nitrosomonas* (Figure 9.8)*,* which are dominant ammonia-oxidizing bacteria (AOB) in wastewater treatment plants. The relative abundance of *Nitrosomonas* was significantly lower in the four test culture samples (ca. 3%), compared to the control (ca. 23%). However, the relative abundance of *Nitrosospira* was significantly higher in the four test culture samples (ca. 20 to 24%), compared to the control (ca. 1%). Thus, *Nitrosomonas* was negatively affected while *Nitrosospira* was enriched by PAA and/or H_2O_2. Unlike the AOB, the relative abundance of the detected nitrite-oxidizing bacteria (NOB), *Nitrobacter* and *Nitrospira,* were very low. The relative abundance of *Nitrobacter* was 0.31 to 0.33% in the control and the culture sample amended with 0.5 mg/L PAA or H_2O_2, while was 0.28 and 0.24% in the culture sample amended with 3 mg/L PAA and H_2O_2, respectively. Thus, *Nitrobacter* was moderately and negatively affected by PAA and H_2O_2, both at 3 mg/L. The relative abundance of *Nitrospira* was very low in all the five samples, ranging from 0.007 to 0.019%, without a particular trend among the samples. The reason of the low abundance of NOB could be that the NOB detected in the culture had a low similarity to the existing NOB species in the database.
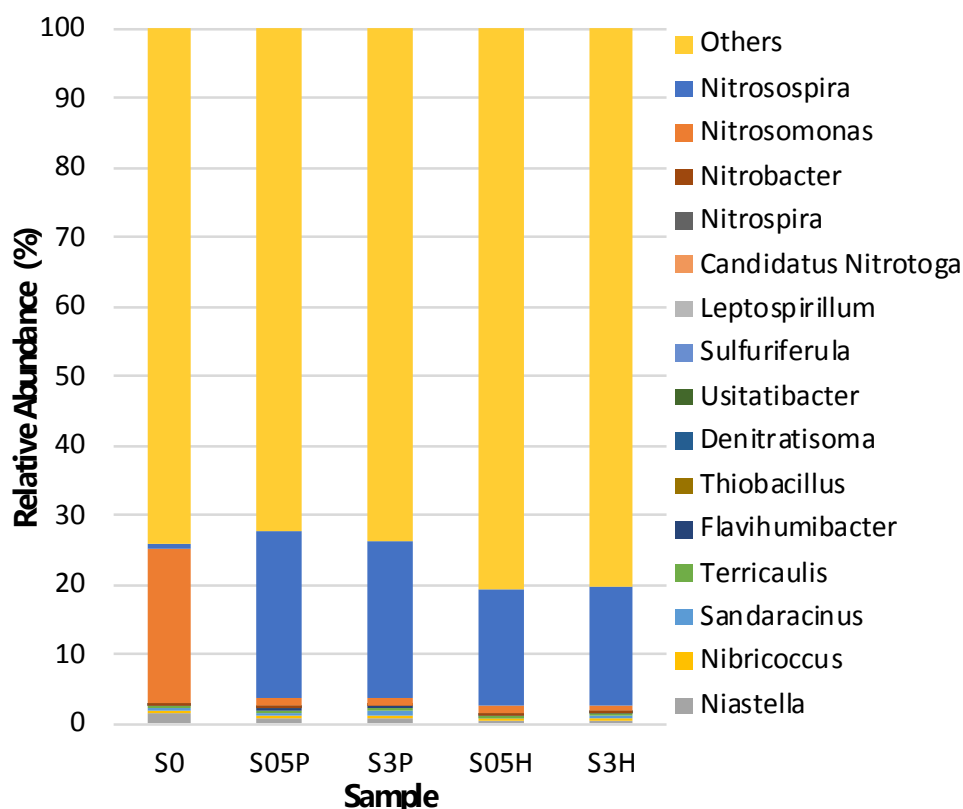
Figure 9.8. Genus level relative abundance in the five nitrifying culture samples.

Abbreviations: S0, PAA solution-free control; S05P and S3P, culture amended with 0.5 and 3 mg/L PAA solution, respectively; S05H and S3H, culture amended with 0.5 and 3 mg/L H_2O_2, respectively.

The effect of PAA and H_2O_2 solution on the transcriptional activities of the nitrifying culture was evaluated, based on the transcription levels of genes involved in nitrogen metabolism, oxidase and oxidoreductase reactions, energy production and conversion, cell membrane protein, cell division, and DNA repair. Table 9.10 summarizes the transcription level of major genes involved in nitrogen metabolism. Compared to the control, the transcription level of a nitrite oxidoreductase (*nxrA*, K00370) in the culture amended with 0.5 mg/L PAA, 0.5 mg/L H_2O_2, and 3 mg/L H_2O_2, decreased by ca. 23, 40, and 38%, while increased by ca. 25% in the culture amended with 3 mg/L PAA. Compared to the control culture, the transcription level of another nitrite

oxidoreductase (*nxrB*, K00371) was upregulated in all four cultures amended with PAA or H_2O_2 solution. When cells are under oxidative stress, they often need more energy to maintain cell membrane structure and avoid error-prone DNA replication. The possible reason for the observed upregulation of the nitrite oxidoreductase (K00370) in the culture amended with 3 mg/L PAA was that the nitrifying bacteria strengthened their nitrite oxidation activity to produce energy and maintain their viability under acute oxidative stress. However, in the condition of mild oxidative stress without facing an energy deficiency, the transcription pattern shifted to stress-related gene expression, such as those for catalase production and membrane biogenesis. Besides nitrite oxidoreductase, the nitrate/nitrite regulator also plays an important role in transporting or sensing nitrite and nitrate. Compared to the control culture, the transcription level of a nitrate/nitrite response regulator (K02479) in the cultures amended with 0.5 mg/L PAA, 0.5 mg/L H_2O_2, and 3 mg/L H_2O_2, increased by ca. 117, 228, and 146%, while decreased by ca. 63% in the culture amended with 3 mg/L PAA. Thus, the culture amended with 3 mg/L PAA had the opposite transcription pattern to that of the other three cultures. These results agree with the observation that 3 mg/L PAA significantly impacted ARR and NPR as discussed in Section 2.1. The transcription level of a nitrogen regulatory protein (K04751) increased by 7- to 8-fold in the culture amended with 0.5 and 3 mg/L PAA and increased by 4- to 5- fold in the culture amended with 0.5 and 3 mg/L H_2O_2, compared to the PAA and H_2O_2-free control culture. Thus, nitrogen regulatory proteins were upregulated under the effect of PAA and H_2O_2. The hydroxylamine oxidase (HAO, K11517) decreased by more than 14-fold in all four culture samples, compared to the control. Hydroxylamine is very unstable and tends to be fast oxidized to nitrite in an oxidizing environment

(Greenwood and Earnshaw, 1997). Thus, it is highly probable that hydroxylamine was
oxidized to nitrite by PAA and/or H_2O_2, resulting in downregulation of the
hydroxylamine oxidase in the four culture samples.

**Table 9.10. Absolute transcription reads number of major genes involved in
nitrogen metabolism in the five nitrifying culture samples [a].**

KO_ID	S0	S05P	S3P	S05H	S3H	Annotation
K00370	1230	952	1532	741	765	narG, narZ, nxrA | nitrate reductase/nitrite oxidoreductase, alpha subunit
K00371	263	635	505	642	534	narH, narY, nxrB | nitrate reductase/nitrite oxidoreductase, beta subunit
K00374	144	73	43	48	25	narI, narV | nitrate reductase gamma subunit
K02479	71	154	26	233	175	narL | two-component system, NarL family, nitrate/nitrite response regulator
K07686	41	2	1	3	0	uhpA | two-component system, NarL family, uhpT operon response regulator UhpA
K07675	30	2	1	0	0	uhpB | two-component system, NarL family, sensor histidine kinase UhpB
K02575	14	29	44	9	18	NRT, narK, nrtP, nasA | MFS transporter, NNP family, nitrate/nitrite transporter
K11618	13	7	6	9	9	liaR | two-component system, NarL family, response regulator LiaR
K11517	76	5	2	3	0	HAO | (S)-2-hydroxy-acid oxidase
K07684	8	12	0	12	2	narL | two-component system, NarL family, nitrate/nitrite response regulator NarL
K07696	3	76	60	23	12	nreC | two-component system, NarL family, response regulator NreC
K02806	327	13	8	14	6	ptsN | nitrogen PTS system EIIA component
K04751	13	120	106	86	70	glnB | nitrogen regulatory protein P-II 1

[a] Sample abbreviations in Figure 9.8 caption.

Table 9.11 summarizes the transcription level of major oxidase genes.
Cytochrome c oxidase subunit 1, 3, and I were significantly higher in the four culture
samples than in the control. Compared to the control, cytochrome c oxidase subunit 1
(COX1, K02256) increased 144, 234, 191, and 126 times in the culture amended with 0.5
and 3 mg/L PAA, and 0.5 and 3 mg/L H_2O_2, respectively. Similarly, cytochrome c
oxidase subunit 3 (COX1, K02262) increased 188, 268, 247, and 161 times in the culture
amended with 0.5 and 3 mg/L PAA, and 0.5 and 3 mg/L H_2O_2, respectively, compared to
the control. However, cytochrome c oxidase subunit III (coxC/ctaE, K02276) decreased

by more than 10 times in the four culture samples, compared to the control. Cytochrome c oxidase, also referred to as Complex IV, is a large transmembrane protein complex found in bacteria, archaea, and the mitochondria of eukaryotes. Cytochrome c oxidase is the last enzyme in the respiratory electron transport chain of cells located in the cell membrane. It receives an electron from each of four cytochrome c molecules, and transfers them to one O_2 molecule, converting molecular oxygen to two molecules of water (Castresana et al., 1994). It is noteworthy that none of the ammonia monooxygenase (*amo*) subunits was detected in the five culture samples, while *Nitrosomonas* and *Nitrosospira* were found in all culture samples as discussed above. Also, methane monooxygenase, homologous to *amo* and able to oxidize ammonia due to its broad substrate specificity (Cabello et al., 2009), was not detected in any of the culture samples. Thus, it is possible that there was an oxidase as an alternative to *amo* playing the role of enzyme in ammonia oxidation to hydroxylamine. Based on the membrane structure of common ammonia-oxidizing bacteria, the potential alternative to *amo* could be an enzyme that could take 2e$^-$ from the quinol/quinone pool and pass them to one of the oxygen atom in O_2 and take another 2e$^-$ from ammonia and pass the 2e$^-$ to another oxygen in O_2 (Figure 9.9) (Cabello, et al., 2009). Thus, in the absence of *amo*, it is reasonable to assume that cytochrome c oxidase can also oxidize ammonia to hydroxylamine by accepting 2e$^-$ from ammonia and 2e$^-$ from cytochrome c or a quinol and transferring the total of 4e$^-$ to an O_2 molecule. Compared to the control culture, catalase-peroxidase (*katG*, K03782) increased by 0.85, 2.29, and 1.67 times in the cultures amended with 0.5 mg/L PAA, 0.5 and 3 mg/L H_2O_2, respectively, while slightly decreased in the culture amended with 3 mg/L PAA. The upregulation of *katG* in the

three culture samples also corresponded to the unimpacted nitrification activity of these three cultures. The slightly down-regulation of *katG* in the culture amended with 3 mg/L PAA agreed with the observed nitrification inhibition. Thus, it is likely that cells up-regulated the catalase-peroxidase gene to defend themselves from oxidative stress when the oxidants level was low, while they were unable to up-regulate this gene when the oxidants level was high, causing lethal cell damage. The transcription level of peroxidase (PXDN, VPO1, K19511) was significantly lower by 9 to 43 times in the four culture samples compared to the control. The expression of peroxidase could have been upregulated when the cells were exposed to peroxides at nonlethal levels. Thus, it is thought that cells upregulated one enzyme to protect themselves from peroxides and downregulated other peroxidases.

Table 9.11. Absolute transcription reads number of major oxidase genes of the five nitrifying culture samples [a].

KO_ID	S0	S05P	S3P	S05H	S3H	Annotation
K02274	3830	9341	7030	5326	4358	coxA, ctaD | cytochrome c oxidase subunit I
K02276	925	91	82	75	44	coxC,ctaE | cytochrome c oxidase subunit III
K00404	721	218	118	223	161	ccoN | cytochrome c oxidase cbb3-type subunit I
K00428	599	53	66	62	57	E1.11.1.5 | cytochrome c peroxidase
K03782	278	514	233	914	742	katG | catalase-peroxidase
K11473	93	417	357	203	135	glcF | glycolate oxidase iron-sulfur subunit
K19511	88	9	2	8	2	PXDN, VPO1 | peroxidase
K02275	48	193	87	71	23	coxB, ctaC | cytochrome c oxidase subunit II
K00278	26	162	122	85	50	nadB | L-aspartate oxidase
K02258	17	1	2	0	0	COX11,ctaG | cytochrome c oxidase assembly protein subunit 11
K02265	16	0	0	0	0	COX5B | cytochrome c oxidase subunit 5b
K02261	5	34	66	50	48	COX2 | cytochrome c oxidase subunit 2
K02495	4	23	11	71	95	hemN,hemZ | oxygen-independent coproporphyrinogen III oxidase
K17893	4	14	27	28	21	AOX1,AOX2 | ubiquinol oxidase
K02256	2	291	471	384	254	COX1 | cytochrome c oxidase subunit 1
K02262	1	189	269	248	162	COX3 | cytochrome c oxidase subunit 3
K22552	0	6	32	18	4	mmcO | multicopper oxidase

[a] Sample abbreviations in Figure 9.8 caption.
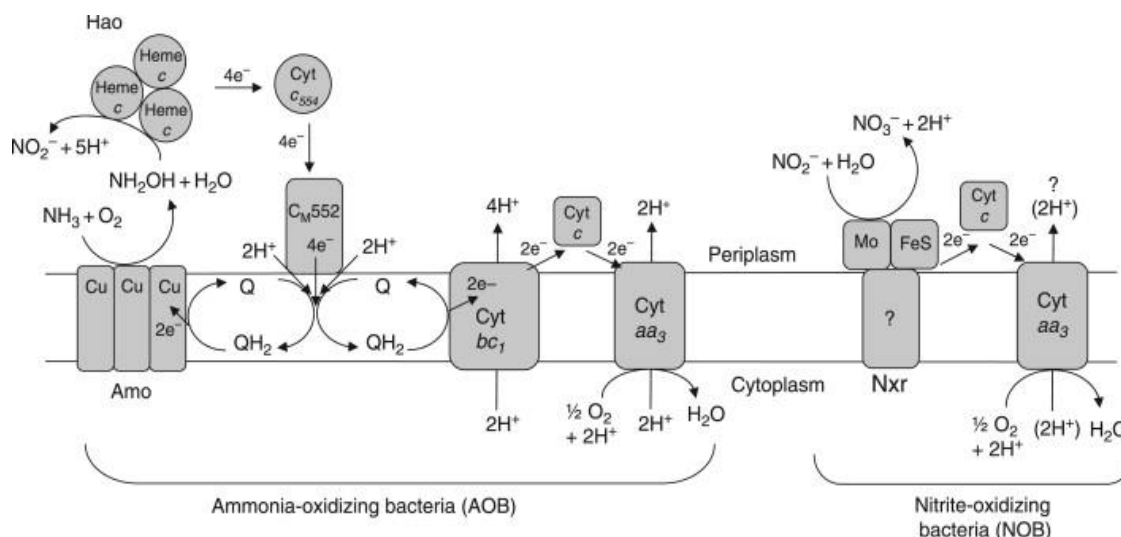
Figure 9.9. Nitrification pathway in chemolithoautotrophic bacteria.

Left, ammonia oxidation by ammonia-oxidizing bacteria (AOB); right, nitrite oxidation by nitrite-oxidizing bacteria (NOB). Location, putative subunit composition and cofactors of the enzymes ammonia monooxygenase (*Amo*), hydroxylamine oxidoreductase (*Hao*), and nitrite oxidoreductase (*Nxr*) are shown. The proton-pumping cytochrome bc1 and cytochrome aa3 complexes are also shown. QH_2/Q represents the membrane quinol/quinone pool. The location of the *Nxr* active site (periplasm or cytoplasm) is still controversial and the H^+-pumping activity of cytochrome *aa3* in NOB is also under discussion (Cabello, et al., 2009).

Table 9.12 summarizes the transcription level of major oxidoreductase genes. Seven major subunits of a NADH-quinone oxidoreductase, *nuo*, were found and changes in their transcription level are discussed. The transcription level of NADH-quinone oxidoreductase subunit D (*nuoD*, K00333), the most abundant one, in the culture amended with 0.5 mg/L PAA was higher by ca. 74% than in the control, while was comparable to the control in the other culture samples. In all four PAA or H_2O_2 amended cultures, the transcription level of subunit F, H, M, and chain 4 of the NADH-quinone oxidoreductase, were all significantly decreased, while the subunit N and C/D of *nuo*

were significantly increased, compared to the control. Overall, the NADH-quinone

oxidoreductase had some subunits upregulated and some downregulated under the effect

of PAA and/or H_2O_2.

Table 9.12. Absolute transcription reads number of major oxidoreductase genes of the five nitrifying culture samples [a].

KO_ID	S0	S05P	S3P	S05H	S3H	Annotation
K00333	1185	2064	1307	1219	907	nuoD | NADH-quinone oxidoreductase subunit D
K00335	607	279	294	453	241	nuoF | NADH-quinone oxidoreductase subunit F
K00337	567	21	15	22	10	nuoH | NADH-quinone oxidoreductase subunit H
K00174	512	168	163	280	145	korA,oorA,oforA | 2-oxoglutarate/2-oxoacid ferredoxin oxidoreductase subunit alpha
K00342	491	34	22	36	16	nuoM | NADH-quinone oxidoreductase subunit M
K00347	353	13	5	12	7	nqrB | Na+-transporting NADH:ubiquinone oxidoreductase subunit B
K17218	310	677	729	179	206	sqr | sulfide:quinone oxidoreductase
K00341	223	202	140	140	100	nuoL | NADH-quinone oxidoreductase subunit L
K03881	211	2	2	0	3	ND4 | NADH-ubiquinone oxidoreductase chain 4
K15977	196	20	13	2	5	K15977 | putative oxidoreductase
K00340	70	5	2	4	1	nuoK | NADH-quinone oxidoreductase subunit K
K00343	55	393	307	184	112	nuoN | NADH-quinone oxidoreductase subunit N
K00330	26	8	4	3	2	nuoA | NADH-quinone oxidoreductase subunit A
K05578	23	1	0	7	3	ndhG | NAD(P)H-quinone oxidoreductase subunit 6
K13378	4	453	260	247	249	nuoCD | NADH-quinone oxidoreductase subunit C/D
K11209	2	89	54	46	35	yghU,yfcG | GSH-dependent disulfide-bond oxidoreductase
K03878	0	59	97	88	66	ND1 | NADH-ubiquinone oxidoreductase chain 1
K00336	0	15	23	35	31	nuoG | NADH-quinone oxidoreductase subunit G

[a] Sample abbreviations in Figure 9.8 caption.

Table 9.13 summarizes the transcription level of the 30 major genes involved in

energy production and conversion. Overall, 16 out of 30 energy-related genes were

upregulated (yellow-shaded) and 14 out of 30 were downregulated. Particularly, all the

ATPase genes in the four culture samples were downregulated compared to the control,

including ATPase subunit alpha, beta, gamma, A and b, ribosome-binding ATPase and a

putative ATPase. ATPases are a class of enzymes that catalyze the decomposition of

adenosine triphosphate (ATP) into adenosine diphosphate (ADP) and a free phosphate

ion (Pi) or the inverse reaction (Martin and Senior, 1980). This dephosphorylation

reaction releases energy used to drive other biochemical reactions that would not

otherwise occur (Riley and Peters, 1981). Thus, energy production activities in all four

culture samples were diminished under the effect of PAA and/or H_2O_2. It is noteworthy

that flagellum-specific ATP synthase (*filI*, K02412) increased 143 and 124 times in the

culture with 0.5 and 3 mg/L PAA addition, respectively, and increased 50 and 34 times in

the culture with 0.5 and 3 mg/L H_2O_2 addition, respectively. ATP synthase is a protein

that catalyzes the formation of the energy storage molecule ATP using ADP and

inorganic phosphate (Pi) (Junge and Nelson, 2015). Thus, energy storage activities

significantly increased under the effect of PAA and/or H_2O_2, which is normal that cells

tend to store energy rather than utilize energy under stressed conditions. The predominant

upregulated genes were ATP-dependent Clp protease ATP-binding subunit ClpA, ClpB,

and ClpX (K03694, K03695, and K03544), and the upregulation was greater in the

culture samples amended with PAA than those amended with H_2O_2. Protease (also called

peptidase or proteinase) is a class of enzymes that catalyze proteolysis that functions as a

precise regulatory mechanism for a broad spectrum of cellular processes, such as the

regulation of stability of key metabolic enzymes and the effective removal of terminally

damaged polypeptides (Porankiewicz et al., 2002). Much of the directed protein turnover

is performed by proteases that require ATP and, of those in bacteria, the Clp protease

from *Escherichia coli* is one of the best characterized to date (Porankiewicz et al., 2002).

Thus, upregulation of ClpA, ClpB, and ClpX in the four culture samples may be the

result of damaged proteins caused by PAA and/or H_2O_2 that require more proteases to

remove them; the damage on proteins caused by PAA was higher than that by H_2O_2. Three genes belonging to the ATP-binding cassette multidrug efflux pump (K18890, K18893, and K18138) were significantly upregulated in the two culture samples amended with PAA and slightly to moderately upregulated in the culture samples amended with H_2O_2. Bacterial multidrug efflux pumps are antibiotic resistance determinants present in all microorganisms. The two main ways of acquiring antibiotic resistance are decreasing the affinity of the target for the antibiotic (mutations in genes encoding the antimicrobial targets) or diminishing the active, intracellular antibiotic concentration. For the latter, the use of energy-dependent efflux pumps to extrude the antibiotics is one of the major mechanisms of antibiotic resistance (Blanco et al., 2016). Therefore, the upregulation of the three multidrug efflux pump genes in the four culture samples indicates that the cells were acquiring resistance to PAA and/or H_2O_2, and the induced resistance was greater in the cultures amended with PAA than with H_2O_2.

Table 9.13. Absolute transcription reads number of 30 major genes involved in energy production and conversion of the five nitrifying culture samples (Upregulated genes are yellow-shaded) [a].

KO_ID	S0	S05P	S3P	S05H	S3H	Annotation
K02132	803	394	88	797	100	ATPeF1A, ATP5A1, ATP1 | F-type H+-transporting ATPase subunit alpha
K02112	736	290	476	470	201	ATPF1B, atpD | F-type H+/Na+-transporting ATPase subunit beta
K02502	613	88	59	45	54	hisZ | ATP phosphoribosyltransferase regulatory subunit
K03695	467	5230	1753	2038	2082	clpB | ATP-dependent Clp protease ATP-binding subunit ClpB
K03694	137	2155	2281	976	811	clpA | ATP-dependent Clp protease ATP-binding subunit ClpA
K03667	9	562	403	200	140	hslU | ATP-dependent HslUV protease ATP-binding subunit HslU
K03544	70	305	295	245	203	clpX,CLPX | ATP-dependent Clp protease ATP-binding subunit ClpX
K16898	1	127	61	72	56	addA | ATP-dependent helicase/nuclease subunit A
K02036	258	7	8	8	10	pstB | phosphate transport system ATP-binding protein
K02065	10	296	210	139	97	mlaF, linL, mkl | phospholipid/cholesterol transport system ATP-binding protein
K02010	54	829	1369	2422	1409	afuC, fbpC | iron(III) transport system ATP-binding protein
K09817	0	48	29	12	13	znuC | zinc transport system ATP-binding protein
K15738	26	887	903	331	312	uup | ABC transport system ATP-binding/permease protein
K09013	239	33	21	25	12	sufC | Fe-S cluster assembly ATP-binding protein
K12371	1	128	51	44	21	dppD | dipeptide transport system ATP-binding protein
K06942	149	25	15	35	8	ychF | ribosome-binding ATPase
K09810	144	17	13	9	0	lolD | lipoprotein-releasing system ATP-binding protein
K06158	96	51	5	61	10	ABCF3 | ATP-binding cassette, subfamily F, member 3
K02109	69	5	3	16	6	ATPF0B, atpF | F-type H+-transporting ATPase subunit b
K02136	42	1	0	2	3	ATPeF1G, ATP5C1, ATP3 | F-type H+-transporting ATPase subunit gamma
K02145	55	1	1	0	0	ATPeV1A, ATP6A | V-type H+-transporting ATPase subunit A
K18890	0	131	90	60	41	mdlB, smdB | ATP-binding cassette, subfamily B, multidrug efflux pump
K18893	66	708	289	118	66	vcaM | ATP-binding cassette, subfamily B, multidrug efflux pump
K18138	11	795	440	324	180	acrB, mexB, adeJ, smeE, mtrD, cmeB | multidrug efflux pump
K03301	64	1	3	2	1	TC.AAA | ATP:ADP antiporter, AAA family
K07478	63	9	11	1	7	ycaJ | putative ATPase
K02412	19	2741	2376	977	677	fliI | flagellum-specific ATP synthase
K23997	13	570	197	118	46	nnr | ADP-dependent NAD(P)H-hydrate dehydratase/epimerase
K01515	3	716	525	341	263	nudF | ADP-ribose pyrophosphatase
K04770	91	1	0	3	0	lonH | Lon-like ATP-dependent protease

[a] Sample abbreviations in Figure 9.8 caption.

Table 9.14 summarizes the transcription level of the major genes related to cell membrane functionality and synthesis. Some membrane-bounded proteins were upregulated and some others were downregulated, without a particular pattern. It is noteworthy that hyperosmotically inducible periplasmic protein (osmY, K04065) was at least 76 times higher in the four culture samples than in the control. The hyperosmotically inducible periplasmic protein of *E. coli*, osmY, was found to be an appropriate carrier of foreign proteins for their extracellular secretion (Gupta et al., 2013). Thus, upregulation of osmY indicates that cells tended to export secreted proteins from intracellular to the extracellular medium under the effect of PAA and/or H_2O_2.

Table 9.14. Absolute transcription reads number of major genes related to cell membrane of the five nitrifying culture samples [a].

KO_ID	S0	S05P	S3P	S05H	S3H	Annotation
K02014	860	1476	1220	1803	1506	TC.FEV.OM | iron complex outer membrane receptor protein
K07403	559	37	30	35	29	nfeD | membrane-bound serine protease (ClpP class)
K08307	499	294	47	417	84	mltD, dniR | membrane-bound lytic murein transglycosylase D
K08305	474	146	64	63	34	mltB | membrane-bound lytic murein transglycosylase B
K07165	197	5	2	7	4	fecR | transmembrane sensor
K12542	84	0	2	3	0	lapC | membrane fusion protein, adhesin transport system
K08304	126	457	391	293	219	mltA | membrane-bound lytic murein transglycosylase A
K05807	122	401	362	152	96	bamD | outer membrane protein assembly factor BamD
K17713	89	4	3	2	0	bamB | outer membrane protein assembly factor BamB
K12538	51	1	1	0	0	hasF, prtF | outer membrane protein, protease secretion system
K12537	41	2	0	0	0	hasE, prtE | membrane fusion protein, protease secretion system
K18133	36	1	0	0	0	K18133,porB | major outer membrane protein P.IB
K07275	10	53	93	9	40	ompW | outer membrane protein
K03926	253	7	8	7	11	cutA | periplasmic divalent cation tolerance protein
K04065	6	823	597	461	492	osmY | hyperosmotically inducible periplasmic protein
K03832	0	57	39	26	19	tonB | periplasmic protein TonB
K03926	253	7	8	7	11	cutA | periplasmic divalent cation tolerance protein
K09796	23	3	5	28	4	pccA | periplasmic copper chaperone A

[a] Sample abbreviations in Figure 9.8 caption.

Table 9.15 summarizes the transcription level of the major genes related to cell division and DNA repair. Compared to the control, the cell division protein ZapA (K09888) in the culture amended with 0.5 and 3 mg/L PAA was 25 and 50 times higher, respectively, and 4 and 8 times higher in the culture amended with 0.5 and 3 mg/L H_2O_2, respectively. Some membrane-bound proteins were upregulated and others were downregulated. The cell division protein ZapD (K18778) in the four culture samples decreased by at least 13 times compared to the control. Similar to cell division proteins, some DNA repair proteins were upregulated and some were downregulated, without a particular pattern.

Table 9.15. Absolute transcription reads number of major genes related to cell division and DNA repair in the five nitrifying culture samples [a].

KO_ID	S0	S05P	S3P	S05H	S3H	Annotation
K03798	2024	867	891	1073	957	ftsH,hflB | cell division protease FtsH
K03531	638	1419	1186	611	501	ftsZ | cell division protein FtsZ
K03590	465	212	191	277	173	ftsA | cell division protein FtsA
K09888	204	5723	10511	995	1741	zapA | cell division protein ZapA
K09811	143	53	51	171	32	ftsX | cell division transport system permease protein
K18778	140	6	1	10	3	zapD | cell division protein ZapD
K06639	99	2	4	4	2	CDC14 | cell division cycle 14
K05589	44	1	2	2	4	ftsB | cell division protein FtsB
K03587	21	797	607	434	302	ftsI | cell division protein FtsI (penicillin-binding protein 3)
K03547	322	337	419	617	294	sbcD,mre11 | DNA repair protein SbcD/Mre11
K04485	200	253	275	99	74	radA,sms | DNA repair protein RadA/Sms
K03630	169	289	293	216	51	radC | DNA repair protein RadC
K03629	163	213	23	279	46	recF | DNA replication and repair protein RecF
K03631	108	38	54	42	22	recN |DNA repair protein RecN (Recombination protein N)
K03546	0	121	60	28	26	sbcC,rad50 | DNA repair protein SbcC/Rad50

[a] Sample abbreviations in Figure 9.8 caption.

9.4 Summary

Direct addition of PAA to aliquots of the enriched nitrifying culture did not significantly affect nitrification at initial PAA concentrations up to 0.5 mg/L, while both the initial ARR and NPR were negatively affected by initial PAA concentrations from 1 to 3 mg/L. Cell lysis was not observed during the batch assay at initial PAA concentrations up to 3 mg/L. The cell viability was higher in batch series amended with 0.2 to 2 mg/L PAA than in the control series, which is attributed to the positive effect of acetic acid on the heterotrophic bacteria. Although the viable heterotrophic bacteria were less than 5% in the enriched mixed culture, their growth rate is much higher than that of the autotrophic nitrifiers; thus, a fast increase in cell viability was observed in batch culture series amended with medium to high PAA levels (i.e., 0.2 to 2 mg/L PAA). However, as the PAA level was increased to 3 mg/L, the cell viability was close to that of the control series. The observed net increase of cell viability during the incubation suggests that all PAA levels suppressed any increase of cell viability of the nitrifiers. The fact that the measured intracellular ROS levels were similar in all culture series suggests that the observed impact of PAA on nitrification was not the result of cell oxidative stress. The decrease in the relative OUR_{NH4} and OUR_{NO2} agrees with the observed negatively-impacted nitrification activities. The negative impact on ammonia oxidation was higher than on nitrite oxidation. Direct addition of H_2O_2 up to 3 mg/L did not impact nitrification, cell viability or the related OURs. Therefore, the impact of directly added PAA solution on the enriched nitrifying culture is attributed to PAA alone or in some combination with H_2O_2. The impact on nitrification was predominantly related to the inhibitory effect of PAA on related enzymes, such as the membrane-bound ammonia

monooxygenase and membrane-associated nitrite oxidoreductase, rather than to loss of cell viability and/or cell lysis. Both PAA and H_2O_2 negatively affected *Nitrosomonas* but not *Nitrosospira*. *Nxr* was downregulated when the PAA level was low while upregulated when the PAA level was high. *Hao* was significantly downregulated in all four culture samples, possibly attributed to hydroxylamine oxidation by PAA and/or H_2O_2. *Amo* was not detected in any of the cultures, suggesting the existence of alternative enzymes to *amo*; cytochrome c oxidase is a possible candidate as an alternative enzyme to *amo*. The downregulation of all major ATPases genes and the upregulation of ATP synthases genes suggests that culture cells tended to store ATP rather than use ATP under the effect of PAA and/or H_2O_2. The upregulation of ATP-dependent protease indicates that protein damage occurred in all four culture samples; the damage caused by PAA was worse than that by H_2O_2. The transcription levels of genes related to cell division and DNA repair did not show a particular pattern among the major genes, suggesting that the functionality of cell division and the integrity of DNA were not significantly affected by PAA or H_2O_2.

CHAPTER 10. CONCLUSIONS AND RECOMMENDATIONS

10.1 Conclusions

Peracetic acid (PAA), as a wide-spectrum effective disinfectant, has been extensively and increasingly used in many industries, especially in poultry processing to control food-borne pathogens. Upsets of biological wastewater treatment processes and failures of whole effluent toxicity (WET) tests have been reported as potentially caused by the excessive use of PAA solutions. However, information related to the fate and effect of PAA on biological wastewater treatment processes commonly used in poultry processing plants is extremely limited.

This study focused on the assessment of the fate of a PAA solution in poultry processing wastewater streams, factors contributing to PAA decomposition, and the evaluation of the effect of PAA on biological treatment processes, such as organic matter degradation, nitrification, and denitrification. On-site monitoring did not detect PAA in dissolved air flotation (DAF) influent and effluent samples collected at mid plant operation shifts; however, up to 25 mg/L PAA was detected in the DAF effluent at the end of the operation shift coinciding with emptying chiller tanks where PAA levels in excess of 1,000 mg/L are typically maintained. The PAA decomposition rate in poultry processing wastewater correlated positively with pH, temperature, wastewater strength and organic content, and negatively with initial PAA concentration. PAA decomposition resulted in equimolar concentrations of acetic acid.

In both the short- and long-term evaluation of PAA effect using a mixed heterotrophic/autotrophic culture, the inhibitory effect of the PAA solution on organic

matter degradation, nitrification and denitrification was dose-dependent, with significant inhibition at PAA ≥ 40 mg/L; fast recovery was observed after direct PAA solution addition ended. Microbial acclimation to PAA did not take place under aerobic conditions, but partial acclimation was observed under anoxic conditions over a long-term operation of semi-continuously fed bioreactors. The impact on nitrification was predominantly attributed to enzyme inhibition than to loss of nitrifiers, whereas the impact on denitrification was attributed to both enzyme inhibition and loss of culture viability. Intracellular reactive oxygen species (ROS) were not the cause of the observed inhibition on nitrification, but contributed to the decrease in denitrification activity. Nevertheless, the capacity of the microbial communities to manage PAA-induced cell oxidative stress increased in both aerobic and anoxic reactors over the long-term operation.

Long-term evaluation of PAA on a continuously-fed, three-reactor biological nitrogen removal (BNR) system showed that continuous, direct addition of PAA at 80 to 200 mg/L in the first, anaerobic reactor did not affect the BNR system performance; however, organic matter degradation and nitrogen removal were severely affected by continuous feeding with wastewater carrying residual PAA at 80 and 200 mg/L. The same pattern of the BNR system recovery from the first and the second system upset resulting from direct or residual PAA addition, respectively, suggest that the BNR system performance did not worsen during the long-term operation with PAA; however, acclimation to PAA was not established either.

Direct addition of PAA at 3 mg/L to a highly enriched nitrifying culture resulted in severe nitrification inhibition not caused by loss of cell viability or cell oxidative stress,

but rather by enzyme inhibition reflected in the culture transcriptional levels. The inhibitory effect of PAA on both ammonia and nitrite oxidation was quantitatively successfully described by a Michaelis-Menten, non-competitive inhibition model.

The outcome of the study provides crucial information for the rational design and operation of biological wastewater treatment processes under the effect of PAA solutions. It also provides information for the poultry processing industry to develop a sound methodology that will ensure the continuous use of PAA solutions to achieve pathogen-free products, while avoiding upsets of biological wastewater treatment processes dealing with PAA-bearing wastewater. With further research on the effect of PAA on biological processes at the cellular and molecular level, the mechanism of the effect caused by PAA will be further elucidated and the application of PAA as an effective disinfectant could be widened.

10.2 Recommendations

10.2.1 Research Recommendations

Several research questions remain in the area of the effect of PAA on biological wastewater treatment processes, especially the possible inhibitory effect of intermediates and byproducts, as well as the inhibitory mechanisms at the cellular and molecular level. Current research related to PAA byproducts predominantly focused on those formed during PAA disinfection of wastewater. Nevertheless, the formation of PAA byproducts in biological wastewater treatment systems has never been examined. Such information

could provide a better insight into the actual inhibition mechanism by PAA. Ketones and aldehydes have been reported as PAA DBPs ((Nurizzo et al., 2005). Thus, it is worthwhile to examine byproducts, such as ketones, aldehydes and other compounds formed during the biological treatment of PAA-bearing wastewater.

This study suggests that the impact caused by PAA on both nitrification and denitrification was related to enzyme inhibition; however, information related to the mechanism of how PAA attacks membrane-associated or intracellular enzymes, as well as how reversible the enzyme inhibition is, is not available. Thus, the effect of PAA on cell enzymes, such as ammonia monooxygenase, nitrite oxidoreductase, catalase, peroxidase, cytochrome c oxidase, and NADH-quinone oxidoreductase should be evaluated both in vivo and in vitro. For vivo evaluation, the PAA effect should be assessed at both lethal and sublethal conditions. The effect of PAA on the activity, relative abundance, structure and post-translation modification of enzymes could be analyzed by proteomics. In addition, the mechanism of PAA reaction with the cell membrane phospholipid bilayer should be investigated.

10.2.2 Development Recommendations

Reported by Kim et al. (2019), significant abatement of recalcitrant pollutants, such as methylene blue, naproxen, and bisphenol-A, by the Fe(II)/PAA process was observed at the same initial Fe(II) and PAA concentration, 0.1 mM. This PAA concentration is equal to 7.6 mg/L PAA, which is far below the PAA concentration that impacted organic matter degradation, nitrification, and denitrification in the mixed heterotrophic culture as discussed in Chapter 6, 7 and 9. As no negative impact was

observed at PAA concentration below 10 mg/L, thus, it is worthwhile to investigate the degradation of recalcitrant pollutants by Fe(II)/PAA in biological wastewater treatment systems. In such case, the degradation products of the recalcitrant pollutants can be further biodegraded at microbially tolerable PAA levels. Cathodic tetracycline degradation and synergistic treatment of various wastewaters in a microbial fuel cell (MFC)-Fenton system has been proposed by Long et al. (2021). As PAA can be activated by Fe (II), generating highly oxidizing radicals (Kim et al., 2019), it is worthwhile to investigate the degradation of recalcitrant organic compounds by applying PAA in similar Fenton-MFC systems.

REFERENCES

American Public Health Association (APHA); American Water Works Association; and Water Environment Federation. (2012) Standard Methods for the Examination of Water and Wastewater, 22nd Ed., Washington, D.C.

Anthonisen, A. C., Loehr, R.C., Prakasam, T.B.S., Srinath, E.G. (1976) Inhibition of nitrification by ammonia and nitrous acid. Journal of Water Pollution Control Federation 48, 835-852.

Baldry, M. G. C. (1983) The bactericidal, fungicidal and sporicidal properties of hydrogen peroxide and peracetic acid. Journal of Applied Bacteriology 54, 417–423.

Baldry, M. G. C., and French, M.S. (1989) Activity of peracetic acid against sewage indicator organisms. Water Science & Technology 21, 1747–1749.

Baskaran, V., Patil, P.K., Antony, M.L., Avunje, S., Nagaraju, V.T., Ghate, S.D., Nathamuni, S., Dineshkumar, N., Alavandi, S.V., and Vijayan, K.K. (2020) Microbial community profiling of ammonia and nitrite oxidizing bacterial enrichments from brackishwater ecosystems for mitigating nitrogen species. Scientific Reports 10, 5201.

Beg, S.A., Siddiqi, R.H., Ilias, S. (1982) Inhibition of nitrification by arsenic, chromium, and fluoride. Journal of Water Pollution Control Federation 54, 482–488.

Blanco, P., Hernando-Amado, S., Reales-Calderon, J. A., Corona, F., Lira, F., Alcalde-Rico, M., Bernardini, A., Sanchez, M. B., & Martinez, J. L. (2016) Bacterial Multidrug Efflux Pumps: Much More Than Antibiotic Resistance Determinants. Microorganisms 4(1), 14.

Block, S.S. (1991) Peroxygen compounds. In S.S. Block (Ed.), *Disinfection, Sterilization and Preservation* (pp. 185–201). Lea & Febiger, Philadelphia, PA.

Boden, R., Hutt, L.P., Rae, A.W. (2017) Reclassification of *Thiobacillus aquaesulis* (Wood & Kelly, 1995) as *Annwoodia aquaesulis* gen. nov., comb. nov., transfer of *Thiobacillus* (Beijerinck, 1904) from the *Hydrogenophilales* to the *Nitrosomonadales*, proposal of *Hydrogenophilalia* class. nov. within the '*Proteobacteria*', and four new families within the orders *Nitrosomonadales* and *Rhodocyclales*. International Journal of Systematic and Evolutionary Microbiology 67, 1191-1205.

Booth, R., Lester, J. (1995) The potential formation of halogenated by-products during peracetic acid treatment of final sewage effluent. Water Research 29, 1793–1801.

Cabello, P., Roldán, M.D., Castillo, F., Moreno-Vivián, C. (2009) Nitrogen Cycle, Editor: Moselio Schaechter, Encyclopedia of Microbiology (Third Edition), 299-321,

Carlson, Curtis A. (1983) Comparison of denitrification by Pseudomonas stutzeri, Pseudomonas aeruginosa, and Paracoccus denitrificans. Applied and Environmental Microbiology 45.4: 1247–1253.

Castresana, J., Lübben, M., Saraste, M., & Higgins, D. G. (1994) Evolution of cytochrome oxidase, an enzyme older than atmospheric oxygen. The EMBO journal 13(11), 2516–2525.

DeAngelis, K.M., Silver, W.L., Thompson, A.W., Firestone, M.K. (2010) Microbial communities acclimate to recurring changes in soil redox potential status. Environmental Microbiology 12, 3137-3149.

De Angelis, M. and Gobbetti, M. (2011) Lactic Acid Bacteria | Lactobacillus spp.: General Characteristics, Editor: John W. Fuquay, Encyclopedia of Dairy Sciences (Second Edition), 78-90.

Dickinson, B.C. and Chang, C.J. (2012) Chemistry and biology of reactive oxygen species in signaling or stress responses. Nature Chemical Biology 7 (8), 504-511.

Dlangamandla, C., Ntwampe, S.K.O., Basitere, M. (2018) A bioflocculant-supported dissolved air floatation system for the removal of suspended solids, lipids and protein matter from poultry slaughterhouse wastewater. Water Science & Technology 78 (2), 452-458.

Domínguez Henao, L., Delli Compagni, R., Turolla, A., Antonelli, M. (2018) Influence of inorganic and organic compounds on the decay of peracetic acid in wastewater disinfection. Chemical Engineering Journal 337, 133-142.

Domínguez Henao, L., Turolla, A., Antonelli, M. (2018) Disinfection by-products formation ecotoxicological effects of effluents treated with peracetic acid: a review. Chemosphere 213, 25-40.

Dul'neva, L.V., Moskvin, A.V. (2005) Kinetics of formation of peroxyacetic acid. Russian Journal of General Chemistry 75, 1125–1130.

Du, P.H., Liu,W., Cao, H.B., Zhao, H. Huang, C.H. (2018) Oxidation of amino acids by peracetic acid: Reaction kinetics, pathways and theoretical calculations. Water Research X 1, 100002.

Enke, T.N., Leventhal, G.E., Metzger, M., Saavedra, J.T., Cordero, O.X. (2018) Microscale ecology regulates particulate organic matter turnover in model marine microbial communities. Nature Communications 9, 2743.

Falsanisi, D., Gehr, R., Santoro, D., Dell'Erba, A., Notarnicola, M., Liberti, L. (2006) Kinetics of PAA demand and its implications on disinfection of wastewaters. Water Quality Research Journal of Canada 41, 398–409.

Finkmann, W., Altendorf, K., Stackebrandt, E., Lipski, A. (2000) Characterization of N_2O- producing *Xanthomonas*-like isolates from biofilters as *Stenotrophomonas nitritireducens* sp. nov., *Luteimonas mephitis* gen. nov., sp. nov. and *Pseudoxanthomonas broegbernensis* gen. nov., sp. nov. International Journal of Systematic and Evolutionary Microbiology 50 (1), 273–282.

Fontoura, R., Daroit, D.J., Corrêa, A.P.F., Moresco, K.S., Santi, L., Beys-da-Silva, W.O., Yates III, J.R., Moreira, J.C.F., Brandelli, A. (2019) Characterization of a novel antioxidant peptide from feather keratin hydrolysates. New Biotechnology 49, 71-76.

Fraser, J. A. L., Godfree, A. F., Jones, F. (1984) Use of peracetic acid in operational sewage sludge disposal to pasture. Water Science & Technology 17, 451–466.

Fu, J., Zhang, Z., Zhu, J. (2020) Study on the diversity of denitrification bacteria treating with wastewater by using PPGC filler on SBMBBR at low temperature. E3S Web of Conferences 158, 04002.

Garrity, G.M., Bell, J.A., and Lilburn, T. (2005) Order I. *Burkholderiales* ord. nov. In: Brenner, D.J., Krieg, N.R., Staley, J.T., and Garrity, G.M. (eds), Bergeys Manual of Systematic Bacteriology, second edition, vol. 2 (The *Proteobacteria*), part C (The Alpha-, Beta-, Delta-, and *Epsilonproteobacteria*), Springer, New York, p. 575.

Gehr, R., Wagner, M., Veerasubramanian, P., Payment, P. (2003) Disinfection efficiency of peracetic acid, UV and ozone after enhanced primary treatment of municipal wastewater. Water Research 37, 4573-4586.

Gheewala, S.H., Pole, R.K., Annachhatre, A.P. (2004) Nitrification modeling in biofilms under inhibitory conditions. Water Research 38, 3179–3188.

Grady C. P. L., G. T. Daigger, Lim H. C. (1999) Biological Wastewater Treatment, 2nd Edition, Marcel Dekker Inc., New York, NY.

Greenwood and Earnshaw. (1997) Chemistry of the Elements. 2nd Edition. Reed Educational and Professional Publishing Ltd. pp. 431–432.

267

Guo, L.J., Zhao, B., An, Q., Tian, M. (2016) Characteristics of a novel aerobic denitrifying bacterium, *Enterobacter cloacae* strain HNR. Applied Biochemistry and Biotechnology 178, 947-959.

Gupta, S., Adlakha, N., Yazdani, S.S. (2013) Efficient extracellular secretion of an endoglucanase and a β-glucosidase in E. coli. Protein Expression and Purification 88(1): 20-25.

Harp, D. L. (2002) Current Technology of Chlorine Analysis for Water and Wastewater: Technical Information Series — Booklet No.17, HACH, Loveland, CO.

Hajaya, M. G., Pavlostathis, S. G. (2012) Fate and effect of benzalkonium chlorides in a continuous-flow biological nitrogen removal system treating poultry processing wastewater. Bioresource Technology 118, 73-81.

Hajaya M.G., Pavlostathis, S.G. (2013) Modeling the fate and effect of benzalkonium chlorides in a continuous-flow biological nitrogen removal system treating poultry processing wastewater. Bioresource Technology 130, 278-287.

Hespell, R.B. and Odelson, D.A. (1978) Metabolism of RNA-Ribose by Bdellovibrio bacteriovorus during intraperiplasmic growth on Escherichia coli. Journal of Bacteriology 136 (3), 936-946.

Hmidet, N., Jemil, N., Ouerfelli, M., Almajano, M.P., Nasri, M. (2019) Antioxidant properties of *Enterobacter cloacae* C3 lipopeptides in vitro and in model food emulsion. Journal of Food Processing and Preservation 44, 14337.

Holmes, D. E., Dang, Y., Smith, J. A. (2018) Nitrogen cycling during wastewater treatment. Advances in Applied Microbiology (Ch. 4), 106, 113-192.

Imlay, J. A. (2008) Cellular defenses against superoxide and hydrogen peroxide. Annual Review of Biochemistry 77, 755-776.

Junge, W., Nelson, N. (2015) ATP synthase. Annual Review of Biochemistry. 84: 631–57.

Kim, J., Zhang, T., Liu, W., Du, P., Dobson, J.T., and Huang, C-H. (2019) Environmental Science & Technology 53 (22), 13312-13322.

Kim, J. C., Oh, E., Kim, J., & Jeon, B. (2015) Regulation of oxidative stress resistance in *Campylobacter jejuni*, a microaerophilic foodborne pathogen. Frontiers in microbiology 6, 751.

Kitis, M. (2004) Disinfection of wastewater with peracetic acid: A review. Environment International 30, 47-55.

Koch, H., Lücker, S., Albertsen, M., Kitzinger, K., Herbold, C., Spieck, E., Nielsen, P.H., Wagner, M., Daims, H. (2015) Expanded metabolic versatility of ubiquitous nitrite-oxidizing bacteria from the genus. Proceedings of the National Academy of Sciences 112 (36), 11371-1376.

Koivunen, J., Heinonen-Tanski, H. (2005) Peracetic acid (PAA) disinfection of primary, secondary and tertiary municipal wastewaters. Water Research 39 (2005), 4445-4453.

Koju, R., Miao, S., Liang, B., Joshi, D.R., Bai, Y., Liu, R., Qu, J. (2020) Transcriptional and metabolic response against hydroxyethane-(1,1-bisphosphonic acid) on bacterial denitrification by a halophilic *Pannonibacter* sp. strain DN. Chemosphere 252, 126478.

Koops, H. P., and A. Pommerening-Roser. (2001) Distribution and ecophysiology of the nitrifying bacteria emphasizing cultured species. FEMS Microbiology Ecology 37:1-9.

Kundu, P., Pramanik, A., Dasgupta, A., Mukherjee, S., Mukherjee, J. (2014) Simultaneous heterotrophic nitrification and aerobic denitrification by *Chryseobacterium* sp. R31 isolated from abattoir wastewater. BioMed Research International 436056.

Kunigk, L., Silva, S.M., Jurkiewicz, C.H. (2012) The influence of temperature and organic matter on the decomposition kinetics of peracetic acid in aqueous solution. Latin American Applied Research 42 (3), 291-297.

Liberti, L., Notarnicola, M. (1999) Advanced treatment and disinfection for municipal wastewater reuse in agriculture. Water Science & Technology 40, 235–245.

Lee, S. H. I., Cappato, L. P., Corassin, C. H., Cruz, A. G., Oliveira, C. A. F. (2016) Effect of peracetic acid on biofilms formed by *Staphylococcus aureus* and *Listeria monocytogenes* isolated from dairy plants. Journal of Dairy Science 99(3), 2384-2390.

Long, S., Zhao, L., Chen, J., Kim, J., Huang, C-H., Pavlostathis, S.G. (2021) Tetracycline inhibition and transformation in microbial fuel cell systems: Performance, transformation intermediates, and microbial community structure, Bioresource Technology 322, 124534.

Luukkonen,T., Heyninck,T., Ramo, J., Lassi,U. (2015) Comparison of organic peracids in wastewater treatment: disinfection, oxidation and corrosion. Water Research 85, 275–285.

Luukkonen, T., Pehkonen, S. O. (2017) Peracids in water treatment: A critical review. Critical Reviews in Environmental Science and Technology 47, 1-39.

Ma, S., Tong, M., Yuan, S., Liu, H. (2019) Responses of the microbial community structure in Fe (II)-bearing sediments to oxygenation: The role of reactive oxygen species. ACS Earth Space Chemistry 3, 738-747.

Martin, S.S., Senior, A.E. (1980) Membrane adenosine triphosphatase activities in rat pancreas. Biochimica et Biophysica Acta (BBA) - Biomembranes. 602 (2): 401–18.

Maszenan, A.M., Seviour, R.J., Patel, B.K.C., Rees, G.N., McDougall, B.M. (1997) *Amaricoccus* gen. nov., a gram-negative coccus occurring in regular packages or tetrads, isolated from activated sludge biomass, and descriptions of *Amaricoccus veronensis* sp. nov., *Amaricoccus tamworthensis* sp. nov., *Amaricoccus macauensis* sp. nov., and *Amaricoccus kaplicensis* sp. nov. International Journal of Systematic Bacteriology 47, 727-734.

Mattle, M. J., Crouzy, B., Brennecke, M., Wigginton, K.R., Perona, P., Kohn, T. (2011) Impact of virus aggregation on inactivation by peracetic acid and implications for other disinfectants. Environmental Science & Technology, 45:7710-7717.

Mergaert, J., Cnockaert, M.C., Swings, J. (2003) *Thermomonas fusca* sp. nov. and *Thermomonas brevis* sp. nov., two mesophilic species isolated from a denitrification reactor with poly(ε-caprolactone) plastic granules as fixed bed, and emended description of the genus *Thermomonas*. International Journal of Systematic and Evolutionary Microbiology 53, 1961–1966.

McFadden, M., Loconsole, J., Schockling, A.J., Nerenberg, R., Pavissich, J.P. (2017) Comparing peracetic acid and hypochlorite for disinfection of combined sewer overflows: Effects of suspended-solids and pH. Science of the Total Environment 599-600, 533-539.

Monarca, S., Richardson, S.D., Feretti, D., Grottolo, M., Thruston, A.D., Zani, C., Navazio, G., Ragazzo, P., Zerbini, I., Alberti, A. (2002) Mutagenicity and disinfection by-products in surface drinking water disinfected with peracetic acid. Environmental Toxicology and Chemistry 21 (2), 309-318.

Morris, D.L. (1948) Quantitative determination of carbohydrates with Dreywood's anthrone reagent. Science 107 (2775), 254-255.

Nurizzo, C., Antonelli, M., Profaizer, M., Romele, L. (2005) By-products in surface and reclaimed water disinfected with various agents. Desalination 176, 241–253.

Pedersen, L.F., Pedersen, P.B., Nielsen, J.L., Nielsen, P.H. (2009) Peracetic acid degradation and effects on nitrification in recirculating aquaculture systems. Aquaculture 296 (3-4), 246-254.

Oslislo, A., Lewandowski, Z. (1985) Inhibition of nitrification in packed bed reactors by selected organic compounds. Water Research 19, 423–426.

Pearson, A., Budin, M., Brocks, J.J. (2003) Phylogenetic and biochemical evidence for sterol synthesis in the bacterium *Gemmata obscuriglobus.* Proceedings of the National Academy of Sciences 100 (26), 15352-15357.

Pedersen, L-F, Pedersen, P.B. (2012) Hydrogen peroxide application to a commercial recirculating aquaculture system. Aquacultural Engineering 46, 40-46.

Pereira da Silva, W., Dias, C.T., Cavallini, G.S., Pereira, D.H. (2020) Peracetic acid: Structural elucidation for applications in wastewater treatment. Water Research 168, 115-143.

Petruk, G., Roxo, M., De Lise, F., Mensitieri, F., Notomista, E., Wink, M., Izzo, V., & Monti, D. M. (2019) The marine Gram-negative bacterium *Novosphingobium sp.* PP1Y as a potential source of novel metabolites with antioxidant activity. Biotechnology letters 41(2), 273–281.

Pinkernell, U., Effkemann, S., Karst, U. (1997) Simultaneous HPLC determination of peroxyacetic acid and hydrogen peroxide. Analytical Chemistry 69:3623-3627.

Popov, E., Eloranta, J., Hietapelto, V., Vuorenpalo, V., Aksela, R., Jakara, J. (2005) Mechanism of decomposition of peracetic acid by manganese ions and diethylene triamine pentaacetic acid (DTPA). Holzforschung 59, 507–513.

R Core Team. (2014) R: A language and environment for statistical computing. R Foundation for Statistical Computing, Vienna, Austria. URL http://www.R-project.org/.

Rice, E. W., Eaton, A. D., Baird, R. B. (2005) Standard Methods for the Examination of Water and Wastewater, 22nd ed.; WEF: Washington, DC.

Riley, M.V., Peters, M.I. (1981) The localization of the anion-sensitive ATPase activity in corneal endothelium. Biochimica et Biophysica Acta (BBA) - Biomembranes, 644(2): 251-256.

Richardson, S.D., Plewa, M.J., Wagner, E.D., Schoeny, R., DeMarini, D.M. (2007) Occurrence, genotoxicity, and carcinogenicity of regulated and emerging disinfection by-products in drinking water: a review and roadmap for research. Mutation Research 636 (1-3), 178-242.

271

Rittmann, B. E., McCarty, P. L. (2001) *Environmental Biotechnology: Principles and Applications*. McGraw-Hill, New York, NY.

Sander, R. (2015) Compilation of Henry's law constants (version 4.0) for water as solvent. Atmospheric Chemistry and Physics 15, 4399-4981.

Santoro, D., R. Gehr, T. A. Bartrand, L. Liberti, M. Notarnicola, A. Dell'Erba, D. Falsanisi, C. N. Haas. (2007) Wastewater disinfection by peracetic acid: Assessment of models for tracking residual measurements and inactivation. Water Environment Research 79 (7): 775-787.

Schroeder, J.P., Klatt, S.F., Schlachter, M., Zablotski, Y., Keuter, S., Spieck, E., Schulz, C. (2015) Impact of ozonation and residual ozone-produced oxidants on the nitrification performance of moving-bed biofilters from marine recirculating aquaculture systems. Aquacultural Engineering 65, 27-36.

Seaver, L.C., Imlay, J.A. (2001) Hydrogen peroxide fluxes and compartmentalization inside growing *Escherichia coli*. Journal of Bacteriology 183 (24), 7182-7189.

Shang, M., Hou, H. (2009) Studies on effect of peracetic acid pretreatment on anaerobic fermentation biogas production from sludge. Asia-Pacific Power and Energy Engineering Conference, DOI: 10.1109/APPEEC.2009.4918789.

Shinoda, Y., Sakai, Y., Uenishi, H., Uchihashi, Y., Hiraishi, A., Yukawa, H., Yurimoto, H., Kato, N. (2004) Aerobic and anaerobic toluene degradation by a newly isolated denitrifying bacterium, *Thauera* sp. strain DNT-1. Applied and Environmental Microbiology 70 (3), 1385-1392.

Sims, G.K., Wander, M.M. (2002) Proteolytic activity under nitrogen or sulfur limitation. Applied Soil Ecology 568: 1–5.

Sin, G., Kaelin, D., Kampschreur, M. J., Takacs, I., Wett, B., Gernaey, K. V., Rieger, L., Siegrist, H., van Loosdrecht, M. C. M. (2008) Modelling nitrite in wastewater treatment systems: A discussion of different modelling concepts. Water Science & Technology 58 (6), 1155-1171.

Soares Cavallini, G., de Campos, S.X., de Souza, J.B., Magno de Souza Vidal, C. (2013) Evaluation of the physical-chemical characteristics of wastewater after disinfection with peracetic acid. Water Air Soil Pollution 224, 1752–1755.

Surmacz-Gorska, J., Gernaey, K., Demuynck, C., Vanrolleghem, P., Verstraete, W. (1996) Nitrification monitoring in activated sludge by oxygen uptake rate (OUR) measurements. Water Research 30, 1228-1236.

Suurnakki, S., Pulkkinen, J.T., Lindholm-Lehto, P.C., Tiirola, M., Aalto, S.L. (2020) The effect of peracetic acid on microbial community, water quality, nitrification and rainbow trout (*Oncorhynchus mykiss*) performance in recirculating aquaculture systems. Aquaculture 516, 734534.

Takashi, C., Nukui, Y., Morishita, Y., Moriya, K. (2017) Morphological bactericidal fast-acting effects of peracetic acid, a high-level disinfectant, against *Staphylococcus aureus* and *Pseudomonas aeruginosa* biofilms in tubing. Antimicrobial Resistance and Infection Control, 6:122

Tchobanoglous, G., Burton, F. L., Stensel, H. D., Tsuchihashi, R. (2014) *Wastewater Engineering: Treatment and Resources Recovery* (Ch. 12). 5th Edition, New York, NY: McGraw-Hill.

Tolleson, W. H., Jackson, L.S., Triplett, O.A., Aluri, B., Cappozzo, J., Banaszewski, K., Chang, C.W., Nguyen, K.T. (2012) Chemical inactivation of protein toxins on food contact surfaces. Journal of Agricultural and Food Chemistry 60, 6627-6640.

Torrentó, C., Urmeneta, J., Otero, N., Soler, A., Viñas, M., Cama, J. (2011) Enhanced denitrification in groundwater and sediments from a nitrate-contaminated aquifer after addition of pyrite. Chemical Geology 287, 90-101.

Trung Tran, T., Bott, N. J., Dai Lam, N., Trung Nguyen, N., Hoang Thi Dang, O., Hoang Le, D., Tung Le, L., & Hoang Chu, H. (2019) The Role of Pseudomonas in Heterotrophic Nitrification: A Case Study on Shrimp Ponds (*Litopenaeus vannamei*) in Soc Trang Province. Microorganisms 7(6), 155.

Wang, D., Yamaki, S., Kawai, Y., Yamazaki, K. (2020) Sanitizing efficacy and antimicrobial mechanism of peracetic acid against T histamine-producing bacterium, *Morganella psychrotolerans*. LWT - Food Science and Technology 126, 109263.

Wang, X., Zeng, R.J., Dai, Y., Peng, Y. and Yuan, Z. (2008) The denitrification capability of cluster 1 *Defluviicoccus vanus*‐related glycogen‐accumulating organisms. Biotechnology Bioengineering 99: 1329-1336.

Wagner, M., Brumelis, D., Gehr, R. (2002) Disinfection of wastewater by hydrogen peroxide or peracetic acid: Development of procedures for measurement of residual disinfectant and application to a physicochemically treated municipal effluent. Water Environment Research 74:33-50.

Wu, L., Zhu, G., Zhang, X., Si, Y. (2020) Silver nanoparticles inhibit denitrification by altering the viability and metabolic activity of *Pseudomonas stutzeri*. Science of the Total Environment 706, 135711.

Yamada, Y. and Yukphan, P. (2008) Genera and species in acetic acid bacteria. International Journal of Food Microbiology 125(1):15-24.

Yang, Y., Tezel, U., Li, K., Pavlostathis, S.G. (2015) Prolonged exposure of mixed aerobic cultures to low temperature and benzalkonium chloride affect the rate and extent of nitrification, Bioresource Technology 179, 193-201.

Yang, Y., Wang, J., Zhu, H., Colvin, V.L., Alvarez, P.J. (2012) Relative susceptibility and transcriptional response of nitrogen cycling bacteria to quantum dots. Environmental Science & Technology 46 (6), 3433-3441.

Young, J.M., Kuykendall, L.D., Martínez-Romero, E., Kerr, A., Sawada, H. (2001) A revision of Rhizobium Frank 1889, with an emended description of the genus, and the inclusion of all species of *Agrobacterium* Conn 1942 and *Allorhizobium undicola de Lajudie* et al. 1998 as new combinations: *Rhizobium radiobacter*, *R. rhizogenes, R. rubi, R. undicola* and *R. vitis.* International Journal of Systematic and Evolutionary Microbiology 51, 89-103.

Yuan, Z., Ni, Y., Van Heiningen, A.R.P. (1997) Kinetics of peracetic acid decomposition. Part I: Spontaneous decomposition at typical pulp bleaching conditions. The Canadian Journal of Chemical Engineering 75:37-41.

Zeng, X., Liu, J., Zhao, J. (2017) Wet oxidation of an industrial high concentration pharmaceutical wastewater using hydrogen peroxide as an oxidant. Journal of Advanced Oxidation Technologies 20160179.

Zhang, C., Brown, P.J.B., Miles, R. J., White, T. A., Grant, D. G., Stella, D., Hu, Z. (2019) Inhibition of regrowth of planktonic and biofilm bacteria after peracetic acid disinfection. Water Research 149, 640-649.

Zhang, T., Wang, T., Mejia-Tickner, B., Kissel, J., Xie, X., and Huang, C-H. (2020) Inactivation of bacteria by peracetic acid combined with ultraviolet irradiation: Mechanism and optimization. Environmental Science & Technology 54(15), 9652-9661.

Zhao, X., Zhang, T., Zhou,Y., Liu, D. (2007) Preparation of peracetic acid from hydrogen peroxide: Part I: Kinetics for peracetic acid synthesis and hydrolysis. Journal of Molecular Catalysis A: Chemical 271, 246–252.

Zhao, X., Chen, K., Hao, J., Liu, D. (2008) Preparation of peracetic acid from hydrogen peroxide, Part II: Kinetics for spontaneous decomposition of peracetic acid in the liquid phase. Journal of Molecular Catalysis A: Chemical 284, 58–68.